UiT
THE ARCTIC UNIVERSITY OF NORWAY

Faculty of Health Sciences
Department of Pharmacy

Development of osmotically active liposomes for nose-to-brain drug delivery

—

Iren Yeeling Wu

A dissertation for the degree of Philosophiae Doctor – August 2019

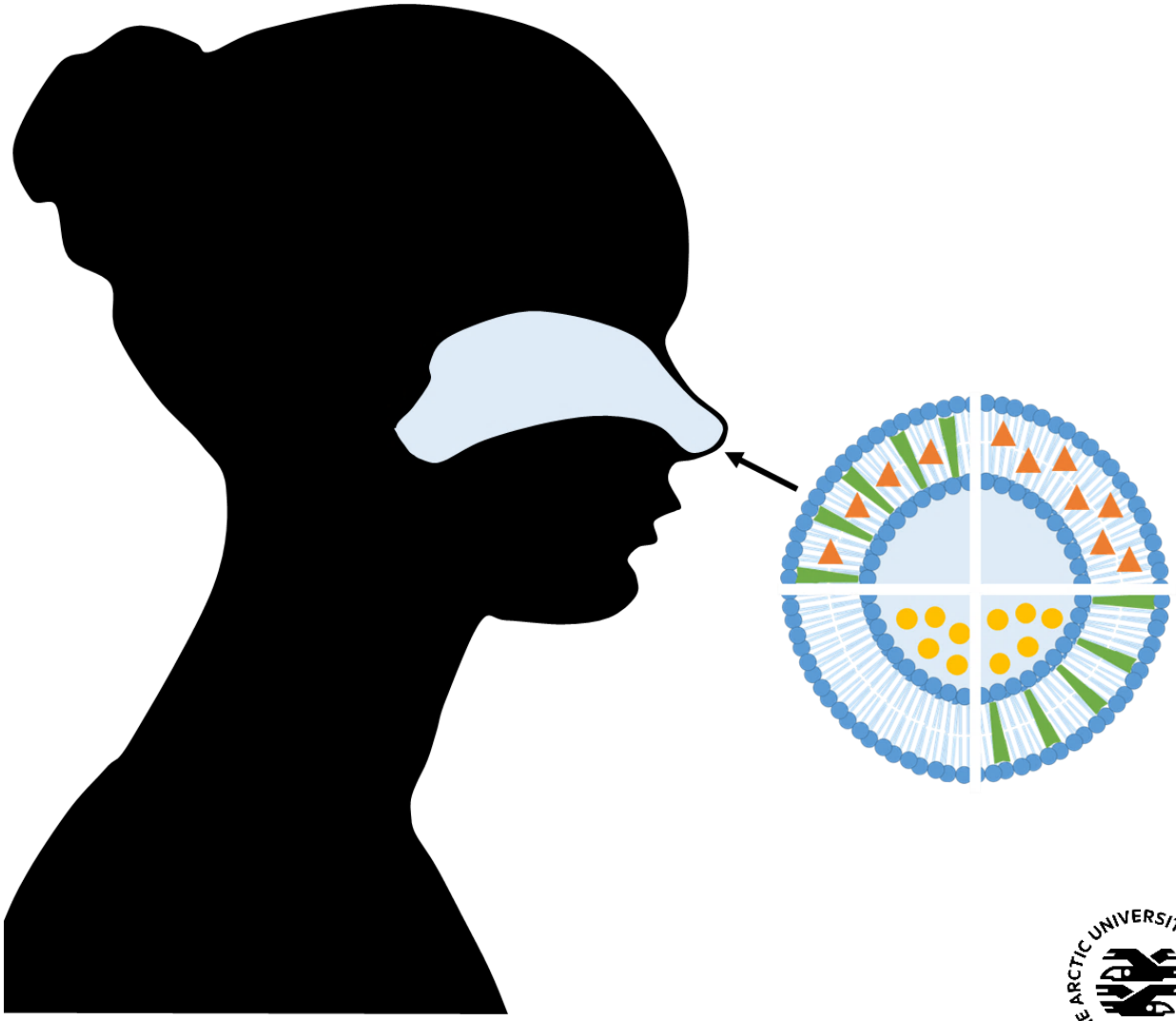

THE ARCTIC UNIVERSITY OF NORWAY • UiT •

Front page content:

Silhouette adapted from http://www.colourbox.com (left) and one unilamellar vesicle comprising various drugs and cholesterol (right).

A dissertation for the degree of Philosophiae Doctor

Development of osmotically active liposomes for nose-to-brain drug delivery

Iren Yeeling Wu

Tromsø, August 2019

Drug Transport and Delivery Research Group
Department of Pharmacy
Faculty of Health Sciences
UiT The Arctic University of Norway
Norway

My liposomal journey

I heard in a lecture about some tiny balls.
Consisting of lipids and fatty walls.
Professor said, “Liposomes are future”, I recall.
So I started my master in liposomes next fall.

Dissolve lipid in methanol and evaporate “all”.
Hydrate film to create vesicle walls.
“Add curcumin, they have potentials”, someone called.
“Liposomes are super, they can entrap them all!”

Sonication and extrusion to make them small.
Most cases sadly on benches, clothes, and walls.
Experiments seemed to go downfall.
Wait – master defended. PhD from next fall?

Osmotically active liposomes, my next call.
Redesigning LUVs formulations with cholesterol.
Franz cell experiments – an immense haul.
Success or not, under tonicity befall.

Even though my journey has come to a stall.
Further dreams for these vesicles are post-nasal.
Start penetrating the brain’s impermeable wall.
Maybe brain diseases can be cured after all.

Iren Yeeling Wu

Acknowledgements

The work presented in this thesis was carried out at the Drug Transport and Delivery Research Group, Department of Pharmacy, UiT The Arctic University of Norway, from September 2015 to August 2019. I am grateful to UiT for financing this project, and I would like to use this opportunity to express my gratitude to everyone that has helped me along the way.

First and foremost, I would like to give my sincere gratitude to my supervisors, Associate Professor Massimiliano Pio di Cagno, and Professor Nataša Škalko-Basnet. Especially to Max for letting me work on his project and guiding me into the fields of nose-to-brain, and Nataša for dedicating her valuable time to supervise, give words of advice and encouragement until the completion of this thesis. It has been a privilege to learn from both of you.

My deepest appreciations to my master students and co-authors, Trygg Einar Nikolaisen and Sonali Bala for their tremendous work in the lab. You have been inspiring, motivating, and I have learned a lot from you. You have helped me to grow both as a researcher and as a person. It has been a great pleasure working with both of you.

I am also thankful to Professor Purusotam Basnet for his generous support and belief in me. I am thankful that you and Nataša saw something in me that I did not know existed. I would never be where I am today, nor started with a PhD without any of you.

I would like to thank my former and current colleagues in the Drug and Transport and Delivery Research Group. I appreciate our lutefisk tradition, lunch in the Botanical garden, hikes, dinners, and chats. Especially thanks to Cris, Jennifer, Laura, Lisa, Margherita, May Wenche, and Sybil for creating the most perfect working environment I could ever ask for in the most stressful period of my life. Special thanks to Sveinung for always wondering how I am doing and updating me about his life.

I want to thank former and current colleagues at the Department of Pharmacy. I appreciate all the scientific meetings and social occasions, especially the knitting evenings and wine lotteries have been my absolute favourites. To my second home “IPSUM”; for not being related to your group, I feel privileged that you call me the “I” in IPSUM and sometimes “IPSHUM”. Thank you for “adopting” Håvard and me. I admire your kind nature and appreciate all the social inclusion. Also, I will miss having morning coffee with you, Elin, Elizabeth, and Lars. This period would never have been the same without you.

On this “journey” I also spent time with people who deserve to be mentioned for their encouragement and tolerant support in me;

To the “Dine and Wine Club” and all the exclusive members there; thank you for being the persons you are and for sharing the same love for food. Even though life is moving us apart in distance, I hope that we will still be able to meet frequently. You are all very precious to me, and you are always welcome to wherever I will be. I am looking forward to more food-related adventures with you.

To “Sangfuglene”; I am grateful that I met you during my studies, and that we have become part of each other lives since then. Even though I am not the best to reply to your messages, I still appreciate that you all take time to send me updates now and then. Special thanks to the mother of Sangfuglene, Lilli, who always has the extra time for me. You are such a considerate person putting others in front of your own needs. All those times spent on comforting, cooking or make me laugh things off during stressful periods are invaluable. It has all contributed a lot to my performance at work and making it able to set work aside when a break was needed. I owe you my deepest gratitude.

To Julia; who I would like to give my deepest heartfelt appreciations to. Whenever sick, sad, happy - you are there! My time in Tromsø would never be this great without you in my life. I am looking forward to be there for you when you need me. Please keep up your fighting spirit because you are one of the strongest persons I know!

To Elenaz Naderkhani and Ingvild Arnesen; for giving me the opportunity to work at the Pharmacy in parallel with my PhD project. Both of you have shown me tremendous support and understanding. Never questioning when I needed time off due to a conference or because of lab work. I would never have been able to combine PhD with pharmacy work if it was not for you always stepping in for me.

Lasts but not least, this will never have happened without the encouragement and support from my family;

To my mother and father; this PhD project is dedicated to both of you. You have always encouraged me to study and follow my dreams. I will forever be in depth to you for all guidance and opportunities you have given me. It has been hard to be away from you, but you have always been in my mind.

To Kit and Natalie; for being my big sisters. I am thankful that I can always tell you everything on my mind. Now, that Jasmin and Augusta are born, I hope I can create the same encouraging and supportive environment you created for me.

To my family in Hong Kong and Australia (in Chinese); 感謝您的支持和鼓勵!

To Family Utstøl Jakobsen (in Norwegian); takk for at dere har vært der for meg i alle disse årene. Det har vært utrolig gøy å være en del av deres liv og ikke minst få ta del i at familien har blitt større. Først Synne, så vår guddatter, Jenny, og nå Ingrid. Uansett hvor vi befinner oss i verden håper jeg at vi får møtt hverandre like mye. Dere er alltids velkomne på besøk!

To Håvard; we have now been part of each other's lives in more than 9 years. I am filled with gratitude for all the patience you have given me. As I promised four years ago, PhD will be the last thing I do for me, and from now on I will always plan according to us. It was a promise and a promise I intend to keep. I am looking forward to all adventures ahead of us.

Last but not least, my dearest Carina; even though we have been apart, maybe by distance but not by heart. I feel that this PhD period has brought us closer together. I will forever be indebted to your interest and support in my project. Maybe in the future, you will continue this work? Maybe my dream of having a paper with Wu CY and Wu IY will be true? Anyhow, what I know is that you have so much potential and I know you will succeed in anything you do in life. You are the smartest person I know, and I am proud to be your sister!

Iren Yeeling Wu

Tromsø, August 2019

Table of contents

Abstract

Central nervous system (CNS) disorders are accounted as the leading cause of disability and the second leading cause of death globally. Despite intense research efforts, CNS therapeutics covering a wide range of CNS disorders are still limited, possibly because of the complex pathophysiology of the CNS disorders and difficulties accessing the brain. One of the major barriers preventing drugs to reach the brain is the blood-brain-barrier (BBB). The BBB is responsible for preventing over 98% of drug molecules from the systemic circulation to reach the brain. Therefore, instead of utilizing the traditional drug administration routes, time and investment have been shifted towards new strategies to overcome the BBB.

One of the innovative and promising strategies is the nose-to-brain delivery approach. Nasally administered drugs have shown to provide therapeutic effect locally, systemically and within the CNS. Despite promising results from *in vivo* studies, the main limitations using the nose as the administration site are related to drug's potency in small volumes applicable to the nose, and the drug's stability and permeability through the nasal mucus. Liposomes as drug carrier system exhibit the ability to entrap a wide range of poorly soluble drugs protecting them from early degradation and clearance. However, the nasal mucus tonicity fluctuates greatly due to its direct exposure to the peripheral milieu, thus influencing liposomes behaviour and their sensitivity to osmotic stress. Our hypothesis was that co-operation between osmotic stress and liposomal behaviour might be utilized to achieve controlled drug delivery systems.

In the present study, we selected two markers and six drugs covering a wide range of relevant physiochemical properties to be entrapped into large unilamellar vesicles (LUVs). The various LUVs were verified to be osmotically active. Both linear and non-linear approximations were used to interpret the *in vitro* diffusion data and showed that release from LUVs was associated with their exposure to osmotic stress. These findings were consistent using the standard regenerated cellulose and biomimetic Permeapad® as the diffusion barriers. To achieve better *in vitro/in vivo* correlations, mucin was introduced into the *in vitro* diffusion study to mimic the nasal environment. Surprisingly, mucin did not affect the osmotic activity of the LUVs, nor had an impact on the drug release from LUVs. LUVs formulated with an increased amount of cholesterol incorporated into the bilayer (up to 25% w/w) showed decreased sensitivity to osmotic stress. However, the liposomes comprising 11% w/w cholesterol were the most stable formulations. Also, these formulations retained relatively good osmotic activity.

The obtained data provide important information on the osmotic activity of liposomes and build the fundament for further development of innovative nose-to-brain drug delivery systems.

Nomenclatures

Abbreviations

AD	Alzheimer's disease
bFGF	Basic fibroblast growth factor
BBB	Blood-brain barrier
BCS	Biopharmaceutics classification system
CHOL	Cholesterol
CNS	Central nervous system
CPP	Cell-penetrating peptide
DALY	Disability-adjusted life year
DMPC	Dimyristoylphosphatidylcholine
DMPG	Dimyristoylphosphatidylglycerol
DOPC	Dioleoylphosphatidylcholine
DSPC	Distearoylphosphocholine
DSPE	Distearoylphosphatidylethanolamine
EE	Entrapment efficiency
EPC	Egg-phosphatidylcholine
GDNF	Glial cell line-derived neurotrophic factor
GI	Gastrointestinal
GUVs	Giant unilamellar vesicles
HSPC	Hydrogenated soy-phosphatidylcholine
IN	Intranasal administration
IV	Intravenous administration
LUVs	Large unilamellar vesicles
MPEG	Methoxypoly(ethylene glycol)
MW	Molecular weight
ND	Not detected
ODA	Octadecylamine
PBS	Phosphate buffer saline
PBS300	Phosphate buffer saline with tonicity of 300 mOsm/kg
PBS65	Phosphate buffer saline with tonicity of 65 mOsm/kg
PCL	Poly(ε-caprolactone)
PEG	Poly(ethylene glycol)
PI	Polydispersity index
PLA	Poly(lactic acid)
PLGA	Poly(lactic-co-glycolic acid)
PO	Peroral administration
RGD	Integrin-binding peptide
SA	Stearylamine
SD	Standard deviation
SL	Soy-lecithin
SPC	Soy-phosphatidylcholine
ZP	ζ-potential

Variables and parameters

$\Delta mOsm/kg$	Difference between the measured osmolality of LUVs formulation and the exposing PBS
ΔT_f	Freezing point
A^-	Conjugate base of a weak acid
A	Surface area
B	Weak base
BH^+	Conjugate acid of a weak base
C^0_d	Initial drug concentration of the formulation
C_a	Drug concentration in the acceptor compartment
D	Diffusion coefficient
HA	Weak acid
i	van't Hoff factor
j	Mass flux
K	Transport constant
K_f	Cryoscopic constant
$\log D_{7.4}$	Distribution coefficient at pH 7.4
$\log P$	Partition coefficient
m	Molality
M_t/M_∞	Fractional permeated drug
n	Transport exponent
$Osm_{(in)}$	Osmolality of the internal environment LUVs
$Osm_{(out)}$	Osmolality of the external environment of LUVs
P_{app}	Apparent permeability coefficient
$P_{app}{}^m$	Apparent permeability coefficient with the presence of mucin
pH	Concentration of hydrogen ions in a solution
pKa	Ionization constant
R	Barrier's resistance
R_0	Ideal gas constant
R_B	Resistance to drug transport through permeable barrier
R_L	Resistance to drug transport through liposomal bilayer
R_T	Total resistance to drug transport
T	Absolute temperature
t	Time
x	Barrier thickness
π	Osmotic pressure
π_{rel}	Relative osmotic pressure

Papers

Paper I[1]:

Wu, I. Y., Škalko-Basnet, N. & di Cagno, M. P. **2017**. Influence of the environmental tonicity perturbations on the release of model compounds from large unilamellar vesicles (LUVs): A mechanistic investigation. *Colloids Surf B,* 157**,** 65-71.

Paper II[2]:

Wu, I. Y., Nikolaisen, T. E., Škalko-Basnet, N. & di Cagno, M. P. **2019b**. The hypotonic environmental changes affect liposomal formulations for nose-to-brain targeted drug delivery. *J Pharm Sci*, 108, 2570-2579.

Paper III[3]:

Wu, I. Y., Bala, S., Škalko-Basnet, N. & di Cagno, M. P. **2019a**. Interpreting non-linear drug diffusion data: Utilizing Korsmeyer-Peppas model to study drug release from liposomes. *Eur J Pharm Sci,* 138, 105026.

[1]© 2017 Elsevier B.V. Reprinted with permission from Elsevier.

[2]© 2019 American Pharmacists Association®. Reprinted with permission from Elsevier.

[3]© 2019 Elsevier B.V. Reprinted with permission from Elsevier.

1 Introduction

Central nervous system CNS) disorders are a broad category of conditions, which according to the International Neuromodulation Society, are defined as;

"…conditions in which the brain does not function as it should, limiting health and the ability to function. The condition may be an inherited metabolic disorder; the result of damage from an infection, a degenerative condition, stroke, a brain tumour or other problem; or arise from unknown or multiple factors" (INS, 2013).

Due to the broad category of conditions which CNS disorders represent, they collectively account as the leading cause of disability and are the second leading cause of death globally (Feigin *et al.*, 2019). In a global burden of disease study published in 2019, the prevalence, incidence, and mortality of 15 most relevant CNS disorders were estimated in 195 countries in the years 1990-2016. It was reported that in 2016, the three major contributors to CNS disability-adjusted life year (DALY) were stroke (42%), migraine (16%), and Alzheimer's and other dementias (10%), as it can be seen in Figure 1.1.

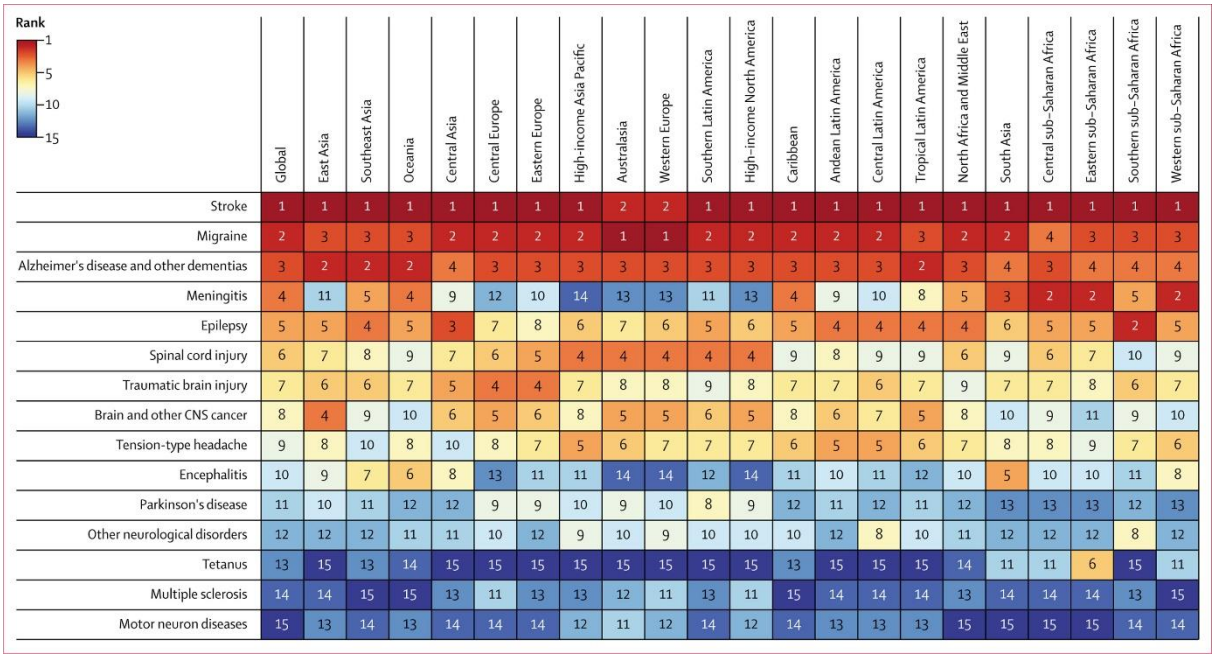

Figure 1.1: Ranking of age-standardized DALYs for CNS disorders by demographic region in 2016. Reproduced from Feigin *et al*., 2019, with permission from Elsevier.

In terms of the absolute number of deaths and DALYs, both values have been increasing with 39 and 15%, respectively, since 1990. On the contrary, age-standardized deaths and DALY values have generally been decreasing for all CNS disorders, suggested to be due to socio-

economic development globally. However, Alzheimer's and other dementias, and Parkinson's disease do not seem to follow this trend and are suggested to continue to develop independently from socio-economic development. The prevalence of Alzheimer's and other dementias are up to 9 times higher than Parkinson's disease and is causing more deaths and DALYs in women compared to men (Feigin *et al.*, 2019). Similar findings were reported in a Norwegian burden of disease study from 2018 (Tollanes *et al.*, 2018). Alzheimer's and other dementias were the second leading cause of deaths ranked after the cardiovascular diseases in 2016. With this alarming percentage, Alzheimer's and other dementias are considered to be one of the most fatal diseases in Norway (Tollanes *et al.*, 2018).

1.1 The global burden of Alzheimer's and other dementias

Due to increasing life expectancy globally, the number of people affected by Alzheimer's and other dementias is estimated to almost double by 2030 (82 million) and triple within the year 2050 (152 million) (ADI, 2018, Alzheimer's Association, 2018, FHI, 2019, WHO, 2019).

Dementia is a syndrome which covers a broad classification of progressive neurodegenerative disorders describing memory impairment and thinking and behavioural disturbances that affect the daily life of patients (WHO, 2019). The most common form of dementia is Alzheimer's disease (AD), representing up to 70% of the cases. According to the World Alzheimer report in 2018, new cases of AD are developed almost every minute in the United States alone (Alzheimer's Association, 2018). Globally, the incidence rates of AD and other dementias are even more alarming, with newly diagnosed patients every three seconds (ADI, 2018). The highest incidence rates are anticipated to be 50% in Asia, 25% in Europe and 20% in America, respectively (ADI, 2018).

In 2017, over 184 billion unpaid hours were spent by family members and caregivers to provide care to people with AD and other dementias in the United States. These hours were estimated to value more than 232 billion USD, emphasizing the great socio-economic burden dementias cause the society (Alzheimer's Association, 2018). The annual estimated global cost of dementia in 2018 was 1 trillion USD and is predicted to be doubled by the year 2030 (ADI, 2018). To decrease the global cost, it is of high necessity to develop more effective CNS diagnostics, therapeutics and prevention measures across the globe (Feigin *et al.*, 2019).

Despite intense research efforts for better CNS therapeutics, it is estimated that approx. 90% of molecules developed by the pharmaceutical industry for the treatment of CNS disorders,

never reach the market (Vlieghe and Khrestchatisky, 2013). Since 1998, 100 drugs have been tested for the treatment of dementia, whereas only four have been authorized for clinical use (ADI, 2018). The low success is presumably because of the complex pathophysiology of AD and other dementias, but most importantly the difficulties potential drugs experience in accessing the brain (Khan *et al.*, 2017, Patel and Patel, 2017).

Therefore, rather than focusing on the discovery of new drugs, the development of new strategies to increase the drug transport to the brain might have a greater impact on the therapy (Li *et al.*, 2017, Wong *et al.*, 2012). Five different barriers in the CNS have been attributed to limit drug access into the brain. They are namely the blood–brain barrier (BBB), the blood–cerebrospinal fluid barrier, the arachnoid barrier, the blood– spinal cord barrier, and the blood–retina barrier (Gorlé *et al.*, 2016). Among all these barriers, the BBB represents the strongest resistance to drug permeation and is the largest interface for blood-to-neuronal extracellular fluid exchange (Abbott *et al.*, 2010). For this reason, in the next section, the BBB's anatomy and functionality in the body will be discussed, before addressing the strategies to overcome the barrier.

1.2 The blood-brain barrier (BBB)

The BBB is a term commonly used to describe the properties of the blood capillaries found in the CNS. The capillaries in the BBB differ from other peripheral capillaries because they are generally thinner (approx. 500 nm in diameter) and more complex (see Figure 1.2).

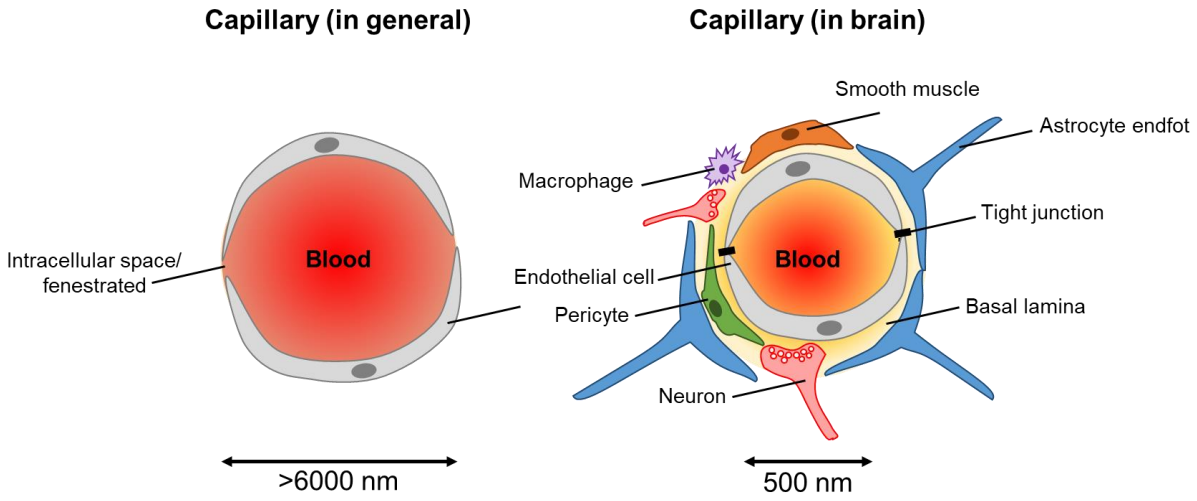

Figure 1.2: Schematic representation of the capillaries generally found in the body and brain. Based on Abbott *et al.*, 2010, Khan *et al.*, 2017.

The main cell types in the BBB are the tightly packed endothelial cells that create the walls of the capillaries. Other types of cells include the mural cells (smooth muscle cells and pericytes), immune cells (macrophage, astrocytes), and neuronal cells (Abbott *et al.*, 2010, Daneman and Prat, 2015). Secrete from astrocytes, endothelial cells, and pericytes create the basal lamina; the microenvironment supporting the efficient signalling between the capillary and the neuronal cells (Daneman and Prat, 2015). The synergistic interplay between the basal lamina and the various cell types contributes to the BBB properties. The BBB is an obstacle for drug transport into the brain, and to understand this, the transport mechanisms across BBB (summarized in Figure 1.3) will be first briefly described in chronological order.

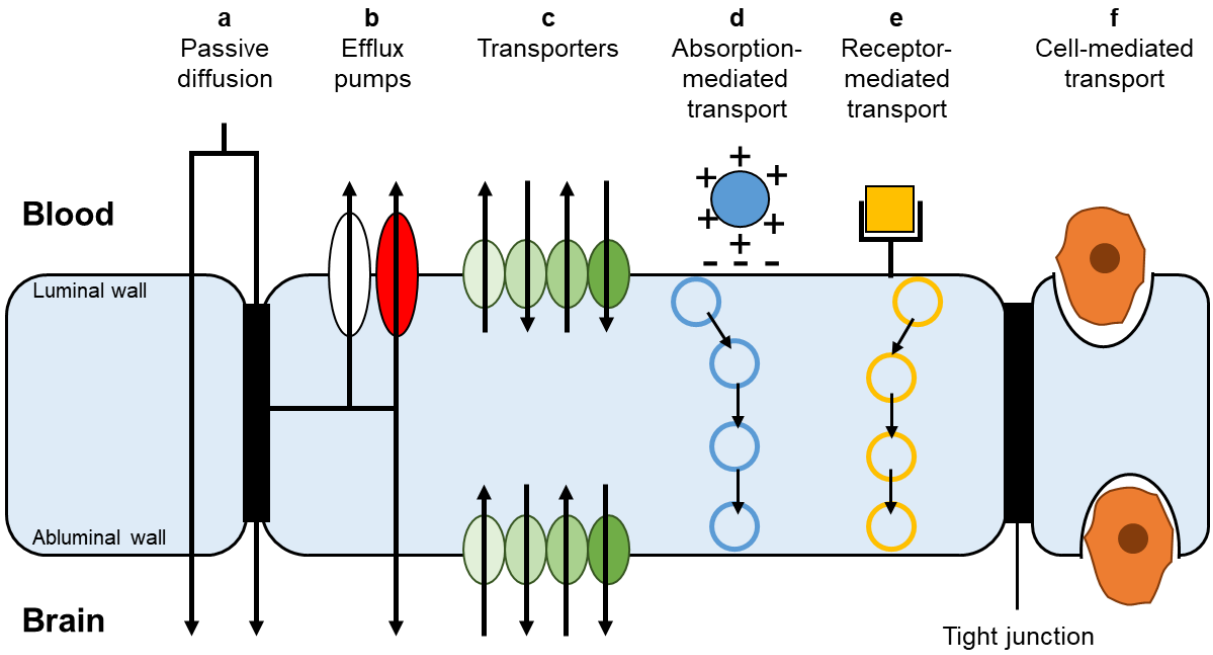

Figure 1.3: Routes of transport across the BBB. Based on Abbott *et al*., 2010, Patel and Patel, 2017.

The passive diffusion process (Figure 1.3a) allows molecules to move across a cellular membrane through their electrochemical gradient (*i.e.* concentration gradient) without the requirement of metabolic energy. It has been observed that small (<500 Da) and lipid soluble compounds (log*P* 1.5-2.7) favour the passive diffusion through the BBB, whereas larger and polar compounds (polar surface area >80 $Å^2$) are not suited for this type of transport (Abbott *et al.*, 2010, Patel and Patel, 2017).

Transporter-mediated transports (Figure 1.3b-c) are important for the control of influx and efflux of poorly permeable solutes that are regarded as either important or not important for the optimal synaptic function of the BBB. Influx of nutrients often follows the facilitated diffusion requiring no energy, whereas the efflux often happens through efflux pumps that consume

ATP. For efficient transport into the brain, transporters expressed on the luminal and/or abluminal wall of the BBB can be utilized (Abbott *et al.*, 2010, Patel and Patel, 2017).

Absorption- and receptor-mediated transports (Figure 1.3d-e) are transports related to the surface interaction between the neuronal endothelial cell and the potential drug. The absorption mediated transport involves electrostatic binding between a cationic compound (*e.g*. IgG, albumin) and the negatively charged endothelial cell membrane. It represents a relatively weak interaction in comparison to receptor-mediated transport, where a specific unit (*e.g.* ligand, peptide) binds covalently to specific receptors expressed on the BBB surface (*e.g*. transferrin, albumin, insulin). In both absorption- and receptor-mediated transport, the surface interaction triggers endocytosis/transcytosis, engulfing the compound, and leading to increased transport across the BBB into the brain (Abbott *et al.*, 2010, Patel and Patel, 2017).

Cell-mediated transports utilize the body's own cells, such as macrophages, monocytes, and neutrophils who are recruited during inflammation (Figure 1.3f). These cells have good ability to travel in the systemic circulation and can pass through the BBB using endocytosis/transcytosis mechanisms to reach the site of inflammation (Abbott *et al.*, 2010, Patel and Patel, 2017).

The transport mechanisms across the BBB are highly selective and strictly controlling the transport of essential ions, nutrients and peptides to maintain brain homeostasis and optimal neuronal function (Abbott *et al.*, 2010, Daneman and Prat, 2015, Patel and Patel, 2017). However, when there is a shift to an imbalance in the BBB, a different situation may occur.

Alterations of the BBB integrity can cause brain damages and have been suggested to be the cause of CNS disorders (Abbott *et al.*, 2010, Daneman and Prat, 2015). Several alterations of the BBB have been proposed. One theory includes the decrease in resistance in tight junctions between the endothelial cells, which allows an increase in paracellular transport of substances that is otherwise hindered. Another theory is that alterations in the transporter systems can directly affect the transport of essential molecules (*i.e.* glucose) which are vital to maintaining brain homeostasis. Alterations in the enzymes expressed in the cytoplasm of neuronal endothelial cells can also be important, as this will hamper the BBB from discarding harmful substances (*i.e.* neurotoxins). Moreover, inflammation has also been suggested to play an essential role in CNS disorders as inflammation might cause structural abnormalities and damage of the BBB, possibly causing a secondary immune response that can reduce the resistances of tight junctions (Abbott *et al.*, 2010, Daneman and Prat, 2015).

Therefore, to develop efficient therapeutics for CNS disorders, the drug transport strategies across BBB must be applicable at disordered state as well as in a healthy state. Moreover, the choice of administration route is important as drug administration following traditional routes (*i.e.* systemic administration) often results in binding of the drug to plasma proteins. Consequently, systemic administration reduces the compounds ability to reach therapeutic concentrations in the brain without reaching intolerable systemic side effects (Patel and Patel, 2017).

In the past, strategies such as direct injection of potential drugs into the brain tissues, cerebrospinal fluid, or spinal cord have been attempted (Abbott *et al.*, 2010). Furthermore, disrupting the BBB using hyperosmotic solution, ultrasound or electromagnetic radiation have also been examined (Patel and Patel, 2017). These invasive ways of drug administration are limited by the requirement for qualified personnel, as well as with the high risk of infection, tissue damage, little patient comfort, and high costs due to hospitalization (Alam *et al.*, 2010, Patel and Patel, 2017).

In the urge for finding new ways to circumvent the BBB, the nasal administration of drugs for the direct delivery to the brain (namely the nose-to-brain drug delivery) seems to be both innovative and promising approach. The nasal route represents a non-invasive administration route and offers therapeutic efficacy locally, systemically, and reaching the CNS (Erdő *et al.*, 2018, Khan *et al.*, 2017, Patel and Patel, 2017).

Before discussing the olfactory and trigeminal nerves` involvement in drug transport from the nasal cavity into the brain, a brief introduction of the nasal anatomy and physiology will be presented.

1.3 Nasal anatomy and physiology

The nose consists of two nasal cavities with a septum of bone and cartilage between them (Crowe *et al.*, 2018, Sahin-Yilmaz and Naclerio, 2011). Each cavity can be further divided into the anterior and posterior part as shown in Figure 1.4.

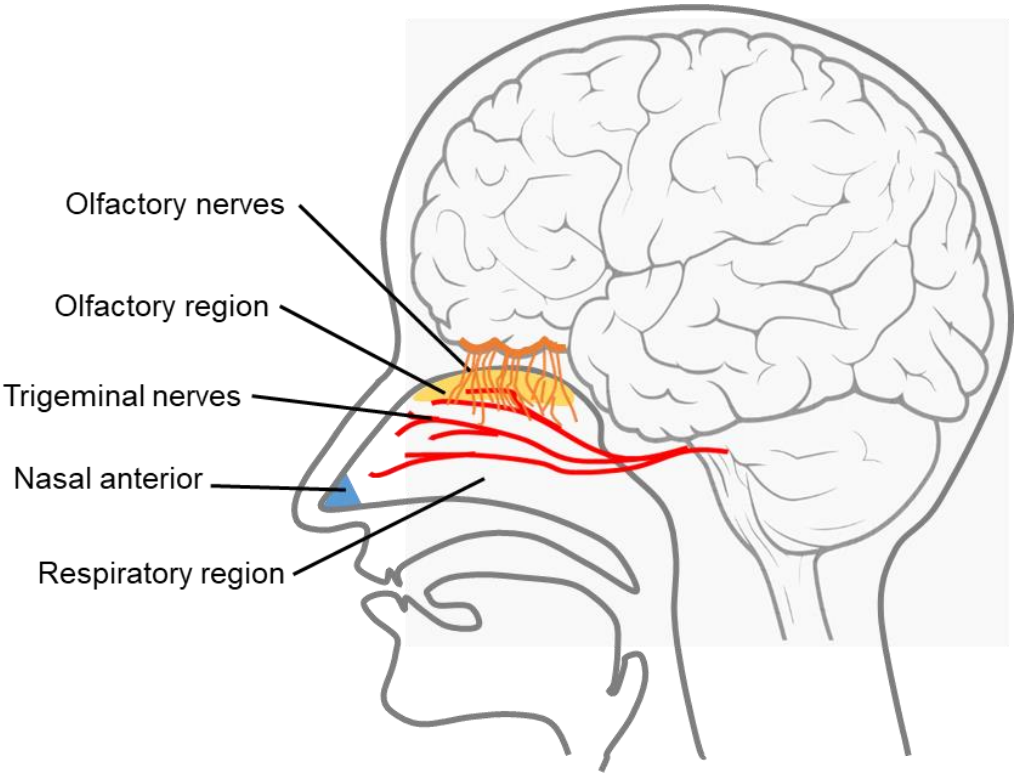

Figure 1.4: Lateral section of the human nose and brain, showing the key regions and nerves relevant for nose-to-brain drug delivery. Based on Djupesland *et al.*, 2014.

The anterior part (0.4% of total nose area) is the area closest to the peripheral environment and creates an opening to the nasal cavity. The posterior part of the nose can be divided into the respiratory and olfactory region and represents approx. 90 and 10% of the total nose area, respectively. The main functions of the nose are to regulate for humidity and temperature of the inhaled air to be transported into the lungs. Along the process, inhaled particles pass through the posterior part of the nose and will be either eliminated or absorbed (Crowe *et al.*, 2018, Illum, 2003, Mistry *et al.*, 2009, Sahin-Yilmaz and Naclerio, 2011).

1.3.1 The respiratory region

The respiratory epithelium consists of four types of cells. The surface is covered by non-ciliated and ciliated cells, the area closest to the epithelium consists of basal cells, and the goblet cells are lined among epithelium cells (see Figure 1.5b).

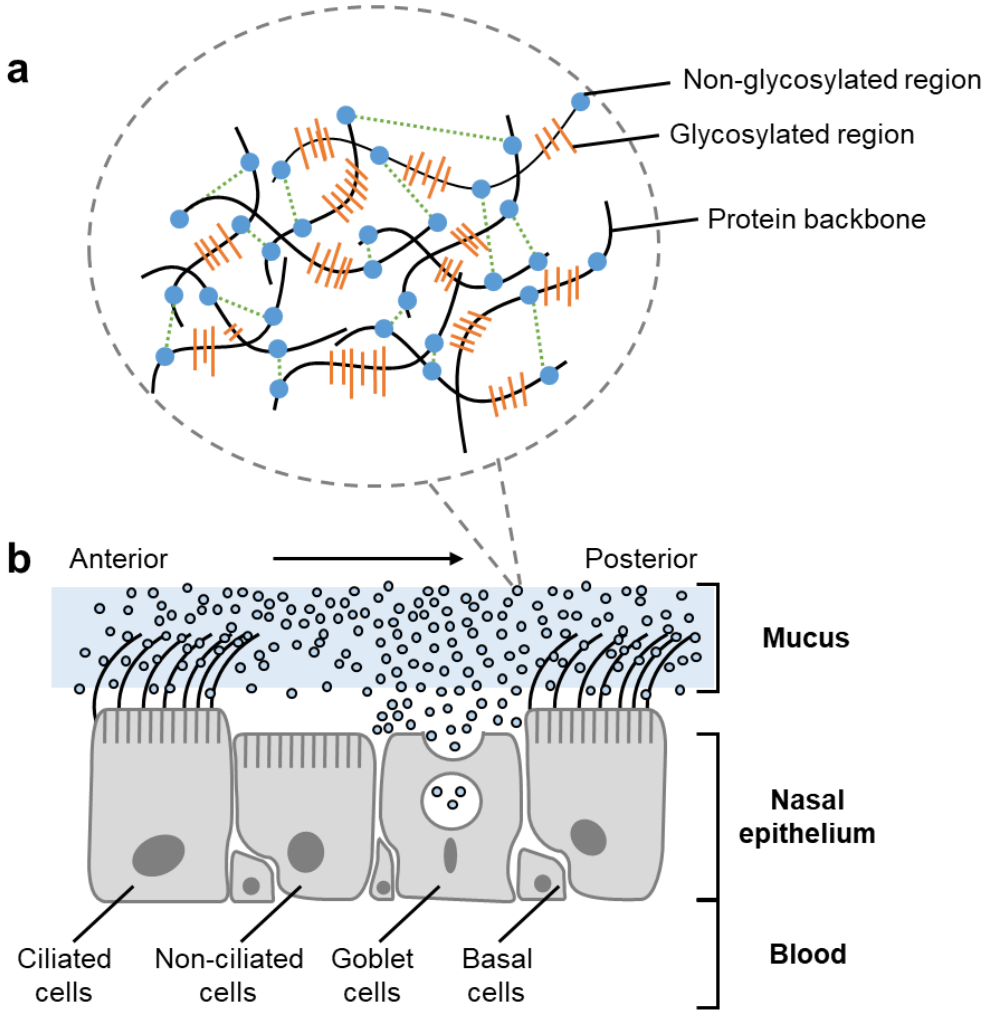

Figure 1.5: Simplified representation of secreted mucin forming the mucus that covers the nasal respiratory epithelium. Based on Lock *et al.*, 2018, Murgia *et al.*, 2018.

The respiratory region is highly vascular, and the cells presented here provide for the transport of water and ions between nasal mucus, cells, and control the cilia movements. Moreover, the goblet cells secrete mucin which is one of the most important components in the nasal mucus (Bansil and Turner, 2018, Crowe *et al.*, 2018).

The nasal mucus is a complexed hydrogel consisting mainly of water (95%) and mucins (2%) (Bansil and Turner, 2018, Quraishi *et al.*, 1998). The primary structure of mucins is the protein backbone consisting of glycosylated and non-glycosylated regions (see Figure 1.5a). The glycosylated regions are covalently bound to oligosaccharide side chains and account for up to 80% of the molecular weight of mucins. For the non-glycosylated regions, cysteine-rich parts serve to form strong bindings with other cysteine-rich regions creating the mesh-like structure of the mucus (Bansil and Turner, 2018, Murgia *et al.*, 2018, Quraishi *et al.*, 1998). Due to

mucin's hydrophilic (glycosylated regions) and hydrophobic nature (protein backbone), various inhaled particles can be entrapped in the mucus, and be prevented from absorption through the nasal epithelium (Bansil and Turner, 2018, Gänger and Schindowski, 2018, Murgia *et al.*, 2018, Quraishi *et al.*, 1998, Taherali *et al.*, 2018).

1.3.2 The olfactory region

The olfactory region is located in the upper part of the human nasal cavities (Figure 1.4, yellow region). Presented in this region are the olfactory nerves, trigeminal (ophthalmic branch) nerves, supporting and basal cells (Crowe *et al.*, 2018). The olfactory epithelium is reported to be the only CNS tissue in direct contact with the peripheral environment (Djupesland *et al.*, 2014). Inhaled particles that come in contact with this nasal region are suggested to give the sensation of smell and associations to taste. Drugs that come in contact with the olfactory region is suggested to be transported directly into the brain (Crowe *et al.*, 2018, Illum, 2003, Mistry *et al.*, 2009).

1.4 Nose-to-brain drug delivery

The most discussed topic considering nose-to-brain drug delivery is the involvement of the olfactory and trigeminal nerves (Crowe *et al.*, 2018, Erdő *et al.*, 2018). These nerves expand themselves, leaving one end in the nasal cavity and the other end in the brain (Crowe *et al.*, 2018). The trigeminal nerves are the largest of the cranial nerves and originates from the brain stem and branch into the ophthalmic, maxillary, and mandibular nerves. It has to be mentioned that the trigeminal (ophthalmic and maxillary branch) nerves are also to be found in the nasal respiratory region (Figure 1.4). Drugs that come in contact with these nerves can be potentially transported into the brain as well (Crowe *et al.*, 2018, Gänger and Schindowski, 2018).

The transport mechanisms behind the involvement of olfactory and trigeminal nerves in nose-to-brain drug delivery are not fully understood, but one theory includes both the extracellular (paracellular) and intracellular (endocytosis, transcytosis) transport mechanisms (Crowe *et al.*, 2018, Erdő *et al.*, 2018, Gänger and Schindowski, 2018). Pre-clinical studies suggest that the rapid onset of action in CNS after intranasal administration (minutes) is due to paracellular transport through the nasal epithelium, leading to direct accumulation in cerebrospinal fluid, and thereby distribution into brain tissues. This transport mechanism is suggested to be more applicable for hydrophilic molecules below 500 Da. The slow onset of action (hours to days) due to neuronal endocytosis and transcytosis transport mechanisms is often reserved for

lipophilic molecules (Crowe *et al.*, 2018, Djupesland *et al.*, 2014, Erdő *et al.*, 2018, Gänger and Schindowski, 2018).

Utilizing nasal drug administration for brain delivery purposes have shown promising outcomes in clinical studies. Nasally administered benzodiazepines (*e.g.* diazepam and midazolam) for the treatment of epileptic seizures have shown to offer more convenience, more rapid onset of drug action and better bioavailability in comparison to intravenous or rectal administration forms (Henney *et al.*, 2014, Kälviäinen, 2015). Clinical studies have also been carried out on nasally administered insulin for the treatment of AD and mild cognitive impairments (Claxton *et al.*, 2013, Craft *et al.*, 2017). Insulin administered daily over a study period up to 16 weeks showed cognitive and memory improvements suggesting direct nose-to-brain delivery (Claxton *et al.*, 2013, Craft *et al.*, 2017). Other clinical studies utilizing the nose-to-brain pathway with positive outcomes are summarized in a review by Erdö and colleagues published in 2018. The positive therapeutic effects have been suggested to be due to a combination of avoidance of first-pass metabolism and renal clearance leading to enhanced drug transport across the BBB (Erdő *et al.*, 2018).

Despite that the nose-to-brain drug delivery offers promising results, the long-term effects and safety of this administration route are still uncertain (Erdő *et al.*, 2018, Schmid *et al.*, 2018). This reflects the limited number of available marketed products.

1.4.1 Nose-to-brain marketed products

In the Norwegian market (Felleskatalogen, 2019), nasally administered drugs with effect site in the brain/CNS are for the chronic pain (fentanyl/Instanyl® from Takeda Pharma AS, Japan) and migraine (sumatriptan/Imigran® from GlaxoSmithKline AS, UK and zolmitriptan/Zomig®, from Grünenthal GmbH, Germany). Only one marketed local anaesthetic is available for intranasal administration (lidocaine/Xylocain®, Aspen Nordic, Denmark). As it can be noticed, the marketed drugs are used for symptomatic treatment rather than therapeutic treatment of CNS disorders, and these nasal formulations are reserved for short treatment periods. This might be due to the many factors that can affect the drug absorption when utilizing nasal route of administration. Moreover, long-term use of some intranasal drugs have shown the occurrence of local side effects such as congestion, nasal irritation, nose bleed and rhinitis (Erdő *et al.*, 2018, Schmid *et al.*, 2018).

Despite the many advantages with nasal administration, the benefit *vs* safety has to be carefully evaluated before developing the nose-to-brain drug delivery system. For this reason,

in the next section, some of the considerations when developing nasal formulations are discussed.

1.4.2 Considerations for nose-to-brain drug delivery

The field of nose-to-brain drug delivery is relatively young, where the first patent involving this administration route was reported only 33 years ago (Crowe *et al.*, 2018). Despite evidence supporting that there might be a direct pathway from the nose to the brain, the transport mechanisms are still not clarified (Crowe *et al.*, 2018). Moreover, different factors might affect the absorption of drugs through nasal epithelium regarding anatomical, physiological, and environmental aspects. In Table 1.1, drug- and formulation-related properties that can affect drug absorption through the nasal epithelium are addressed (Khan *et al.*, 2017).

Table 1.1: List of drug- and formulation-related properties that can affect drug absorption through the nasal epithelium.

	Properties	For optimal absorption through nasal epithelium
Drug-related	Molecular size[1]	<300 Da: little influenced by nasal mucus <500 Da: cross nasal mucus and epithelium >1000 Da: should be formulated with absorption enhancer
	p*Ka*[1]	Unionized (salt or ester form) preferred
	Solubility[1]	Extracellularly: hydrophilic preferred Intracellularly: lipophilic preferred
Formulation-related	Absorption enhancers[1,2]	Surfactants (*e.g.* phospholipids), cationic polymers (*e.g.* chitosan), enzyme inhibitors, nanotechnology (*e.g.* liposomes), tight junction modulators, cell-penetrating peptides
	Absorption time[1]	Within 20 min
	Dosage volume[1]	Maximum 200 µL per nostril
	Dosage form[1,3]	Semi-solid > liquid
	p*H*[4,5]	p*H* 4.6-6.5: favoured p*H* 3-10: minimal cellular and ciliary damage *in situ* in rats
	Tonicity[5,6]	Isotonic and hypertonic (300-600 mOsm/kg): minimal cell and ciliary abnormalities

Information summarized from [1]Khan *et al*., 2017, [2]Ghadiri *et al*., 2019, [3]Gänger and Schindowski, 2018, [4]Ohwaki *et al*., 1987, [5]Pujara *et al*., 1995, [6]Homer *et al*., 2000.

As indicated in Table 1.1, not all drugs are chemically suited for nasal administration, as the transport across the nasal epithelium is highly restricted to drugs with certain molecular sizes and solubility profiles (Khan *et al.*, 2017). The main barrier regarding drug absorption through the nasal epithelium is the nasal mucus (Murgia *et al.*, 2018, Taherali *et al.*, 2018). The ciliary action beats 1000 strokes per minute moving the mucus from the anterior to the posterior part of the nasal cavity and clears the nose from particles (Gänger and Schindowski, 2018, Illum, 2003, Murgia *et al.*, 2018, Taherali *et al.*, 2018). The fraction of drug absorbed through the

nasal epithelium is thus highly dependent on the compound's solubility and metabolic stability in the mucus, and the drug should be absorbed through the epithelium within 20 min to avoid for elimination due to ciliary movements (Ghadiri *et al.*, 2019).

Nasal formulations with the ability to slow down the ciliary action, and protect the drug from early degradation and elimination would be attractive when it comes to designing intranasal formulations. This can be achieved by the use of absorption enhancers in the drug formulation (Ghadiri *et al.*, 2019, Gänger and Schindowski, 2018, Sonvico *et al.*, 2018). Some of the promising absorption enhancers include surfactants and cationic polymers (Ghadiri *et al.*, 2019, Illum, 2003). Surfactants (*i.e.* fatty acids, phospholipids, and non-ionic surfactants) have shown to be promising in improving the paracellular drug transport across nasal epithelium with minimal nasal epithelium and mucosa damage *in vitro* and *in vivo* (Ghadiri *et al.*, 2019). Among the cationic polymers, the chitosan-based ones have shown good mucoadhesive properties, increasing residence time on the nasal mucosa, and thereby allowing more drug transport through the nasal epithelium. Additionally, chitosan has shown good biocompatibility, biodegradability, and low toxicity profiles, making it currently attractive for use in nasal formulations (Ghadiri *et al.*, 2019).

In recent years, it has also been proposed that to optimize the brain drug delivery, combining nasal administration with nanotechnology-based drug formulation might be an advantage (Bourganis *et al.*, 2018, Gänger and Schindowski, 2018, Khan *et al.*, 2017, Patel and Patel, 2017, Sonvico *et al.*, 2018).

1.5 Nanotechnology for nose-to-brain drug delivery

Nano size is 10^{-9} of a meter. Applying nanotechnology for biomedical and pharmaceutical purposes is a field that is currently rapidly evolving. The first nanoparticulate drug delivery system was approved by the FDA in 1996 and since then, a total of 50 nanopharmaceuticals are available for use in the clinical practice (Kapoor *et al.*, 2017, Ventola, 2017). The interest in using nanotechnology-based delivery systems (called nanocarriers) to deliver drugs to the CNS has gained momentum in the recent years (Bourganis *et al.*, 2018, Khan *et al.*, 2017, Li *et al.*, 2017). Various animal studies have shown that drugs formulated within nanocarriers can enhance drug distribution into the brain, improve drug efficacy, and reduce drug-related side effects (Bourganis *et al.*, 2018, Khan *et al.*, 2017, Li *et al.*, 2017, Patel and Patel, 2017).

Nanocarriers are attractive for their ability to enhance the solubility and potency of potential drugs, which are often required for the dosage volumes that are applicable for nasal administration (Erdő *et al.*, 2018). Depending on the preparation method, the potential drug can be adsorbed to, covalently attached to, or entrapped within the carrier (Li *et al.*, 2017). Drug formulated with a nanocarrier can, therefore, be protected from early degradation, thus increasing the drug retention time in the nose (Li *et al.*, 2017). In addition, an increase in the absorption of compounds through the nasal olfactory or trigeminal nerves might be expected (Khan *et al.*, 2017, Patel and Patel, 2017).

The nanocarriers are promising drug delivery systems that can be re-engineered and tailored to express certain physiochemical properties with minimal alterations of the potential drug (Bourganis *et al.*, 2018, Li *et al.*, 2017). Yet, maximal therapeutic benefits are only achieved if the nanocarrier design can ensure optimal available dose at the target site at the right time (Bourganis *et al.*, 2018). An overview of the advantages and disadvantages of some of the major nanocarrier systems considering nose-to-brain targeting purposes are shown in Table 1.2.

Table 1.2: Some advantages and disadvantages of lipid- and polymer-based nanocarriers for nose-to-brain drug delivery.

Nanosystems	Nanocarriers	Advantages	Disadvantages
Lipid-based	Exosomes[1]	Good stability, minimal immune responses, natural and non-toxic	Limited knowledge of optimal composition and loading procedure
	Liposomes [1,2,4,5]	Biocompatible, biodegradable, increase BBB transport, low toxic, drug protective, provide controlled release, suitable for surface modifications and various molecules	(Conventional liposomes) Low stability, immunogenic and passive delivery.
	Nanoemulsions [1,2,4,5]	Biocompatible, increase BBB transport, suitable for surface modifications, promote the delivery of small molecules, suitable for various molecules	Thermodynamically unstable and surfactant concentration-dependent toxicity
	Nanostructured lipid carriers[3,4] (liquid core)	Low toxicity, high drug loading and stability, provide controlled release, enhance biodistribution	Absorption through the respiratory epithelium
	Solid lipid nanoparticles [1-5]	Biocompatible, biodegradable, increase stability and BBB transport, non-toxic, provide controlled release, suitable for surface modifications and macromolecules	Hydrophobic, low entrapment efficiency, immunogenic, storage-related problems and limited knowledge on neurotoxicity
Polymer-based	Dendrimers[1,4]	Increase BBB transport, suitable for surface modifications and tailorable	Limited knowledge of biocompatibility and toxicity
	Micelles[1,2,4,5]	Good stability, increase BBB transport and suitable for various molecules	Limited knowledge of biocompatibility
	Microcarriers[2]	Compatible with other drug delivery systems and mucoadhesive	Dependent on head position during administration
	Nanogels[1,2,4,5]	Compatible with other drug delivery systems, enhance deposition in the nasal cavity, increase BBB transport, provide controlled release and suitable for various molecules	Not suited for hydrophobic drugs
	Polymeric nanoparticles [1,2,4,5]	Increase mucus permeation, nasal residence time and BBB transport. Suitable for surface modifications and tailorable. Natural polymers are cost-effective, low toxicity and biodegradable	Limited knowledge of catabolites and immunologic responses. Issues regarding nasal irritation and toxicity
	Polymersomes[1]	Good stability, suitable for surface modifications and various molecules	Limited knowledge

Information summarized from [1]Li *et al*., 2017, [2]Khan *et al*., 2017, [3]Selvaraj *et al*., 2018, [4]Wong *et al*., 2012, [5]Bourganis *et al*., 2018.

As shown in Table 1.2, both the lipid- and polymer-based nanocarrier systems offer advantages related to increased BBB transport (Li *et al.*, 2017, Patel and Patel, 2017). On the other hand, limited knowledge on the biocompatibility, immunogenicity, and toxicity are disadvantages seen for several polymer-based nanosystems.

Natural polymers (*e.g.* alginate, chitosan) are currently preferred in nasal dosage forms due to their relatively low cost, low toxicity and good biodegradability compared to the synthetic polymers (Bourganis *et al.*, 2018, Ghadiri *et al.*, 2019, Sonvico *et al.*, 2018). However, due to their natural origin, batch-to-batch variation may occur. Several synthetic biodegradable polymers are approved by the FDA for human use, and they include poly(lactic-co-glycolic acid) (PLGA), poly(lactic acid) (PLA), poly(ethylene glycol) (PEG), and poly(ε-caprolactone) (PCL) (Marin *et al.*, 2013). To our knowledge, the most studied polymer-based nanosystems for nose-to-brain delivery purposes appears to be dominated by the above mentioned synthetic polymers (Bourganis *et al.*, 2018, Gänger and Schindowski, 2018, Li *et al.*, 2017, Sonvico *et al.*, 2018). Although polymer-based nanocarriers show promising properties, no more focus will be given to this topic in this thesis as we have chosen to focus on the liposomes. Liposomes provide advantages over many other nanoparticulate drug delivery systems because of their low batch-to-batch variation, simple manufacturing, scalable manufacturing possibilities and good biocompatibility (Daraee *et al.*, 2016, Sharma *et al.*, 2018).

1.5.1 General introduction to liposomes

Liposomes are lipid-based vesicles in the nanometric range, consisting of unilamellar or multilamellar phospholipid bilayers surrounding an aqueous core. They were first described in the 1960s (Bangham and Horne, 1964) and originally, liposomes were used as simple models to study biological membranes. For these reasons, the first liposomal formulations were extremely simple, consisting of only phospholipids, before eventually adding cholesterol and drugs, as demonstrated in Figure 1.6 (de Gier *et al.*, 1968, Immordino *et al.*, 2006).

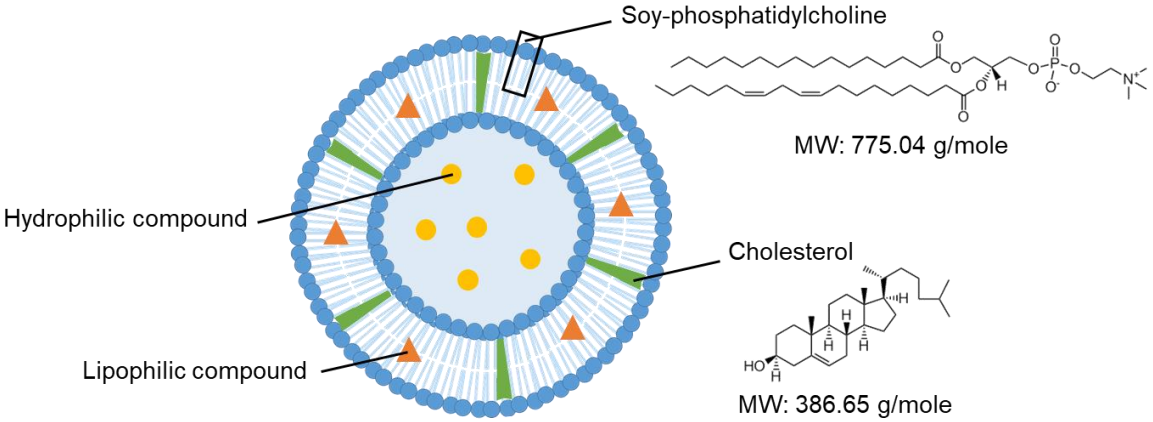

Figure 1.6: Schematic representation of one unilamellar vesicle comprising drugs and cholesterol.

The first liposome-based drug reached the market in 1996, and liposomes have since then been extensively studied for drug delivery purposes. In fact, liposomes are currently representing 60% of all the nanosystems in clinical use, and are the most investigated nanocarrier for drug delivery purposes (Ventola, 2017). The current focus of liposomes development is towards design and creation of sophisticated liposomes for active drug delivery purposes (Nisini *et al.*, 2018, Noble *et al.*, 2014, Riaz *et al.*, 2018, Ross *et al.*, 2018). In the last decade, liposomes have been expanding into the field of nose-to-brain drug delivery due to their promising carrier properties involving good biocompatibility, and tailorable possibilities (Bourganis *et al.*, 2018, Li *et al.*, 2017).

1.5.2 Liposomes for nose-to-brain drug delivery

Liposomes for nose-to-brain drug delivery is a relatively new field, where the first experiments carried out *in vivo* appeared in 2007 (Wattanathorn *et al.*, 2007). Since then, several pre-clinical studies have shown that drug-loaded liposomal formulations administered via the nose increase drug transport into the brain, reduce drug-related systemic side effects and improved the drug's therapeutic efficacy *in vivo* (Bourganis *et al.*, 2018, Erdő *et al.*, 2018, Vieira and Gamarra, 2016). A summary of some nasally administered liposomal drug formulations for brain delivery (focused on *in vivo* rat studies) is represented in Table 1.3.

Table 1.3: Short summary of some nasally administered liposomal drug formulations for brain delivery performed on rats.

Disease	Study period	Liposome composition (ratio)	Active ingredient (hydro-/lipophilic character)	Liposomes characteristics	Major findings	Reference
Alzheimer's	8 hours	DSPC:CHOL:PEG (1:2:0.5 w/w/w)	Donepezil (hydrophilic)	Size: 102 nm ZP: -28 mV EE: 85% Unilamellarity: yes	Liposomes protected drug from early degradation, safe to nasal epithelium, reduced systemic and GI side effects. IN increased CNS distribution in comparison to PO.	Al Asmari *et al.*, 2016
	12 hours	SL:CHOL (4:1 mol/mol)	Rivastigmine (hydrophilic)	Size: 10 000 nm ZP: ND EE: 80% Unilamellarity: no	Liposomes provided good stability (up to 3 months) and prolonged drug release. IN increased drug concentration in plasma and CNS in comparison to PO.	Arumugam *et al.*, 2008
	10 days	SPC:CHOL (3:0.02 w/w)	Galanthamine (hydrophilic)	Size: 112 nm ZP: -49 mV EE: 84% Unilamellarity: no	Liposomes improved therapeutic efficacy, did not exhibit cytotoxic profiles and reduced systemic and GI side effects. IN and liposomes increased BBB transport in comparison to PO and drug solution.	Li *et al.*, 2012
	3 weeks	EPC:CHOL (not specified)	Quercetin (lipophilic)	Size: ND ZP: ND EE: ND Unilamellarity: ND	IN of liposomes with drug showed neuroprotective and neurotropic effects. Liposomes enhanced the antioxidant properties of drug when entrapped within liposomes.	Phachonpai *et al.*, 2010
	4-7 days	EPC:CHOL (1:1 mol/mol) EPC:CHOL:DSPE-PEG-CPP (1:1:0.06 mol/mol/mol)	Rivastigmine (hydrophilic)	Size: 166 nm ZP: -10.5 mV EE: 33% Unilamellarity: ND Size: 179 nm ZP: -9 mV EE: 31% Unilamellarity: ND	Surface-modified liposomes increased BBB transport. Liposomes provided good stability (up to 4 weeks), prolonged drug release and no alterations in ciliary movement/nasal epithelium. Surface modified liposomes might be cleared out faster than conventional liposomes.	Yang *et al.*, 2013
	7-11 days	EPC:DSPE-PEG2000:CHOL (20:1:5 mol/mol/mol)	H102 peptide (hydrophilic)	Size: 112 nm ZP: -3 mV EE: 71% Unilamellarity: yes	Liposomes protected the peptide from early degradation and provided prolonged peptide release. IN compared to IV increased peptide concentration in CNS and therapeutic efficacy.	Zheng *et al.*, 2015

Table 1.3: (continued).

Disease	Study period	Liposome composition (ratio)	Active ingredient (hydro-/lipophilic character)	Liposomes characteristics	Major findings	Reference
Anxiety	4 weeks	EPC:CHOL (not specified)	Quercetin (lipophilic)	Size: ND ZP: ND EE: ND Unilamellarity: ND	IN of liposomes with drug showed decreased anxiolytic-like activity and enhanced cognitive effects in comparison to liposomes without drug.	Wattanathorn *et al.*, 2007
CNS iron deficiency	7 days	SL:CHOL (5:1 w/w)	Ferric ammonium citrate (hydrophilic)	Size: 40 nm ZP: -48 mV EE: 97% Unilamellarity: yes	Liposomes increased iron concentration in CNS. Liposomes did not alter nasal epithelium, brain cell, and lung epithelial cell morphology.	Guo *et al.*, 2017
Ischemic stroke	3 days	HSPC:CHOL (4:1 w/w)	bFGF (hydrophilic)	Size: 128 nm ZP: -15 mV EE: 84% Unilamellarity: yes	Liposomes increased therapeutic efficacy. Growth factor was transported to CNS with similar efficacy as from liposomal formulation and solution, whereas IN had higher CNS distribution in comparison to IV.	Zhao *et al.*, 2016
Pain	5 days	DMPC:DMPG:RGD (1:1:0.01 mol/mol/mol)	Fentanyl (lipophilic)	Size: 96 nm ZP: assumed negative at p*H* 7 EE: 80% Unilamellarity: ND	Surface modified liposomes expressed higher binding to nasal epithelial cells. Liposomes provided prolonged drug release and improved therapeutic efficacy. IN decreased drug concentration in plasma (assuming drug accumulation in the CNS).	Hoekman *et al.*, 2014
Parkinson's	3-4 weeks	DOPC:CHOL:SA (50:30:5 mol/mol/mol)	GDNF (hydrophilic)	Size: 149 nm ZP: 30 mV EE: 95% Unilamellarity: ND	IN of liposomes increased CNS distribution, improved therapeutic efficacy and decreased side effects. However, the liposomal formulation was therapeutically not better in comparison to the solution.	Migliore *et al.*, 2014
	8 weeks	SL:CHOL:ODA (20:5:1 w/w/w)	bFGF (hydrophilic)	Size: ND ZP: ND EE: >82% Unilamellarity: ND	Liposomes increased the amount of growth factor into CNS in comparison to the solution. Liposomes increased therapeutic efficacy. Liposomes did not alter cell viability.	Yang *et al.*, 2016

Table 1.3: (continued).

Disease	Study period	Liposome composition (ratio)	Active ingredient (hydro-/lipophilic character)	Liposomes characteristics	Major findings	Reference
Schizophrenia	2 days	SPC:CHOL (2:1, 4:1, 8:1 mol/mol) SPC:CHOL:SA (8:1:0.25, 8:1:0.5, 8:1:1, 8:1:2 mol/mol/mol) SPC:CHOL:DSPE-MPEG (8:1:0.05, 8:1:0.10, 8:1:0.20 mol/mol/mol)	Risperidone (lipophilic)	Size: 91-106 nm ZP: -50 to -54 mV EE: 30-50% Unilamellarity: yes Size: 99-209 nm ZP: 16-22 mV EE: 44-51% Unilamellarity: yes Size: 99-116 nm ZP: -29 to -37 mV EE: 54-59% Unilamellarity: yes	Liposomes increased biodistribution of the drug into the CNS in comparison to the solution. Amount of drug that reached the brain was highest for surface-modified liposomes, middle for cationic liposomes and lowest for conventional liposomes. IN provided sustained release profile in comparison to IV.	Narayan *et al.*, 2016

bFGF, basic fibroblast growth factor; CHOL, cholesterol; CPP, cell-penetrating peptide; DMPC, dimyristoylphosphatidylcholine; DMPG, dimyristoylphosphatidylglycerol; DOPC, dioleoylphosphatidylcholine; DSPC, distearoylphosphocholine; DSPE, distearoylphosphatidylethanolamine; EPC, egg-phosphatidylcholine; GDNF, glial cell line-derived neurotrophic factor; GI, gastrointestinal; HSPC, hydrogenated soy-phosphatidylcholine; IN, intranasal administration; IV, intravenous administration; MPEG, methoxypoly(ethylene glycol); ND, not detected; ODA, octadecylamine; PEG, poly(ethylene glycol); PO, peroral administration; RGD, integrin binding peptide; SA, stearylamine; SL, soy-lecithin; SPC, soy-phosphatidylcholine.

The human nose consists of approx. 60 µm thick mucus layer, respiratory epithelium and olfactory epithelium covering the surface area of 160 and 10 cm^2, respectively (Bourganis *et al.*, 2018, Crowe *et al.*, 2018, Erdő *et al.*, 2018). The animal models commonly used for intranasal drug administration have been dogs, pigs, mice, monkeys, rabbits, rats, and sheep (Erdő *et al.*, 2018). The rat's nasal anatomy is the most different from humans in terms of shorter nasal length (2 *vs* 8 cm), and smaller nasal epithelium surface area (14 *vs* 160 cm^2) (Erdő *et al.*, 2018). However, the rat's olfactory epithelium surface area is approx. 7 cm^2, relatively comparable to the humans of 10 cm^2 (Bourganis *et al.*, 2018). Perhaps that is why most pre-clinical *in vivo* studies on liposomal nose-to-brain drug delivery have been performed on rats.

As pointed out in Table 1.3, liposomal sizes in the range from 40 nm (Guo *et al.*, 2017) up to 10 000 nm (Arumugam *et al.*, 2008) have been studied for nose-to-brain drug delivery, but a significant portion was restricted to sizes between 100-200 nm. The most common lipid used in the listed liposomal formulations appeared to be the uncharged phosphatidylcholine, often in combination with the stabilizing agent, cholesterol. Almost half of the listed studies were of more "sophisticated" liposomes, where the surfaces of the nanocarriers were modified (Al Asmari *et al.*, 2016, Hoekman *et al.* 2014, Narayan *et al.*, 2016, Yang *et al.*, 2013, Zheng *et al.*, 2015). Surprisingly, these complex liposomes did not necessarily show extraordinary improvement in brain transport, side effect profiles or neurological functions in comparison to the conventional liposomes or drug solution (Migliore *et al.*, 2014, Yang *et al*., 2013). One reason might be the slow drug release kinetics from these liposomal carriers for both hydrophilic and lipophilic compounds (Arumugam *et al.*, 2008, Hoekman *et al.*, 2014, Narayan *et al.*, 2016, Yang *et al.*, 2013, Zheng *et al.*, 2015). Another important variable might be the physiological aspects using the nose as the administration site.

1.5.3 Challenges for nose-to-brain drug delivery

The mucociliary clearance rate influences the contact time between the drug formulation and the nasal epithelium, which have a direct influence on the distribution into the brain. Many of the studies reported in Table 1.3 were conducted under general anaesthesia and/or drug administered in a determined position (Arumugam *et al.*, 2008, Guo *et al.*, 2017, Hoekman *et al.*, 2014, Li *et al.*, 2012, Phachonpai *et al.* 2010, Yang *et al.*, 2013, Yang *et al.*, 2016, Zhao *et al.*, 2016). It has been emphasized that both of these variables might influence the mucociliary function, making it hard to draw comparisons between the therapeutic effects between studies (Djupesland *et al.*, 2014, Wu *et al.*, 2008). Moreover, since the mucociliary clearance rate is

up to four times faster in rats, the rat animal model might underestimate the efficiency of the nose-to-brain pathway (Djupesland *et al.*, 2014, Wu *et al.*, 2008).

Importantly, liposomes administered via the nasal route will be directly exposed to the nasal mucus. Under normal physiological conditions, the human nasal mucus tonicity is approx. 300 mOsm/kg (Pedersen *et al.*, 2007). This value can change considerably as the nasal mucus is rather sensitive to the surrounding environment (*e.g.* air humidity, temperature) (Quraishi *et al.*, 1998). It has been reported that hyperventilation in dry air can increase the nasal tonicity up to 450 mOsm/kg (Pedersen *et al.*, 2007). These changes are highly relevant for liposomal drug formulations as they are colloidal systems. Changes in the dispersing media can cause changes at the liposome level, and therefore their release properties. We have focused on utilizing the changes in tonicity as a mean to control the drug delivery from nasally administered liposomes. To fully understand the consequences of the changes in tonicity on drug release from liposomes, the next section will discuss some of the important features relevant to the drug release.

1.6 Colligative properties

Physical phenomena that are mainly influenced by the number of solute molecules in a solution are called colligative properties (Sinko and Singh, 2011). The most important colligative properties are vapour pressure depression, boiling point elevation, freezing point depression, and osmotic pressure (Sinko and Singh, 2011).

The term colligative comes from the Latin word "*colligatus*" that means connected. In fact, the characterization of one of these parameters allows the immediate determination of all the others. For instance, the normal freezing, or melting point of a pure compound is the temperature at which the solid and liquid phases are in equilibrium under a pressure of 1 atm. In this equilibrium, the tendency for a solid to pass into the liquid state, or *vice versa*, is the same. If a solute is added into the liquid at normal freezing point, the temperature lowering (namely, freezing point depression) is required to re-establish the equilibrium between solid and liquid. In other words, the freezing point depression (or melting point elevation) is *colligatus* with the solute concentration in solution (Sinko and Singh, 2011). The new freezing point (ΔT_f) can be calculated using Equation 1.1;

$$\Delta T_f = mK_f \qquad \textbf{Equation 1.1}$$

where m describes the molality of solute, and K_f the cryoscopic constant.

It is known that the liposomal membranes are semi-permeable, and allow neutral, poorly polarized, and small molecules to passively diffuse through, whereas ions, highly polarized small molecules, and large molecules will not, as shown in Figure 1.7 (Bangham *et al.*, 1967, Paula *et al.*, 1996).

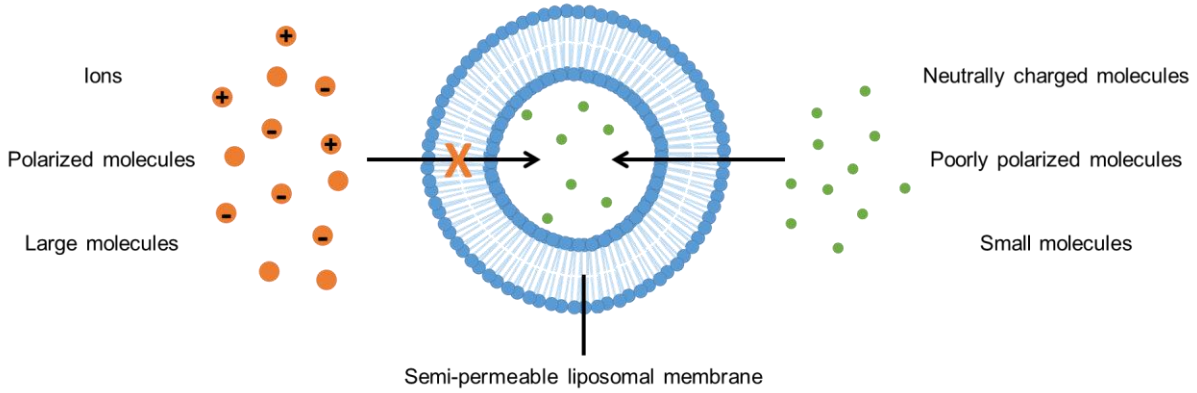

Figure 1.7: Simplified representation of the semi-permeable nature of the liposomal membrane.

As illustrated in Figure 1.7, the passive migration of solvent molecules through the semi-permeable membrane is generally called osmosis, and it is initiated by the different chemical potential between the two sides of the membrane (Sinko and Singh, 2011). Specifically, solvent molecules will diffuse from the side with higher chemical potential (*i.e.* low solute concentration) to the regions with lower chemical potential (*i.e.* high solute concentration) until equilibrium is reached (Sinko and Singh, 2011). Due to osmosis, a pressure (namely, osmotic pressure) is created on the liposomal membrane (Sinko and Singh, 2011).

1.6.1 Osmotic pressure

The osmotic pressure (π) describes the excess pressure applied to a solution to prevent the solvents from passing through the membrane (Sinko and Singh, 2011). The first equation describing osmotic pressure was proposed by Jacobus van't Hoff (Equation 1.2). In this equation, the osmotic pressure is related to the ideal gas constant (R_0), the absolute temperature (T), and solute concentration in a system (n/V) (Sinko and Singh, 2011);

$$\pi = \frac{n}{V} R_0 T \qquad \textbf{Equation 1.2}$$

As it can be seen from Equation 1.2, changes in the solute concentration can proportionally change the π.

It was later found out by Morse and others that if the solute concentration was expressed in molality (*m*) rather than molarity, the calculated theoretical osmotic pressure fitted better to experimental findings (Equation 1.3, (Sinko and Singh, 2011));

$$\pi = mR_0T$$ **Equation 1.3**

When solutes dissolving in a determined solvent are the electrolytes, the Morse equation becomes;

$$\pi = imR_0T$$ **Equation 1.4**

In Equation 1.4, *i* represents the number of dissociating ions (namely, the van't Hoff factor). For non-electrolytes, such as glucose, *i* remains to be 1, whereas sodium chloride which can dissociate into sodium and chloride ions in solution has *i*=2. It has to be kept in mind that *i* is a value for ideal conditions that do not take into account some not totally dissociating compounds, and possibly ion pairings in solution. The measured *i*, and *i* for ideal conditions might for these reasons deviate for some compounds. However, for strong electrolytes such as sodium chloride, *i* can be considered to be equal to 2 (Sinko and Singh, 2011).

The osmotic pressure created on the liposomal membrane is relevant when it comes to the development of liposomal drug delivery systems since the osmotic pressure can cause the liposomes to shrink, or swell due to their close vesicle structures (see Figure 1.8) (Alam Shibly *et al.*, 2016, Fujiwara and Yanagisawa, 2014, Mui *et al.*, 1993, Ohno *et al.*, 2009).

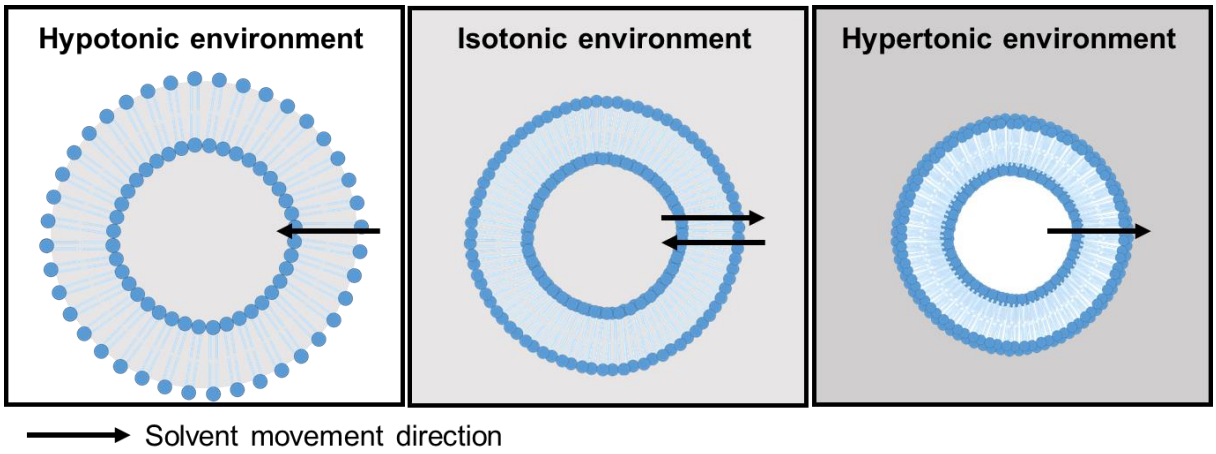

Figure 1.8: Simplified representation of the solvent diffusion process across the liposomal membrane under the influence of different environment.

As schematically presented in Figure 1.8, due to the migration of the solvent, the liposomes swell in a hypotonic environment and shrink in a hypertonic environment. Because of the liposomal size changes, and consequently the changes in the liposomal membrane rigidity, the drug release kinetics from the liposomes might be affected (Ahumada *et al.*, 2015, Chabanon *et al.*, 2017).

In order to achieve controlled drug diffusion across any barrier, it is necessary to understand the release mechanism from liposomes. To study the release from liposomes, drug diffusion studies can be applied (Solomon *et al.*, 2017).

1.7 Drug diffusion study

Passive diffusion is the movement of molecules due to chemical potential (*i.e.* concentration) gradient. Let us consider the movement of drug molecules dissolved in water that are all located on one side of a compartment divided by the physical permeable barrier (Figure 1.9). Solute molecules will move from the compartment from areas with high drug concentration (with higher chemical potential, donor compartment) to low drug concentration (namely, acceptor compartment) (Sinko and Singh, 2011). In this situation, the drug diffusion can be assumed to be in just one direction, and the degree of drug diffusion across the barrier can be affected by the barrier properties (*e.g.* barrier structure, interaction) (Brandl *et al.*, 2007, Brodin *et al.*, 2010).

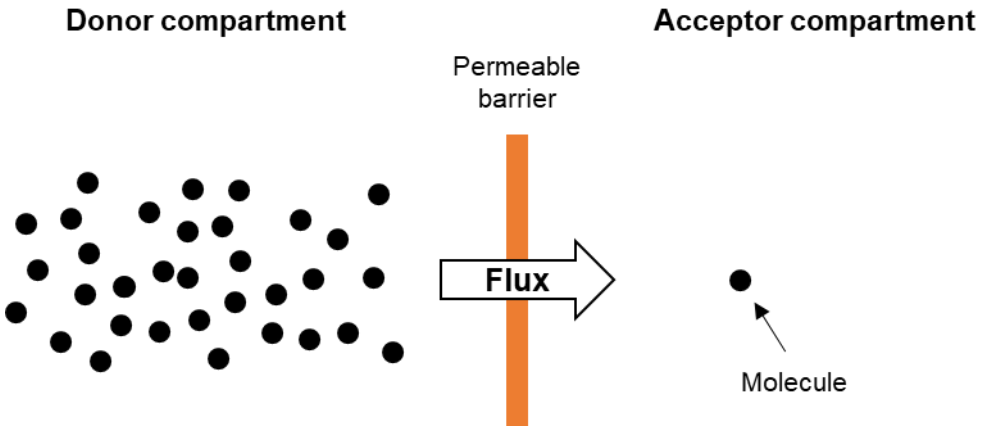

Figure 1.9: Simplified representation of the one-directional movement of molecules across a physical permeable barrier.

One common way to describe drug diffusion across a barrier is by using the concept of flux. Mass flux (*j*) is defined as the mass variation over time (*dm/dt*) across a defined surface area (*A*) as shown in Equation 1.5;

$$j = \frac{dm}{dt} \cdot \frac{1}{A} \qquad \textbf{Equation 1.5}$$

The net drug diffusion across a barrier can be categorized into the steady, and non-steady state conditions. The steady state condition, in which the flux is considered to be constant over the experimental time interval, is preferential. In this case, the simplified version of Fick's first law (Equation 1.6) is considered acceptable (Brodin *et al.*, 2010);

$$j = D\frac{(C_d^0 - C_a)}{x} \qquad \textbf{Equation 1.6}$$

In this equation, *D* represents the diffusion coefficient, (C^0_d-C_a) the drug concentration difference between the two sides of a barrier with thickness = *x*. From Equation 1.6, the flux is proportional to the concentration gradient. If (C^0_d-C_a)/*x* = constant, a zero order diffusion kinetic is established, and the experimental data can be therefore fitted by the linear regression models (see Figure 1.10) (Brodin *et al.*, 2010, Nothnagel and Wacker, 2018).

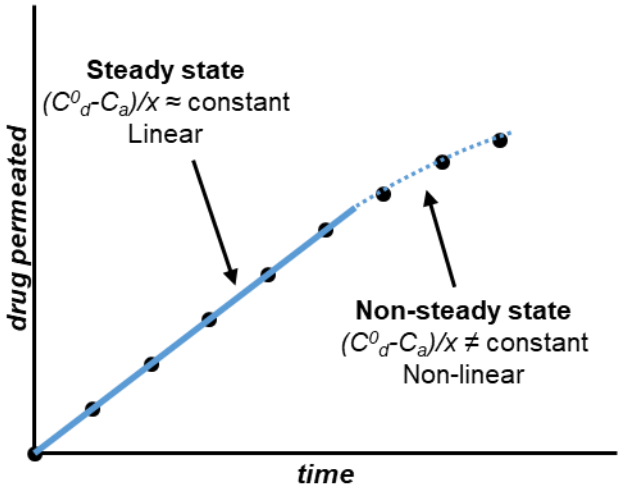

Figure 1.10: Example of a drug diffusion profile representing steady state and non-steady state conditions.

Apparent permeability coefficient (P_{app}) is commonly used to quantify the ability of molecules in crossing barriers (Brodin *et al.*, 2010). The constant flux in *in vitro* diffusion studies can be achieved by creating a large enough and constant concentration gradient between the donor

and acceptor compartment. This is usually achieved by working under sink conditions, therefore by constant removal of accumulated material in the acceptor compartment. It is generally considered sink condition when the concentration in the acceptor compartment is kept <10% of the donor drug concentration under the whole study period (Brodin *et al.*, 2010). Under these premises, the amount of drug applied in donor compartment is assumed to be constant over the whole experiment, and the concentration difference (C^0_d-C_a) can be assumed to be equal to the initial drug concentration of the formulation (C^0_d) (Brodin *et al.*, 2010). Apparent permeability is then calculated according to Equation 1.7;

$$P_{app} = \frac{dm}{dt} \cdot \frac{1}{A} \cdot \frac{1}{C_d^0}$$ **Equation 1.7**

It is sometimes convenient to highlight the barrier's resistance (*R*) to drug permeation. *R* is the inverse of the permeability, as shown in Equation 1.8;

$$R = \frac{1}{P_{app}}$$ **Equation 1.8**

For studying the release from nanocarriers, the standard way to treat diffusion data is based on semi-empirical approaches, where experimental data (*e.g.* obtained from *in vitro* drug diffusion study) are fitted to mathematical models (Jain and Jain, 2016). By quantifying the amount of drug that permeates the diffusion barrier, the diffusion data can be fitted to linear, and non-linear regression models to predict drug release from the nanocarrier (Jain and Jain, 2016, Nothnagel and Wacker, 2018).

1.7.1 Drug release from liposomes

In the case of drug-loaded liposomal dispersions, drug molecules need to cross two physical barriers (first the liposomal bilayer, and thereafter the diffusion barrier) in order to accumulate into the acceptor compartment. In this case, the net drug transport across the diffusion barrier is considered to be dependent on two diffusion mechanisms (see Figure 1.11, (Wacker, 2017)).

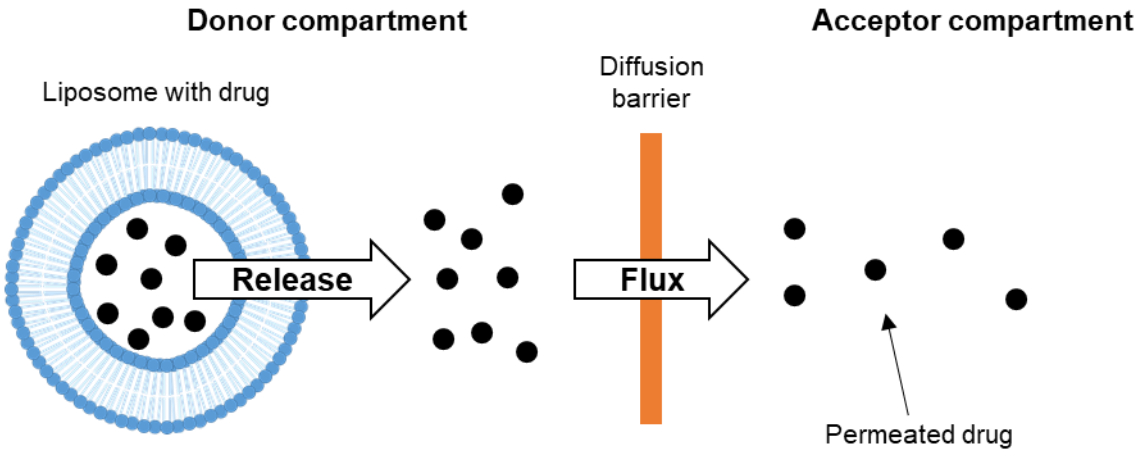

Figure 1.11: Simplified representation of the currently used semi-empirical approach where drug permeation across a diffusion barrier is used to predict the drug release mechanism from the liposome.

Three possible outcomes can be expected when discussing drug release from liposomes (Jain and Jain, 2016);

i) Release rate ≈ flux: constant concentration gradient across the diffusion barrier giving a (close to) perfect zero order diffusional curve. In this situation, linear regression models could be used.

ii) Release rate < flux: reduced concentration gradient across the diffusion barrier giving a first, or pseudo order diffusional curve. The nanocarrier is contributing to a sustained drug release. In this situation, non-linear regression models should be used.

iii) Release rate > flux: increased concentration gradient across the diffusion barrier giving a positive deviation from the linear diffusional curve. The nanocarrier is enhancing the net transport of the drug across the diffusion barrier. In this situation, non-linear regression models should be used.

1.7.1.1 Linear approximation

Based on the assumption that the total resistance to drug transport of drug-loaded liposomes is caused by the sum of single resistances (caused by each of the physical barriers involved), the liposomal bilayer's contribution to drug transport can be calculated using Equation 1.9;

$$R_L = R_T - R_B \qquad \textbf{Equation 1.9}$$

where the total resistance to drug transport (R_T, calculated from $1/P_{app}$ of drug-loaded liposomes), and the resistance to drug transport through permeable barrier (R_B, measured

from $1/P_{app}$ of drug reference solutions) can be predetermined to calculate the resistance to drug transport through liposomal bilayer (R_L).

This linear approximation of the drug diffusion data might lead to wrong interpretations as the concentration gradient across the diffusion barrier might not be constant under the whole study period when the drug is formulated with liposomes (non-steady state). This can be due to the presence of the unentrapped drug in the liposomal formulation, reversible drug binding to the carrier, and interaction between drug and the barrier (Modi and Anderson, 2013, Nothnagel and Wacker, 2018). The presence of unentrapped drug can be solved by the removal of freely unentrapped drug from a liposomal drug formulation so the drug diffusion across the diffusion barrier represents the direct release from the nanocarrier. However, it should also be taken into consideration that the most common methods to remove freely unentrapped drug are based on passive diffusion principles. The removal of the freely unentrapped drug might introduce the system to a new shift in drug concentration equilibrium across the liposomal barrier which can complicate the interpretation of the drug release from the nanocarrier (Nothnagel and Wacker, 2018). For these reasons, it has become more common to fit the *in vitro* diffusion data to non-linear regression models (Jain and Jain, 2016).

1.7.1.2 Non-linear approximation

Some of the most common non-linear mathematical models to describe drug release phenomena from semi-solid dosage forms are the Higuchi and the Korsmeyer-Peppas model (Costa and Sousa Lobo, 2001, Jain and Jain, 2016). Experimental data are fitted to any of the above-mentioned models taking into account different variables such as the surface area of dosage form, or the solubility of the drug (Higuchi) (Costa and Sousa Lobo, 2001, Jain and Jain, 2016).

The Korsmeyer-Peppas model is commonly used to analyse the release mechanism from nanocarriers which is unknown, or when more than one type of release phenomena might be involved (*e.g.* drug release affected by geometry, swelling, or shrinkage of the nanocarrier) (Costa and Sousa Lobo, 2001). The *in vitro* diffusion data are plotted as the fractional permeated drug (M_t/M_∞ up to 60%) over time (t) and fitted to the Korsmeyer-Peppas equation (Equation 1.10, (Korsmeyer *et al.*, 1983));

$$\frac{M_t}{M_\infty} = K \cdot t^n \qquad \textbf{Equation 1.10}$$

From the fitted curve to Korsmeyer-Peppas equation, the transport constant (*K*), and transport exponent (*n*) provide information related to the drug formulation such as drug properties, structural characteristics of the nanocarriers, and drug release mechanism. The most interesting variable is the exponent value, *n,* that can be used to indicate how far the migration process is from Fickian diffusion (Korsmeyer *et al.*, 1983).

When the exponent *n*=1, it is evident from Equation 1.10 that the drug release rate is directly dependent on time. In this situation, the release kinetics correspond to zero order, and the diffusion is non-Fickian (see also Figure 1.12).

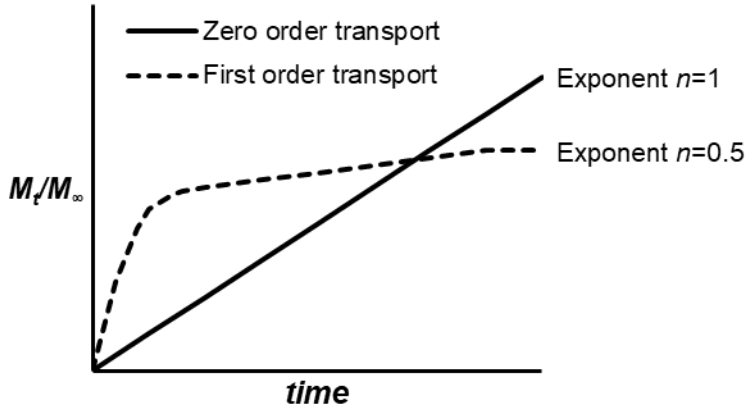

Figure 1.12: Simplified representation of the diffusion curves that can be expected when discussing drug release from liposomes.

On the contrary, if the exponent *n*=0.5, the drug release rate is dependent on the square root of the time. In this situation, the release kinetics correspond more to the first order, and the diffusion is approximated to exhibit Fickian behaviour (Ritger and Peppas, 1987). The interpretation of the exponent *n* is a bit more complicated when it falls in between 0.5 and 1. When 0.5<*n*<1, the release kinetics correspond to pseudo-first order and can describe both phenomena of Fickian- and non-Fickian-controlled drug release.

We have selected markers and drugs to cover a wide range of relevant physiochemical properties to challenge the liposomes suitability to be used as osmotically active liposomes for nose-to-brain drug delivery. This to prove that controlled release from liposomes can be achieved by controlling the environment surrounding the liposomes.

1.8 Fluorescent markers and drugs used in this study

1.8.1 Fluorescent markers

In the development of a drug formulation, it is common to start formulation development applying markers to verify a concept before using drugs. The fluorescent markers (Figure 1.13) were chosen because of their physiochemical properties and known applicability when studying lipid membrane properties (Ahumada *et al.*, 2015, Chabanon *et al.*, 2017, Maherani *et al.*, 2013, Oglecka *et al.*, 2014). Both calcein and rhodamine are reported to be successfully entrapped into liposomes and give bright fluorescent signals (Chabanon *et al.*, 2017, Maherani *et al.*, 2013).

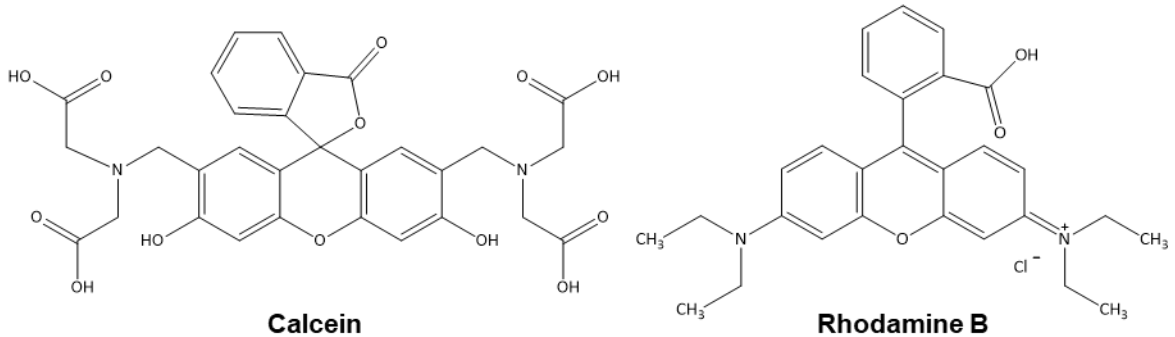

Calcein
MW: 622.5 g/mol
log$D_{7.4}$: -3.3[a]
p*Ka*: 1.8[b]

Rhodamine B
MW: 479.0 g/mol
log$D_{7.4}$: 2.3[c]
p*Ka*: 3.1[d]

Figure 1.13: Molecular structures and general physiochemical properties of the fluorescent markers used in this thesis. Information summarized from [a]Maherani *et al*., 2013, [b]Flaten *et al*. 2006, [c]Toropainen *et al*., 2001, [d]Pittman *et al*., 2001.

Calcein is a hydrophilic marker, which upon entrapment, is localized in the liposomal aqueous core (Flaten *et al.*, 2006, Maherani *et al.*, 2013). The other fluorescent marker of choice was rhodamine, a lipophilic marker which can be incorporated in the phospholipid bilayer of liposomes (Pittman *et al.*, 2001, Toropainen *et al.*, 2001). As a result of the different osmotic gradient across a liposomal membrane, an increase or decrease of the fluorescence intensity can be promoted by the changes in the liposomal inner volume due to osmosis (Ahumada *et al.*, 2015, Chabanon *et al.*, 2017, Maherani *et al.*, 2013). This provides important information on the mechanism of release from liposomes and is the first step that needs to be validated before proceeding with the development of drug-loaded liposomal formulations.

1.8.2 Drugs

As a recap to the previous section (Section 1.2), the controlled microenvironment is essential to maintain optimal neuronal functions in the brain. Alterations of the BBB structure and/or duration of an imbalance in the microenvironment might contribute to the development of CNS disorders (Abbott *et al.*, 2010, Daneman and Prat, 2015). It has been proposed that BBB alterations might be due to elevated oxidative stress levels, or inflammation in the brain (Patel, 2016, Stephenson *et al.*, 2018). Epidemiological observation indicates that long-term administration of anti-inflammatory drugs (>1 year) showed delayed or lower risk of CNS disorder development such as Alzheimer's disease, Parkinson's disease, and multiple sclerosis (Aisen, 2002, Onatibia-Astibia *et al.*, 2017). Therefore, anti-inflammatory drugs have been proposed to be potential candidates to prevent and/or treat several CNS disorders (McCaulley and Grush, 2015, Onatibia-Astibia *et al.*, 2017).

Despite promising pre-clinical results, the statistical evidence that anti-inflammatory drugs can prevent and/or treat any CNS disorders are still clinically unproven (McCaulley and Grush, 2015, Onatibia-Astibia *et al.*, 2017). It has been suggested that these failures might be related to patient selection, drug selection, drug dosage, therapy duration, but more importantly the low drug delivery across the BBB when utilizing the conventional administration routes (Lehrer, 2014, McCaulley and Grush, 2015, Onatibia-Astibia *et al.*, 2017).

The therapeutic effect of anti-inflammatory drugs might be enhanced by utilizing liposomes and the nasal administration route. Even though it was beyond the scope of this thesis to investigate the therapeutic effects associated with nose-to-brain drug delivery, it was important to select the relevant drugs to be formulated into liposomes that might have great potential for the treatment and/or prevention of a wide range of CNS disorders. For this reason, six already marketed drugs with anti-inflammatory properties were chosen (see Figure 1.14) (McCaulley and Grush, 2015, Onatibia-Astibia *et al.*, 2017).

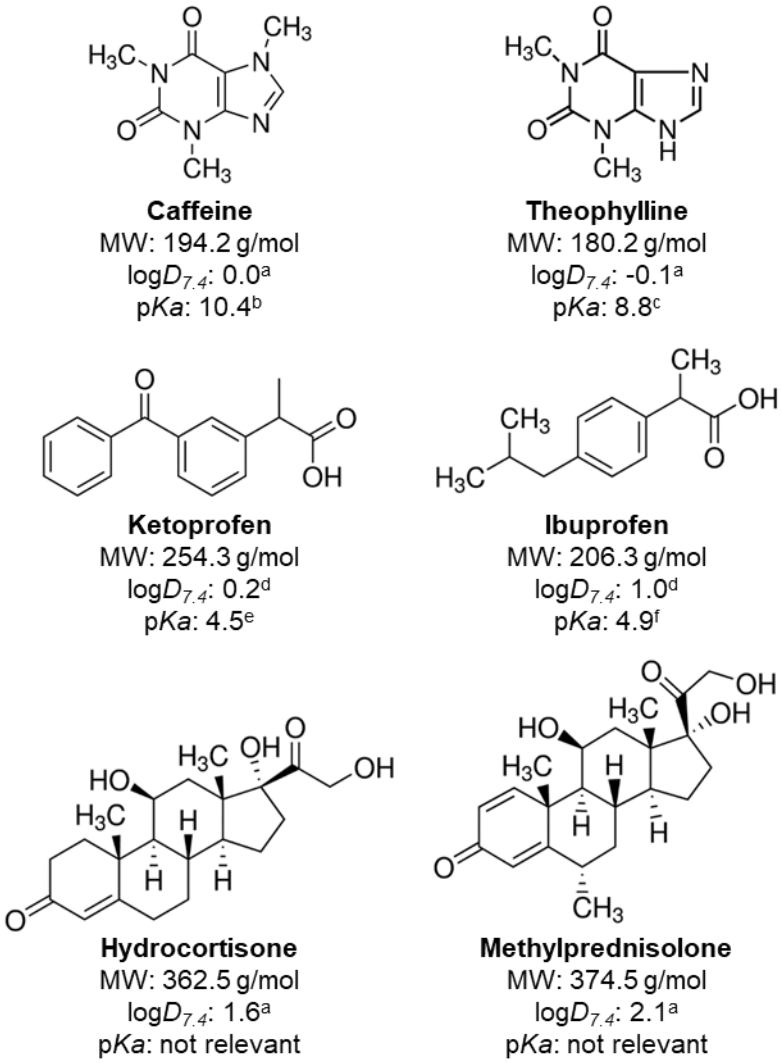

Figure 1.14: Molecular structures and general physiochemical properties of the drugs used in this thesis. Information summarized from [a]Zhu *et al*., 2002, [b]PubChem, 2019a, [c]PubChem, 2019d, [d]Stein *et al*., 2011, [e]PubChem, 2019c, [f]PubChem, 2019b.

As presented in Figure 1.14, the different drugs selected for this study expressed different physiochemical properties such as partition coefficient (log$D_{7.4}$) and ionization constant (p*Ka*). Two of the parameters that can be used to predict the bioavailability of a drug are the permeability (can be expressed as log$D_{7.4}$) and solubility (can be expressed as p*Ka*) (Ashford, 2013).

The partition coefficient describes the concentration ratio of a chemical entity between two immiscible solvents at equilibrium. The most common solvent system is octan-1-ol/water. The octan-1-ol phase mimics the short hydrocarbon chains that make up in many biological barriers, whereas the water phase mimics the aqueous environment. Therefore, the partition coefficient of a drug can be used to estimate the permeability of a drug (Gaisford, 2013).

The degree of the partitioning of partially ionizable solutes is better described by log*D* which take into account the p*H* of the aqueous phase (Gaisford, 2013). Since we aimed to perform all the experiments in this study at physiological p*H*, the log*D* at p*H* 7.4 (log$D_{7.4}$) of each of the selected drugs are represented in Figure 1.14.

The log$D_{7.4}$ is not only providing information related to the permeability across biological barriers, but it can also be used to predict the drugs' localization inside liposomes. A log$D_{7.4}$ above 1 indicates that more drug is favourably distributed in the octan-1-ol in comparison to the aqueous phase, and these drugs will most likely incorporate in the liposomal bilayer (Nii and Ishii, 2005). On the contrary, log$D_{7.4}$ below 1 indicates that more drug is distributed in the aqueous phase, and will most likely be entrapped in the inner core of liposomes (Xu *et al.*, 2012).

The ionization constant (p*Ka*) describes the number of dissociated (*i.e.* ions) and undissociated molecules in a solution, a collective term used for both weakly acidic and basic drugs. Whether a drug molecule is dissociated or not in a solution is highly dependent on the p*H* of the solution. The relationship between p*H* and p*Ka* can be described using the Henderson-Hasselbach equations. The equation for a weak acid is shown in Equation 1.11;

$$\mathrm{p}H = \mathrm{p}Ka + \log\frac{[A^-]}{[HA]} \qquad \textbf{Equation 1.11}$$

From Equation 1.11, the experimental p*H* and the p*Ka* of a drug molecule can be used to find the ratio between the weak acid (*HA*) and the conjugate base (A^-). When p*H* is greater than p*Ka* of a drug molecule (p*H*>p*Ka*), the drug will be dissociated, yielding the charged conjugate base. On the other hand, when p*H* is less than p*Ka* (p*H*<p*Ka*), most of the drug will be in the uncharged weak acid form in a solution. The Henderson-Hasselbach equation for a weak base is shown in Equation 1.12;

$$\mathrm{p}H = \mathrm{p}Ka + \log\frac{[B]}{[BH^+]} \qquad \textbf{Equation 1.12}$$

From Equation 1.12, p*H*>p*Ka* yields the uncharged weak base (*B*) form in solution, and p*H*<p*Ka* yields the charged conjugate acid (BH^+). The relationship between dissociated and undissociated molecules in a solution is relevant as it is directly linked to the drug's aqueous solubility (Aulton, 2013).

Introduction

The relationship between bioavailability, permeability, and solubility can be explained by the biopharmaceutics classification system (BCS) (Wu and Benet, 2005). For the oral route of drug administration, the drug has to be dissolved in order to be absorbed. For this reason, the BCS classifies drugs according to their aqueous solubility at gastric p*H* range, and permeability across the gut wall (Ashford, 2013).

The four BCS classes are;

1) high solubility and high permeability
2) low solubility and high permeability
3) high solubility and low permeability
4) low solubility and low permeability.

The main purpose of the BCS was to replace *in vivo* bioavailability study with *in vitro* data. Even though the BCS original purpose was focused on oral dosage forms, BCS is currently used by regulatory authorities as a guide to approve generics and is used by scientists as a guide to design drug delivery systems for any route of administration (Ashford, 2013).

Generally, BCS class 1 drugs are the most preferable. In this category, the drugs have high solubility and high permeability. Unless the drugs form insoluble complexes with biological fluids or undergo rapid clearance *in vivo*, these drugs will be rapidly absorbed and show good bioavailability. The BCS class 1 drugs selected for this study were the caffeine, theophylline, hydrocortisone and methylprednisolone (Ashford, 2013, Benet *et al.*, 2011). The second most preferable is BCS class 2 drugs. In this category, the drugs have low solubility but high permeability. These drugs are strictly limited by the drug's dissolution rate and will likely not show good bioavailability unless assisted by the right formulation that enhance the drugs' solubility profile (Ashford, 2013). The BCS class 2 drugs selected for this study were the ketoprofen and ibuprofen (Benet *et al.*, 2011). BCS class 3 and 4 drugs have limitation regarding low permeability and can be problematic to achieve good bioavailability (Ashford, 2013, Benet *et al.*, 2011). None of the selected drugs for this study were in these two classes.

To summarize, all the drugs included in this study were mainly chosen due to their reported anti-inflammatory properties and potentials in the prevention and/or treatment of CNS disorders. All have not been, up to now, proven clinically relevant which might be contributed to non-ideal study design, or sub-optimal administration route. It was also important to choose the drugs with different physiochemical properties to be entrapped within liposomes. The selected six different drugs exhibited log$D_{7.4}$ ranging from ~0 to 2, and p*Ka* ranging from 4.5 to 10.4, considered to be relevant for this study.

2 Aims of the study

The general aim of this project was to develop osmotically active liposomes suitable for nose-to-brain drug delivery.

For these reasons, the specific aims during the project have been to;

i) Investigate if large unilamellar vesicles (LUVs) made from soy-phosphatidylcholine are osmotically active in terms of size and release when formulated with;
    - Fluorescent markers (calcein and rhodamine)
    - Drugs (caffeine, theophylline, ketoprofen, ibuprofen, hydrocortisone, and methylprednisolone)

ii) Evaluate the drug release from LUVs using;
    - Low retention diffusion barrier (regenerated cellulose)
    - High retention diffusion barrier (biomimetic Permeapad®)

iii) Analyse the *in vitro* diffusion data using;
    - Linear regression (zero order model)
    - Non-linear regression (Korsmeyer-Peppas model)

iv) Evaluate the effect of cholesterol incorporation in the liposomal bilayer on the drug release from LUVs

v) Evaluate the effect of mucin on the drug release from LUVs

vi) Evaluate the stability of the liposomal formulations upon storage.

3 Summary of papers

3.1 Paper I

The aim of Paper I was to investigate the underlying mechanisms on how changes in the environmental tonicity could influence the liposomal size and release. The graphical abstract of this paper is represented in Figure 3.1.

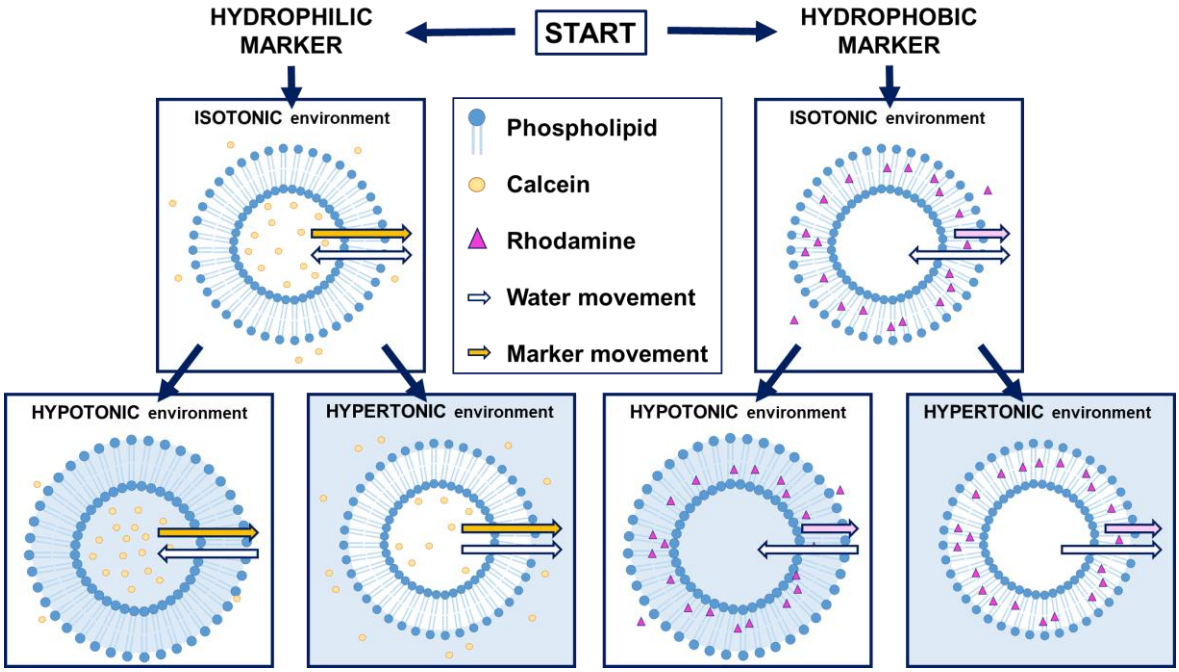

Figure 3.1: Graphical abstract for Paper I. Reproduced from Wu *et al*., 2017, with permission from Elsevier.

In Paper I, liposomes were prepared in phosphate buffer saline (PBS, p*H* 7.4) with an osmolality of 65 and 300 mOsm/kg, respectively. Giant unilamellar vesicles (GUVs) were prepared using a swelling method modified from Mocho *et al.* (1996) followed with extrusion to obtain large unilamellar vesicles (LUVs) within acceptable sizes for nasal administration (around 400 nm). To ensure the lamellarity of the LUVs, phase contrast microscopy was employed and confirmed the liposomal integrity (unpublished results). Entrapped within the LUVs were two fluorescent markers of different physiochemical properties, namely calcein (hydrophilic) and rhodamine (lipophilic).

The LUVs were exposed to PBS of different tonicity to generate a different gradient of salt concentration within the internal and external environment of the liposomes. This was based on the assumption that the measured osmolality of the PBS used to prepare the LUVs would represent the inner core tonicity, whereas the osmolality of the PBS that LUVs were exposed

to would represent the external environment tonicity. The relative osmotic pressure (π_{rel}), generated on the liposomal surfaces was expressed as negative or positive π_{rel} to describe the water influx or efflux into/from liposomes, respectively.

Liposomal sizes were monitored after LUVs were exposed to different environment. The LUVs seemed to be more susceptible to osmotic swelling than shrinking, and size changes were more evident for empty and calcein-LUVs in comparison to rhodamine-LUVs. These findings were in agreement with the marker's different physiochemical characteristics; the lipophilic compound (rhodamine) contributes to more rigid liposomal bilayer and reduces liposomes sensitivity to osmotic stress. On the other hand, calcein (hydrophilic) have no such effect as it is localized in the aqueous core.

The flux of marker through the regenerated cellulose barrier (using Franz diffusion cell set-up) was monitored to describe the release from the liposomes. The marker flux across the diffusion barrier seemed to correlate with changes in the π_{rel}. Decreased amount of calcein diffused through the diffusion barrier when LUVs were exposed to hypotonic environment, whereas the enhanced amount of calcein diffused in a hypertonic environment (when compared to isotonic condition). These results indicated that the release from LUVs was dependent on the interplay between the water flux and marker release direction (probably due to the hydrophilic nature of calcein). Rhodamine-LUVs, on the other hand, were generally less affected by the changes in π_{rel}.

The LUVs seemed to be suitable to entrap various compounds and showed promising carrier properties in terms of their osmotic activity. It would be, therefore, interesting to explore this phenomenon further by entrapping the LUVs with various drugs and investigate more thoroughly how the different degrees of environmental tonicity perturbations change the drug release from liposomes.

3.2 Paper II

The aim of Paper II was to focus on detailed hypotonic exposures of LUVs entrapping six drugs of different physiochemical properties (caffeine, hydrocortisone, ibuprofen, ketoprofen, methylprednisolone, and theophylline). The graphical abstract of this paper is represented in Figure 3.2.

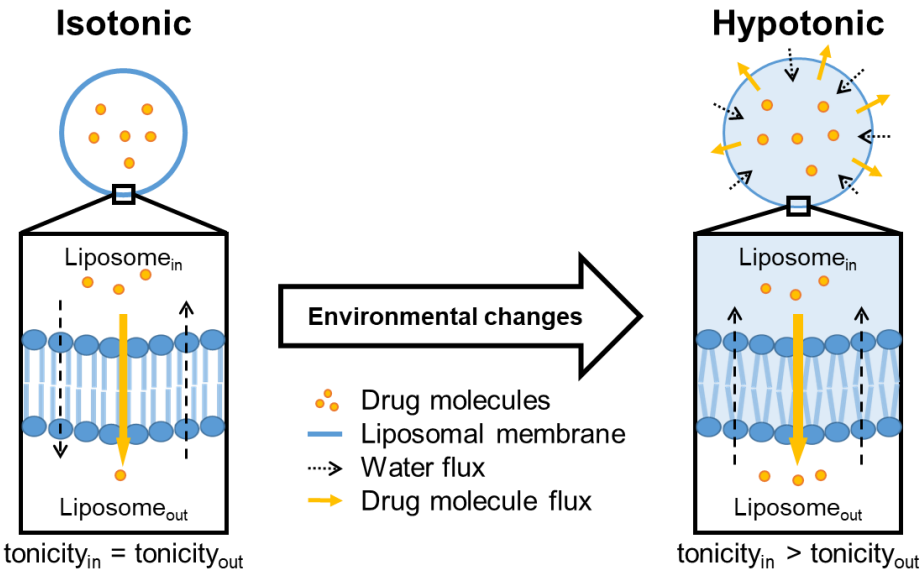

Figure 3.2: Graphical abstract for Paper II. Reproduced from Wu *et al*., 2019b, with permission from Elsevier.

The nasal mucus is in direct contact with the surrounding environment and the tonicity of the nasal mucus is relatively inconsistent and highly alterable. For these reasons, the physiological condition of the nose such as tonicity is an important parameter to consider if liposomal drug formulations are intended for nasal administration.

A similar methodology was applied for the investigation of drug release as described in Wu *et al*. (2017) by using the Franz diffusion cell set-up. Unlike the previous paper, the tonicity of the prepared LUVs formulations were measured instead of being calculated. To our surprise, liposomes itself acted as strong tonicity enhancers increasing the total tonicity of the whole formulation with 350-400 mOsm/kg. From these observations, the measured osmolality of the whole LUVs dispersion was assumed to represent the tonicity of the inner core of the liposomes.

The PBS used to create different external environment was adjusted according to the measured osmolality of LUVs, and in total, seven different degrees of hypotonic environment

ranging from 0 up to 650 mOsm/kg in differences between the LUVs and the external environment were created (Δ*mOsm/kg*). After the exposure of LUVs to hypotonic environment, the size distribution was monitored and vesicle populations of bigger sizes could be detected for the most hypotonic environment, indicating swelling of the LUVs.

Similarly to findings in Paper I, the changes in drug diffusion across the regenerated cellulose barrier were most apparent for the hydrophilic drugs in comparison to the lipophilic/hydrophobic drugs. More importantly, all drug-loaded LUVs exposed to hypotonic environment (Δ*mOsm/kg* approx. 300) exhibited a significant increase in the apparent permeability (P_{app}) across the diffusion barrier, indicating that the tonicity perturbations played an essential role in the drug release from liposomes. To better describe the changes in the drug release, the P_{app} was expressed as the resistance to drug transport through liposomal bilayer (R_L) to better highlight the contribution given by the liposomal carrier.

The further research scope was to optimize the liposomal formulation and investigate if similar behaviour could be found when a more biomimetic diffusion barrier was used. We also wanted to investigate the LUVs' response to both hypotonic and hypertonic environment.

3.3 Paper III

The aim of Paper III was to clarify the dynamics behind the influence of tonicity perturbations on the changes in drug release from liposomes. The graphical abstract of this paper is represented in Figure 3.3.

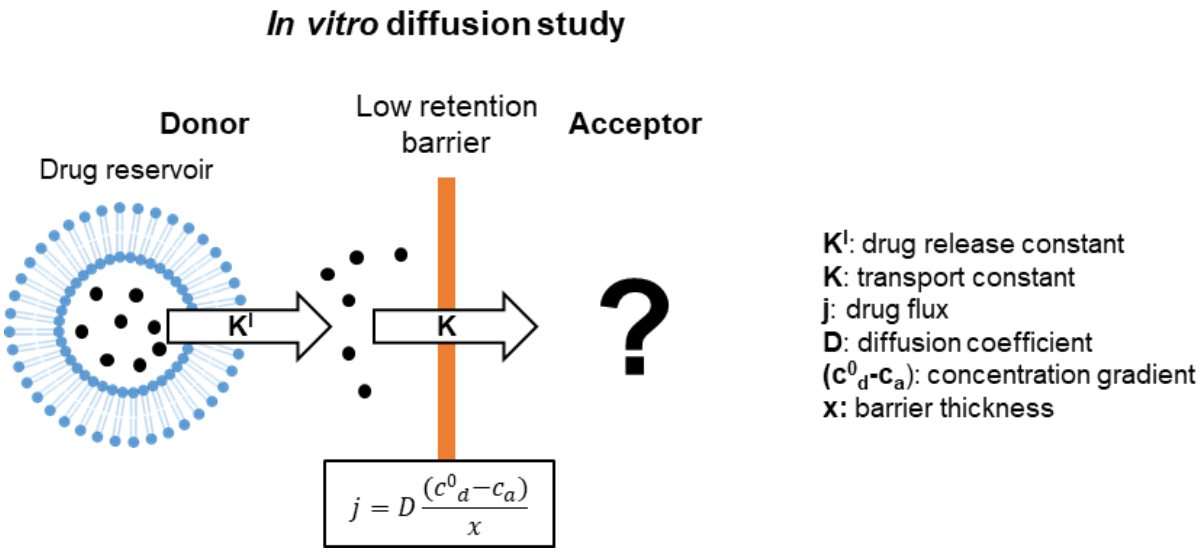

Figure 3.3: Graphical abstract for Paper III. Reproduced from Wu *et al*., 2019a, with permission from Elsevier.

For this study, LUVs were prepared to entrap individually either caffeine or hydrocortisone, and with various amounts of cholesterol incorporated in the lipid bilayer (11 and 25% w/w). The *in vitro* diffusion study was carried out utilizing both the standard regenerated cellulose and the innovative biomimetic Permeapad® barrier to achieve better *in vitro*/*in vivo* correlation for the nasal environment. The LUVs were exposed to 300 mOsm/kg differences between initial LUVs and external environment (the optimal tonicity difference according to Paper II). Both linear regression (zero order) and non-linear regression (Korsmeyer-Peppas) models were used to treat the experimentally determined diffusion data to predict the release from liposomes.

Similar to Papers I and II, the amount of diffused drug through the diffusion barrier changed according to the tonicity perturbations of the external environment surrounding the LUVs. For instance, an increased amount of drug diffused through the diffusion barriers when LUVs were exposed to a hypotonic environment. On the other hand, decreased drug diffusion was detected in the hypertonic environment.

Summary of papers

The drug diffusion rate through the regenerated cellulose barrier was higher when compared to Permeapad® barrier, which can be explained by the different structures of the diffusion barriers. The regenerated cellulose exhibits low retention to drug diffusion (controlled by drug concentration gradient). On the other hand, Permeapad® barrier is a thicker barrier containing lipids that exhibit higher retention to drug diffusion.

The structural changes of the liposomes (incorporation of cholesterol) and its direct effect on the drug diffusion rate across the diffusion barrier were strongly correlated. The incorporation of cholesterol in liposomal bilayer seemed to limit the LUVs' sensitivity to osmotic stress.

The *in vitro* diffusion data interpreted using the zero order and Korsmeyer-Peppas model were in good agreement. Both models provided important information related to the release from liposomes. Korsmeyer-Peppas model offered additional advantages as being less time-consuming due to avoidance of the need for reference experiments including drug solutions, which the zero order model required.

This paper confirmed the necessity to use both linear and non-linear regression models during the assessment of drug release phenomena from liposomes. The Korsmeyer-Peppas model was found to be suitable for this study to improve the interpretation of drug release from LUVs under osmotic stress. In terms of stability upon storage, LUVs with 11% w/w cholesterol were found to be superior in comparison to 0 and 25% w/w, respectively. These findings can be utilized in the development of liposomal formulations intended for nose-to-brain drug delivery.

4 Experimental section

Materials and Methods employed in this thesis are described in Papers I-III. The first part of this section describes the calculation used to determine the relative osmotic pressure (π_{rel}) generated on the liposomal membrane, used in Paper I. The latter part of this section provides information on the preliminary experiments with mucin that are not included in the Papers I-III.

4.1 Osmotic pressure calculations

As previously described in Section 1.6, the osmotic pressure can be calculated using the van't Hoff and the Morse equation. The equations propose that the difference in salt concentration on both sides of a semi-permeable membrane will generate an osmotic pressure on the membrane. As the internal and external environment of liposomes can have different salt concentrations, this assumption may apply to liposomal membranes as well.

In this study, the measured salt concentration of the PBS used to prepare the liposomes, and the PBS used to expose the liposomes were represented as the internal and external osmolality of LUVs. Based on this assumption, an adaptation of the van't Hoff and Morse equation could be expressed as followed (Equation 4.1);

$$\pi_{rel} = (Osm_{(out)} - Osm_{(in)})R_0T \qquad \textbf{Equation 4.1}$$

In Equation 4.1, the R_0 represents the ideal gas constant, T the absolute temperature, and $Osm_{(out)}$-$Osm_{(in)}$ represents the osmolality difference between the external and internal environment of LUVs. A positive π_{rel} indicates that the LUVs are exposed to a hypertonic environment, causing solvent molecules to migrate from the inner core to the external environment of the liposome. On the contrary, a negative π_{rel} indicates that the LUVs are exposed to a hypotonic environment, causing solvent molecules to migrate from an external environment to the internal core of liposomes.

4.2 Experiments involving mucin

When performing *in vitro* diffusion study, it is important to tailor the experimental conditions as close as possible to the real biological conditions to obtain good *in vitro/in vivo* correlation. We have already described in Paper III the use of the Permeapad® barrier for the purpose to mimic

the nasal epithelium. Furthermore, we also wanted to include mucin in our experiments to mimic nasal mucus.

One of the main constituents of nasal mucus is mucin (Bansil and Turner, 2018, Quraishi *et al.*, 1998). The purified porcine stomach mucin type III is commonly used for *in vitro* studies due to the resemblance to human mucins in terms of structure and molecular weight (Groo and Lagarce, 2014, Lock *et al.*, 2018). Within the range of mucin concentration used in this study, the purified mucins were considered suitable for the determination of drug diffusion hindrances caused by the electrostatic and hydrophobic interactions (Lock *et al.*, 2018, Murgia *et al.*, 2018).

4.2.1 Preparation of mucin dispersions

Mucin from porcine stomach type III (bound sialic acid 0.5-1.5%, partially purified, Sigma-Aldrich Chemie GmbH, Steinheim, Nordrhein-Westfalen, Germany) was dispersed in PBS at a concentration of 1 mg/mL, following previous reports (Chen *et al.*, 2013, Qiang *et al.*, 2012). At this mucin concentration, the mucin was homogeneously dispersed in the PBS. The osmolality and p*H* of PBS before and after the addition of mucin were measured using a Semi-Micro Osmometer Model 4602 (Knauer, Berlin, Germany) and SensION™ +PH31 p*H* meter (Hach Company, Barcelona, Spain), respectively. To avoid mucin degradation when dispersed in PBS, mucin dispersions were stored at 4°C and protected from direct sunlight and used within 7 days after preparation.

4.2.2 *In vitro* diffusion study in the presence of mucin

The diffusion study was performed as previously described by Wu *et al.* (2019a). For the *in vitro* diffusion studies involving mucin, mucin dispersion (0.3 mL, concentration of 1 mg/mL) was added on top of the different diffusion barriers (regenerated cellulose or Permeapad® barrier) instead of PBS before LUVs dispersion was added (0.5 mL). The total concentration of mucin was approx. 0.4 mg/mL in the donor compartment at the start of the experiment (t=0) in agreement with previously reported conditions (Khatri *et al.*, 2008). The diffusion study was conducted under the same conditions as in the experiments where mucin was not included.

5 Results and discussions

This thesis aimed to develop osmotically active liposomes for nose-to-brain drug delivery. The rationale for using liposomes as a drug delivery system is already described in Section 1.5.

As previously discussed, a sufficient amount of drug needs to be efficiently absorbed through the nasal epithelium to obtain therapeutic levels of a drug in the brain (Bourganis *et al.*, 2018, Khan *et al.*, 2017). To achieve controllable permeation across any biological barriers, it is of great importance to first understand the drug release from the nanocarrier when drug is delivered via nanocarrier. One of the major challenges considering the development of nasally administered liposomal drug formulations is the nasal mucus. Nasal mucus tonicity is known to fluctuate greatly due to its sensitivity to the environmental and physiological factors (Quraishi *et al.*, 1998). The liposomal membrane has a semi-permeable nature (Bangham *et al.*, 1967, Paula *et al.*, 1996), and liposomes that come in direct contact with mucus might undergo unpredictable behaviour due to the tonicity differences that can take place.

Therefore, the work was carried out by firstly validating the liposomes' susceptibility to osmotic stress. Once validated, a wider range of liposomal formulations and the tonicity differences between the formulation and external tonicity were screened, which assisted us to choose the relevant drugs and tonicity differences to investigate. We then tried to optimize the experimental condition to better mimic the nasal environment by using the newly developed Permeapad® barrier and mucin. Simultaneously, more advanced liposomal formulations were prepared by incorporating various amounts of cholesterol, and their drug release and stability upon storage were evaluated. All these variables were considered important for the development of osmotically active liposomes for nose-to-brain drug delivery.

On those grounds, in the first part of Results and discussions, the focus is put on the general characteristics of all LUVs dispersions prepared throughout this project.

5.1 Characterization of liposomes (Papers I-III)

Among the different nanoparticulate drug delivery systems proposed for nose-to-brain drug delivery, liposomes exhibit low toxicity to the nasal mucosa and epithelium (Li *et al.*, 2017, Patel and Patel, 2017). Liposomes are promising drug carriers for brain targeting as they can be tailored in composition (*e.g.* type of lipid, dispersing medium and stabilizing agent) to achieve preferable characteristics (Daraee *et al.*, 2016). The LUVs characteristics are important in-process controls considering the development of liposomal formulations and

should be determined before the formulation testing stage. In this section, LUVs characteristics such as the formulation tonicity, size, lamellarity, surface charge, and drug entrapment are discussed in the respective order.

Liposomes were prepared in PBS of different tonicity (0, 65 and 300 mOsm/kg, respectively) to obtain LUVs with different inner core tonicity. In Paper I, we assumed that the inner core tonicity of LUVs would be equivalent to the tonicity of the hydrating medium used to prepare the LUVs. This is an iterative assumption found in the literature (Ahumada *et al.*, 2015, Boroske *et al.*, 1981, Fujiwara and Yanagisawa, 2014, Mui *et al.*, 1993, Ohno *et al.*, 2009, Sabin *et al.*, 2006). Two of the most common tonicity enhancing agents are sucrose and salt (*e.g.* KCl, NaCl). Sucrose and NaCl are suggested to slowly permeate through liposomal membranes, and can, therefore, create a tonicity imbalance across the liposomal bilayer (Paula *et al.*, 1996). Exposing liposomes to different environmental tonicity after reconstruction generates a relative osmotic pressure (π_{rel}) on the liposomal membrane. We decided to calculate the π_{rel} following Equation 4.1, in agreement with a similar approach suggested by Jackman *et al.* (2013). As described by Jackman and colleagues, the sign of the osmotic pressure can be arbitrary (Jackman *et al.*, 2013). In Paper I, we decided to present π_{rel} as either positive or negative if the salt concentration outside the liposomes was higher or lower than the inner core salt concentration, respectively.

To our later knowledge and rather surprisingly, liposomes acted as strong tonicity agents. The presence of liposomes in the formulation increased the formulation tonicity up to 400 mOsm/kg in comparison to the plain PBS. For instance, empty liposomes prepared in PBS65 expressed tonicity of approx. 410 mOsm/kg, whereas liposomes prepared with PBS300 expressed formulation tonicity around 700 mOsm/kg. The present findings emphasize that the buffer tonicity used to prepare the liposomes is not necessarily equivalent to the inner core tonicity of the vesicles, which should be taken into consideration when comparing studies. The implications of these findings concerning size and release will be later addressed in Sections 5.2 and 5.4.

Early work in liposomes field has reported that liposomes are susceptible to osmosis (Bangham *et al.*, 1965, Bangham *et al.*, 1967) and that for liposomes smaller than 1000 nm, vesicles keep their spherical shape upon swelling and shrinkage (Boroske *et al.*, 1981). To study the direct influence the tonicity perturbations have on the liposomal bilayer, unilamellar vesicles have been suggested as more suitable due to their simple membrane construction in comparison to multilamellar vesicles (Mui *et al.*, 1993, Sun *et al.*, 1986). For these reasons, this thesis aimed to utilize large unilamellar vesicles; therefore a modified swelling method for

the rapid preparation of giant unilamellar vesicles was used (Moscho *et al.*, 1996). To confirm the vesicles spheroid structure, phase contrast microscopy was employed.

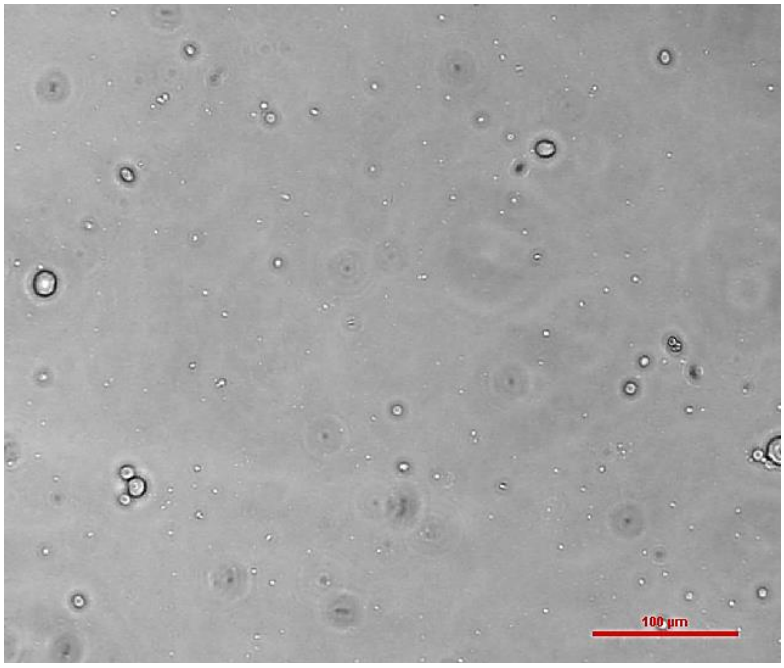

Figure 5.1: Phase contrast image of empty GUVs before extrusion. The bar shows 100 µm (unpublished results).

In Figure 5.1, the phase contrast image of empty giant unilamellar vesicles right after reconstruction is shown. Images of the higher resolution were unachievable with the available microscope in the laboratory. However, the image illustrates that the liposomes were spherical.

The extrusion method was chosen to optimize the distribution and size of liposomes. The extrusion method was found to be a convenient and well-suited method to achieve desired vesicle sizes and acceptably narrow PI (<0.5) for our purposes. Photon correlation spectroscopy (PCS) is a commonly used technique to quantify liposomal sizes and PI in a dispersion. The general rule of thumb is that the PI value below 0.7 is considered acceptable, and PI of 0.3 for a liposomal dispersion suggests rather homogeneous size distribution (Danaei *et al.*, 2018).

Some of the liposomal formulations exhibited large size variations and PI, especially for the marker-loaded LUVs (Paper I). This illuminates some of the PCS technique's limitations, including its shortage to provide information regarding the morphology and shape of the particles (*e.g*. elongated, spherical, *etc.*). Moreover, the aggregation of particles during the measurement tends to be measured as one single particle. Upon realizing that LUVs acted as tonicity enhancing agents, diluting the LUVs to the correct intensity before size measurements

might have induced small scale of liposomal swelling which might influence the size measurements.

The determination of ζ-potential (ZP) of nanocarriers has become a standard measurement of liposomal characteristics. Small changes in temperature, p*H*, ionic strength and solvent might all contribute to a dramatic change in ZP (Smith *et al.*, 2017), and therefore the same medium used to prepare the LUVs was used to dilute the sample before measurement. The most negative ZP values were observed for LUVs prepared in distilled water, and a linear relationship between the osmolality of the different PBS used and measured ZP could be observed (Papers I-II). The presence of cholesterol in the LUVs dispersions had minimal effects on the ZP as expected since all formulations retained neutral ZP values (Paper III). These results are the result of the zero net charge of phosphatidylcholine, and cholesterol being uncharged (Aniket *et al.*, 2014, Li *et al.*, 2015).

The entrapment efficiency (EE) is a very important parameter during the development of liposomal drug delivery systems, as it can influence the available dose at the administration site (Bourganis *et al.*, 2018, Khan *et al.*, 2017). It was beyond the scope of this thesis to optimize the EE of the loaded liposomes, but for better comparisons, different drugs with different physiochemical properties were chosen to be entrapped individually into LUVs. This resulted in drug-loaded LUVs with a range of EE but a constant total marker/drug concentration of 2 mM. As expected, the EE of the LUVs dispersions were the lowest for the hydrophilic (caffeine and theophylline), middle for lipophilic (ibuprofen and ketoprofen) and highest for hydrophobic drugs (hydrocortisone and methylprednisolone) (Akbarzadeh *et al.*, 2013, Nii and Ishii, 2005, Xu *et al.*, 2012).

We prepared LUVs with cholesterol to investigate its effects on drug release and stability upon storage. Cholesterol can be used as a stabilizing agent in liposomal formulations due to its steroid structure forming hydrophobic interactions with the hydrocarbon chains of the phospholipids (McIntosh, 1978, Milon *et al.*, 1986). As a result, cholesterol contributes to a more densely packed liposomal membrane which can influence the liposomes as a carrier (Briuglia *et al.*, 2015, de Gier *et al.*, 1968). Lipophilic compounds might compete with cholesterol to be embedded within the lipid membrane. In this situation, the compound with the strongest affinity to the liposomal membrane will remain highly incorporated, thus influencing the EE (Ali *et al.*, 2010). In terms of developing osmotically active liposomes, cholesterol might hinder the free solvent movement across the liposomal membrane (Allen and Cleland, 1980). Consequently, cholesterol can alter the sensitivity of liposomes to osmotic stress.

Based on these results, we managed to successfully prepare different LUVs formulations for different purposes throughout this study. Liposomes were prepared to exhibit various formulation tonicity (*i.e.* 410 or 700 mOsm/kg) to generate different salt concentration gradients with the external environment of LUVs. We prepared different LUVs comprising various markers, drugs, and cholesterol for a thorough screening, and comparison. In the following section, the results obtained to prove the LUVs osmotic activity are discussed.

5.2 Effect of tonicity perturbations on liposomal size (Papers I-II)

The first papers mentioning osmotic properties of liposomes were published in the 1960s by Bangham and colleagues, where they proved that liposomes prepared of egg-phosphatidylcholine could retain different concentrations of univalent (*e.g.* K^-, Na^-, Cl^-, I^-, F^-, NO_3^-) and divalent (*e.g.* SO^{2-}, HPO_4^{2-}) ions. They also described the relationship between the rate of ion diffusion across liposomal bilayer as a function of the ion size and charge (Bangham *et al.*, 1965, Bangham *et al.*, 1967). Due to the slower ion diffusion rate across the liposomal bilayer in comparison to water molecules, water could influx or efflux the liposomes and cause the liposomes to shrink or swell (Bangham *et al.*, 1967).

Since then, a considerable amount of research has been carried out to investigate the influencing factors related to the swelling or shrinking of liposomes. Findings support that osmotic stress influences larger unilamellar vesicles (>100 nm) to a greater extent than smaller unilamellar vesicles (<100 nm) (Hallett *et al.*, 1993, Mui *et al.*, 1993). It has been suggested that unilamellar vesicles remain spherical shapes upon swelling or shrinking (Boroske *et al.*, 1981, Reeves and Dowben, 1970).

As the liposomal composition, shape and original size can all influence the liposome sensitivity to tonicity perturbations, the first set of experiments focused on verifying the osmotic activity of the LUVs. If size changes could be detected, it would indicate the liposome susceptibility to solvent permeation, therefore liposomes being osmotically active. In the following section, the first sets of results indicating that marker-loaded LUVs are osmotically active are discussed (Figure 5.2). As a continuation of Paper I, the results obtained for the drug-loaded LUVs are presented (Figure 5.3).

Exposure of unilamellar vesicles to the hypotonic environment has been reported to induce liposomal swelling (Mui *et al.*, 1993, Oglecka *et al.*, 2014), whereas exposure to hypertonic environment induces liposomal shrinkage (Boroske *et al.*, 1981, Ohno *et al.*, 2009). The

apparent size changes are directly dependent on the exposure time, and unilamellar vesicles exposed to small concentration differences (Δ*mOsm/kg* up to 400) have shown size change saturation after approx. 1 hour (Fujiwara and Yanagisawa, 2014, Sun *et al.*, 1986). For these reasons, we decided to monitor the LUVs for at least 70 min and the average sizes of the LUVs at different environment were plotted as a function of time as shown in Figure 5.2.

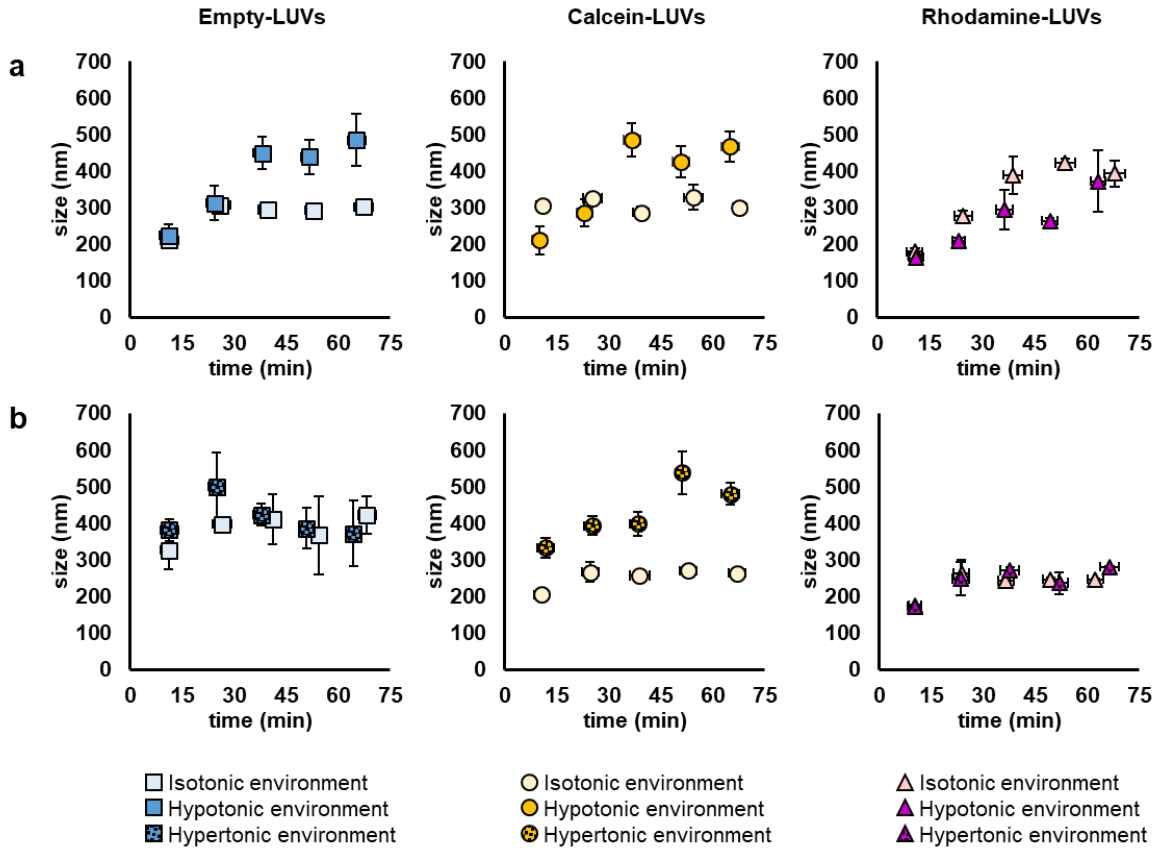

Figure 5.2: Average liposomal sizes before and after exposure to the hypotonic and hypertonic environment. LUVs prepared in a) PBS300 and b) PBS65 were exposed to PBS65 and PBS300, respectively. Results represent mean ± SD (n=2). Adapted from Wu *et al.*, 2017, with permission from Elsevier.

In Figure 5.2, larger liposomal sizes could be detected when LUVs were exposed to a hypotonic environment in comparison to the isotonic environment, and the size enlargement became more apparent with time, reaching a plateau after 45 min. These results were in a good agreement with the literature (Mui *et al.*, 1993, Oglecka *et al.*, 2014). On the contrary to our presumption and literature (Boroske *et al.*, 1981, Ohno *et al.*, 2009), the shrinking behaviour of marker-LUVs after their exposure to the hypertonic environment could not be observed, and calcein-LUVs showed even larger sizes.

Deviations between our results and the literature can arise from several factors. Sabin *et al.* (2006) proposed that liposomal aggregation often affects liposomes exhibiting neutral surface. Furthermore, the LUVs were exposed to PBS of different osmolality, thus different amounts of ions that can neutralize the liposomal surfaces. The shrinking behaviour of liposomes might be masked by aggregated liposomes, disturbing the size detection measurements when the PCS technique was used. We could notice that the PI of each size measurement increased with time, especially for those LUVs exposed to the hypotonic environment, and, in some cases, the PI rose from 0.3 up to 1. This indicated that presenting the distributional results rather than the mean size might provide a better interpretation of the vesicle size, which was later implemented in Paper II.

For Paper I, we calculated the π_{rel} based on the assumption that the liposomal inner core tonicity was equivalent to the tonicity of the PBS used to prepare the liposomes. However, we later realized that the LUVs acted as the tonicity agent when in a dispersion. To the best of our knowledge, this phenomenon has never been reported in the literature before. If the tonicity of the formulation is representing the liposomal inner core tonicity, Figure 5.2 can be reinterpreted. What was earlier assumed to be a hypertonic environment in Figure 5.2b will, in fact, be a low-hypotonic environment ($\Delta mOsm/kg$ assumed to be approx. 100). This better explains the size enlargements observed for calcein-LUVs and the lack of size decrements of empty- and rhodamine-LUVs. Rhodamine is a lipophilic marker ($\log D_{7.4}$ of 2.3 (Toropainen *et al.*, 2001)) that incorporates itself in the liposomal bilayer, contributing to the stabilization of the vesicle membrane. Consequently, rhodamine-LUVs might be less sensitive to osmotic stress. Calcein is a hydrophilic marker ($\log D_{7.4}$ of -3.3 (Maherani *et al.*, 2013)) which is localized in the aqueous inner core. As seen in Table 3 (Paper I), the calcein-LUVs expressed a more neutral ZP (-2.8 mV) than empty-LUVs (-12 mV) indicating that calcein can be adsorbed onto the vesicle surfaces. As this might contribute to a relatively neutral liposomal membrane, this might enhance the liposomal osmotic sensitivity. Water permeation across liposomal membranes has been reported to be the highest for the positively charged membranes, middle for the uncharged, and the lowest for the negatively charged (Allen and Cleland, 1980, Bangham *et al.*, 1967, Biondi *et al.*, 1991).

To provide deeper insight into the findings in Paper I, we decided to proceed with a more detailed screening of six drug-loaded LUVs formulations. Instead of using the π_{rel} as in Paper I, we used the $\Delta mOsm/kg$. The $\Delta mOsm/kg$ was determined as the difference between the measured osmolality of LUVs formulation and the exposing PBS. In Figure 5.3, the size distributions of all drug-loaded LUVs taken at different time points and environment are represented.

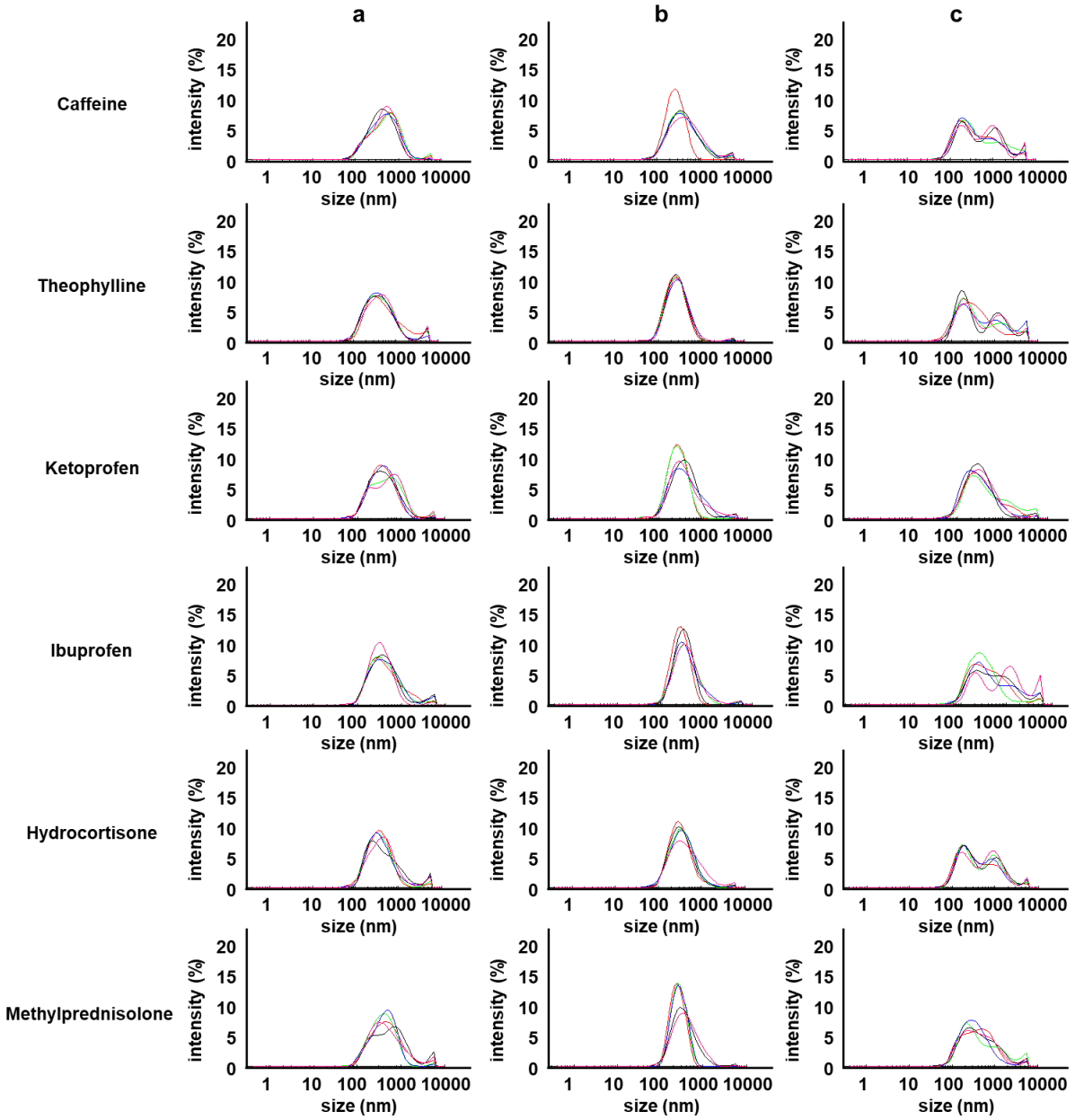

Figure 5.3: Size distributions of drug-loaded LUVs in a) isotonic, b) low-hypotonic, and c) hypotonic environment (Δ*mOsm/kg* of 3±2, 419±19, and 648±19, respectively). Each line represents the mean size distribution (n=2) measured at five different time points within 90 min. Adapted from Wu *et al*., 2019b, with permission from Elsevier.

In agreement with the findings in Paper I, the drug-loaded LUVs exhibited size enlargement when exposed to hypotonic environment. Based on the distributional curves, no lysis of LUVs could be observed, even up to the maximum osmolality difference between the LUVs formulation and external tonicity (Δ*mOsm/kg* around 650). Earlier reports have indicated that the maximum difference in the concentration LUVs can withstand before lysis strongly depends on the phospholipid used to prepare the liposomes. For instance, LUVs of egg-

phosphatidylcholine and cholesterol (approx. 50% mol/mol) rupture at ∆*mOsm/kg* greater than 650 (Mui *et al.*, 1993) while LUVs of dioleoylphosphatidylcholine rupture at ∆*mOsm/kg* of 2000 (Alam Shibly *et al.*, 2016). The obtained data verified that the increment in liposomal size correlated with the degree of difference between the inner and external environment of LUVs. It was, therefore, interesting to see if tonicity perturbations could alter the release kinetics from the liposomes.

Before discussing the drug release from liposomes, it is important to point out that currently there is no standard method to determine the release from liposomes (Nothnagel and Wacker, 2018, Wacker, 2017). The common methods utilize techniques such as filtration, ultracentrifugation, or solid phase extraction to separate the free unentrapped drug from liposomal drug (Nothnagel and Wacker, 2018). The common limitation associated with these techniques is the risk of disrupting the nanocarrier due to exposure to mechanical forces during the separation procedure (Solomon *et al.*, 2017).

In the present study, we used the Franz diffusion cell set-up to study release from the liposomes. This method relies on the drug's ability to diffuse across a barrier that separates the donor and acceptor compartment. Due to lower risk of exposure to mechanical forces, this method is considered to be more gentle and is currently one of the preferred methods to study drug release from liposomes (Solomon *et al.*, 2017). The downside of the method is that drug needs to diffuse through several physical barriers before reaching the acceptor compartment. One way to adjust for this is to compare the release profile of a liposomal formulation with a reference diffusion of free drug solution (Nothnagel and Wacker, 2018, Wacker, 2017). For this reason, before going deeper into the release from liposomes, a short discussion on the experimentally collected diffusion data for marker and drug solutions is presented.

5.3 Diffusion study with solutions (Papers I-III)

The markers and drugs were prepared individually in a buffer solution of 65 or 300 mOsm/kg tonicity (PBS65 or PBS300, respectively) as represented in Table 5.1.

Table 5.1. Apparent permeability coefficient (P_{app}) and total permeated marker/drug from free solution through regenerated cellulose barrier. Results represent mean ± SD (n≥3). Adapted from Wu *et al*. 2017, Wu *et al*. 2019a and Wu *et al*. 2019b, with permission from Elsevier.

Reproduced from	Marker/drug	PBS	P_{app} (10^{-5} cm/sec)	Total permeated after 4 hours (%)
Paper I	Calcein	65	0.68 ± 0.06	37.10 ± 7.80
		300	0.90 ± 0.07	46.97 ± 4.17
	Rhodamine	65	1.55 ± 0.06	83.06 ± 2.61
		300	1.61 ± 0.11	86.22 ± 3.68
Paper II	Caffeine	65	6.18 ± 0.13	63.08 ± 0.94
		300	6.10 ± 0.20	63.90 ± 1.58
	Theophylline	65	6.34 ± 0.19	65.96 ± 2.59
		300	6.25 ± 0.27	64.66 ± 1.39
	Ketoprofen	65	4.43 ± 0.16	46.75 ± 1.30
		300	4.82 ± 0.27	51.37 ± 2.68
	Ibuprofen	65	4.69 ± 0.29	49.25 ± 3.33
		300	4.60 ± 0.34	48.56 ± 3.50
	Hydrocortisone	65	5.25 ± 0.59	59.24 ± 4.28
		300	4.53 ± 0.33	51.79 ± 3.93
	Methylprednisolone	65	4.96 ± 0.41	62.39 ± 7.19
		300	4.48 ± 0.67	54.15 ± 7.39
Paper III[a]	Caffeine	65	2.79 ± 0.14	32.09 ± 1.61
	Hydrocortisone	65	1.12 ± 0.09	15.23 ± 2.18

[a]Permeapad® barrier.

As highlighted in Table 5.1, we used the regenerated cellulose barrier in the first two papers (Papers I-II), whereas in Paper III we additionally used the innovative biomimetic Permeapad® barrier as a diffusion barrier. If we first look at the findings reported in Paper I, we can see that the P_{app} values for marker solutions were greater in PBS300 in comparison to PBS65, whereas opposite trends were found for the drug solutions in Paper II. This might be related to the Franz diffusion cell set-up where marker or drug in the donor compartment diffuse one-sidedly across a diffusion barrier before being collected in the acceptor compartment. Diffusion data obtained using this experimental set-up are sensitive to barrier-related influences (Brandl *et al.*, 2007, Brodin *et al.*, 2010). For instance, ions and charged molecules can interact with the barrier, and influence the barrier's susceptibility to permeation (Benavente, 1984). It has been reported that regenerated cellulose exhibits slightly negative surface charge, and allows neutral molecules rather than charged molecules to permeate (Benavente, 1984, Coday *et al.*, 2015). Both markers used in this study are strongly ionized at p*H* 7.4 (p*Ka* of 1.8 and 3.1 for calcein

and rhodamine, respectively) (Flaten *et al.*, 2006, Pittman *et al.*, 2001), whereas ketoprofen and ibuprofen ionize at p*H*>4.5 and 4.9, respectively (PubChem, 2019c, PubChem, 2019b). We believe that the greater fluctuations in P_{app} values of marker solutions correlate with the considerably greater number of dissociated ions at experimental p*H*, thus influencing the permeation through regenerated cellulose barrier in comparison to the drugs.

In Table 5.1 it can be observed that the Permeapad® was a more restrictive barrier allowing less drug to diffuse in comparison to the regenerated cellulose barrier. The regenerated cellulose barrier is a low retention barrier allowing molecules to diffuse across as long as a concentration gradient is retained (Bartels *et al.*, 2005, Benavente, 1984, Nothnagel and Wacker, 2018). On the other hand, the biomimetic Permeapad® barrier consists of a lipid layer in between two support sheets (di Cagno and Bauer-Brandl, 2014). When the barrier comes in contact with an aqueous solution, the lipid layer is assumed to create tightly packed vesicles mimicking the structure of biological membranes (di Cagno *et al.*, 2015), thus the Permeapad® barrier represents a thicker barrier that can provide higher retention to drug permeation.

These data indicate that the PBS (*e.g.* p*H*, tonicity) plays a major role in the diffusion across barriers, as well as the type of the diffusion barrier used. It emphasizes the importance of selecting the correct conditions as a reference to interpret release from liposomes, as small variations in the experimental set-up can have a considerable effect on the P_{app}. For this reason, we ensured that the reference experiment was performed in the respective PBS used in the formulation. In the following section, a relationship between the tonicity perturbation and changes in release kinetics from liposomes are discussed in more details (Papers I-II).

5.4 Tonicity perturbation and liposomal release (Papers I-III)

As shown and discussed in the previous section (Section 5.2), we verified that the LUVs were osmotically active, and we suspected that tonicity perturbations might as well influence the drug release from liposomes (Ahumada *et al.*, 2015, Ohno *et al.*, 2009, Wolfram *et al.*, 2014).

In the earliest reports, water or ion permeation changes across the liposomal membrane for shrunken or swollen liposomes consisting of synthetic or natural origin phosphatidylcholine have been extensively described (Abuin *et al.*, 1995, Bangham *et al.*, 1967, Biondi *et al.*, 1991, Paula *et al.*, 1996, Polozov *et al.*, 2001). Attempts in controlling the liposomal leakage under their exposure to osmotic stress have also been tried using cholesterol, PEGylation, and surfactants (Allen and Cleland, 1980, Cipolla *et al.*, 2014, Leite *et al.*, 2018, Milon *et al.*, 1986,

Wolfram *et al.*, 2014). In more recent years, the burst and pulsating leakage from giant unilamellar vesicles have been observed when liposomes were exposed to the extreme hypotonic environment ($\Delta mOsm/kg$ >2000) (Alam Shibly *et al.*, 2016, Chabanon *et al.*, 2017, Oglecka *et al.*, 2014). In spite of the efforts put in preventing leakage from liposomes upon osmotic stress, rather few studies have tried to investigate if osmotic stress can be used to control the release from liposomes. An explanation might be that the currently marketed liposomal products are developed for parenteral routes (Bulbake *et al.*, 2017, Choi and Han, 2018). We agree that for parenteral routes, the tonicity perturbations will be rather irrelevant due to the body homeostasis. Moreover, immunogenicity, opsonisation and reticuloendothelial system are more common challenges the liposomes are facing when administered parenterally (Sercombe *et al.*, 2015).

As previously discussed in Section 1.3, the nasal epithelium provides a great platform for drug absorption to the brain overcoming the BBB and systemic side effects (Erdő *et al.*, 2018, Khan *et al.*, 2017, Patel and Patel, 2017). However, most of the nasal epithelium is covered with nasal mucus, which creates a large obstacle to efficient drug absorption. The nasal mucus directly captures inhaled drugs, which can challenge the drug's stability and permeability across the mucus layer (Ghadiri *et al.*, 2019). It becomes even more complex when the nasal mucus is exposed to constant change due to direct contact with the peripheral environment. The changes in either humidity, temperature, lifestyle (*e.g*. cigarette smoking) and nasal condition (*e.g*. inflammation, rhinitis, sinusitis) are all associated with changed mucociliary clearance rate, nasal mucus rheology as well as tonicity exploited in the nasal cavity (Pedersen *et al.*, 2007, Quraishi *et al.*, 1998, Taherali *et al.*, 2018). For these reasons, it is necessary to take into account the possibility of osmotic influences when developing liposomes for nose-to-brain drug delivery. It would be even greater if osmotic stress can be utilized to direct the release from liposomes.

In this project, the mass transport across the diffusion barrier was monitored over time, and the accumulated diffused amount was analysed to predict the release kinetics from liposomes. In Paper I, the changes of fluorescent marker release from liposomes were determined by monitoring the marker flux across the regenerated cellulose barrier as a function of change in π_{rel} (see Figure 3 in Paper I). From the data, it was evident that the release was changing more drastically for calcein-LUVs than for rhodamine-LUVs, presumably due to the marker's localization inside the LUVs and its solubility.

To our later knowledge, the presence of LUVs changed the formulation tonicity with an increase of approx. 350-400 mOsm/kg. Even though we did not exactly measure the marker-

loaded LUVs formulations used for the diffusion study, measurement of empty liposome formulations in PBS65 and PBS300 suggests that the initial tonicity should have been approx. 410 or 700 mOsm/kg, respectively. If reanalysing the marker-loaded LUVs release data, assuming that the tonicity of the LUVs formulation was representing the liposomal inner core tonicity, all the LUVs formulations were probably exposed to different degrees of hypotonicity. In Figure 5.4, the flux in a different environment as a function of $\Delta mOsm/kg$ is displayed. With a new representation of the diffusion data, the conclusions made in Paper I remain the same, however, we could postulate more on the findings.

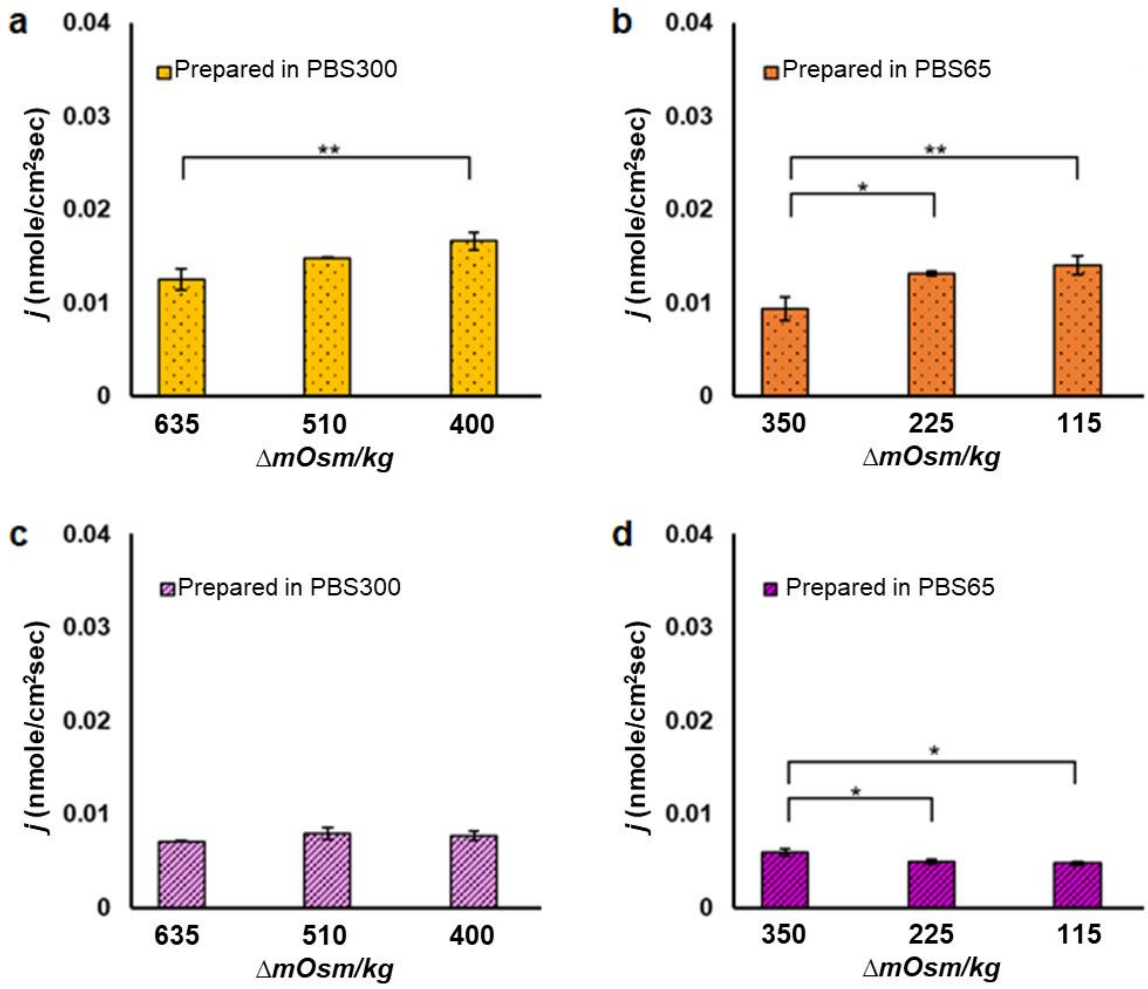

Figure 5.4: Flux (*j*) under the influence of hypotonic environmental changes. Results represent mean ± SD (n=3), and a statistically significant difference in *j* (**p*≤0.050, ***p*≤0.010, ****p*≤0.001) between the highlighted bars. Adapted from Wu *et al*., 2017, with permission from Elsevier.

As already mentioned, calcein is a hydrophilic marker (Maherani *et al.*, 2013). It is by now generally accepted that solvent influx into the LUVs can cause the liposomes to swell, thus stretching the liposomal membrane, and allowing more of the entrapped content to be released (Ahumada *et al.*, 2015, Alam Shibly *et al.*, 2016, Allen and Cleland, 1980, Ertel *et al.*, 1993).

As it can be seen from Figure 5.4a-b, we repeatedly saw that the flux of calcein is decreasing with an increasing degree of hypotonic exposure. These findings might be related to the direction of solvent migration. As the marker concentration gradient across the liposomal bilayer can be disturbed due to the solvent influx, it seems possible that a decrease in the release can occur, especially for hydrophilic compounds. On the contrary, rhodamine is a lipophilic drug that is highly incorporated within the liposomal bilayer. The rhodamine-LUVs were somehow less sensitive to environmental changes since smaller variations in flux were found in comparison to calcein-LUVs. These results correspond well with previous studies, where compounds incorporated into the liposomal bilayer increase the membrane rigidity, thus decreasing sensitivity to osmotic influences (Ali *et al.*, 2010, Leite *et al.*, 2018).

We also observed that the calcein flux across the diffusion barrier for the LUVs formulation prepared in PBS300 was higher than for LUVs prepared in PBS65. Again, the diffusion seemed to be highly influenced by the presence of ions, similarly to the data obtained from solutions that have already been discussed in Section 5.3.

A more insightful way to report *in vitro* diffusion data is using the permeability across a barrier (namely, P_{app}), or R (inverse of P_{app}) instead of the mass flux (j) (Baker *et al.*, 2010). In Paper II, the focus was to achieve a more detailed screening of the influences the hypotonic environment had on the drug release from liposomes. Since we could see in Paper I that the hydrophilic marker was more susceptible to tonicity changes in comparison to lipophilic marker, six different drugs with different log$D_{7.4}$ were chosen to be entrapped individually into LUVs. The tonicity difference between the LUVs and external environment was reported as $\Delta mOsm/kg$ instead of the π_{rel} for simplicity. Moreover, the R_L calculations were implemented, and the obtained results are represented in Figure 5.5.

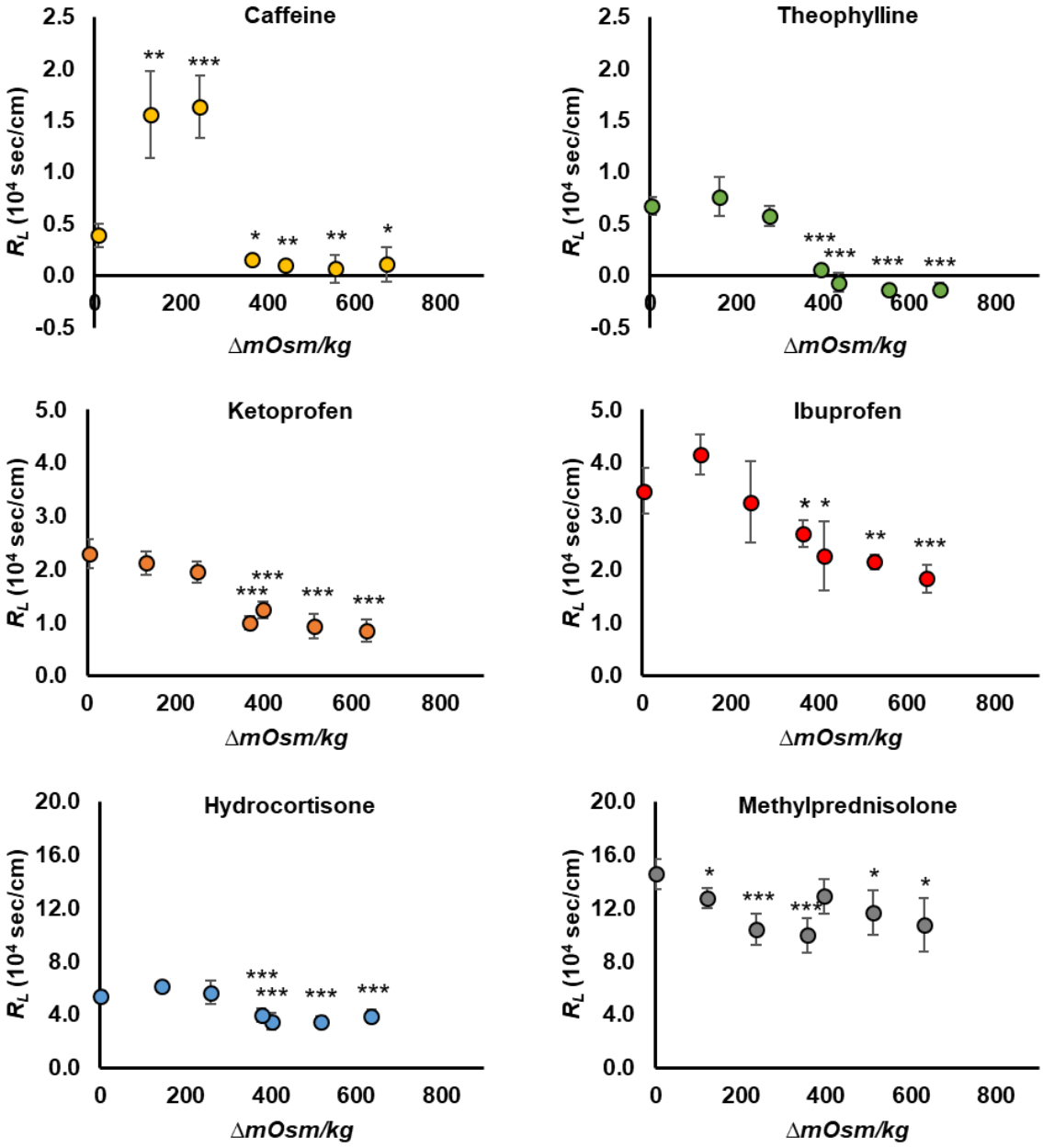

Figure 5.5: Resistance to drug transport through liposomal bilayer (R_L) under the influence of hypotonic environmental changes. Results represent mean ± SD (n=4), and a statistically significant difference in R_L (*p≤0.050, **p≤0.010 and ***p≤0.001) when compared to the isotonic environment. Adapted from Wu *et al.*, 2019b, with permission from Elsevier.

As highlighted by Figure 5.5, the R_L obtained for the different LUVs formulations in an isotonic environment (Δ*mOsm/kg* approx. 0) expressed the lowest values for the hydrophilic drugs (caffeine and theophylline) and the highest for the hydrophobic drugs (hydrocortisone and methylprednisolone). The higher R_L for hydrophobic compounds in comparison to hydrophilic compounds is not surprising since the hydrophobic compounds are tightly incorporated within the liposomal bilayer and will experience more difficulties to become released. A linear

correlation could be found between the R_L and the different degrees of hypotonic environment, and a significant drop in R_L (p<0.05) could be observed for all of the formulations at $\Delta mOsm/kg$ around 300 mOsm/kg. Decreasing R_L values indicate that more drug permeates the liposomal bilayer when the vesicles swell. Interestingly, an increase in R_L could be observed at differences lesser than 300 mOsm/kg for caffeine and theophylline. These results demonstrate two things. First, hydrophilic compounds are highly influenced by solvent flux direction probably due to their hydrophilic nature. These findings are directly in line with our previous findings (Paper I). Second, when large enough difference is created between the LUVs and the external environment ($\Delta mOsm/kg$ around 300), the release from liposomes for both hydrophilic and hydrophobic compounds will overrule the effect of solvent influx.

The present findings confirmed that changes in tonicity (within nasal environment) can be used to alter the release from LUVs. However, both Papers I and II have been casting more light on LUVs exposed to a hypotonic environment, and not addressing hypertonic environmental influences as thoroughly. Sun *et al*. (1986) suggested that tonicity induced liposomal shrinking is often more complexed than liposomal swelling. To get a deeper understanding of the release from swollen and shrunken liposomes, we decided to test all formulations in both hypotonic and hypertonic environment. We also decided to focus on the development at: i) formulation level, ii) experimental set-up level, and iii) data interpretation level, which will be more closely discussed in the next sections.

5.5 The effect of liposomal composition on drug release (Paper III)

Based on the findings so far, the LUVs seemed to be responsive to osmotic stress when the difference between LUVs and external environment showed a $\Delta mOsm/kg$ of 300. For simplicity, we prepared all LUVs formulations in PBS65 to obtain dispersions with tonicity around 400 mOsm/kg to be used in both environment. We chose to focus on one hydrophilic (caffeine) and one lipophilic (hydrocortisone) drug to be entrapped into LUVs with various amounts of cholesterol incorporated in the liposomal bilayer (up to 25% w/w).

Cholesterol is a component in most of the currently available marketed liposomal products (Bulbake *et al.*, 2017), and also within the liposomal formulations designed for nose-to-brain drug delivery (see Table 1.3). Early liposomal research showed that the increase of cholesterol content within the liposomal bilayer was correlated with a decrease in membrane elastic properties, thus influencing the permeability of water and small molecules through the liposomal bilayer (Allen and Cleland, 1980, McIntosh, 1978). The incorporation of cholesterol

into liposomal bilayers has shown to delay the release of both hydrophilic and lipophilic compounds from liposomes (Ali *et al.*, 2010, Briuglia *et al.*, 2015, Grit and Crommelin, 1993). With the manipulation of the phospholipid and cholesterol content, liposomes can be altered to exhibit favourable drug release profiles (Briuglia *et al.*, 2015). It has been estimated that liposomes consisting of phosphatidylcholine can incorporate up to 50% w/w cholesterol (Sułkowski *et al.*, 2005). Therefore, the release of the liposomal drug (localized either in the aqueous core or in liposomal bilayer) was examined by preparing LUVs with various amounts of incorporated cholesterol (up to 25% w/w).

All the results for cholesterol-containing liposomes experiments are summarized in Figures 5.6-5.8. The *in vitro* diffusion studies were performed employing different diffusion barriers; a synthetic (regenerated cellulose) and a biomimetic (Permeapad®). Synthetic barriers (*e.g.* regenerated cellulose) are convenient and cost-effective and are often preferred in the early stage of drug development. However, the synthetic barriers do not include/consider the lipid effect which plays a major role in all biological tissues, including the nasal epithelium. For this reason, we decided to use the newly developed biomimetic Permeapad® barrier due to its higher similarity to the nasal epithelium (di Cagno *et al.*, 2015). Moreover, Permeapad® barriers have shown good reproducibility, stability at a wide range of p*H*, and tolerance to different surfactants and co-solvents (Bibi *et al.*, 2015, Bibi *et al.*, 2016). With a relatively long shelf life (1 year), the Permeapad® barriers are handy, requiring no hydration or cutting before use, which is often required for the synthetic diffusion barriers.

As a continuation of Paper II, we calculated the R_L values for the various formulations, diffusion barriers, and external environment as it can be seen in Figure 5.6. The R_L values were calculated by normalizing with the reference experiment involving free drug solution using the method established in Paper II.

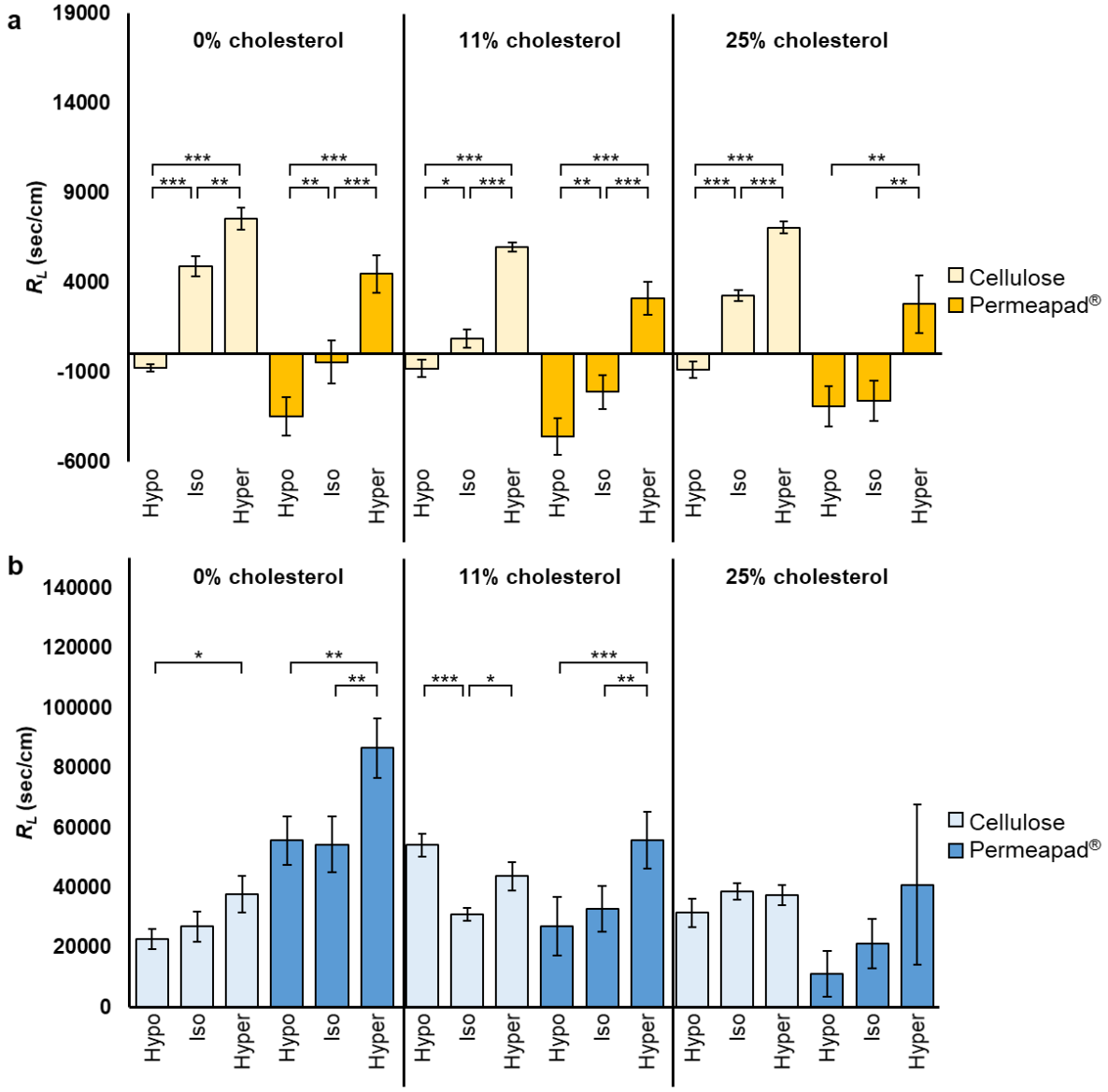

Figure 5.6: Resistance to drug transport through liposomal bilayer (R_L) of LUVs comprising a) caffeine, b) hydrocortisone, and various amounts of cholesterol (0-25% w/w). The regenerated cellulose and Permeapad® barriers were used as diffusion barriers. LUVs were exposed to isotonic, hypotonic, and hypertonic environment ($\Delta mOsm/kg$ of 0, -300, and 300 between LUVs formulation and external environment, respectively). Results represent the mean ± SD (n=3), and a statistically significant difference in R_L (*p≤0.050, **p≤0.010, ***p≤0.001) between the highlighted bars. Adapted from Wu *et al*., 2019a, with permission from Elsevier.

As illustrated in Figure 5.6, the external environment plays an essential role in R_L. The lowest R_L values were found in a hypotonic and the highest values for the hypertonic environment. Lower R_L indicates a higher release from the liposomes. Even though the liposomal size changes in the different environment were not carried out for these formulations, a clear indication of the relation between the release changes and the liposomal swelling and shrinking

in the hypotonic or hypertonic environment, respectively, can be seen. These findings are in great accordance with our earlier reports (Papers I-II), and important for the understanding of the release kinetics from liposomes. Interestingly, the R_L trends could be observed independently of the amount of incorporated cholesterol and the diffusion barrier used. However, the R_L with respect to the different environment fluctuated less for the formulations with 25% w/w cholesterol, or if the Permeapad® barrier was used. Other reports also confirm the negative effect the increasing levels of cholesterol have on the release from liposomes (Ali *et al.*, 2010, Allen and Cleland, 1980, Briuglia *et al.*, 2015). The differences between regenerated cellulose and Permeapad® barriers might be related to the different ion transport rate through the diffusion barriers. Previous observations of filling the acceptor compartment to a Franz cell with distilled water, and the donor compartment with PBS300 has shown ion diffusing across the regenerated cellulose barrier with almost twice as fast rate as compared to the rate across the Permeapad® barrier (43 vs 26 mOsm/kg hour, unpublished results).

We noticed in Paper II that the drug diffusion profiles showed deviation from linearity over time, especially for the LUVs exposed to osmotic stress. Ali *et al*. (2010) have also reported similar observations, where the drug release profile of several lipophilic drugs changed from zero order to first order profile for cholesterol-containing liposomes. In Paper II, we only used the linear part of the curve to calculate the R_L (the first 2.5 hours). This is a rather precarious assumption as relatively few data points are proving its linearity. Hence, a non-linear regression approximation was introduced in Paper III to elaborate on the collected diffusion data. The Korsmeyer-Peppas model was chosen as it could fit a larger portion of the collected experimental data (M_t/M_∞ up to 60%). Moreover, it can provide information related to the structural characteristics of the nanocarrier (transport constant, K), and the release mechanism from the nanocarrier (transport exponent, n).

The experimentally obtained diffusion data were fitted to the Korsmeyer-Peppas equation (Equation 1.10), and the predicted curve showed a good fit with the experimental data (R^2 ≥0.96). The slope of the fitted curve represents the K and describes the constant drug diffusion across a barrier. The higher K the higher release from liposomes can be assumed. In Figure 5.7, all the K obtained for the various LUVs formulations are represented.

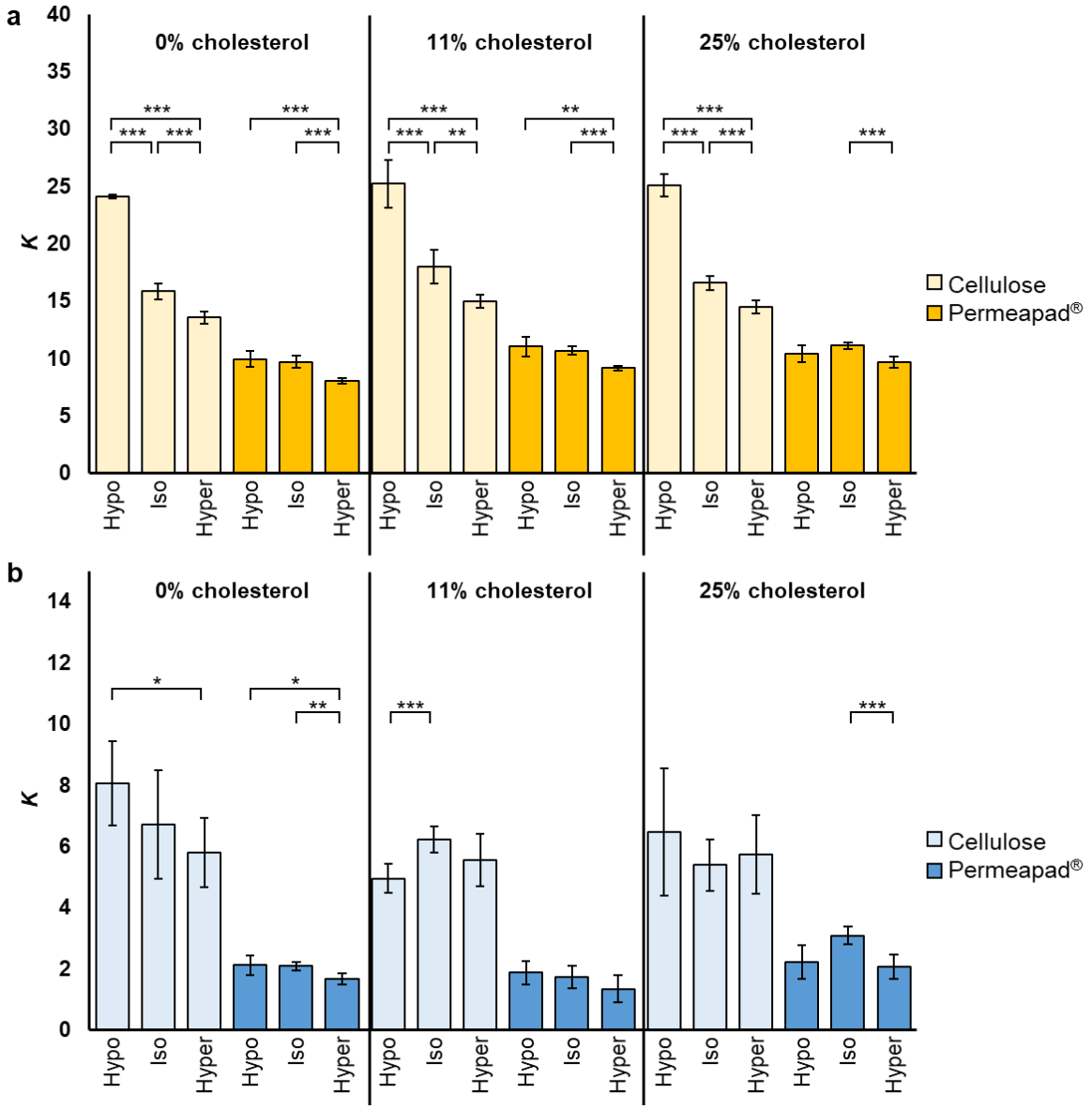

Figure 5.7: Transport constant (*K*) of LUVs comprising a) caffeine, b) hydrocortisone, and various amounts of cholesterol (0-25% w/w). The regenerated cellulose and Permeapad® barriers were used as diffusion barriers. LUVs were exposed to isotonic, hypotonic, and hypertonic environment (Δ*mOsm/kg* of 0, -300, and 300 between LUVs formulation and external environment, respectively). Results represent the mean ± SD (n=3), and a statistically significant difference in *K* (**p*≤0.050, ***p*≤0.010, ****p*≤0.001) between the highlighted bars. Adapted from Wu *et al.*, 2019a, with permission from Elsevier.

As seen in Figure 5.7, a trend starting from the highest *K* for hypotonic, middle for isotonic, and lowest for hypertonic environment could be observed. As higher *K* indicates a higher release, the trend of *K* should exhibit the opposite trend of R_L (Figure 5.6) if zero order data treatment was the optimal approach. As implied, differences were observed especially for the LUVs formulations containing cholesterol and when using Permeapad® as a diffusion barrier.

This indicates that the cumulative released drug was elapsing with time, and confirms the necessity of a non-linear regression model. Further, changes in *K* were generally smaller for Permeapad® in comparison to regenerated cellulose as a diffusion barrier. Regenerated cellulose barrier (due to its low retention to drug diffusion) might therewith be excellent in detecting formulation-related diffusional changes. On the other hand, it might not provide the best *in vitro/in vivo* correlations as the diffusion trends obtained using the regenerated cellulose barrier were rather different from results obtained using a more biomimetic barrier.

In regards to transport exponent *n,* the order of the curve describes the release mechanism from the liposomes. As a recap to the previous section (Section 1.7), if the drug release is only controlled by Fickian diffusion, a graph of cumulative percentage of released drug *vs* square root of time will originate a straight line ($n \leq 0.5$). On the other hand, no linear relationship gives $n > 0.5$ and indicates a non-Fickian-controlled diffusion mechanism (Costa and Sousa Lobo, 2001, Jain and Jain, 2016). In Figure 5.8, all the obtained *n* are represented. Generally, lower *n* values could be observed for the caffeine experiments (Figure 5.8a) in comparison to the hydrocortisone experiments (Figure 5.8b). This indicates that the release of caffeine was more indicating a Fickian-controlled diffusion mechanism in comparison to hydrocortisone, which might be explainable by different lipophilicity and solubility.

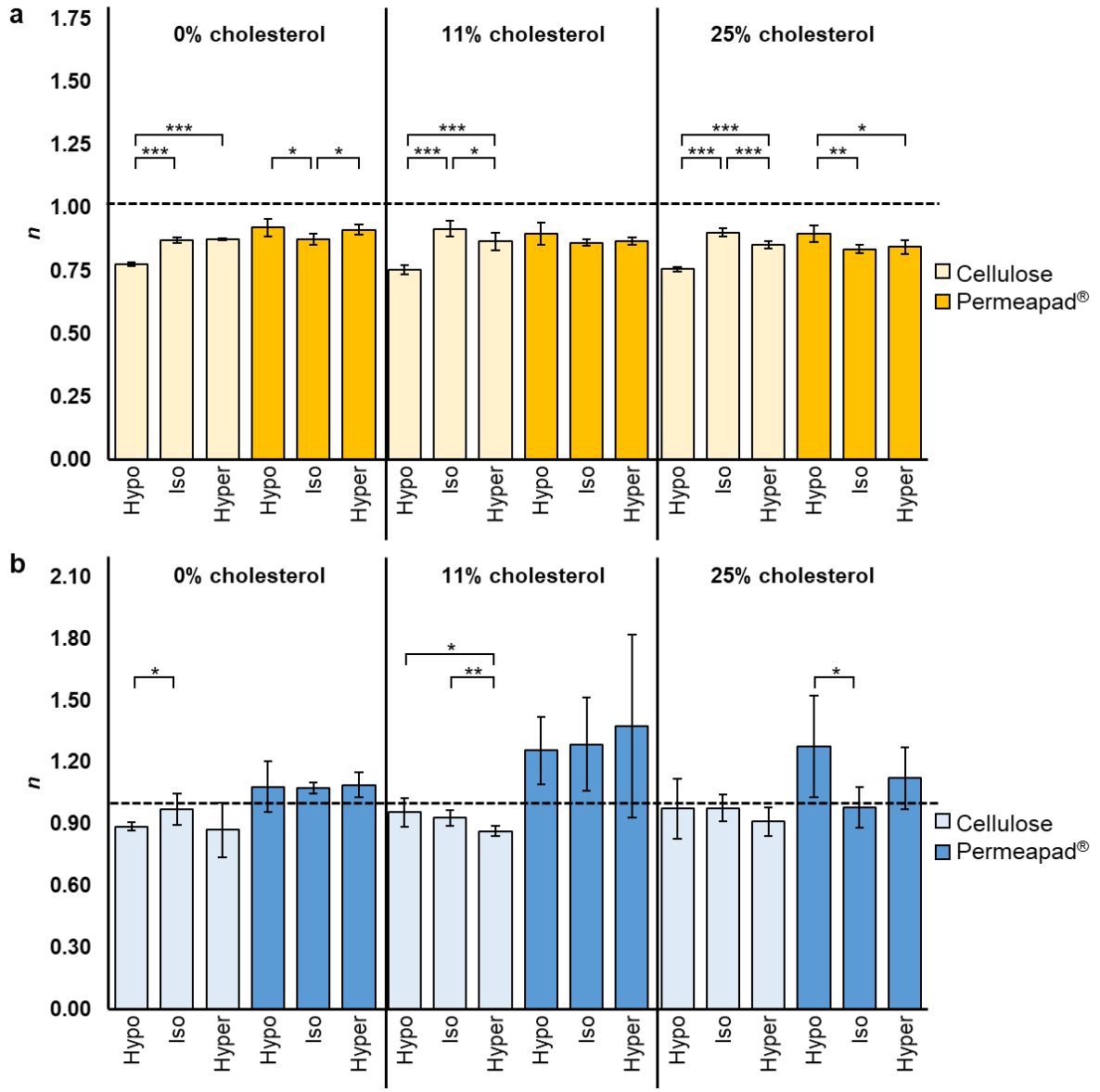

Figure 5.8: Transport exponent (*n*) of LUVs comprising a) caffeine, b) hydrocortisone, and various amounts of cholesterol (0-25% w/w). The regenerated cellulose and Permeapad® barriers were used as diffusion barriers. LUVs were exposed to isotonic, hypotonic, and hypertonic environment (Δ*mOsm/kg* of 0, -300, and 300 between LUVs formulation and external environment, respectively). Results represent the mean ± SD (n=3), and a statistically significant difference in *n* (**p*≤0.050, ***p*≤0.010, ****p*≤0.001) between the highlighted bars. Adapted from Wu *et al*., 2019a, with permission from Elsevier.

For the experiments carried out utilizing regenerated cellulose barrier, most of the obtained *n* was between 0.5 and 1, which describes both Fickian- and non-Fickian-controlled diffusion mechanisms (Figure 5.8). This was expected as the liposomal barrier (a boundary layer) may influence the passive diffusion across a diffusion barrier. The caffeine experiments involving liposomes incorporating various amounts of cholesterol showed the lowest *n* in hypotonic and higher *n* in isotonic/hypertonic environment. Lower *n* indicates a more Fickian-controlled drug

release. In other words, the boundary layer which the liposomal carrier originally represented was affecting less the liposomal release when liposomes became more stretched in a hypotonic environment. The *n* values for hydrocortisone-LUVs were generally higher than for the caffeine-LUVs, and the *n* varied less according to environmental changes. These results are in agreement with the drug's lipophilicity, and the findings in Papers I and II, as previously discussed. Another important finding was that *n* was the closest to 1 for the experiments carried out using Permeapad® barrier. Hydrocortisone-LUVs with 11 and 25% w/w cholesterol showed *n* greater than 1, indicating that the liposomes enhanced the drug transport across the diffusion barrier. The possible explanations could be the liposomes affinity for the Permeapad® barrier or the presence of cholesterol (Leite *et al.*, 2018). Compared to the LUVs formulations without cholesterol, the presence of cholesterol in liposomal bilayer seems to provide superior diffusion across the Permeapad® barrier.

In summary, these data demonstrate how the release from liposomes can be manipulated by careful tailoring of the lipid and cholesterol content of liposomes. Both linear and non-linear regression models should be used to achieve a more accurate interpretation of the diffusion data. The Korsmeyer-Peppas model was, in comparison to the zero order approach, more timesaving since it did not require reference experiments using drug solutions to normalize the data. Diffusion data for LUVs under osmotic stress fitted well with the Korsmeyer-Peppas model and gave equal to or better results than the currently accepted for the linear regression approximation. Different diffusion profiles could be observed when utilizing the regenerated cellulose and Permeapad® barriers. While the low retention diffusion barrier allows monitoring of release changes on the formulation level, the Permeapad® barrier recognized the lipid and retention effect, which are highly relevant considering the net transport across biological barriers. Due to the great differences in drug diffusion between the synthetic and biomimetic barrier, we wanted to introduce mucin to our experiments to further mimic the nasal environment and determine the influence of the mucin presence on the release from liposomes.

5.6 The effect of mucin on drug permeation (preliminary results)

In the first part of experiments involving mucin, we needed to select the mucin concentration to use in our experiments. In the literature, 1 mg/mL mucin dispersions have been used to study the binding of liposomes to mucin (porcine stomach type III) intended for nasal administration (Chen *et al.*, 2013, Qiang *et al.*, 2012). Using this as a reference, we screened mucin dispersions at concentrations ranging from 0.1 to 1.9 mg/mL. We found out that

1 mg/mL was the highest mucin concentration achievable without altering the original PBS tonicity. A representation of the measured osmolality and p*H* of PBS before and after the addition of mucin are shown in Table 5.2.

Table 5.2: Experimentally determined osmolality and p*H* of the prepared PBS and mucin dispersions used for the *in vitro* diffusion study with mucin present. Results represent mean ± SD (n≥2).

				PBS		Mucin dispersion (1 mg/mL)	
LUVs	**Cholesterol (% of lipid weight)**	**Osmolality of LUVs (mOsm/kg)[a]**	**PBS type**	**Osmolality (mOsm/kg)[a]**	**p*H*[a]**	**Osmolality (mOsm/kg)**	**p*H***
Caffeine	0	420 ± 11	Hypo	119 ± 10	7.5 ± 0.1	123 ± 19	7.5 ± 0.0
			Iso	418 ± 10	7.3 ± 0.0	422 ± 24	7.3 ± 0.0
			Hyper	718 ± 12	7.2 ± 0.0	727 ± 19	7.2 ± 0.0
	11	392 ± 12	Hypo	95 ± 16	7.6 ± 0.0	73 ± 3*	7.6 ± 0.0
			Iso	386 ± 5	7.3 ± 0.0	363 ± 3***	7.3 ± 0.0
			Hyper	693 ± 23	7.2 ± 0.0	663 ± 6*	7.2 ± 0.0
	25	388 ± 4	Hypo	88 ± 8	7.5 ± 0.0	90 ± 5	7.5 ± 0.0
			Iso	393 ± 4	7.3 ± 0.0	380 ± 5**	7.3 ± 0.0
			Hyper	692 ± 8	7.2 ± 0.0	650 ± 10***	7.2 ± 0.0
Ketoprofen	0	394 ± 7	Hypo	95 ± 5	7.6 ± 0.0	91 ± 5	7.5 ± 0.0
			Iso	394 ± 7	7.4 ± 0.0	390 ± 13	7.3 ± 0.0
			Hyper	695 ± 5	7.2 ± 0.0	675 ± 14*	7.1 ± 0.0
Hydro-cortisone	0	383 ± 5	Hypo	85 ± 5	7.6 ± 0.0	83 ± 8	7.6 ± 0.0
			Iso	385 ± 5	7.3 ± 0.0	359 ± 9***	7.3 ± 0.0
			Hyper	685 ± 5	7.2 ± 0.0	667 ± 17	7.2 ± 0.0
	11	405 ± 5	Hypo	105 ± 5	7.6 ± 0.0	105 ± 16	7.6 ± 0.0
			Iso	405 ± 5	7.3 ± 0.0	402 ± 13	7.4 ± 0.0
			Hyper	705 ± 5	7.2 ± 0.0	703 ± 15	7.2 ± 0.0
	25	383 ± 19	Hypo	86 ± 16	7.6 ± 0.0	85 ± 5	7.6 ± 0.0
			Iso	385 ± 16	7.3 ± 0.0	380 ± 11	7.4 ± 0.0
			Hyper	687 ± 15	7.2 ± 0.0	685 ± 5	7.2 ± 0.0

A statistically significant difference in osmolality (*p≤0.050, **p≤0.010, ***p≤0.001) between PBS before and after addition of mucin.

[a]Adapted from Wu *et al*. 2019a, with permission from Elsevier.

As demonstrated in Table 5.2, the osmolality of the PBS after the addition of mucin varied more, and, in some cases, caused a significant alteration of the PBS tonicity. These changes are rather hard to explain as the same batch of mucin was used during the whole study. The changes might be related to the biological origin of mucin, or possibility that mucin influence the readings of the osmometer. To limit mucin degradation upon storage, the mucin dispersions were always used within 7 days after original preparation.

Results and discussions

To understand the influence of mucin on drug diffusion across diffusion barriers, reference experiments were carried out similarly to those established in Papers II and III. The P_{app} of marker/drug solutions determined without the presence of mucin are already discussed in Section 5.3. To investigate mucin's effect on drug diffusion across the different diffusion barriers, we carried the diffusion study of drug solutions in the presence of mucin, and the results are summarized in Table 5.3.

Table 5.3: Apparent permeability coefficient of drug solutions in the presence of mucin ($P_{app}{}^{m}$). Results represent mean ± SD (n≥2).

		Absence of mucin	Presence of 0.4 mg/mL mucin		
Drug	**PBS**	**P_{app} (10^{-5} cm/sec)**	**$P_{app}{}^{m}$ (10^{-5} cm/sec)**	**Total permeated after 4 hours (%)**	**P_{app}-$P_{app}{}^{m}$ (10^{-5} cm/sec)**
Caffeine	65 [a]	6.18 ± 0.13[c]	5.78 ± 0.89	85.70 ± 18.78	-0.4
	65[b]	2.79 ± 0.14[c]	3.49 ± 0.11	35.79 ± 0.95	0.7
Ketoprofen	65 [a]	4.82 ± 2.48	4.43 ± 0.33	70.77 ± 17.88	-0.4
	65[b]	1.18 ± 1.98	1.32 ± 0.02	13.80 ± 0.81	0.1
Hydrocortisone	65 [a]	5.25 ± 0.59[c]	3.34 ± 0.80	52.03 ± 6.08	-1.9
	65[b]	1.12 ± 0.09[c]	1.18 ± 0.36	14.24 ± 3.23	0.1

[a]Regenerated cellulose barrier.

[b]Permeapad® barrier.

[c]P_{app} replotted from Table 5.1.

As highlighted in Table 5.3, the $P_{app}{}^{m}$ values determined in the presence of mucin were lower than the P_{app} values in the experiments utilizing the regenerated cellulose barrier as a diffusion barrier ($P_{app}{}^{m}<P_{app}$). The opposite trend was found when the Permeapad® barrier was used ($P_{app}{}^{m}>P_{app}$). These findings indicate that mucin plays a major role in the drug diffusion across barriers, and different diffusion trends can be observed based on the type of the diffusion barrier used. These data emphasize the importance of selecting the correct reference experiment, as small changes in the experimental set-up can result in large variations in P_{app} or $P_{app}{}^{m}$, and lead to misleading interpretations of the release from liposomes (Jain and Jain, 2016, Modi and Anderson, 2013). We decided to use the reciprocal function of $P_{app}{}^{m}$ to calculate the R_L for experiments performed in the presence of mucin. The obtained R_L values for caffeine- and hydrocortisone-LUVs are represented in Figure 5.9.

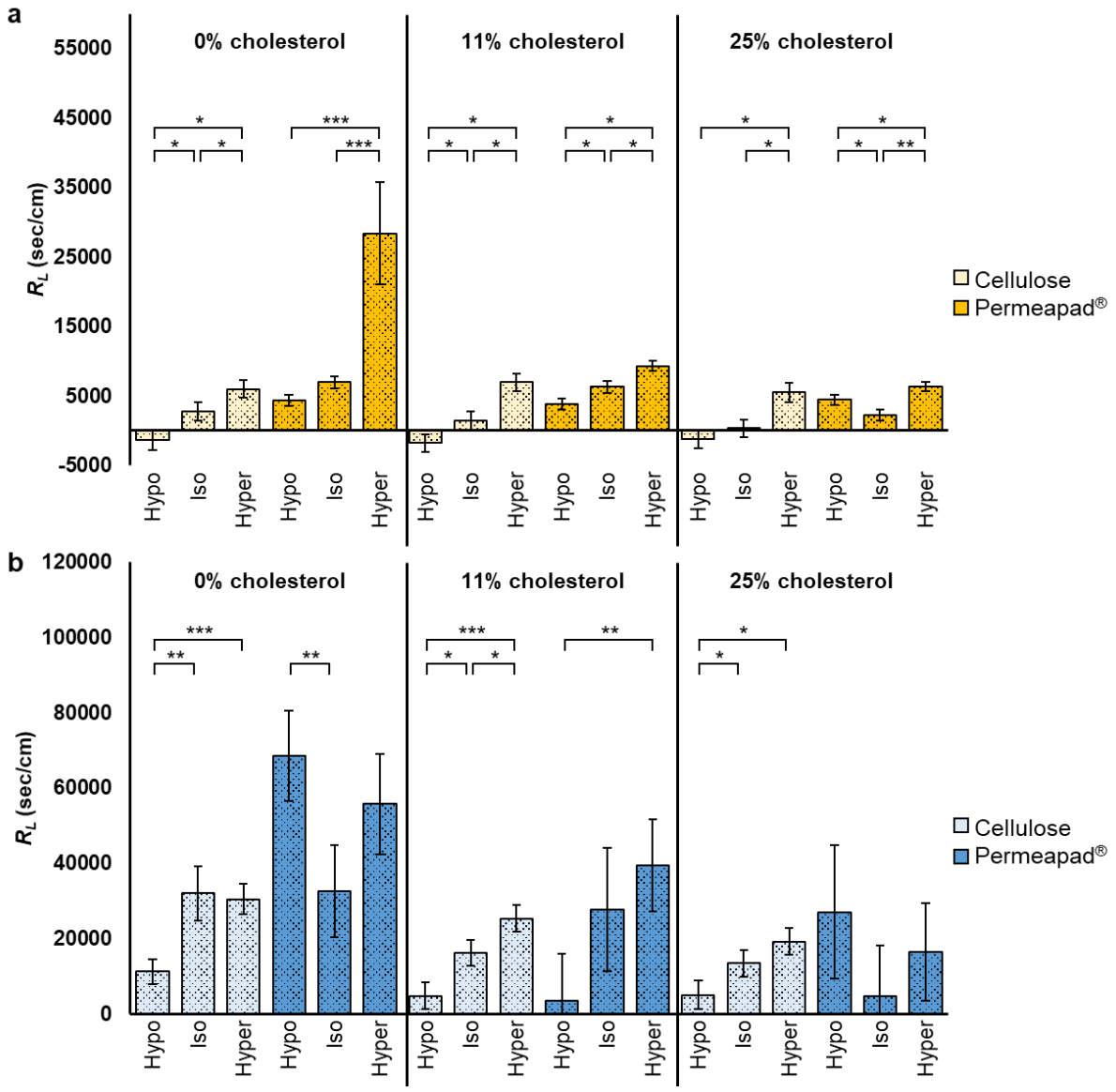

Figure 5.9: Resistance to drug transport through liposomal bilayer (R_L) of LUVs comprising a) caffeine, b) hydrocortisone, and various amounts of cholesterol (0-25% w/w). A total of 0.12 mg mucin was added on top of the regenerated cellulose and Permeapad® barriers. LUVs were exposed to isotonic, hypotonic, and hypertonic environment ($\Delta mOsm/kg$ of 0, -300, and 300 between LUVs formulation and external environment, respectively). Results represent the mean ± SD (n=3), and a statistically significant difference in R_L (*p≤0.050, **p≤0.010, ***p≤0.001) between the highlighted bars.

The R_L showed a similar trend to one observed for the experiments without mucin (Figure 5.6), indicating that the LUVs remained osmotically active even in the presence of mucin. The LUVs formulations without cholesterol showed the greatest differences in R_L values between the results obtained using regenerated cellulose and Permeapad® barriers, whereas the presence of cholesterol in liposomal bilayers reduced these differences. To ensure that the zero order approximation is applicable, we also applied the Korsmeyer-Peppas model to fit our

experimental data. The obtained *K* and *n* are represented in Figures 5.10 and 5.11, respectively.

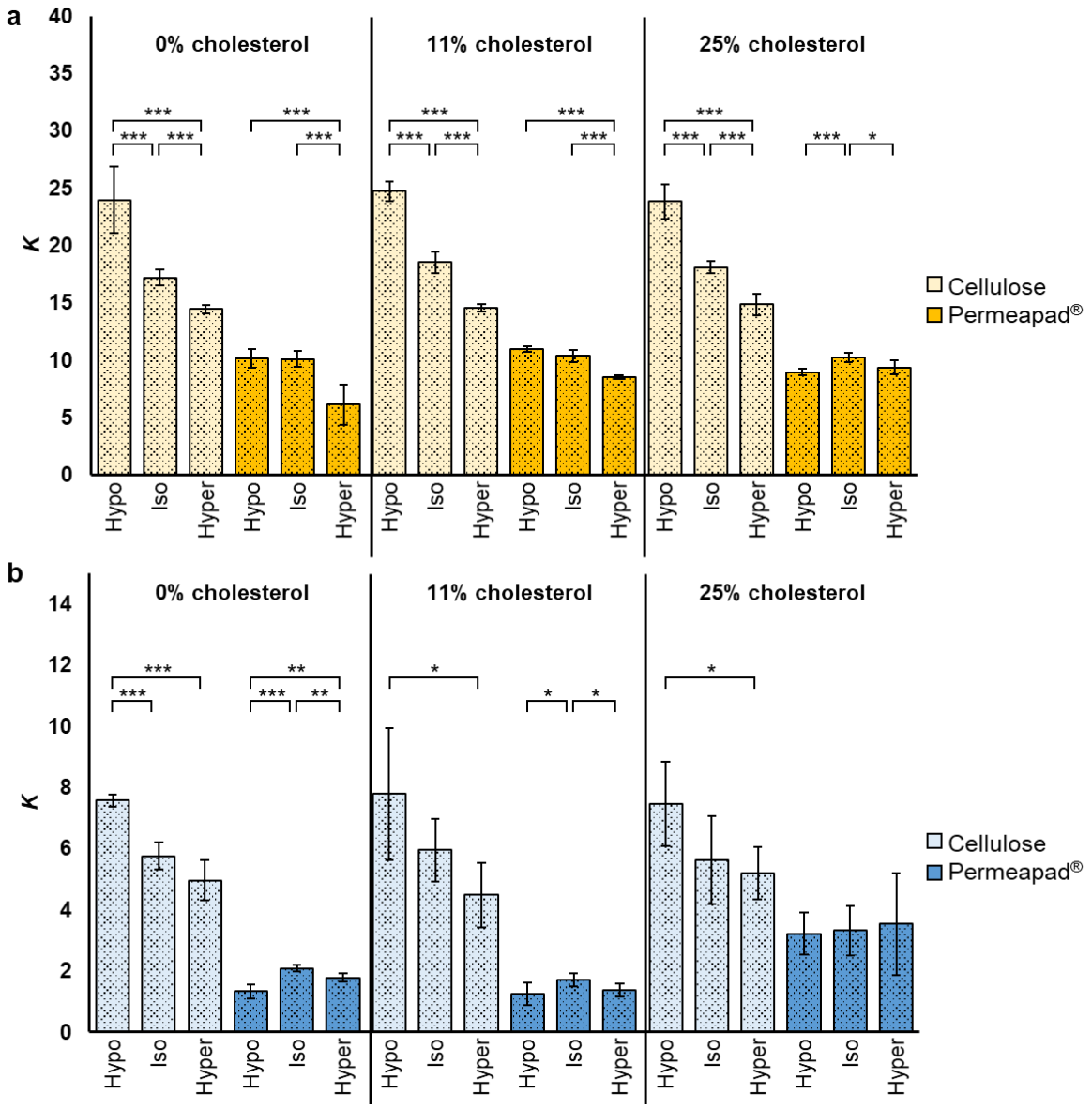

Figure 5.10: Transport constant (*K*) of LUVs comprising a) caffeine, b) hydrocortisone, and various amounts of cholesterol (0-25% w/w). A total of 0.12 mg mucin was added on top of the regenerated cellulose and Permeapad® barriers. LUVs were exposed to isotonic, hypotonic, and hypertonic environment (Δ*mOsm/kg* of 0, -300, and 300 between LUVs formulation and external environment, respectively). Results represent the mean ± SD (n=3), and a statistically significant difference in *K* (*$p \leq 0.050$, **$p \leq 0.010$, ***$p \leq 0.001$) between the highlighted bars.

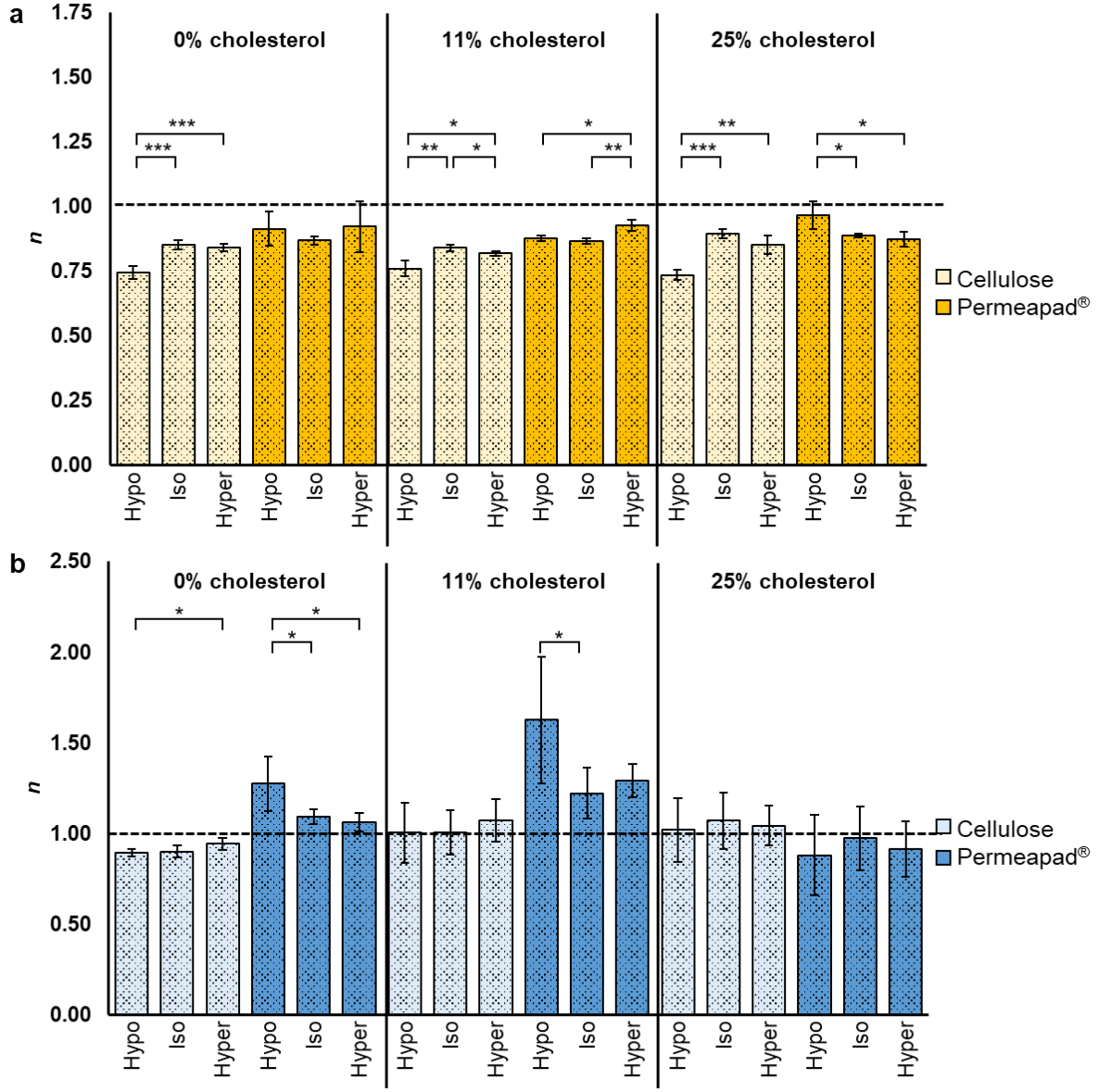

Figure 5.11: Transport exponent (*n*) of LUVs comprising a) caffeine, b) hydrocortisone, and various amounts of cholesterol (0-25% w/w). A total of 0.12 mg mucin was added on top of the regenerated cellulose and Permeapad® barriers. LUVs were exposed to isotonic, hypotonic, and hypertonic environment (Δ*mOsm/kg* of 0, -300, and 300 between LUVs formulation and external environment, respectively). Results represent the mean ± SD (n=3), and a statistically significant difference in *n* (**p*≤0.050, ***p*≤0.010, ****p*≤0.001) between the highlighted bars.

Again, the experimental data showed a good fit with the predicted curve (R^2 of 0.97-1.00). The *K* and *n* values obtained in the caffeine experiments were close to identical to the experiments carried out without the mucin (Figures 5.7-5.8). Hydrocortisone experiments showed decreasing *K* values starting from the hypotonic to hypertonic environment for experiments using the regenerated cellulose as a barrier. This trend was not as apparent for the experiments conducted in the absence of mucin. The results suggest that mucin might

enhance the LUVs' osmotic activity even when cholesterol was incorporated within liposomal bilayers. Permeapad® experiments indicated a relatively stable *K* for all environment highlighting that even though the release from liposomes alters due to tonicity perturbations, the net transport across a biomimetic barrier (and possibly biological barrier) are not much different. In retrospect, we should have carried the experiments with Permeapad® for a longer time (more than 4 hours) due to the barrier's inherent nature of expressing high retention to drug diffusion. The longer study would probably provide more apparent differences in the diffusion across the Permeapad® barrier over time. However, due to the awareness that nasal mucus renews every 20 min (Illum, 2003, Taherali *et al.*, 2018), we believed that experiments over a total of 4 hours were sufficient at this point in the project.

Considering the mucin concentrations used in this study, the mucin content was sufficient to cause drug diffusion hindrances because of electrostatic and hydrophobic interactions (Lock *et al.*, 2018, Murgia *et al.*, 2018). Mucin had generally little effect on the *n* of caffeine which seems to be explainable by caffeine's good permeability across cellulose and lipid barriers (di Cagno *et al.*, 2015, Flaten *et al.*, 2006). Due to caffeine's small molecular size (MW of 194.2 g/mol), the mucin was not an obstacle to diffusion. On the other hand, due to the larger molecular size and more lipophilic nature of hydrocortisone (MW of 362.5 g/mol), it was not surprising that the *n* of hydrocortisone was more affected. An increase in *n* can be explained by increased interaction between drug and mucin resulting in a stronger boundary layer, shifting the release mechanism away from a Fickian-controlled diffusion mechanism.

As both investigated drugs are neutral at p*H* 7.4, we also performed some preliminary study with ketoprofen. Ketoprofen is ionized at p*H*>4.5 (PubChem, 2019c), conferring to a negatively charged ketoprofen molecule at high p*H*. Due to the demanding manual work required to obtain these data, we have only been able to screen the ketoprofen-LUVs free of cholesterol. The R_L, *K*, and *n* are all summarized in Figure 1.12.

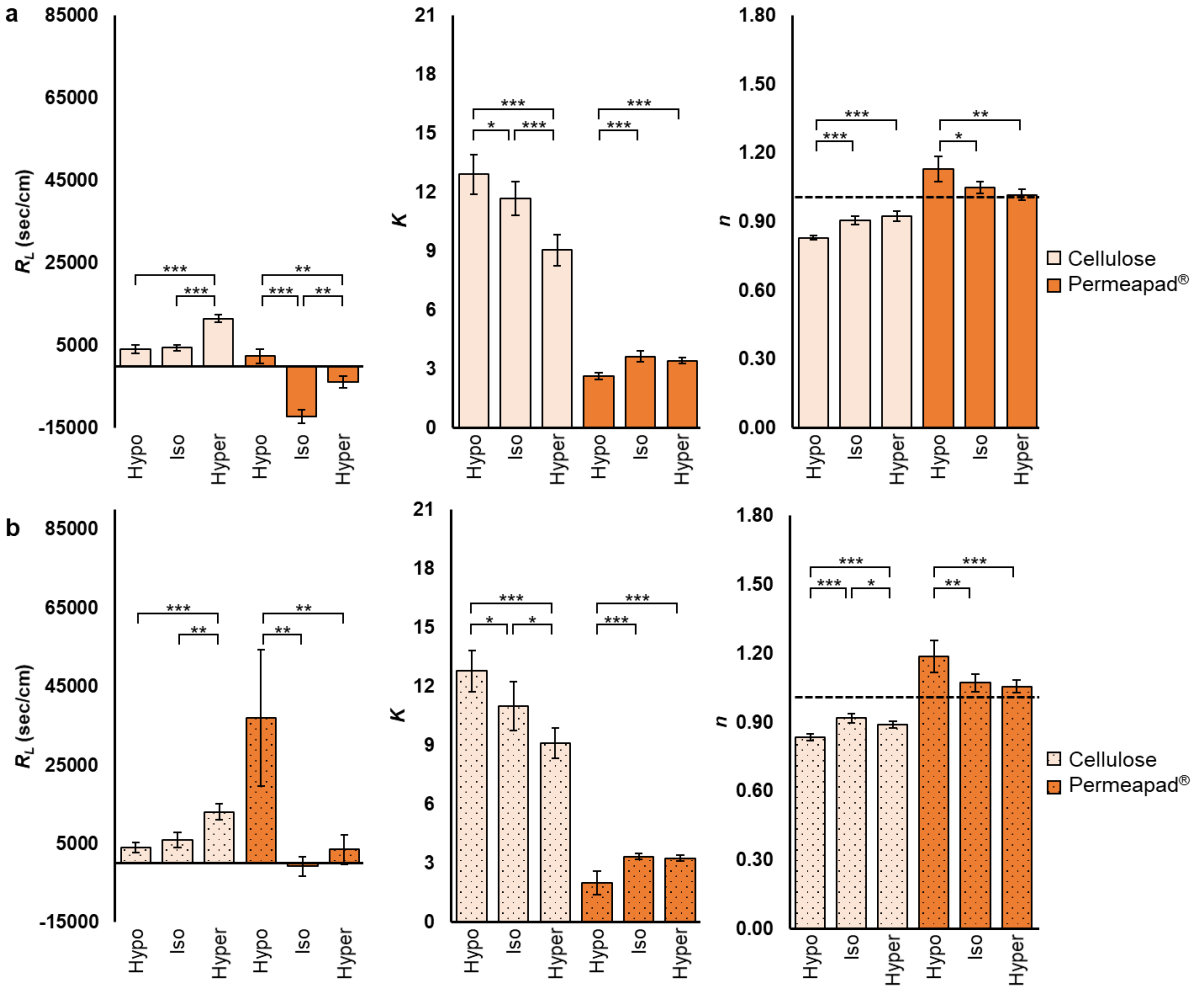

Figure 5.12: Resistance to drug transport through liposomal bilayer (R_L), transport constant (K), and transport exponent (n) of ketoprofen-LUVs (0% w/w cholesterol). Experiments were conducted with the a) absence and b) presence of mucin (a total of 0.12 mg mucin was added) on top of the regenerated cellulose and Permeapad® barriers. LUVs were exposed to isotonic, hypotonic, and hypertonic environment (Δ*mOsm/kg* of 0, -300, and 300 between LUVs formulation and external environment, respectively). Results represent the mean ± SD (n=3), and a statistically significant difference in n (*p≤0.050, **p≤0.010, ***p≤0.001) between the highlighted bars.

Considering Figure 1.12, if we first focus on the results obtained using regenerated cellulose as a diffusion barrier and starting from the hypotonic to the hypertonic environment, we can see that;

1) R_L increased (liposomal bilayer resists more to drug transport) which correlates with

2) K decreased (less drug diffuses across diffusion barrier), and

3) n increased (release mechanism from liposomes shifts towards non-Fickian diffusion).

This trend remained independently of the mucin absence (Figure 1.12a) or presence (Figure 1.12b) and indicated that both linear and non-linear regression can be used to interpret the diffusion data obtained using regenerated cellulose as a diffusion barrier.

On the other hand, the Permeapad® experiments were more complex. First, the highest R_L values were found in the hypotonic environment, in disagreement with the findings for caffeine- and hydrocortisone-LUVs (previously shown the lowest R_L values, Paper III). The difference in R_L between the isotonic and hypotonic environment could be as great as 37000 sec/cm. Second, the *K* showed a trend with increasing values going from the hypotonic to hypertonic environment, indicating that upon liposomal shrinkage, the release was enhanced (correlate with decreasing trend of *n*). The large deviations between the caffeine/hydrocortisone and ketoprofen results might be due to the drugs' charge. As previously described, caffeine and hydrocortisone are both neutral at experimental p*H*, whereas ketoprofen is negatively charged. Charge-related corruptions of the Brownian movement of drug molecules might play an essential role in the net drug transport across the different diffusion barriers (Newby *et al.*, 2018). To our surprise, the ketoprofen results did not differ regardless of the mucin presence. This might be due to the negative charge of both ketoprofen and mucin at experimental p*H* resulting in little mucin influence on the ketoprofen drug diffusion (Newby *et al.*, 2018, Taherali *et al.*, 2018). It is too preliminary to draw any conclusions, but it seemed that using the non-linear regression model to interpret the diffusion data might be a more appropriate model to use, whereas the linear regression model provided the worst fit when investigating release from swollen or shrunken ketoprofen-LUVs.

To summarize, the presence of mucin in the diffusion study did not change the osmotic activity of LUVs, and in some cases, it seemed to even contribute to the higher osmotic activity. In agreement with our previous reports (Paper III), the obtained R_L and *K* values showed that the drug release was enhanced when LUVs were exposed to a hypotonic environment, and the release decreased in the hypertonic environment for LUVs containing uncharged drugs. The presence of cholesterol in LUVs hampered their sensitivity to osmotic stress. For the negatively charged drug, ketoprofen, diffusion across the regenerated cellulose and Permeapad® barrier differed and showed different trends. When the net transport of ketoprofen changed in the different environment using the regenerated cellulose barrier, the net transport across Permeapad® barrier remained similar. The ketoprofen results might indicate that the osmotically active LUVs contribute to rather small diffusional changes across real biological barriers and that the drugs' lipophilicity and charge might be larger contributors to the net transport across lipid-containing barriers, especially in the presence of mucin. It would be,

therefore, highly relevant to verify the diffusion across Permeapad® barrier with more drugs before any conclusions can be made.

Furthermore, liposomal physical stability is a crucial factor that needs to be addressed during the liposomal drug formulation development. For this reason, we followed the formulation's stability upon storage.

5.7 Stability study (Paper III and preliminary results)

Liposomes developed to enter the market as pharmaceutical products must be stable during the storage period. The stability issue was beyond the scope of Papers I and II, but we started to follow the stability for caffeine- and hydrocortisone-LUVs in Paper III. In this section, the focus will also be given to our preliminary stability results obtained for the ketoprofen-LUVs (0% w/w cholesterol, Table 5.4) which was used in the experiments involving mucin.

Table 5.4: Characterization of LUVs dispersions during storage at 6 and 22°C over 65 days, respectively. Results represent mean ± SD (n=2).

Storage temperature	Day	Osmolality (mOsm/kg)	Size (nm)	PI	ZP (mV)	EE (%)
6°C	3	398 ± 15	291 ± 49	0.26 ± 0.03	-7.2 ± 0.5	33 ± 2
6°C	14	395 ± 17	266 ± 41	0.24 ± 0.02	-6.8 ± 0.4*	42 ± 2***
	35	385 ± 17	267 ± 40	0.23 ± 0.02	-7.0 ± 0.5	36 ± 1
	65	383 ± 21	253 ± 38	0.24 ± 0.02	-8.2 ± 0.7***	46 ± 3***
22°C	14	400 ± 12	258 ± 38	0.20 ± 0.02*	-9.1 ± 0.7***	39 ± 3**
	35	398 ± 15	288 ± 46	0.25 ± 0.03	-10.5 ± 1.3***	41 ± 2**
	65	390 ± 18	250 ± 34	0.20 ± 0.02*	-26.3 ± 13.4***	57 ± 9***

A statistically significant difference in means (* $p \leq 0.050$, ** $p \leq 0.010$, *** $p \leq 0.001$) when compared to day 3 measurements.

For the development of osmosis-controlled liposomes, it is crucial that the formulations maintain constant tonicity upon storage. Caffeine- and hydrocortisone-LUVs prepared in this study with various amounts of cholesterol incorporated (0-25% w/w, Paper III, results not shown), and ketoprofen-LUVs (0% w/w cholesterol, Table 5.4) all indicated stable osmolality upon storage at both conditions up to 65 days. This finding is highly relevant for further formulation development.

In terms of size, PI and EE, LUVs stored at 6°C were more stable than those stored at 22°C, as expected (Grit and Crommelin, 1993). Upon storage at lower temperatures, the lipid bilayer elasticity is suggested to decrease and contribute to more stable colloidal dispersions (Tayebi

et al., 2012). The addition of cholesterol within liposomes has also been suggested to reduce liposomal leakage due to an increase in the dense packing of the phospholipids (de Gier *et al.*, 1968). The stabilizing effect of cholesterol on ketoprofen-LUVs has not been confirmed yet, but as indicated in Table 5.4, the EE of ketoprofen-LUVs (free of cholesterol) varied significantly upon storage ($p<0.01$). Introducing cholesterol into the ketoprofen-LUVs might be beneficial to achieve more stable dispersions as suggested by the literature (Briuglia *et al.*, 2015, Grit and Crommelin, 1993).

Alterations in ZP values measured for ketoprofen-LUVs upon storage (Table 5.4) matched the results obtained for caffeine- and hydrocortisone-LUVs (Paper III). The more negative ZP obtained after storage might indicate liposomal membrane degradation which is commonly observed for the liposomes composed of phospholipids of natural origin (Li *et al.*, 2015). If the liposomal membrane is degraded, the visual perception of the liposomal dispersion might change. For this reason, pictures were taken of the different LUVs formulations after 65 days of storage. The pictures of caffeine- and hydrocortisone-LUVs are not included in this section as they have been extensively discussed in Paper III. Instead, the focus was on the preliminary formulations of ketoprofen-LUVs (see Figure 5.13).

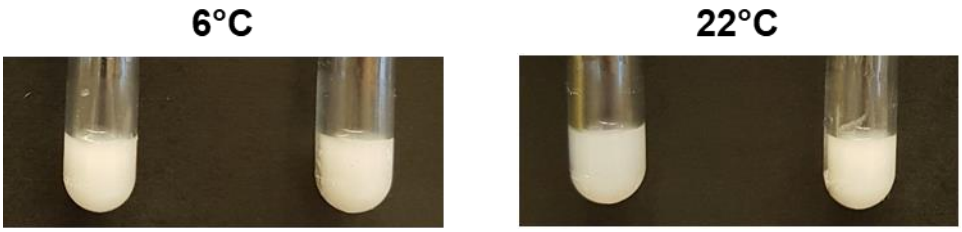

Figure 5.13: Photographs of ketoprofen-LUVs (0% w/w cholesterol) after 65 days of storage at 6 and 22°C. Each tube represents one replicate out of a total of two replicates (n=2).

As illustrated in Figure 5.13, all the dispersions appeared bright and white in colour. However, for one of the ketoprofen-LUVs stored at 22°C (left tube) were slightly more translucent indicating a possible change in liposomal integrity. Better pictures were not achievable with the camera available in the laboratory. However, these pictures might be of assistance to understand the stability issues regarding liposomal dispersions. It also suggests that with the use of better camera and more frequent monitoring might provide more extensive information about the liposomal integrity in the dispersion upon storage.

Considering all the variables measured, caffeine- and hydrocortisone-LUVs with 11% w/w cholesterol were found to be the most stable formulations in comparison to 0 and 25% w/w cholesterol. Even though the stabilizing effect of cholesterol was not investigated for

ketoprofen-LUVs, preliminary results suggest that cholesterol might be beneficial to reduce leakage from these LUVs. Collectively, the stability results obtained so far might be important for the further development of drug-loaded LUVs. More importantly, all the formulations exhibited stable tonicity at all storage conditions making them suitable for the development of osmotically active LUVs for nose-to-brain targeted drug delivery.

6 Conclusions

We have proven that liposomal release can be manipulated by tonicity environment and can be used for the development of nose-to-brain drug delivery systems. In detail, the following conclusions can be drawn:

Large unilamellar vesicles (LUVs) consisting of soy-phosphatidylcholine and cholesterol swelled and shrank when exposed to the hypotonic and hypertonic environment, respectively, proving their osmotic activity. The liposomal release of both hydrophilic and lipophilic compounds changed due to tonicity perturbations, particularly at tonicity difference greater than 300 mOsm/kg. The presence of cholesterol in the LUVs formulations reduced the LUVs' osmotic sensitivity, however, liposomes with 11% w/w cholesterol maintained a relatively good osmotic activity in addition to being the most stable formulations upon storage.

For better mimicking the nasal epithelium, the biomimetic Permeapad® was used as a diffusion barrier and compared to the standard regenerated cellulose barrier. The drug diffusion profiles were different through the two barrier types. We suggest that regenerated cellulose is sensitive to detect small diffusional changes on the liposome level, whereas the Permeapad® is superior in detecting the net transport across lipid-containing barriers. To additionally improve the experimental set-up, studies involving mucin were carried out to mimic the nasal environment. Mucin maintained the LUVs' osmotic activity and expressed low hindrance to drug diffusion.

Both zero order and Korsmeyer-Peppas models can be used to interpret the *in vitro* diffusion data of LUVs. Korsmeyer-Peppas model offered additional advantages, by being less time-consuming since reference experiments using drug solutions are omitted, which are compulsory for the zero order model. The Korsmeyer-Peppas model was found to be suitable to improve the diffusion data interpretation of LUVs experiencing osmotic stress.

In summary, these results provide a fundament and can be utilized for the further development of liposomal formulations for nose-to-brain drug delivery.

7 Future perspectives

We have carried out studies to prove that LUVs are osmotically active within tonicity that resemble nasal environment. In the future, it would be valuable to determine the liposomal lipid content and tailor the liposomal lipid composition.

Furthermore, more drugs with a wider range of physiochemical properties should be tested to validate our hypothesis. The use of Permeapad® barrier as a diffusion barrier and mucin to simulate the nasal environment are worth investigating in more detail. In particular, substituting the porcine mucin type III with more gel-forming mucin (*e.g.* MUC5B, MUC5AC, MUC2 found in the nasal cavity) and the use of different mucin concentrations should be thoroughly screened.

In this thesis, the stability of the formulations upon storage were evaluated in PBS at two different temperature conditions. The stability of the liposomes in nasal enzymes, plasma, and brain homogenate will be of equivalent importance to verify if the liposomes are susceptible for nose-to-brain drug administration.

We have only focused on LUVs of sizes between 200-400 nm, but the confirmation of the osmotic activity of smaller or larger liposomes might be of value as well. It would be also beneficial to investigate different surface modifications to increase the mucoadhesion and absorption through the nasal epithelium.

The ideal nasal formulation should not affect mucus secretion or cause morphologic changes on the nasal epithelium while serving its purpose of improving the mucoadhesion and absorption through the nasal epithelium. Further cell experiments, *in vivo* and clinical studies, are required to confirm the lack of formulation toxicity as a nasal irritant or inhibition of mucin secretion.

8 References

Abbott, N. J., Patabendige, A. A. K., Dolman, D. E. M., Yusof, S. R.*, et al.* **2010**. Structure and function of the blood–brain barrier. *Neurobiol Dis,* 37**,** 13-25.

Abuin, E. B., Campos, A. M., Lissi, E. A. & Disalvo, E. A. **1995**. Osmotic response of large unilamellar vesicles of phosphatidylcholine: Factors determining the rate of the process and the properties of the shrunken vesicles. *J Colloid Interface Sci,* 171**,** 406-412.

ADI - Alzheimer's Disease International. **2018**. World Alzheimer report 2018 [Report]. Available from: https://www.alz.co.uk/research/world-report-2018 [Accessed on: June 01, 2019].

Ahumada, M., Calderon, C., Alvarez, C., Lanio, M. E.*, et al.* **2015**. Response of unilamellar DPPC and DPPC:SM vesicles to hypo and hyper osmotic shocks: A comparison. *Chem Phys Lipids,* 188**,** 54-60.

Aisen, P. S. **2002**. The potential of anti-inflammatory drugs for the treatment of Alzheimer's disease. *Lancet Neurol,* 1**,** 279-284.

Akbarzadeh, A., Rezaei-Sadabady, R., Davaran, S., Joo, S. W.*, et al.* **2013**. Liposome: Classification, preparation, and applications. *Nanoscale Res Lett,* 8**,** 102-111.

Al Asmari, A. K., Ullah, Z., Tariq, M. & Fatani, A. **2016**. Preparation, characterization, and in vivo evaluation of intranasally administered liposomal formulation of donepezil. *Drug Des Devel Ther,* 10**,** 205-215.

Alam, M. I., Beg, S., Samad, A., Baboota, S.*, et al.* **2010**. Strategy for effective brain drug delivery. *Eur J Pharm Sci,* 40**,** 385-403.

Alam Shibly, S. U., Ghatak, C., Sayem Karal, M. A., Moniruzzaman, M.*, et al.* **2016**. Experimental estimation of membrane tension induced by osmotic pressure. *Biophys J,* 111**,** 2190-2201.

Ali, M. H., Kirby, D. J., Mohammed, A. R. & Perrie, Y. **2010**. Solubilisation of drugs within liposomal bilayers: Alternatives to cholesterol as a membrane stabilising agent. *J Pharm Pharmacol,* 62**,** 1646-1655.

Allen, T. M. & Cleland, L. G. **1980**. Serum-induced leakage of liposome contents. *Biochim Biophys Acta Biomembr,* 597**,** 418-426.

Alzheimer's Association. **2018**. 2018 Alzheimer's disease facts and figures [Report]. Available from: https://doi.org/10.1016/j.jalz.2018.02.001 [Accessed on: May 21, 2019].

Aniket, M., Vivek, D., Paraskevi, K., Tapani, V.*, et al.* **2014**. Cholesterol level affects surface charge of lipid membranes in saline solution. *Sci Rep,* 4**,** 1-5.

Arumugam, K., Subramanian, G. S., Mallayasamy, S. R., Averineni, R. K.*, et al.* **2008**. A study of rivastigmine liposomes for delivery into the brain through intranasal route. *Acta Pharm,* 58**,** 287-297.

Ashford, M. **2013**. Chapter 21: Assessment of biopharmaceutical properties. In: *Aulton's pharmaceutics: The design and manufacture of medicines.* 4th ed. Edinburgh: Churchill Livingstone, 334-354.

References

Aulton, M. E. **2013**. Chapter 3: Properties of solutions. In: *Aulton's pharmaceutics: The design and manufacture of medicines.* 4th ed. Edinburgh: Churchill Livingstone, 38-48.

Baker, R. W., Wijmans, J. G. & Huang, Y. **2010**. Permeability, permeance and selectivity: A preferred way of reporting pervaporation performance data. *J Memb Sci,* 348**,** 346-352.

Bangham, A. D., de Gier, J. & Greville, G. D. **1967**. Osmotic properties and water permeability of phospholipid liquid crystals. *Chem Phys Lipids,* 1**,** 225-246.

Bangham, A. D. & Horne, R. W. **1964**. Negative staining of phospholipids and their structural modification by surface-active agents as observed in the electron microscope. *J Mol Biol,* 688**,** 660-688.

Bangham, A. D., Standish, M. M. & Watkins, J. C. **1965**. Diffusion of univalent ions across the lamellae of swollen phospholipids. *J Mol Biol,* 13**,** 238-257.

Bansil, R. & Turner, B. S. **2018**. The biology of mucus: Composition, synthesis and organization. *Adv Drug Deliv Rev,* 124**,** 3-15.

Bartels, C., Franks, R., Rybar, S., Schierach, M.*, et al.* **2005**. The effect of feed ionic strength on salt passage through reverse osmosis membranes. *Desalination,* 184**,** 185-195.

Benavente, J. **1984**. A study of membrane potentials across a cellophane membrane for different electrolytes. *J Non-Equilib Thermodyn,* 9**,** 217-224.

Benet, L. Z., Broccatelli, F. & Oprea, T. I. **2011**. BDDCS applied to over 900 drugs. *AAPS J,* 13**,** 519-547.

Bibi, H. A., di Cagno, M., Holm, R. & Bauer-Brandl, A. **2015**. Permeapad™ for investigation of passive drug permeability: The effect of surfactants, co-solvents and simulated intestinal fluids (FaSSIF and FeSSIF). *Int J Pharm,* 493**,** 192-197.

Bibi, H. A., Holm, R. & Bauer-Brandl, A. **2016**. Use of Permeapad® for prediction of buccal absorption: A comparison to in vitro, ex vivo and in vivo method. *Eur J Pharm Sci,* 93**,** 399-404.

Biondi, A. C., Féliz, M. R. & Disalvo, E. A. **1991**. Surface changes induced by osmotic stress and its influence on the glycerol permeability in lipid bilayers. *Biochim Biophys Acta Biomembr,* 1069**,** 5-13.

Boroske, E., Elwenspoek, M. & Helfrich, W. **1981**. Osmotic shrinkage of giant egg-lecithin vesicles. *Biophys J,* 34**,** 95-109.

Bourganis, V., Kammona, O., Alexopoulos, A. & Kiparissides, C. **2018**. Recent advances in carrier mediated nose-to-brain delivery of pharmaceutics. *Eur J Pharm Biopharm,* 128**,** 337-362.

Brandl, M., Flaten, G. E., Bauer-Brandl, A. & Begley, T. P. **2007**. Passive diffusion across membranes. In: *Wiley encyclopedia of chemical biology.* Hoboken: John Wiley & Sons, Inc., 1-10.

Briuglia, M. L., Rotella, C., McFarlane, A. & Lamprou, D. A. **2015**. Influence of cholesterol on liposome stability and on in vitro drug release. *Drug Deliv Transl Res,* 5**,** 231-242.

Brodin, B., Steffansen, B. & Uhd Nielsen, C. **2010**. Chapter 3.2 Passive diffusion of drug substances: The concepts of flux and permeability. In: *Molecular biopharmaceutics:*

Aspects of drug characterisation, drug delivery and dosage form evaluation. London: Pharmaceutical Press, 135-152.

Bulbake, U., Doppalapudi, S., Kommineni, N. & Khan, W. **2017**. Liposomal formulations in clinical use: An updated review. *Pharmaceutics,* 9**,** 12.

Chabanon, M., Ho, J. C. S., Liedberg, B., Parikh, A. N.*, et al.* **2017**. Pulsatile lipid vesicles under osmotic stress. *Biophys J,* 112**,** 1682-1691.

Chen, L., Zhu, J., Li, Y., Lu, J.*, et al.* **2013**. Enhanced nasal mucosal delivery and immunogenicity of anti-caries DNA vaccine through incorporation of anionic liposomes in chitosan/DNA complexes. *PLoS One,* 8**,** e71953.

Choi, Y. H. & Han, H. K. **2018**. Nanomedicines: Current status and future perspectives in aspect of drug delivery and pharmacokinetics. *J Pharm Investig,* 48**,** 43-60.

Cipolla, D., Wu, H., Gonda, I., Eastman, S.*, et al.* **2014**. Modifying the release properties of liposomes toward personalized medicine. *J Pharm Sci,* 103**,** 1851-1862.

Claxton, A., Baker, L. D., Wilkinson, C. W., Trittschuh, E. H.*, et al.* **2013**. Sex and ApoE genotype differences in treatment response to two doses of intranasal insulin in adults with mild cognitive impairment or Alzheimer's disease. *J Alzheimers Dis,* 35**,** 789-797.

Coday, B. D., Luxbacher, T., Childress, A. E., Almaraz, N.*, et al.* **2015**. Indirect determination of zeta potential at high ionic strength: Specific application to semipermeable polymeric membranes. *J Memb Sci,* 478**,** 58-64.

Costa, P. & Sousa Lobo, J. M. **2001**. Modeling and comparison of dissolution profiles. *Eur J Pharm Sci,* 13**,** 123-133.

Craft, S., Claxton, A., Baker, L. D., Hanson, A. J.*, et al.* **2017**. Effects of regular and long-acting insulin on cognition and Alzheimer's disease biomarkers: A pilot clinical trial. *J Alzheimers Dis,* 57**,** 1325-1334.

Crowe, T. P., Greenlee, M. H. W., Kanthasamy, A. G. & Hsu, W. H. **2018**. Mechanism of intranasal drug delivery directly to the brain. *Life Sci,* 195**,** 44-52.

Danaei, M., Dehghankhold, M., Ataei, S., Hasanzadeh Davarani, F.*, et al.* **2018**. Impact of particle size and polydispersity index on the clinical applications of lipidic nanocarrier systems. *Pharmaceutics,* 10**,** 57.

Daneman, R. & Prat, A. **2015**. The blood-brain barrier. *Cold Spring Harb Perspect Biol,* 7**,** a020412.

Daraee, H., Etemadi, A., Kouhi, M., Alimirzalu, S.*, et al.* **2016**. Application of liposomes in medicine and drug delivery. *Artif Cells Nanomed Biotechnol,* 44**,** 381-391.

de Gier, J., Mandersloot, J. G. & Van Deenen, L. L. M. **1968**. Lipid composition and permeability of liposomes. *Biochim Biophys Acta Biomembr,* 150**,** 666-675.

di Cagno, M. & Bauer-Brandl, A. **2014**. Assembly for assessing drug permeability with adjustable biomimetic properties. WO 2016/078667 A1.

di Cagno, M., Bibi, H. A. & Bauer-Brandl, A. **2015**. New biomimetic barrier Permeapad™ for efficient investigation of passive permeability of drugs. *Eur J Pharm Sci,* 73**,** 29-34.

References

Djupesland, P. G., Messina, J. C. & Mahmoud, R. A. **2014**. The nasal approach to delivering treatment for brain diseases: An anatomic, physiologic, and delivery technology overview. *Ther deliv,* 5**,** 709-733.

Erdő, F., Bors, L. A., Farkas, D., Bajza, Á.*, et al.* **2018**. Evaluation of intranasal delivery route of drug administration for brain targeting. *Brain Res Bull,* 143**,** 155-170.

Ertel, A., Marangoni, A. G., Marsh, J., Hallett, F. R.*, et al.* **1993**. Mechanical properties of vesicles. I. Coordinated analysis of osmotic swelling and lysis. *Biophys J,* 64**,** 426-434.

Feigin, V. L., Nichols, E., Alam, T., Bannick, M. S.*, et al.* **2019**. Global, regional, and national burden of neurological disorders, 1990–2016: A systematic analysis for the global burden of disease study 2016. *Lancet Neurol,* 18**,** 459-480.

Felleskatalogen. **2019**. ATC-register Nervesystemet [Online]. Available from: https://www.felleskatalogen.no/medisin/atc-register/N [Accessed on: June 06, 2019].

FHI - Norwegian Institute of Public Health. **2019**. Life expectancy in Norway [Online]. Available from: https://www.fhi.no/en/op/hin/population/life-expectancy/ [Accessed on: May 21, 2019].

Flaten, G. E., Dhanikula, A. B., Luthman, K. & Brandl, M. **2006**. Drug permeability across a phospholipid vesicle based barrier: A novel approach for studying passive diffusion. *Eur J Pharm Sci,* 27**,** 80-90.

Fujiwara, K. & Yanagisawa, M. **2014**. Generation of giant unilamellar liposomes containing biomacromolecules at physiological intracellular concentrations using hypertonic conditions. *ACS Synth Biol,* 3**,** 870-874.

Gaisford, S. **2013**. Chapter 23: Pharmaceutical preformulation. In: *Aulton's pharmaceutics: The design and manufacture of medicines.* 4th ed. Edinburgh: Churchill Livingstone, 367-394.

Gänger, S. & Schindowski, K. **2018**. Tailoring formulations for intranasal nose-to-brain delivery: A review on architecture, physico-chemical characteristics and mucociliary clearance of the nasal olfactory mucosa. *Pharmaceutics,* 10**,** 116.

Ghadiri, M., Young, P. M. & Traini, D. **2019**. Strategies to enhance drug absorption via nasal and pulmonary routes. *Pharmaceutics,* 11**,** 113.

Gorlé, N., Van Cauwenberghe, C., Libert, C. & Vandenbroucke, R. E. **2016**. The effect of aging on brain barriers and the consequences for Alzheimer's disease development. *Mamm Genome,* 27**,** 407-420.

Grit, M. & Crommelin, D. J. A. **1993**. Chemical stability of liposomes: Implications for their physical stability. *Chem Phys Lipids,* 64**,** 3-18.

Groo, A.-C. & Lagarce, F. **2014**. Mucus models to evaluate nanomedicines for diffusion. *Drug Discov Today,* 19**,** 1097-1108.

Guo, X., Zheng, H., Guo, Y., Wang, Y.*, et al.* **2017**. Nasal delivery of nanoliposome-encapsulated ferric ammonium citrate can increase the iron content of rat brain. *J Nanobiotechnology,* 15**,** 42.

Hallett, F. R., Marsh, J., Nickel, B. G. & Wood, J. M. **1993**. Mechanical properties of vesicles II. A model for osmotic swelling and lysis. *Biophys J,* 64**,** 435-442.

References

Henney, H. R., Sperling, M. R., Rabinowicz, A. L., Bream, G.*, et al.* **2014**. Assessment of pharmacokinetics and tolerability of intranasal diazepam relative to rectal gel in healthy adults. *Epilepsy Res,* 108**,** 1204-1211.

Hoekman, J. D., Srivastava, P. & Ho, R. J. Y. **2014**. Aerosol-stable peptide-coated liposome nanoparticles: A proof-of-concept study with opioid fentanyl in enhancing analgesic effects and reducing plasma drug exposure. *J Pharm Sci,* 103**,** 2231-2239.

Homer, J. J., Dowley, A. C., Condon, L., El‐Jassar, P.*, et al.* **2000**. The effect of hypertonicity on nasal mucociliary clearance. *Clin Otolaryngol Allied Sci,* 25**,** 558-560.

Illum, L. **2003**. Nasal drug delivery - Possibilities, problems and solutions. *J Control Release,* 87**,** 187-198.

Immordino, M. L., Dosio, F. & Cattel, L. **2006**. Stealth liposomes: Review of the basic science, rationale, and clinical applications, existing and potential. *Int J Nanomed,* 1**,** 297-315.

INS - International Neuromodulation Society. **2013**. Central nervous system disease [Online]. Available from: https://www.neuromodulation.com/central-nervous-system-disease-definition [Accessed on: May 19, 2019].

Jackman, J. A., Choi, J. H., Zhdanov, V. P. & Cho, N. J. **2013**. Influence of osmotic pressure on adhesion of lipid vesicles to solid supports. *Langmuir,* 29**,** 11375-11384.

Jain, A. & Jain, S. K. **2016**. In vitro release model fitting of liposomes: An insight. *Chem Phys Lipids,* 201**,** 28-40.

Kälviäinen, R. **2015**. Intranasal therapies for acute seizures. *Epilepsy Behav,* 49**,** 303-306.

Kapoor, M., Lee, S. L. & Tyner, K. M. **2017**. Liposomal drug product development and quality: Current US experience and perspective. *AAPS J,* 19**,** 632-641.

Khan, A. R., Liu, M., Khan, M. W. & Zhai, G. **2017**. Progress in brain targeting drug delivery system by nasal route. *J Control Release,* 268**,** 364-389.

Khatri, K., Goyal, A. K., Gupta, P. N., Mishra, N.*, et al.* **2008**. Surface modified liposomes for nasal delivery of DNA vaccine. *Vaccine,* 26**,** 2225-2233.

Korsmeyer, R. W., Gurny, R., Doelker, E., Buri, P.*, et al.* **1983**. Mechanisms of solute release from porous hydrophilic polymers. *Int J Pharm,* 15**,** 25-35.

Lehrer, S. **2014**. Nasal NSAIDs for Alzheimer's disease. *Am J Alzheimers Dis Other Demen,* 29**,** 401-403.

Leite, N. B., Martins, D. B., Fazani, V. E., Vieira, M. R.*, et al.* **2018**. Cholesterol modulates curcumin partitioning and membrane effects. *Biochim Biophys Acta Biomembr,* 1860**,** 2320-2328.

Li, J., Wang, X., Zhang, T., Wang, C.*, et al.* **2015**. A review on phospholipids and their main applications in drug delivery systems. *Asian J Pharm Sci,* 10**,** 81-98.

Li, W., Zhou, Y., Zhao, N., Hao, B.*, et al.* **2012**. Pharmacokinetic behavior and efficiency of acetylcholinesterase inhibition in rat brain after intranasal administration of galanthamine hydrobromide loaded flexible liposomes. *Environ Toxicol Pharmacol,* 34**,** 272-279.

References

Li, X., Tsibouklis, J., Weng, T., Zhang, B.*, et al.* **2017**. Nano carriers for drug transport across the blood-brain barrier. *J Drug Target,* 25**,** 17-28.

Lock, J. Y., Carlson, T. L. & Carrier, R. L. **2018**. Mucus models to evaluate the diffusion of drugs and particles. *Adv Drug Deliv Rev,* 124**,** 34-49.

Maherani, B., Arab-Tehrany, E., Kheirolomoom, A., Geny, D.*, et al.* **2013**. Calcein release behavior from liposomal bilayer; Influence of physicochemical/mechanical/structural properties of lipids. *Biochimie,* 95**,** 2018-2033.

Marin, E., Briceño, M. I. & Caballero-George, C. **2013**. Critical evaluation of biodegradable polymers used in nanodrugs. *Int J Nanomed,* 8**,** 3071-3090.

McCaulley, M. E. & Grush, K. A. **2015**. Alzheimer's disease: Exploring the role of inflammation and implications for treatment. *Int J Alzheimers Dis,* 2015**,** 515248.

McIntosh, T. J. **1978**. The effect of cholesterol on the structure of phosphatidylcholine bilayers. *Biochim Biophys Acta Biomembr,* 513**,** 43-58.

Migliore, M. M., Ortiz, R., Dye, S., Campbell, R. B.*, et al.* **2014**. Neurotrophic and neuroprotective efficacy of intranasal GDNF in a rat model of Parkinson's disease. *Neuroscience,* 274**,** 11-23.

Milon, A., Lazrak, T., Albrecht, A. M., Wolff, G.*, et al.* **1986**. Osmotic swelling of unilamellar vesicles by the stopped-flow light scattering method. Influence of vesicle size, solute, temperature, cholesterol and three α,ω-dihydroxycarotenoids. *Biochim Biophys Acta Biomembr,* 859**,** 1-9.

Mistry, A., Stolnik, S. & Illum, L. **2009**. Nanoparticles for direct nose-to-brain delivery of drugs. *Int J Pharm,* 379**,** 146-157.

Modi, S. & Anderson, B. D. **2013**. Determination of drug release kinetics from nanoparticles: Overcoming pitfalls of the dynamic dialysis method. *Mol Pharm,* 10**,** 3076-3089.

Moscho, A., Orwar, O., Chiu, D. T., Modi, B. P.*, et al.* **1996**. Rapid preparation of giant unilamellar vesicles. *Proc Natl Acad Sci,* 93**,** 11443-11447.

Mui, B. L., Cullis, P. R., Evans, E. A. & Madden, T. D. **1993**. Osmotic properties of large unilamellar vesicles prepared by extrusion. *Biophys J,* 64**,** 443-453.

Murgia, X., Loretz, B., Hartwig, O., Hittinger, M.*, et al.* **2018**. The role of mucus on drug transport and its potential to affect therapeutic outcomes. *Adv Drug Deliv Rev,* 124**,** 82-97.

Narayan, R., Singh, M., Ranjan, O., Nayak, Y.*, et al.* **2016**. Development of risperidone liposomes for brain targeting through intranasal route. *Life Sci,* 163**,** 38-45.

Newby, J. M., Seim, I., Lysy, M., Ling, Y.*, et al.* **2018**. Technological strategies to estimate and control diffusive passage times through the mucus barrier in mucosal drug delivery. *Adv Drug Deliv Rev,* 124**,** 64-81.

Nii, T. & Ishii, F. **2005**. Encapsulation efficiency of water-soluble and insoluble drugs in liposomes prepared by the microencapsulation vesicle method. *Int J Pharm,* 298**,** 198-205.

References

Nisini, R., Poerio, N., Mariotti, S., De Santis, F.*, et al.* **2018**. The multirole of liposomes in therapy and prevention of infectious diseases. *Front Immunol,* 9**,** 155.

Noble, G. T., Stefanick, J. F., Ashley, J. D., Kiziltepe, T.*, et al.* **2014**. Ligand-targeted liposome design: Challenges and fundamental considerations. *Trends Biotechnol,* 32**,** 32-45.

Nothnagel, L. & Wacker, M. G. **2018**. How to measure release from nanosized carriers? *Eur J Pharm Sci,* 120**,** 199-211.

Oglecka, K., Rangamani, P., Liedberg, B., Kraut, R. S.*, et al.* **2014**. Oscillatory phase separation in giant lipid vesicles induced by transmembrane osmotic differentials. *Elife,* 3**,** e03695.

Ohno, M., Hamada, T., Takiguchi, K. & Homma, M. **2009**. Dynamic behavior of giant liposomes at desired osmotic pressures. *Langmuir,* 25**,** 11680-11685.

Ohwaki, T., Ando, H., Kakimoto, F., Uesugi, K.*, et al.* **1987**. Effects of dose, pH, and osmolarity on nasal absorption of secretin in rats II: Histological aspects of the nasal mucosa in relation to the absorption variation due to the effects of pH and osmolarity. *J Pharm Sci,* 76**,** 695-698.

Onatibia-Astibia, A., Franco, R. & Martinez-Pinilla, E. **2017**. Health benefits of methylxanthines in neurodegenerative diseases. *Mol Nutr Food Res,* 61**,** 1600670.

Patel, M. **2016**. Targeting oxidative stress in central nervous system disorders. *Trends Pharmacol Sci,* 37**,** 768-778.

Patel, M. M. & Patel, B. M. **2017**. Crossing the blood-brain barrier: Recent advances in drug delivery to the brain. *CNS Drugs,* 31**,** 109-133.

Paula, S., Volkov, A. G., Van Hoek, A. N., Haines, T. H.*, et al.* **1996**. Permeation of protons, potassium ions, and small polar molecules through phospholipid bilayers as a function of membrane thickness. *Biophys J,* 70**,** 339-348.

Pedersen, P. S., Braunstein, T. H., Jorgensen, A., Larsen, P. L.*, et al.* **2007**. Stimulation of aquaporin-5 and transepithelial water permeability in human airway epithelium by hyperosmotic stress. *Pflugers Arch,* 453**,** 777-785.

Phachonpai, W., Wattanathorn, J., Muchimapura, S., Tong-Un, T.*, et al.* **2010**. Neuroprotective effect of quercetin encapsulated liposomes: a novel therapeutic strategy against Alzheimer's disease. *Am J Appl Sci,* 7**,** 480-485.

Pittman, J. L., Schrum, K. F. & Gilman, S. D. **2001**. On-line monitoring of electroosmotic flow for capillary electrophoretic separations. *Analyst,* 126**,** 1240-1247.

Polozov, I. V., Anantharamaiah, G. M., Segrest, J. P. & Epand, R. M. **2001**. Osmotically induced membrane tension modulates membrane permeabilization by class L amphipathic helical peptides: Nucleation model of defect formation. *Biophys J,* 81**,** 949-959.

PubChem - National Center for Biotechnology Information Compound Database. **2019a**. Caffeine, CID=2519 [Online]. Available from: https://pubchem.ncbi.nlm.nih.gov/compound/2519 [Accessed on: May 14, 2019].

References

PubChem - National Center for Biotechnology Information Compound Database. **2019b**. Ibuprofen, CID=3672 [Online]. Available from: https://pubchem.ncbi.nlm.nih.gov/compound/3672 [Accessed on: May 14, 2019].

PubChem - National Center for Biotechnology Information Compound Database. **2019c**. Ketoprofen, CID=3825 [Online]. Available from: https://pubchem.ncbi.nlm.nih.gov/compound/3825 [Accessed on: May 14, 2019].

PubChem - National Center for Biotechnology Information Compound Database. **2019d**. Theophylline, CID=2153 [Online]. Available from: https://pubchem.ncbi.nlm.nih.gov/compound/2153 [Accessed on: May 14, 2019].

Pujara, C. P., Shao, Z., Duncan, M. R. & Mitra, A. K. **1995**. Effects of formulation variables on nasal epithelial cell integrity: Biochemical evaluations. *Int J Pharm,* 114**,** 197-203.

Qiang, F., Shin, H. J., Lee, B. J. & Han, H. K. **2012**. Enhanced systemic exposure of fexofenadine via the intranasal administration of chitosan-coated liposome. *Int J Pharm,* 430**,** 161-166.

Quraishi, M. S., Jones, N. S. & Mason, J. **1998**. The rheology of nasal mucus: A review. *Clin Otolaryngol Allied Sci,* 23**,** 403-413.

Reeves, J. P. & Dowben, R. M. **1970**. Water permeability of phospholipid vesicles. *J Membr Biol,* 3**,** 123-141.

Riaz, M. K., Riaz, M. A., Zhang, X., Lin, C.*, et al.* **2018**. Surface functionalization and targeting strategies of liposomes in solid tumor therapy: A review. *Int J Mol Sci,* 19**,** 195.

Ritger, P. L. & Peppas, N. A. **1987**. A simple equation for description of solute release I. Fickian and non-Fickian release from non-swellable devices in the form of slabs, spheres, cylinders or discs. *J Control Release,* 5**,** 23-36.

Ross, C., Taylor, M., Fullwood, N. & Allsop, D. **2018**. Liposome delivery systems for the treatment of Alzheimer's disease. *Int J Nanomed,* 13**,** 8507-8522.

Sabin, J., Prieto, G., Ruso, J. M., Hidalgo-Alvarez, R.*, et al.* **2006**. Size and stability of liposomes: A possible role of hydration and osmotic forces. *Eur Phys J E,* 20**,** 401-408.

Sahin-Yilmaz, A. & Naclerio, R. M. **2011**. Anatomy and physiology of the upper airway. *Proc Am Thorac Soc,* 8**,** 31-39.

Schmid, V., Kullmann, S., Gfrörer, W., Hund, V.*, et al.* **2018**. Safety of intranasal human insulin: A review. *Diabetes Obes Metab,* 20**,** 1563-1577.

Selvaraj, K., Gowthamarajan, K. & Karri, V. **2018**. Nose to brain transport pathways an overview: Potential of nanostructured lipid carriers in nose to brain targeting. *Artif Cells Nanomed Biotechnol,* 46**,** 2088-2095.

Sercombe, L., Veerati, T., Moheimani, F., Wu, S. Y.*, et al.* **2015**. Advances and challenges of liposome assisted drug delivery. *Front Pharmacol,* 6**,** 1-13.

Sharma, D., Ali, A. A. E. & Trivedi, L. R. **2018**. An updated review on: Liposomes as drug delivery system. *Pharmatutor,* 6**,** 50-62.

Sinko, P. J. & Singh, Y. **2011**. Chapter 5: Nonelectrolytes. In: *Martin's physical pharmacy and pharmaceutical sciences: Physical chemical and biopharmaceutical principles in the*

pharmaceutical sciences. 6th ed. Philadelphia: Wolters Kluwer/Lippincott Williams & Wilkins, 109-128.

Smith, M. C., Crist, R. M., Clogston, J. D. & McNeil, S. E. **2017**. Zeta potential: A case study of cationic, anionic, and neutral liposomes. *Anal Bioanal Chem,* 409**,** 5779-5787.

Solomon, D., Gupta, N., Mulla, N. S., Shukla, S.*, et al.* **2017**. Role of in vitro release methods in liposomal formulation development: Challenges and regulatory perspective. *AAPS J,* 19**,** 1669-1681.

Sonvico, F., Clementino, A., Buttini, F., Colombo, G.*, et al.* **2018**. Surface-modified nanocarriers for nose-to-brain delivery: From bioadhesion to targeting. *Pharmaceutics,* 10**,** 34.

Stein, P. C., di Cagno, M. & Bauer-Brandl, A. **2011**. A novel method for the investigation of liquid/liquid distribution coefficients and interface permeabilities applied to the water-octanol-drug system. *Pharm Res,* 28**,** 2140-2146.

Stephenson, J., Nutma, E., van der Valk, P. & Amor, S. **2018**. Inflammation in CNS neurodegenerative diseases. *Immunol,* 154**,** 204-219.

Sułkowski, W. W., Pentak, D., Nowak, K. & Sułkowska, A. **2005**. The influence of temperature, cholesterol content and pH on liposome stability. *J Mol Struc,* 744-747**,** 737-747.

Sun, S. T., Milon, A., Tanaka, T., Ourisson, G.*, et al.* **1986**. Osmotic swelling of unilamellar vesicles by the stopped-flow light scattering method. Elastic properties of vesicles. *Biochim Biophys Acta Biomembr,* 860**,** 525-530.

Taherali, F., Varum, F. & Basit, A. W. **2018**. A slippery slope: On the origin, role and physiology of mucus. *Adv Drug Deliv Rev,* 124**,** 16-33.

Tayebi, L., Vashaee, D. & Parikh, A. N. **2012**. Stability of uni- and multillamellar spherical vesicles. *Chemphyschem,* 13**,** 314-22.

Tollanes, M. C., Knudsen, A. K., Vollset, S. E., Kinge, J. M.*, et al.* **2018**. Sykdomsbyrden i Norge i 2016. *Tidsskr Nor Laegeforen,* 138**,** 1-12.

Toropainen, E., Ranta, V. P., Talvitie, A., Suhonen, P.*, et al.* **2001**. Culture model of human corneal epithelium for prediction of ocular drug absorption. *Invest Ophthalmol Vis Sci,* 42**,** 2942-2948.

Ventola, C. L. **2017**. Progress in nanomedicine: Approved and investigational nanodrugs. *Pharm Ther,* 42**,** 742-755.

Vieira, D. B. & Gamarra, L. F. **2016**. Getting into the brain: Liposome-based strategies for effective drug delivery across the blood-brain barrier. *Int J Nanomed,* 11**,** 5381-5414.

Vlieghe, P. & Khrestchatisky, M. **2013**. Medicinal chemistry based approaches and nanotechnology-based systems to improve CNS drug targeting and delivery. *Med Res Rev,* 33**,** 457-516.

Wacker, M. G. **2017**. Challenges in the drug release testing of next-generation nanomedicines - What do we know? *Mater Today Proc,* 4**,** 214-217.

References

Wattanathorn, J., Phachonpai, W., Priprem, A. & Suthiparinyanont, S. **2007**. Intranasal administration of quercetin liposome decreases anxiety-like behavior and increases spatial memory. *Am J Agric Biol Sci,* 2**,** 31-35.

WHO - World Health Organization. **2019**. Dementia [Online]. Available from: http://www.who.int/news-room/fact-sheets/detail/dementia [Accessed on: May 20, 2019].

Wolfram, J., Suri, K., Yang, Y., Shen, J.*, et al.* **2014**. Shrinkage of pegylated and non-pegylated liposomes in serum. *Colloids Surf B,* 114**,** 294-300.

Wong, H. L., Wu, X. Y. & Bendayan, R. **2012**. Nanotechnological advances for the delivery of CNS therapeutics. *Adv Drug Deliv Rev,* 64**,** 686-700.

Wu, C. Y. & Benet, L. Z. **2005**. Predicting drug disposition via application of BCS: Transport/absorption/elimination interplay and development of a biopharmaceutics drug disposition classification system. *Pharm Res,* 22**,** 11-23.

Wu, H., Hu, K. & Jiang, X. **2008**. From nose to brain: Understanding transport capacity and transport rate of drugs. *Expert Opin Drug Deliv,* 5**,** 1159-1168.

Wu, I. Y., Bala, S., Škalko-Basnet, N. & di Cagno, M. P. **2019a**. Interpreting non-linear drug diffusion data: Utilizing Korsmeyer-Peppas model to study drug release from liposomes. *Eur J Pharm Sci,* 138**,** 105026.

Wu, I. Y., Nikolaisen, T. E., Škalko-Basnet, N. & di Cagno, M. P. **2019b**. The hypotonic environmental changes affect liposomal formulations for nose-to-brain targeted drug delivery. *J Pharm Sci,* 108**,** 2570-2579.

Wu, I. Y., Škalko-Basnet, N. & di Cagno, M. P. **2017**. Influence of the environmental tonicity perturbations on the release of model compounds from large unilamellar vesicles (LUVs): A mechanistic investigation. *Colloids Surf B,* 157**,** 65-71.

Xu, X., Khan, M. A. & Burgess, D. J. **2012**. Predicting hydrophilic drug encapsulation inside unilamellar liposomes. *Int J Pharm,* 423**,** 410-418.

Yang, P. H., Zhu, J. X., Huang, Y. D., Zhang, X. Y.*, et al.* **2016**. Human basic fibroblast growth factor inhibits Tau phosphorylation via the PI3K/Akt-GSK3beta signaling pathway in a 6-hydroxydopamine-induced model of Parkinson's disease. *Neurodegener Dis,* 16**,** 357-369.

Yang, Z.-Z., Zhang, Y.-Q., Wang, Z.-Z., Wu, K.*, et al.* **2013**. Enhanced brain distribution and pharmacodynamics of rivastigmine by liposomes following intranasal administration. *Int J Pharm,* 452**,** 344-354.

Zhao, Y. Z., Lin, M., Lin, Q., Yang, W.*, et al.* **2016**. Intranasal delivery of bFGF with nanoliposomes enhances in vivo neuroprotection and neural injury recovery in a rodent stroke model. *J Control Release,* 224**,** 165-175.

Zheng, X., Shao, X., Zhang, C., Tan, Y.*, et al.* **2015**. Intranasal H102 peptide-loaded liposomes for brain delivery to treat Alzheimer's disease. *Pharm Res,* 32**,** 3837-3849.

Zhu, C., Jiang, L., Chen, T.-M. & Hwang, K.-K. **2002**. A comparative study of artificial membrane permeability assay for high throughput profiling of drug absorption potential. *Eur J Med Chem,* 37**,** 399-407.

Paper I

Colloids and Surfaces B: Biointerfaces 157 (2017) 65–71

Contents lists available at ScienceDirect

Colloids and Surfaces B: Biointerfaces

journal homepage: www.elsevier.com/locate/colsurfb

Protocols

Influence of the environmental tonicity perturbations on the release of model compounds from large unilamellar vesicles (LUVs): A mechanistic investigation

Iren Yeeling Wu, Nataša Škalko-Basnet, Massimiliano Pio di Cagno *

Drug Transport and Delivery Research Group, Department of Pharmacy, University of Tromsø The Arctic University of Norway, Universitetsvegen 57, 9037 Tromsø, Norway

ARTICLE INFO

Article history:
Received 24 March 2017
Received in revised form 19 May 2017
Accepted 24 May 2017
Available online 26 May 2017

Keywords:
LUVs
Calcein
Rhodamine
Osmotic pressure
Tonicity
Release kinetics

ABSTRACT

In this work, the influence of environmental tonicity perturbations on the size and release kinetics of model markers from liposomes (calcein and rhodamine) was investigated. Large unilamellar vesicles (LUVs) were prepared from a mixture composed of organic solvents containing dissolved phosphatidylcholine and phosphate buffered saline (PBS, pH 7.4). Organic phase was removed by rotary evaporation and the obtained liposomal dispersions were extruded to reduce the liposomal sizes to approx. 400 nm. The LUVs were exposed to PBS of different tonicity to induce water migration, and consequently, generate an osmotic pressure on the vesicle membranes. The markers release kinetics were studied by the dialysis method employing Franz diffusion cells. LUVs appeared to be more susceptible to the osmotic swelling than the shrinking and the size changes were significantly more pronounced for calcein-loaded LUVs in comparison to rhodamine-loaded LUVs. The calcein release from LUVs was highly affected by the water influx/efflux, whereas rhodamine release was less affected by the tonicity perturbations. Mechanistically, it appeared that hydrophilic molecules (calcein) followed the water flux, whereas lipophilic molecules (rhodamine) seemed to be more affected by the changes in LUVs size and consequent alteration of the tightness of the phospholipid bilayer (where the lipophilic marker was imbedded in). These results demonstrate that the different tonicity (within the inner core and external environment of vesicles) can enhance/hamper the diffusion of a marker from LUVs and that osmotically active liposomes could be used as a novel controlled drug delivery system.

1. Introduction

Since their first description [1], several applications of liposomes have been proposed, among which their use as drug carrier remains the most studied [2,3]. Currently, liposomes account for a significant portion of the market share in nanomedicine [4].

Liposomes are spherical vesicles consisting of single or multiple phospholipid bilayers surrounding an aqueous core. Due to the amphiphilic nature of the phospholipids, liposomes have the ability to entrap both hydrophilic and lipophilic compounds [5]. The liposomal membranes are semipermeable, allowing neutral, poorly polarized and small molecules to diffuse through it, whereas ions, highly polarized small molecules and large molecules will not [6,7].

Liposomes are appealing for drug delivery because of their ability to solubilize poorly water-soluble compounds [8,9]. Chemical entities confined into liposomes are less subjected to early degradation and elimination, and an improved drug distribution compared to non-entrapped drugs can be achieved [10]. The shape and properties of liposomes are similar to human cells, which provide good compatibility and low toxicity [10].

As all systems composed by semipermeable membranes, liposomes shape and size can be subjected to osmosis. Osmotic pressure (π) is defined as the force that applies on the surface of a semipermeable membrane when water diffuses through it due to the different tonicity between the solutions on the two side of the membrane. In these conditions, water diffuses from the side with lowest solute concentration (higher chemical potential) to the regions of highest solute concentration (lower chemical potential) until the equilibrium is reached [11]. If liposomes are exposed to a hypertonic environment, water effluxes through the phospholipid bilayer to the external environment, generating a positive

* Corresponding author.
E-mail address: massimiliano.p.cagno@uit.no (M.P. di Cagno).

http://dx.doi.org/10.1016/j.colsurfb.2017.05.062
0927-7765/

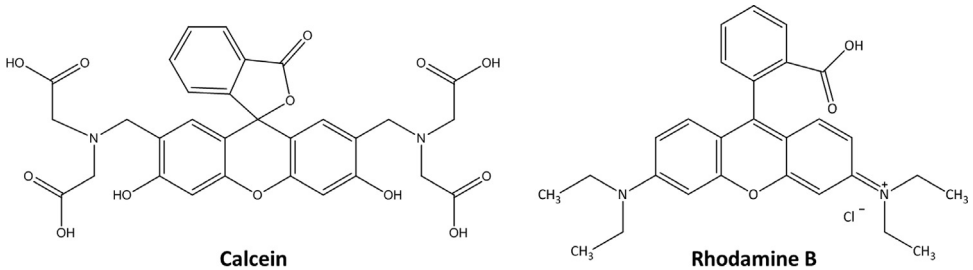

Fig. 1. Molecular structure, molecular weight (MW), partition coefficient (Log P) and dissociation constant (pKa) of calcein and rhodamine B.

osmotic pressure and induces size reduction [12]. On the contrary, when liposomes are exposed to a hypotonic environment, water influxes from the external environment, generating a negative osmotic pressure and size enlargement [12].

The influence of osmotic stress on lipid bilayers has been investigated on different vesicle models such as multilamellar vesicles [6,13] and large unilamellar vesicles (LUVs) [14–16]. Unilamellar vesicles are reported to be an appropriate model system to study the permeability properties associated with osmotic swelling or shrinking [6,13,15]. However, to the best of our knowledge, the influence that the environmental tonicity perturbations have on the release of chemical entities from liposomes has not been clarified yet.

The aim of this study was to verify if, and to which extent, the environmental tonicity perturbations affect the release kinetic of model substances from LUVs.

For this reason, two chemically different fluorescent markers (calcein and rhodamine) were used to study their release kinetics form LUVs. Fluorescent markers of different solubility were chosen to simplify the mechanistic study [17–20]. Calcein is a hydrophilic marker that can be entrapped in the inner aqueous core of LUVs [19], whereas rhodamine is a lipophilic marker (Log P of 2 [21]) that is expected to be incorporated in the phospholipid bilayer of LUVs.

2. Materials and methods

2.1. Materials

Calcein and rhodamine B (Fig. 1 reports the chemical structure of both markers together with meaningful physicochemical characteristics [19,21–23]), disodium hydrogen phosphate dihydrate ($Na_2HPO_4{\cdot}2H_2O$), sodium chloride (NaCl), sodium hydroxide (NaOH), sodium dihydrogen phosphate monohydrate ($NaH_2PO_4{\cdot}H_2O$), chloroform, ethanol (96%, v/v), methanol and non-ionic surfactant Triton X-100 were purchased from Sigma-Aldrich Chemie GmbH (Steinheim, Germany). Soy phosphatidylcholine S100 (SPC) was a gift from Lipoid GmbH (Ludwigshafen, Germany).

2.2. Phosphate buffer saline (PBS) preparation

A 74 mM phosphate buffer saline (PBS) solution (buffer 300) was prepared dissolving 22.5 g $NaH_2PO_4{\cdot}H_2O$ and 36.8 g $Na_2HPO_4{\cdot}2H_2O$ in 5 L distilled water. The pH was adjusted to 7.4 with NaOH, whereas NaCl was employed to fix tonicity at 300 mOsm (Semi-Micro Osmometer K-7400, Knauer, Berlin, Germany). Buffer 300 was diluted with distilled water in order to obtain two other solutions (buffer 190 and 65 respectively, Table 1) with lower tonicity.

Table 1
Measured tonicity, pH (mean ± SD, n = 3) and calculated concentrations of the different types of PBS used.

PBS type	Tonicity (mOsm)	pH	Concentration (mM)
300	300 ± 4	7.40 ± 0.02	74
190	187 ± 3	7.46 ± 0.02	44
65	65 ± 1	7.56 ± 0.01	15

2.3. Liposomes preparation

LUV dispersions were prepared following a method previously described [24,25] with some modifications. In brief, 0.2 mL methanol was mixed with 1 mL SPC/chloroform solution (200 mg/mL) in a 50 mL round bottom flask. PBS (10.5 mL) was gently added, and the organic phase was subsequently removed by rotary evaporation (40 °C, 40 rpm and 0.1 bar for 90 min) (Büchi R-124 rotavapor equipped with Büchi vacuum pump V-500 and Büchi B-480 water bath, Büchi Labortechnik AG, Flawil, Switzerland). All liposomal dispersions were prepared employing buffer 300 (74 mM, Table 1) or, alternatively, buffer 65 (15 mM, Table 1). LUV dispersions were spontaneously formed after the removal of organic phase. In order to reduce liposomal sizes, the dispersions were extruded at room temperature (23–25 °C) through polycarbonate membrane filters (lowest pore-size of 400 nm, Nuclepore Track-Etched Membranes, Whatman International Ltd., Buckinghamshire, UK). To load the fluorescent markers in liposomes, calcein was dissolved in PBS (obtaining a calcein solution with a concentration of 2 mM) prior to the lipid film reconstitution. Differently, for the preparation of rhodamine-LUVs, the marker was dissolved in chloroform together with lipid (rhodamine-lipid molar ratio approx. 1:1).

2.4. Size and surface potential analysis

Photon correlation spectroscopy (PCS) (Nicomp Submicron Particle Sizer 370, PSS Nicomp Particle Sizing Systems, California, USA) was employed for the determination of LUV size distributions after the extrusion. Samples were diluted to a count rate of 250–350 kHz at room temperature (23–25 °C), and each sample was measured in three parallels. Size changes of LUVs induced by tonicity perturbations were measured on the Zetasizer Nano Zen 2600 (Malvern, Worcestershire, UK). Samples were diluted 1/100 (v/v) with PBS 300 (or alternatively PBS 65) previous analysis and LUV dispersions were filtered to remove eventual impurities. Experiments were performed over a period of 70 min at 25 °C in duplicates (n = 2), and each sample was measured in three parallels. The ζ-potential (ZP) of LUVs was measured on the Zetasizer Nano Zen 2600 (Malvern). The respective dispersions were diluted 1/20 (v/v) with filtrated

deionized water. All analyses were performed at 25 °C in duplicates (n = 2), and each of the samples was measured in three parallels.

2.5. Entrapment efficiency determination

Entrapment efficiency of liposome dispersions was estimated combining a dialysis method to quantify the unentrapped marker concentration (C_{free}) with a sedimentation method for estimating the volume occupied and unoccupied by LUVs. For quantification of the unentrapped marker concentration (C_{free}), the method previously described by di Cagno and Luppi [9] was employed. In brief, lower compartment (donor) of a Franz diffusion cell (diffusional area of 0.64 cm^2, jacketed flat ground joint, PermeGear Ink, Hellertown, USA) was filled with liposomal dispersion (5 mL) whereas the upper compartment (acceptor) was filled with the corresponding PBS (1 mL). A cellulose hydrate membrane (Visking dialysis tubing MWCO 12–14 kDa, Medicell International Ltd., London, UK) was placed between the donor and acceptor compartment and used as dialysis barrier. The system was let to equilibrium at room temperature (23–25 °C) over a period of 48 h. The concentration of the marker in the acceptor compartment (C_{free}) was quantified by fluorescence spectroscopy (FLUOstar/POLARstar Galaxy fluorometer, BMG Technologies, Offenburg, Germany). Excitation and emission wavelengths were 485 nm and 520 nm for calcein, and 544 nm and 590 nm for rhodamine, respectively. In order to evaluate the ratio between liposome-occupied and liposome-unoccupied volume, non-dialyzed liposomal dispersions were centrifuged (30 min, 10 °C, 200 000*g*, Beckman model L8–70 M with SW 60 Ti rotor, Beckman Instruments, California, USA) in order to precipitate the vesicles. The liposome-unoccupied volume was used together with the unentrapped marker concentration (C_{free}) to quantify the total amount of unentrapped marker (i.e. not entrapped in liposomes, M_{free}). In order to determine the initial amount of marker in original dispersions (M_{tot}), LUVs were destroyed by adding 5% (v/v) triton/PBS solution for calcein-loaded liposomes or, alternatively, a 50% (v/v) methanol/PBS solution for the rhodamine-loaded LUVs, and the total concentration of marker in the liposomal dispersion (C_{tot}) was quantified by the fluorescence spectroscopy. The entrapment efficiency (EE) was calculated by using the following equation:

$$EE\,(\%) = \frac{M_{tot} - M_{free}}{M_{tot}} * 100 \quad (1)$$

where M_{tot} represents the total amount of marker in the original dispersion and M_{free} is the amount of unentrapped marker. Experiments were performed in duplicates (n = 2) and each sample was measured in four parallels.

2.6. In vitro release of fluorescent markers from LUVs

Release studies of fluorescent markers were performed by Franz diffusion cells (Standard 1.77 cm^2 diffusional area jacketed flat ground joint, PermeGear Ink, Hellertown, USA) equipped with cellulose hydrate membrane (Visking dialysis tubing MWCO 12–14 kDa, Medicell) in between donor and acceptor (12 mL) compartment. Experiments were performed at 35 °C (Julabo F12-ED, Julabo Laboratechnik, Seelback, Germany) in triplicates (n = 3) and each sample was analysed in two parallels. At time zero (t = 0 h, starting of the experiment) dialyzed liposomal dispersion (0.8 mL) was added to the donor compartment. As control experiments, solutions of calcein (2 mM) or rhodamine (1 mM) prepared in both buffer 300 and 65 were employed. Samplings (0.5 mL) were carried out at intervals of 1 h over a period of 8 h. Equal volumes of PBS were reintroduced into the acceptor compartment after withdrawal of samples in order to maintain sink condition. The concentration of the markers in the acceptor compartment was detected by fluorescence spectroscopy (see Section 2.5) and the cumulative amount of diffused marker over time calculated. The flux of each of the marker through the cellulose hydrate membrane (J) was determined by Eq. (2) [26]:

$$J = \frac{dm}{dt} * \frac{1}{A} \quad (2)$$

where dm/dt represents the variation of mass over time and A is the diffusional area. For each marker, the apparent permeability coefficient (P_{app}) was calculated using Eq. (3):

$$P_{app} = \frac{J}{C} \quad (3)$$

where C represents the initial marker concentration. P_{app} was calculated with either the total initial marker concentration in the dispersion (C_{tot}) or, alternatively, the initial concentration of the unentrapped marker (C_{free}, named $P^{ø}_{app}$) [9]. As control, the apparent permeability coefficient of the markers from solutions (P^{0}app) were measured.

Table 2
Types of PBS inside (inner core) and outside (external environment) LUVs and relative osmotic pressures generated. Relative osmotic pressures (π_{rel}) were calculated employing Eq. (1).

PBS type		π_{rel}
Inner core LUVs	External environment LUVs	(bar)
300	300	0
300	190	−3
300	65	−6
65	65	0
65	190	3
65	300	6

2.7. Osmotic pressure calculation

In this work, the relative osmotic pressure (π_{rel}) was estimated by Eq. (4) as:

$$\pi_{rel} = R * T * \left(Osm_{(out)} - Osm_{(in)}\right) \quad (4)$$

where R represents the gas constant, T is the absolute temperature and $Osm_{(out)} - Osm_{(in)}$ is the difference between the external and internal osmolality (units of mOsm) of LUVs. Based on Eq. (4), a positive relative osmotic pressure (Table 2) is produced when the water diffuses from the internal core of liposomes to the external environment ($Osm_{(in)} < Osm_{(out)}$) and negative relative osmotic pressure (Table 2) when the water diffuses from the external environment to the internal core ($Osm_{(in)} > Osm_{(out)}$) [12].

2.8. Statistical evaluation

Student's *t*-test was performed to evaluate a significance in the collected data. A p value ≤ 0.05 was considered as significantly different.

3. Results

3.1. LUV dispersions characterization

The relevant characteristics of the different LUV dispersions prepared are summarized in Table 3. Liposomal size distributions varied between the different types of dispersions prepared. Empty LUVs show similar size distributions when prepared in different PBS, whereas calcein and rhodamine-LUVs expressed differences in size distributions. For both calcein- and rhodamine-loaded LUVs, tonicity of the PBS seemed to have a significant effect ($p < 0.05$) on liposome sizes. Moreover, the PBS composition appeared to have a

Table 3
Size, polydispersity index (PI), ζ-potential (ZP) and entrapment efficiency (EE) of LUVs prepared in different types of PBS. Results are reported as mean ± SD.

Marker	Dispersing PBS type	Size (nm)	PI	ZP (mV)	EE (%)
	0	309 ± 20	0.10 ± 0.01	−20.4 ± 0.8	–
	65	327 ± 52	0.32 ± 0.09	–	–
	300	393 ± 92	0.33 ± 0.04	−12.0 ± 1.6	–
Calcein	65	649 ± 8	0.44 ± 0.04	−2.8 ± 0.4	41 ± 5.3
	300	449 ± 20	0.30 ± 0.02	−0.5 ± 0.2	43 ± 0.6
Rhodamine	65	386 ± 8	0.15 ± 0.00	−16.7 ± 0.4	85 ± 0.6
	300	762 ± 104	0.42 ± 0.06	−8.6 ± 0.3	89 ± 0.7

Table 4
Apparent permeability coefficients (P^0_{app}) through cellulose hydrate membrane of calcein and rhodamine measured from two different PBS type solutions. Experiments were conducted at neutral pH and the results are reported as mean ± SD (n = 3).

	P^0_{app} (10^{-5} cm/sec)	
PBS type	Calcein	Rhodamine
300	0.90 ± 0.07	1.61 ± 0.11
65	0.68 ± 0.06	1.55 ± 0.06

great impact on the repulsive electrokinetic potential (ZP) in all dispersions. Specifically, empty LUVs and rhodamine-LUVs appeared to preserve the partial negative potentials at tested tonicity (buffer 65 and 300), whereas calcein-LUVs surface potentials remained almost neutral. The overall entrapment efficiency were approx. 2-fold higher for rhodamine in comparison to calcein (Table 3).

3.2. Effect of the dispersing media tonicity on liposomal size distributions

The changes in size distributions of LUV dispersions after their exposure to PBS with varied tonicity are reported in Fig. 2. As a control, LUV size distributions in the isotonic environment are also reported (white symbols). For empty LUVs prepared in buffer 300 (Fig. 2A, upper line), a significant increase in size over time was observed when LUVs were exposed to the hypotonic environment (buffer 65) in comparison to the isotonic environment. In hypertonic environment (Fig. 2A, lower line), no significant differences were detected. For calcein-loaded LUVs, size enlargement was measured for both LUV dispersions (buffer 300 and 65 respectively) after the exposure to a dispersing medium of different tonicity (buffer 65 and 300 respectively, Fig. 2B). For rhodamine-LUVs (both buffer 300 and 65), no significant changes in vesicle sizes were observed after exposure to the hypertonic or hypotonic environment (buffer 65 and 300 respectively, Fig. 2C) in comparison to the respective isotonic environment (white symbols).

3.3. In vitro release study

As it can be seen in Table 4, rhodamine (in solution) exhibited a higher apparent permeability coefficient in comparison to calcein (in solution). Interestingly, the tonicity of the PBS had a strong influence on the calcein permeability. In buffer 300, the apparent permeability of calcein was approx. 24% higher than in buffer 65 (level of significance). For rhodamine, a similar trend was observed. Dialysis method is a common method used to estimate the kinetics of drug release from nanocarriers [27]. This method is based on the assumptions that the accumulation of the drug in the sink receiver (i.e. acceptor chamber of Franz cell) is directly proportional to the kinetics of drug release from the carrier. The relationship between the flux of markers through cellulose hydrate membrane and the calculated relative osmotic pressure is shown in Fig. 3. As it can be seen, calcein flux through cellulose membrane was highly influenced by the PBS in which the calcein-LUV dispersions were prepared (same trend as for the calcein in solutions) and by the relative osmotic pressure that was generated when LUVs were dispersed in non-isotonic dispersing medium. When calcein-LUVs were prepared in buffer 300, the flux of calcein through semipermeable membrane was significantly ($p < 0.05$) higher (approx. 44%) in comparison to buffer 65 (Fig. 3A). Interestingly, the flux of calcein through the cellulose membrane decreased (Fig. 3A, light-grey columns) when influx of water molecules increased (i.e. negative osmotic pressures). On the contrary, when a positive osmotic pressure was applied (i.e. efflux of water molecules from LUVs), a significant increase in the calcein flux was observed (Fig. 3A, dark-grey columns). Interestingly, the flux of lipophilic marker (rhodamine) through the cellulose hydrate membrane seemed to be less affected by the differences in the PBS tonicity and osmotic pressures generated on the LUV membranes (Fig. 3B). A significant ($p < 0.05$) decrease in rhodamine flux through cellulose hydrate membrane was observed only when a positive osmotic pressure (i.e. efflux of water molecules) applied. These changes were however minimal in comparison to the changes found for calcein. The normalized fluxes over the initial concentration of the markers in the LUV dispersions (i.e. apparent permeability coefficients) are reported in Table 5. For calcein, both estimated values of permeability coefficients (P_{app} and $P^{ø}_{app}$) were quite comparable to the P^0_{app} (calcein in solution, Table 4). For rhodamine, $P^{ø}_{app}$ (i.e. calculated using the unentrapped marker concentration) was in the same order of magnitude as reference values (P^0app, Table 4) whereas, the P_{app} values (i.e. calculated using the total initial concentration of rhodamine) were 5-fold lower in comparison to P^0_{app} (Table 4).

4. Discussion

Photon correlation spectroscopy is a common method employed for analysing liposomal size [28,29]. Some of the LUV dispersions loaded with marker remain unexpectedly large after the extrusion through 400 nm pore size filter (Table 3). This could be due to the aggregation that often affects the colloidal dispersions, and even more when the dispersed particles own neutral surface potentials [30]. Liposomal aggregation is the result of an interplay between the van der Waals forces (attractive) and repulsive electrokinetic potential [16,31,32]. With increasing electrolyte concentration, the changes in the electrostatic repulsion of liposomes can be estimated by the direct determination of ζ-potential (ZP) of liposomes [16,33]. In this study, a decreased ZP seemed to induce aggregation for rhodamine-LUVs, whereas calcein-LUVs exhibited a different trend (Table 3), probably due to the different physicochemical characteristics of the markers (Fig. 1).

An expected lower ZP (Table 3) was observed for LUV dispersions prepared in buffer 300 in comparison to buffer 65, probably due to the ion shell formation [16,33]. Rhodamine-loaded and empty LUVs expressed a negative ZP at investigated tonicities (Table 3). Since rhodamine is lipophilic (Log P of 2) [21] and zwitterionic at neutral pH [34], it is reasonable to think that this compound is imbedded into the lipid-bilayer, producing limited effects on the surface potential of liposomes. Differently, the ZP of calcein-LUVs was almost neutral at investigated tonicities, implicating that highly hydrophilic (Log P of −4 [19]) and highly polarized marker (negatively charged at neutral pH, pKa of 1.8) [22] might contribute somehow to strengthening of the ion shell surrounding LUVs.

The entrapment efficiency (EE) of the markers into LUVs was determined by standard centrifugation method and was 13% for calcein and 79% for rhodamine, respectively. These results were in accordance with the literature for rhodamine (and lipophilic compounds in general) [35], whereas, for calcein they were rather

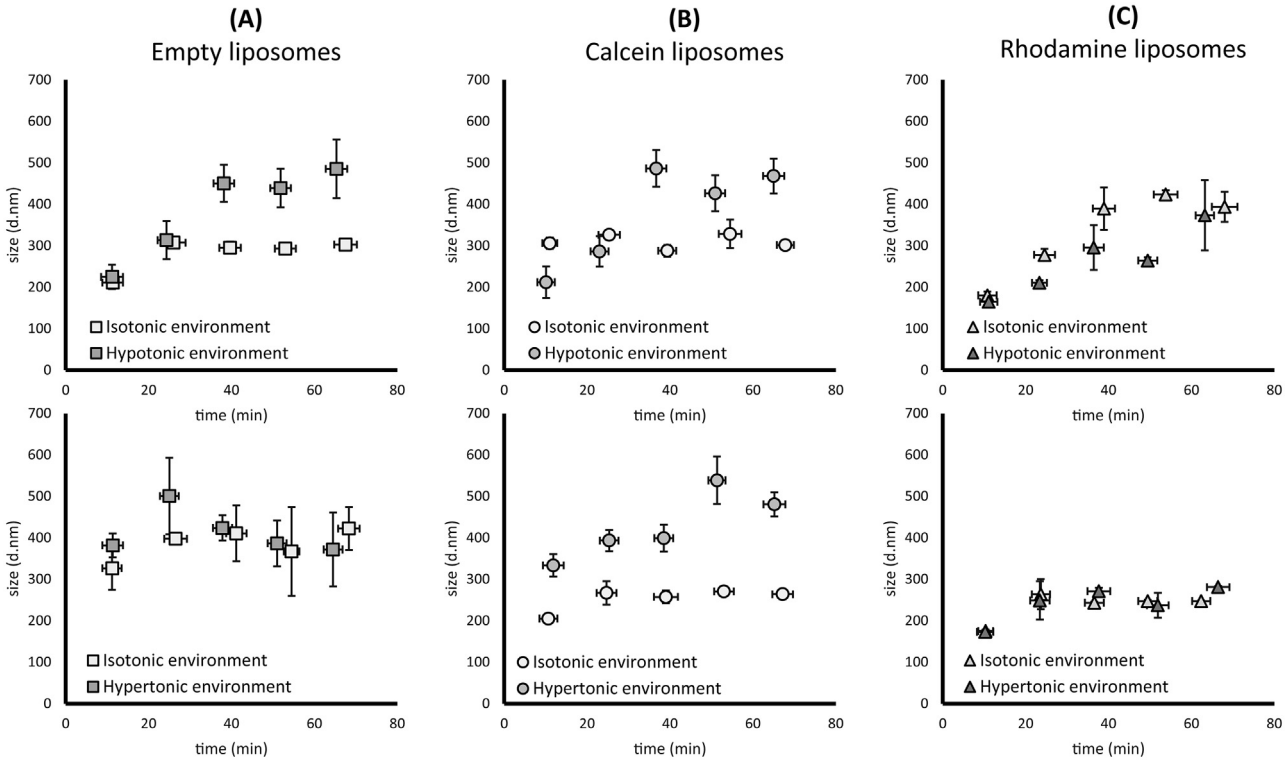

Fig. 2. Size distributional changes of LUVs (empty, calcein-loaded and rhodamine-loaded) prepared in buffer 300 (upper line) and buffer 65 (lower line) after exposure to hypotonic and hypertonic environment (buffer 65 and 300 respectively). Results are reported as mean ± SD (n = 2).

Table 5
Apparent permeability coefficients of calcein and rhodamine through cellulose hydrate membrane measured under tonicity imbalance condition between internal and external environment of LUVs. For the calculations, the total marker concentration in the LUV dispersion (P_{app}) and, alternatively, the unentrapped marker concentration (i.e. molecular dissolved marker concentration (P^{o}_{app})) were employed. Results are reported as mean ± SD (n = 3).

		Calcein		Rhodamine	
Dispersing PBS type	π_{rel}(bar)	$P_{app}(10^{-5}$ cm/sec)	$P^{o}_{app}(10^{-5}$ cm/sec)	$P_{app}(10^{-5}$ cm/sec)	$P^{o}_{app}(10^{-5}$ cm/sec)
300	0	**0.86 ± 0.05**	**1.34 ± 0.08**	**0.33 ± 0.02**	**2.22 ± 0.14**
	−3	0.76 ± 0.00	1.20 ± 0.00	0.35 ± 0.03	2.29 ± 0.17
	−6	0.65 ± 0.06	1.01 ± 0.09	0.31 ± 0.00	2.05 ± 0.02
–					
65	0	**0.47 ± 0.06**	**0.75 ± 0.10**	**0.36 ± 0.02**	**2.48 ± 0.17**
	3	0.65 ± 0.01	1.06 ± 0.02	0.30 ± 0.01	2.06 ± 0.10
	6	0.70 ± 0.05	1.13 ± 0.08	0.29 ± 0.01	2.00 ± 0.09

Isotonic conditions are reported in bold.

low in comparison to previous reports [35]. Applying the dialysis/centrifugation method, an entrapment of approx. 40% was found for calcein and approx. 85% for rhodamine, respectively. Interestingly, the different methods gave relatively similar EE of rhodamine, while they differed a lot for calcein-LUVs. This finding could be explained by the different chemical nature of the two markers (Fig. 1). Rhodamine is a quite lipophilic marker (Log P of 2 [21]) and expected to be incorporated in the lipid bilayer. On the other hand, calcein is extremely hydrophilic at neutral pH (Log P of −4 [19]) and is expected to be entrapped in the liposomal inner aqueous core. It is reasonable that liposomes rupture could influence EE of calcein during ultracentrifugation, whereas rhodamine-LUVs could be more resistant to damage.

Swelling and shrinking are standard responses of liposomes to the environmental tonicity changes. They reflect the ability of phospholipid bilayers to exchange water molecules within internal and external environment, inducing volume changes [6,7,13,15]. In this study, a significant size increase over time was observed when empty and calcein-loaded LUVs were exposed to the hypotonic environment (Fig. 2A, B, upper line) as a result of water influx into the LUVs in comparison to isotonic environment. These findings are in agreement with reported literature on other unilamellar vesicle systems composed of either same phospholipid [15,28] or other phospholipids [36]. The fact that no significant size decrement was measurable when liposomes were exposed to the hypertonic environment might be related to the physical limitation associated to shrinking of liposomes (Fig. 2A, B, lower line) [37]. The increased size of calcein-LUVs in comparison to their size in the isotonic environment might be due to liposomal aggregation that occurs due to neutral surface charge of LUVs and that hampered the detection of size decrement (Fig. 2B, lower line). Rhodamine-LUVs showed no significant size changes before and after the alteration of the environmental tonicity in comparison to isotonic environments (Fig. 2C). This could be explained by the lipophilic nature of rhodamine in comparison to the hydrophilic calcein. Similarly to cholesterol, rhodamine might also contribute to a more rigid and impermeable membrane retaining the incorporated marker [38].

Regarding the marker release studies, the control permeability of both markers through the cellulose hydrate membrane (P^{0}_{app}) was surprisingly higher in the PBS with the highest tonicity

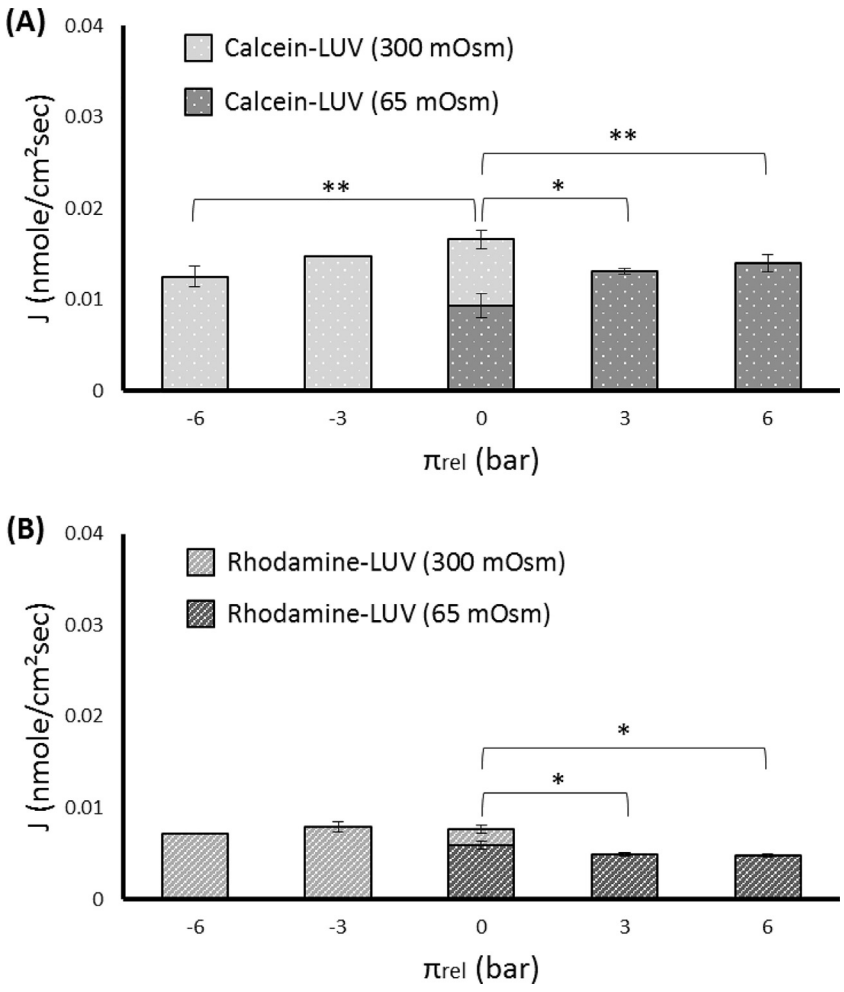

Fig. 3. Correlation between the relative osmotic pressures (π_{rel}) (generated by the difference in tonicity between internal and external environment of LUVs) and the observed fluxes of calcein (A) and rhodamine (B) in LUV dispersions (2 mM total marker concentration). Results are reported as mean ± SD (n = 3, $^{*}p \leq 0.05$, $^{**}p \leq 0.01$).

(Table 4). The same trend was observed when the markers were loaded into LUVs (Fig. 3, central bars). This phenomenon could be related to the nature of the barrier utilized for the release study. The cellulose hydrate membranes are reported to express a slightly negative charge [39,40]. This could reduce the flux of calcein and rhodamine (to a minor extent, Table 4) due to the electrostatic repulsion; more evident for calcein (negatively charged at this pH). It is plausible that in high tonicity (PBS 300), the negative potential of the barrier is neutralized by the ion deposition, improving the flux of the markers [41].

When liposomal dispersions were studied, the flux of calcein through cellulose hydrate membrane was highly affected by the induced osmotic changes (Fig. 3A). At positive osmotic pressures (i.e. efflux of water molecules), the flux of calcein increased, whereas at negative osmotic pressure (i.e. influx of water molecule) it decreased. This phenomenon could be explained by the marker/water flux interplay through the lipid bilayer. When positive osmotic pressure was applied, the flux of water and calcein were both directed outwards (synergistic effect), in agreement with reported literature, even though the lipid composition in the comparing studies differed [36,42]. On the other hand, when negative osmotic pressure applied, the marker still followed the concentration gradient (directed outwards) but the flux of water was directed inwards (antagonistic effect). While the flux of calcein was directly correlated to the osmotic pressure, the rhodamine flux was relatively stable and only slightly influenced by positive osmotic pressures (Fig. 3B). This phenomenon could be due to the fact that rhodamine is a lipophilic compound that is primarily incorporated in the phospholipid bilayer of LUVs. When positive osmotic pressure was applied (i.e. efflux water), liposomal membrane could become tightly packed hampering/reducing the marker release.

Table 5 reports the normalization of all fluxes according to the initial concentration of the markers in the liposomal dispersions. To have a better understanding of the mechanism involved, all fluxes were normalized according to the initial concentration of markers (total and unentrapped marker concentration) in the dispersion. For calcein, the permeability coefficients normalized over the total (P_{app}) or unentrapped marker concentration ($P^{ø}_{app}$) were similar and comparable to the reference value (P^{0}_{app}, Table 4). On the other hand, for rhodamine, only $P^{ø}_{app}$ (Table 5) were in the same order of magnitude as the control permeability (P^{0}_{app}, Table 4). These results are in agreement with previous finding [9] supporting the theory that for the lipophilic substances, the freely molecularly dissolved fraction of the drug is the primary contributor to the permeability.

5. Conclusion

This study shows that tonicity perturbations affect the release of hydrophilic and, to a minor extent, lipophilic markers from LUVs. The sizes, as well as the release kinetics of the two different markers loaded inside LUVs were altered by the tonicity differences. LUV dispersions seemed to be more susceptible to the osmotic swelling than shrinking. Size changes were more evident for empty

and calcein-LUVs in comparison to rhodamine-LUVs. The release of calcein from LUVs was highly influenced by the environmental tonicity changes, whereas the release of rhodamine was less affected. In conclusion, these results demonstrate that different tonicity (within inner core and external environment of LUVs) can enhance/hamper the release of markers from LUVs and that osmotically active liposomes could be used as a new controlled drug delivery system.

Acknowledgements

The authors thank Lipoid (Ludwigshafen, Germany) for free lipid samples. This research did not receive any specific grant from funding agencies in the public, commercial, or not-for-profit sectors.

References

[1] A.D. Bangham, R.W. Horne, Negative staining of phospholipids and their structural modification by surface-active agents as observed in the electron microscope, J. Mol. Biol. 8 (1964) 660–668, http://dx.doi.org/10.1016/S0022-2836(64)80115-7.
[2] M.L. Etheridge, S.A. Campbell, A.G. Erdman, C.L. Haynes, S.M. Wolf, J. McCullough, The big picture on nanomedicine: the state of investigational and approved nanomedicine products, Nanomed.: Nanotechnol. Biol. Med. 9 (2013) 1–14, http://dx.doi.org/10.1016/j.nano.2012.05.013.
[3] J.C. Kraft, J.P. Freeling, Z. Wang, R.J.Y. Ho, Emerging research and clinical development trends of liposome and lipid nanoparticle drug delivery systems, J. Pharm. Sci. 103 (2014) 29–52, http://dx.doi.org/10.1002/jps.23773.
[4] M. Kapoor, S.L. Lee, K.M. Tyner, Liposomal drug product development and quality: current US experience and perspective, AAPS J. 19 (3) (2017) 632–641, http://dx.doi.org/10.1208/s12248-017-0049-9.
[5] R.R.C. New, Chapter 1: Introduction Liposomes: A Practical Approach, vol. 58, IRL Press, Oxford, 1990, pp. 1–32.
[6] M. Ohno, T. Hamada, K. Takiguchi, M. Homma, Dynamic behavior of giant liposomes at desired osmotic pressures, Langmuir 25 (2009) 11680–11685, http://dx.doi.org/10.1021/la900777g.
[7] S. Paula, A.G. Volkov, A.N. Van Hoek, T.H. Haines, D.W. Deamer, Permeation of protons, potassium ions, and small polar molecules through phospholipid bilayers as a function of membrane thickness, Biophys. J. 70 (1996) 339–348, http://dx.doi.org/10.1016/s0006-3495(96)79575-9.
[8] M. di Cagno, J. Styskala, J. Hlaváč, M. Brandl, A. Bauer-Brandl, N. Skalko-Basnet, Liposomal solubilization of new 3-hydroxy-quinolinone derivatives with promising anticancer activity: a screening method to identify maximum incorporation capacity, J. Liposome Res. 21 (2011) 272–278, http://dx.doi.org/10.3109/08982104.2010.550265.
[9] M. di Cagno, B. Luppi, Drug supersaturation states induced by polymeric micelles and liposomes: a mechanistic investigation into permeability enhancements, Eur. J. Pharm. Sci. 48 (2013) 775–780, http://dx.doi.org/10.1016/j.ejps.2013.01.006.
[10] T.M. Allen, P.R. Cullis, Liposomal drug delivery systems: from concept to clinical applications, Adv. Drug Deliv. Rev. 65 (2013) 36–48, http://dx.doi.org/10.1016/j.addr.2012.09.037.
[11] A. Martin, P. Bustamante, A.H.C. Chun, Chapter 5: Solutions of nonelectrolytes, in: Martin's Physical Pharmacy and Pharmaceutical Sciences: Physical Chemical and Biopharmaceutical Principles in the Pharmaceutical Sciences, 4th ed., Lippincott Williams & Wilkins, Philadelphia, 1993, pp. 116–119.
[12] J.A. Jackman, J.H. Choi, V.P. Zhdanov, N.J. Cho, Influence of osmotic pressure on adhesion of lipid vesicles to solid supports, Langmuir 29 (2013) 11375–11384, http://dx.doi.org/10.1021/la4017992.
[13] E. Boroske, M. Elwenspoek, W. Helfrich, Osmotic shrinkage of giant egg-lecithin vesicles, Biophys. J. 34 (1981) 95–109, http://dx.doi.org/10.1016/s0006-3495(81)84839-4.
[14] E.B. Abuin, A.M. Campos, E.A. Lissi, E.A. Disalvo, Osmotic response of large unilamellar vesicles of phosphatidylcholine: factors determining the rate of the process and the properties of the shrunken vesicles, J. Colloid Interface Sci. 171 (1995) 406–412, http://dx.doi.org/10.1006/jcis.1995.1197.
[15] B.L. Mui, P.R. Cullis, E.A. Evans, T.D. Madden, Osmotic properties of large unilamellar vesicles prepared by extrusion, Biophys. J. 64 (1993) 443–453, http://dx.doi.org/10.1016/S0006-3495(93)81385-7.
[16] J. Sabin, G. Prieto, J.M. Ruso, R. Hidalgo-Alvarez, F. Sarmiento, Size and stability of liposomes: a possible role of hydration and osmotic forces, Eur. Phys. J. E 20 (2006) 401–408, http://dx.doi.org/10.1140/epje/i2006-10029-9.
[17] T. Katsu, Application of calcein-loaded liposomes for the determination of membrane channel size, Biol. Pharm. Bull. 22 (1999) 978–980, http://dx.doi.org/10.1248/bpb.22.978.
[18] B.R. Lentz, Use of fluorescent probes to monitor molecular order and motions within liposome bilayers, Chem. Phys. Lipids 64 (1993) 99–116, http://dx.doi.org/10.1016/0009-3084(93)90060-G.
[19] B. Maherani, E. Arab-Tehrany, A. Kheirolomoom, D. Geny, M. Linder, Calcein release behavior from liposomal bilayer; influence of physicochemical/mechanical/structural properties of lipids, Biochimie 95 (2013) 2018–2033, http://dx.doi.org/10.1016/j.biochi.2013.07.006.
[20] T. Shimanouchi, H. Ishii, N. Yoshimoto, H. Umakoshi, R. Kuboi, Calcein permeation across phosphatidylcholine bilayer membrane: effects of membrane fluidity, liposome size, and immobilization, Colloids Surf. B: Biointerfaces 73 (2009) 156–160, http://dx.doi.org/10.1016/j.colsurfb.2009.05.014.
[21] Y.G. Anissimov, X. Zhao, M.S. Roberts, A.V. Zvyagin, Fluorescence recovery after photo-bleaching as a method to determine local diffusion coefficient in the stratum corneum, Int. J. Pharm. 435 (2012) 93–97, http://dx.doi.org/10.1016/j.ijpharm.2012.01.055.
[22] G.E. Flaten, A.B. Dhanikula, K. Luthman, M. Brandl, Drug permeability across a phospholipid vesicle based barrier: a novel approach for studying passive diffusion, Eur. J. Pharm. Sci. 27 (2006) 80–90, http://dx.doi.org/10.1016/j.ejps.2005.08.007.
[23] J.L. Pittman, K.F. Schrum, S.D. Gilman, On-line monitoring of electroosmotic flow for capillary electrophoretic separations, Analyst 126 (2001) 1240–1247, http://dx.doi.org/10.1039/B103316F.
[24] A. Moscho, O. Orwar, D.T. Chiu, B.P. Modi, R.N. Zare, Rapid preparation of giant unilamellar vesicles, Proc. Natl. Acad. Sci. U. S. A. 93 (1996) 11443–11447, http://dx.doi.org/10.1073/pnas.93.21.11443.
[25] D. Stelzl, T.T. Nielsen, T. Hansen, M. di Cagno, β-CD-dextran polymer for efficient sequestration of cholesterol from phospholipid bilayers: mechanistic and safe-toxicity investigations, Int. J. Pharm. 496 (2015) 896–902, http://dx.doi.org/10.1016/j.ijpharm.2015.10.041.
[26] B. Steffansen, B. Brodin, C. Uhd Nielsen, Chapter 3.2: Passive diffusion of drug substances: the concepts of flux and permeability, in: Molecular Biopharmaceutics: Aspects of Drug Characterisation, Drug Delivery and Dosage Form Evaluation, Pharmaceutical Press, London, 2010, pp. 135–152.
[27] S. Modi, B.D. Anderson, Determination of drug release kinetics from nanoparticles: overcoming pitfalls of the dynamic dialysis method, Mol. Pharm. 10 (2013) 3076–3089, http://dx.doi.org/10.1021/mp400154a.
[28] C.A. Rutkowski, L.M. Williams, T.H. Haines, H.Z. Cummins, The elasticity of synthetic phospholipid vesicles obtained by photon correlation spectroscopy, Biochemistry 30 (1991) 5688–5696, http://dx.doi.org/10.1021/bi00237a008.
[29] J. Pencer, G.F. White, F.R. Hallett, Osmotically induced shape changes of large unilamellar vesicles measured by dynamic light scattering, Biophys. J. 81 (2001) 2716–2728, http://dx.doi.org/10.1016/s0006-3495(01)75914-0.
[30] J.N. Israelachvili, Chapter 14: Electrostatic forces between surfaces in liquids, in: Intermolecular and Surface Forces, 3rd ed., Academic Press, Boston, 2011, pp. 291–340, http://dx.doi.org/10.1016/B978-0-12-391927-4.10014-3.
[31] F. Bordi, C. Cametti, Salt-induced aggregation in cationic liposome aqueous suspensions resulting in multi-step self-assembling complexes, Colloids Surf. B: Biointerfaces 26 (2002) 341–350, http://dx.doi.org/10.1016/S0927-7765(02)00018-8.
[32] N. Ostrowsky, D. Sornette, Interaction between neutral vesicles: the importance of bilayer fluidity, Colloids Surf. 14 (1985) 231–238, http://dx.doi.org/10.1016/0166-6622(85)80217-1.
[33] F.J. Carrión, A. De La Maza, J.L. Parra, The Influence of ionic strength and lipid bilayer charge on the stability of liposomes, J. Colloid Interface Sci. 164 (1994) 78–87, http://dx.doi.org/10.1006/jcis.1994.1145.
[34] R.W. Ramette, E.B. Sandell, Rhodamine B equilibria, J. Am. Chem. Soc. 78 (1956) 4872–4878, http://dx.doi.org/10.1021/ja01600a017.
[35] A. Akbarzadeh, R. Rezaei-Sadabady, S. Davaran, S.W. Joo, N. Zarghami, Y. Hanifehpour, M. Samiei, M. Kouhi, K. Nejati-Koshki, Liposome: classification, preparation, and applications, Nanoscale Res. Lett. 8 (2013) 102, http://dx.doi.org/10.1186/1556-276X-8-102.
[36] M. Ahumada, C. Calderon, C. Alvarez, M.E. Lanio, E.A. Lissi, Response of unilamellar DPPC and DPPC:SM vesicles to hypo and hyper osmotic shocks: a comparison, Chem. Phys. Lipids 188 (2015) 54–60, http://dx.doi.org/10.1016/j.chemphyslip.2015.05.001.
[37] L. Tayebi, D. Vashaee, A.N. Parikh, Stability of uni- and multillamellar spherical vesicles, Chemphyschem 13 (2012) 314–322, http://dx.doi.org/10.1002/cphc.201100573.
[38] J. De Gier, J.G. Mandersloot, L.L.M. Van Deenen, Lipid composition and permeability of liposomes, Biochim. Biophys. Acta (BBA) Biomembr. 150 (1968) 666–675, http://dx.doi.org/10.1016/0005-2736(68)90056-4.
[39] J. Benavente, A study of membrane potentials across a cellophane membrane for different electrolytes, J. Non-Equilib. Thermodyn. 9 (1984) 217–224, http://dx.doi.org/10.1515/jnet.1984.9.3.217.
[40] B.D. Coday, T. Luxbacher, A.E. Childress, N. Almaraz, P. Xu, T.Y. Cath, Indirect determination of zeta potential at high ionic strength: specific application to semipermeable polymeric membranes, J. Membr. Sci. 478 (2015) 58–64, http://dx.doi.org/10.1016/j.memsci.2014.12.047.
[41] C. Bartels, R. Franks, S. Rybar, M. Schierach, M. Wilf, The effect of feed ionic strength on salt passage through reverse osmosis membranes, Desalination 184 (2005) 185–195, http://dx.doi.org/10.1016/j.desal.2005.04.032.
[42] E.A. Disalvo, A.M. Campos, E. Abuin, E.A. Lissi, Surface changes induced by osmotic shrinkage on large unilamellar vesicles, Chem. Phys. Lipids 84 (1996) 35–45, http://dx.doi.org/10.1016/S0009-3084(96)02617-5.

Paper II

Journal of Pharmaceutical Sciences 108 (2019) 2570-2579

Contents lists available at ScienceDirect

Journal of Pharmaceutical Sciences

journal homepage: www.jpharmsci.org

Pharmaceutics, Drug Delivery and Pharmaceutical Technology

The Hypotonic Environmental Changes Affect Liposomal Formulations for Nose-to-Brain Targeted Drug Delivery

Iren Yeeling Wu [1], Trygg Einar Nikolaisen [1], Nataša Škalko-Basnet [1], Massimiliano Pio di Cagno [1, 2, *]

[1] Drug Transport and Delivery Research Group, Department of Pharmacy, University of Tromsø—The Arctic University of Norway, Universitetsvegen 57, 9037 Tromsø, Norway

[2] Department of Pharmacy, Faculty of Mathematics and Natural Sciences, University of Oslo, Sem Sælands vei 3, 0371 Oslo, Norway

ARTICLE INFO

Article history:
Received 31 January 2019
Revised 8 March 2019
Accepted 8 March 2019
Available online 16 March 2019

Keywords:
liposomes
osmotic pressure
particle size
passive diffusion
controlled release
membrane resistance
drug transport
drug delivery system

ABSTRACT

Systemic administration of drugs is ineffective in the treatment of central nervous system disorders because of the blood-brain barrier. Nasal administration has been suggested as an alternative administration route as drugs absorbed in the olfactory epithelium bypass the blood-brain barrier and reach the brain within minutes. However, the nasal mucosa properties (e.g., tonicity, pH) are not constant because of physiological and environmental factors, and this might limit the therapeutic outcome of nanocarrier-based formulations. To shine light on the impact of environmental ionic strength on nanocarrier-based formulations, we have studied how liposomal formulations respond to the change of tonicity of the external environment. Large unilamellar vesicles loaded with 6 different drugs were exposed to different hypotonic environments, creating an osmotic gradient within the inner core and external environment of the liposomes up to 650 mOsm/kg. Both size and polydispersity of liposomes were significantly affected by tonicity changes. Moreover, the release kinetics of hydrophilic and lipophilic drugs were largely enhanced by hypotonic environments. These results clearly demonstrate that the environmental ionic strength has an impact on liposomal formulation stability and drug release kinetics and it should be considered when liposomal formulations for nose-to-brain targeted drug delivery are designed.

Introduction

Standard therapies for the treatment of the majority of central nervous system (CNS) disorders (i.e., Alzheimer's disease, multiple sclerosis, Parkinson's disease, etc.) are based on daily systemic administration of drugs. The most serious limitation of systemic administration of drugs is that the blood-brain barrier (BBB) prevents drugs from reaching the CNS.[1-3] The BBB consists of tightly packed endothelial cells separating the systemic circulation from the neuronal cells. It is estimated that the BBB limits the access to the brain for 98% of small molecules and 100% of large ones.[4] To overcome these limitations, alternative routes of drug administration to the brain have lately emerged. One of the most promising routes of administration appears to be the nose-to-brain targeted drug administration.[5,6] The nasal epithelium is divided into the olfactory and respiratory region.[5-7] Drugs that are absorbed through the olfactory region have the potential to avoid systemic elimination (i.e., first-pass metabolism, renal clearance etc.), reach the cerebrospinal fluid, and accumulate in the brain bypassing the BBB.[5-8] This route of drug administration is unfortunately limited by low absorption through the olfactory epithelium because of the limited surface area, early enzymatic degradation, and rapid ciliary clearance.[9] However, new research has shown that liposomes can optimize nose-to-brain targeted drug delivery.[10] Liposomes are spherical vesicles consisting of single or multiple phospholipid bilayers surrounding an aqueous core.[11,12] Liposomes for nose-to-brain targeted delivery have shown to protect drugs from early degradation and elimination because of their ability to entrap both hydrophilic and lipophilic compounds.[13,14] Recent *in vivo* studies in rats have shown that liposomal formulations administered via the nose reduce systemic side effects, improve apparent neurological

Abbreviations used: CNS, central nervous system; EE, entrapment efficiency; LUVs, large unilamellar vesicles; PBS, phosphate buffered saline; PI, polydispersity index; R_B, resistance to drug transport through regenerated cellulose barrier; R_L, resistance to drug transport through liposomal bilayer; R_T, total resistance to drug transport; SD, standard deviation; SPC, soy-phosphatidylcholine; ZP, ζ-potential; ΔmOsm/kg, tonicity difference between the inner core and external environment of liposomes.

Conflicts of interest: None.

* *Correspondence to:* Massimiliano Pio di Cagno (Telephone: +47-22856598).
E-mail address: m.p.d.cagno@farmasi.uio.no (M.P. di Cagno).

https://doi.org/10.1016/j.xphs.2019.03.006
0022-3549/

functions, and enhance cognitive functions for the treatment of Alzheimer's and Parkinson's disease.[10,15] Despite the promising results, liposome-based formulations intended for nose-to-brain targeted drug delivery seem to show inconsistent improvement in the therapeutic effects when compared with other nanoparticulate systems.[16,17] It has been suggested that one of the reasons might be the slow drug release kinetics (for both hydrophilic and lipophilic compounds) from the liposomal carrier.[18-20] Another important variable is related to physiological changes at the nasal mucosal level. In fact, as the mucus is directly open to the external milieu, environmental factors such as air humidity or temperature can perturb the mucus properties such as viscosity, pH, and most importantly, tonicity.[21,22] These alterations might also occur during the inflammation state.[23] It is well accepted that liposomal phospholipid bilayer allows small neutral molecules to pass through it to equalize the chemical activity gradient.[24-26] For instance, when the ionic strength of the liposomal core is higher than the outside environment, water molecules will diffuse through the lipid bilayer from the outside to the inside of the liposomes (following the chemical activity gradient). As a result of solvent movement, an osmotic pressure is generated on the liposomal surfaces and liposomes swell (water influx).[27-29] We have recently proved that the release of a medium-sized hydrophilic marker (calcein) and lipophilic marker (rhodamine) from large unilamellar vesicles (LUVs) is influenced by osmotic stress.[30] Specifically, we proved that the release of a hydrophilic marker from LUVs was significantly more affected by the tonicity perturbations in comparison with a lipophilic marker. This suggests that the magnitude of these changes could be related to the interplay between the changes in liposomal size and the direction of water flux through the liposomal membrane (water influx or efflux). The aim of this study was therefore to verify how the changes in environmental ionic strength might influence liposomal formulations designed for nasal administration. Specifically, we investigated how the exposure of LUVs to hypotonic environment affects the drug release kinetics of 6 active pharmaceutical ingredients (caffeine, hydrocortisone, ibuprofen, ketoprofen, methylprednisolone, and theophylline). The drugs were chosen to cover a range of relevant physiochemical properties (different partition coefficients and ionization constants, see Table 1) within potential candidates in the treatment or prevention of the Alzheimer's disease.[37,38] The liposomal dispersions were characterized in terms of size, ζ-potential (ZP), and entrapment efficiency (EE), whereas drug release kinetics in uneven tonicities were studied by the classic Franz cell diffusion system equipped with regenerated cellulose barriers.

Materials and Methods

Materials

Caffeine, hydrocortisone, ibuprofen, ketoprofen, methylprednisolone, theophylline, disodium hydrogen phosphate dihydrate ($Na_2HPO_4 \cdot 2H_2O$), sodium chloride (NaCl), sodium hydroxide (NaOH), sodium dihydrogen phosphate monohydrate ($NaH_2PO_4 \cdot H_2O$), chloroform, and methanol were purchased from Sigma-Aldrich Chemie GmbH (Steinheim, Nordrhein-Westfalen, Germany). Lipoid S100 (soy-phosphatidylcholine [SPC] >94%) was kindly provided by Lipoid GmbH (Ludwigshafen, Rheinland-Pfalz, Germany).

Table 1
Molecular Weight (MW), Dissociation Constant (*pKa*), Distribution Coefficient at pH 7.4 ($logD_{7.4}$) and Wavelength of Maximum Absorbance (λ_{max}) of the Investigated Drugs

Drug	MW (g/mole)	*pKa*	$logD_{7.4}$	λ_{max} (nm)
Caffeine	194.2	10.4[31]	0.0[32]	273
Theophylline	180.2	8.8[33]	−0.1[32]	272
Ketoprofen	254.3	4.5[34]	0.2[35]	261
Ibuprofen	206.3	4.9[36]	1.0[35]	222
Hydrocortisone	362.5	Not relevant	1.5[32]	247
Methylprednisolone	374.5	Not relevant	2.1[32]	248

Table 2
Experimentally Determined Osmolality, pH, and Calculated Phosphate Concentration for Each of the PBS Solutions Employed

Buffer Solution	Osmolality (mOsm/kg)	pH	Phosphate (mM)
PBS700	707 ± 6	7.21 ± 0.01	74 ± 0
PBS300	298 ± 12	7.39 ± 0.03	74 ± 0
PBS190	183 ± 2	7.49 ± 0.04	44 ± 0
PBS65	64 ± 3	7.60 ± 0.04	15 ± 0

Results represent mean ± SD ($n = 5$).

Preparation of Phosphate Buffered Saline

Phosphate buffered saline (PBS) solutions were prepared following a method previously described.[30] In brief, a 300 mOsm/kg neutral (pH 7.4) buffer (PBS300) was obtained by dissolving $NaH_2PO_4 \cdot H_2O$, $Na_2HPO_4 \cdot 2H_2O$, NaOH, and NaCl (4.5 g/L, 7.4 g/L, 0.8 g/L, and 4.4 g/L, respectively) in distilled water. PBS300 was diluted 3:5 or 1:5 (v/v) with distilled water to achieve buffer solutions with reduced ionic strength (approx. 190 and 65 mOsm/kg, see Table 2). The ionic strength of PBS300 was increased by adding droplets of a 200 g/L NaCl solution (dissolved in PBS300) until a tonicity of 700 mOsm/kg tonicity was reached (PBS700). The measured osmolality (Semi-Micro Osmometer K-7400; Knauer, Berlin, Germany) and pH (sensION™ + PH31 pH meter; Hach, Barcelona, Spain) of the different PBS solutions used in this study are represented in Table 2.

Preparation of LUVs

LUV dispersions were prepared following a method previously described.[30] A buffer solution (10 mL, PBS300 or PBS65) was gently added on top of an organic phase containing methanol (0.2 mL) and SPC/chloroform solution (200 mg/mL, 1 mL) in a 50-mL round bottom flask. LUV formulations containing caffeine, ibuprofen, ketoprofen, or theophylline were prepared by dissolving the drug (2 mM concentration) in the aqueous phase (PBS300 or PBS65, respectively), whereas LUVs with hydrocortisone or methylprednisolone were prepared by dissolving the drug in the SPC/chloroform solution (drug-lipid ratio approx. 0.035 w/w). Unilamellar vesicles (containing 20 mg/mL lipid and 2 mM drug) were spontaneously formed after the removal of the organic phase by rotary evaporation (40°C, 40 rpm, 0.1 bar, 90 min, Büchi R-124 rotavapor equipped with Büchi vacuum pump V-700 and Büchi B-480 water bath; Büchi Labortechnik AG, Flawil, Switzerland). Liposomal dispersions were subsequently extruded through polycarbonate membrane filters (5 × 800 nm and 10 × 400 nm, Nuclepore Track-Etched Membranes; Whatman International Ltd., Maidstone, Kent, UK) at room temperature (23°C-25°C) to obtain vesicles of homogeneous sizes.

Size Characterization

LUVs' size distribution was measured by photon correlation spectroscopy (angle of 173°, 25°C, Zetasizer Nano Zen 2600; Malvern Panalytical, Malvern, Worcestershire, UK). Before analysis, each LUV dispersion was diluted 1:100 (v/v) with the same buffer used to prepare LUVs and filtered through polyethersulfone

membrane filters (0.2 μm pore size; VWR International, Radnor, PA). Analysis were performed in 4 replicates ($n = 4$), where each sample was measured thrice. For the investigation of LUV sizes in non-isotonic conditions, LUV dispersions (prepared from PBS300 with measured tonicity of approx. 710 mOsm/kg) were diluted 1:100 (v/v) with hypotonic buffers (PBS300 or PBS65, Table 2) and sizes were detected at intervals (approx. every 15 min) over a period of 90 min. Each experiment was repeated twice ($n = 2$), and each sample was measured 3 times.

ζ-Potential Characterization

The electrokinetic potential (ζ-potential [ZP]) of LUVs was measured by a Zetasizer Nano Zen 2600 (Malvern Panalytical) following a procedure previously described.[30] LUV dispersions were diluted 1:20 (v/v) with filtrated deionized water (0.2 μm pore size; VWR International, Radnor, PA) prior measurements, and analysis were conducted at room temperature (23°C-25°C). Measurements were performed in 4 replicates ($n = 4$), where each sample was measured thrice.

Entrapment Efficiency of Drugs

LUVs were separated from the supernatant (containing freely unentrapped drug) by ultracentrifugation (200,000 ×*g*, 10°C, 30 min, Beckman model L8-70M with SW 60 Ti rotor; Beckman Instruments, Brea, CA). The pellet obtained after ultracentrifugation was dissolved in 1 mL methanol, and drug concentration was quantified in the supernatant as well as in the pellet solutions by UV-visible spectroscopy using a Microtiter plate reader (Spectra Max 190 Microplate Spectrophotometer; Molecular Devices, Sunnyvale, CA) (see Table 1 for the specific detection wavelengths of each drug). EE was calculated using Equation 1:

$$EE\ (\%) = \frac{M_{LUVs}}{M_{LUVs} + M_{free}} \cdot 100 \quad (1)$$

where M_{LUVs} represents the amount of liposomal entrapped drug (i.e., recovered in the pellet) and M_{free} represents the amount of freely unentrapped drug (i.e., detected in the supernatant). The drug recovery was determined from the total amount of drug (entrapped and unentrapped drug in LUVs) after centrifugation in comparison to the nominal amount of drug in the LUVs (i.e., initial total drug content before centrifugation). Analyses were performed in minimum duplicates ($n \geq 2$), whereas 3 samples of each batch were measured 4 times.

In Vitro Drug Transport Study

Drug transport studies were conducted using the Franz diffusion cell system (0.64 cm^2 diffusional area jacketed flat ground joint; PermeGear, Hellertown, PA) following a method previously used.[30] In brief, the acceptor chamber was filled with 5 mL PBS (see Table 2). Regenerated cellulose barriers (VISKING dialysis tubing MWCO 12-14 kDa; Medicell Membranes Ltd., London, UK) were placed between acceptor and donor chambers. The experiment started by adding 0.8 mL of a liposomal dispersion (containing 20 mg/mL lipid, 2 mM total drug concentration) or, alternatively, drug solution (a.k.a. reference) to the donor chamber. In the case of soluble or poorly soluble compounds (caffeine, ibuprofen, ketoprofen, theophylline), 2 mM reference aqueous solution was used, whereas for very poorly soluble drug (hydrocortisone and methylprednisolone), saturated suspension (1 mg/mL) was used to maintain a consistent concentration gradient between donor and acceptor compartments. The thermodynamic solubility was predetermined to be 1 mM and 0.3 mM for hydrocortisone and methylprednisolone in PBS (both PBS65 and PBS300), respectively. Samplings (0.5 mL) from the acceptor chamber were carried out at intervals of 30 min over a period of 4 h. After withdrawal of samples, equal volumes of the respective PBS (with same tonicity) were reintroduced into the acceptor chamber to maintain sink condition. At the end of the experiment, drug concentrations in the acceptor and donor chambers were quantified by UV-visible spectroscopy (see Entrapment Efficiency of Drugs). The cumulative amount of diffused drug over time was calculated, and the linear part of the slope (representing steady state condition) was used to determine the apparent permeability coefficient (P, cm/s) as shown in Equation 2 rearranged from Brodin et al.[39]:

$$P = \frac{dm}{dt} \times \frac{1}{A} \times \frac{1}{c_d} \quad (2)$$

where dm/dt represents the rate of mass transfer of free drug molecules over time, A is the diffusional area, and c_d represents the initial total drug concentration in the formulation.

Resistance to Drug Transport Through Phospholipid Bilayer Calculation (R_L)

The resistance to drug transport of a compound through a barrier can be defined as the reciprocal function of P as shown in Equation 3.[40,41]

$$R = \frac{1}{P} \quad (3)$$

In a permeation process where different layers need to be crossed, the total resistance to drug transport (R_T) can be calculated from the sum of the single resistances (of each of the barriers involved) to transport. In the case of LUV dispersion studies, drug molecules need to first cross the liposomal bilayer, representing the first resistance to drug transport (R_L, Fig. 1). Second, drug molecules need to cross the regenerated cellulose (dialysis) barrier encountering a second resistance to drug transport, namely R_B (Fig. 1). Based on this assumption, measuring the total resistance to drug transport (R_T) and R_B (measured in the reference experiment with drug solutions), R_L can be calculated by Equation 4:

$$R_L = R_T - R_B \quad (4)$$

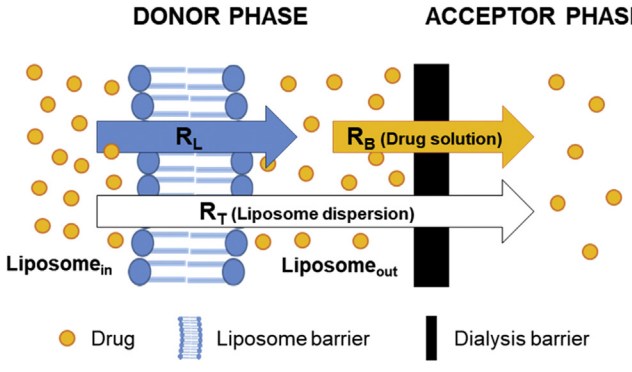

Figure 1. Schematic representation of the passive diffusion setup. R_B represents the resistance to drug transport through the regenerated cellulose barrier (measured for drug in solution), whereas R_T represents the total resistance to drug transport (measured for liposome dispersion) and R_L represents the resistance to drug transport through the liposomal bilayer (calculated with Eq. 4).

Table 3
Measured Tonicity, Size, Polydispersity Index (PI), ζ-potential (ZP), Entrapment Efficiency (EE), and Drug Recovery for All Formulations Investigated

Drug	Buffer Solution	Tonicity (mOsm/kg)	Size (nm)	PI	ZP (mV)	EE (%)	Drug Recovery (%)
Caffeine	PBS65	430 ± 17	288 ± 53	0.34 ± 0.03	−2.99 ± 0.85	22 ± 4	97 ± 3
	PBS300	719 ± 18	262 ± 42	0.27 ± 0.03*	−0.87 ± 0.95***	18 ± 3*	99 ± 1
Theophylline	PBS65	455 ± 6	341 ± 72	0.37 ± 0.04	−1.99 ± 0.93	30 ± 0	100 ± 3
	PBS300	719 ± 22	327 ± 62	0.31 ± 0.04	−0.08 ± 1.28***	23 ± 6*	103 ± 3
Ketoprofen	PBS65	429 ± 4	368 ± 68	0.34 ± 0.03	−5.40 ± 0.98	42 ± 1	97 ± 2
	PBS300	718 ± 28	249 ± 36***	0.22 ± 0.02**	−3.97 ± 0.98	41 ± 4	98 ± 1
Ibuprofen	PBS65	429 ± 1	252 ± 36	0.22 ± 0.02	−8.68 ± 1.05	56 ± 4	99 ± 3
	PBS300	686 ± 23	246 ± 33	0.20 ± 0.02*	−6.26 ± 1.01**	46 ± 9*	101 ± 1
Hydrocortisone	PBS65	437 ± 6	332 ± 60	0.31 ± 0.03	−5.86 ± 1.10	77 ± 3	94 ± 5
	PBS300	718 ± 14	314 ± 58	0.32 ± 0.03	−2.49 ± 0.95*	74 ± 7	97 ± 4
Methylprednisolone	PBS65	425 ± 7	285 ± 46	0.29 ± 0.03	−3.12 ± 0.91	85 ± 3	97 ± 3
	PBS300	701 ± 9	256 ± 35***	0.20 ± 0.02***	−0.75 ± 0.94***	84 ± 5	97 ± 3

Results represent mean ± SD ($n \geq 2$).
Significant difference ($^{*}p \leq 0.050$, $^{**}p \leq 0.010$, $^{***}p \leq 0.001$) between the LUVs prepared in PBS300 in comparison with PBS65.

Statistical Data Evaluation

Two-sample Student's *t*-test assuming unequal variances was used to determine the significant differences between the mean of 2 data sets. A value of p below or equal to 0.050 was considered as statistically significant.

Results

LUVs Characterization

The most relevant physical characteristics of the different liposomal dispersions studied are summarized in Table 3.

LUV dispersions prepared in PBS300 exhibited a tonicity of approximately 710 mOsm/kg, whereas in PBS65, the tonicity of LUV dispersions was found to be between 425 and 455 mOsm/kg. In all dispersions, the liposome average sizes and polydispersity index (PI) were higher when prepared in PBS with lower ionic strength (65 mOsm/kg in respect to 300 mOsm/kg). The size differences were found significant for ketoprofen- ($p = 0.001$) and methylprednisolone-LUVs ($p = 0.000$). The same trend could be found for PI in addition to significant difference for caffeine- ($p = 0.042$) and ibuprofen-LUVs ($p = 0.020$). The ZP of all LUV dispersions prepared was close to neutral and significantly more negative ($p \leq 0.026$) for the dispersion prepared in PBS65 in comparison with PBS300. EE was rather low for caffeine and theophylline (18%-30%) with significant enhanced entrapment for the LUVs prepared in PBS65 in comparison with PBS300 ($p = 0.040$ and 0.014, respectively). We determined medium-high entrapment for ketoprofen and ibuprofen (41%-56%) and considerably higher entrapment for hydrocortisone and methylprednisolone (above 74%).

Effect of the Ionic Strength on LUV Sizes

The changes in LUV size distributions after the exposure to isotonic (a) and hypotonic environments (b and c) are reported in Figures 2 and 3. As it can be seen, LUVs were quite homogeneous in isotonic and low-hypotonic conditions (up to approx. 410 mOsm/kg differences, Figs. 2a and 2b). When exposed to a higher tonicity gradient (approx. 650 mOsm/kg difference between initial LUV dispersion and external environment tonicity), the liposomal dispersions clearly indicated enlargement of the size. Similarly, the PI was relatively constant over time for LUVs in the isotonic and low-hypotonic conditions (Figs. 3a and 3b). When the tonicity gradient between initial LUV dispersion and external environment of LUVs increased to approximately 650 mOsm/kg (Fig. 3c), an increase in PI (as well as standard deviation) was observed over time for all formulations tested.

In Vitro *Transport Study*

Drug Solutions

The initial drug concentration, tonicity, and the resistance to drug transport through the regenerated cellulose barrier (R_B) are presented in Table 4. As shown in Table 4, R_B was not significantly affected by the tonicity of the PBS used to prepare the solutions. The lowest R_B were found for caffeine and theophylline (around 1.6×10^4 s/cm), whereas for all other drugs (hydrocortisone, ibuprofen, ketoprofen, and methylprednisolone), R_B was slightly higher and between 1.9×10^4 and 2.3×10^4 s/cm (Table 4).

LUV Dispersions

The phospholipid bilayer's resistance to drug transport (R_L) over the tonicity gradient is reported in Figure 4. As the tonicity gradient between initial LUV dispersion and external environment of liposomes increases (ΔmOsm/kg), a decrease in the R_L was observed for all drugs to a different extent (Fig. 4). For caffeine and theophylline, a drastic shift in resistance was detected at a tonicity gradient of approximately 400 mOsm/kg, whereas for the other drugs, the decrement in R_L seemed to be more gradual. A significant decrease in R_L ($p \leq 0.026$) could be found for all the LUV dispersions prepared at tonicity differences around 300 and 400 mOsm/kg with the exceptions of caffeine and methylprednisolone. Only in the case of caffeine, the liposomal bilayer produced significantly higher resistance ($p \leq 0.009$) at low-hypotonic conditions (Fig. 4, upper-left) but not in isotonic conditions. For methylprednisolone, a significant decrease in R_L ($p = 0.026$) was already apparent at tonicity differences around 100 mOsm/kg. For all LUV dispersions prepared, the reduction in R_L at the highest concentration gradient (approx. 650 mOsm/kg) was found significantly different (p-value between 0.000 and 0.037) compared with the lowest concentration gradient (0 mOsm/kg, isotonic condition). The overall reduction in R_L was found to be between 75% and 114% for the hydrophilic drugs (caffeine and theophylline), between 49% and 65% for the lipophilic drugs (ibuprofen and ketoprofen), and approximately 27% for the hydrophobic drugs (methylprednisolone and hydrocortisone).

Discussion

LUVs Characterization

The LUVs were prepared using natural lipid (SPC) and PBS (adjusted to physiological pH and tonicities) to achieve LUV

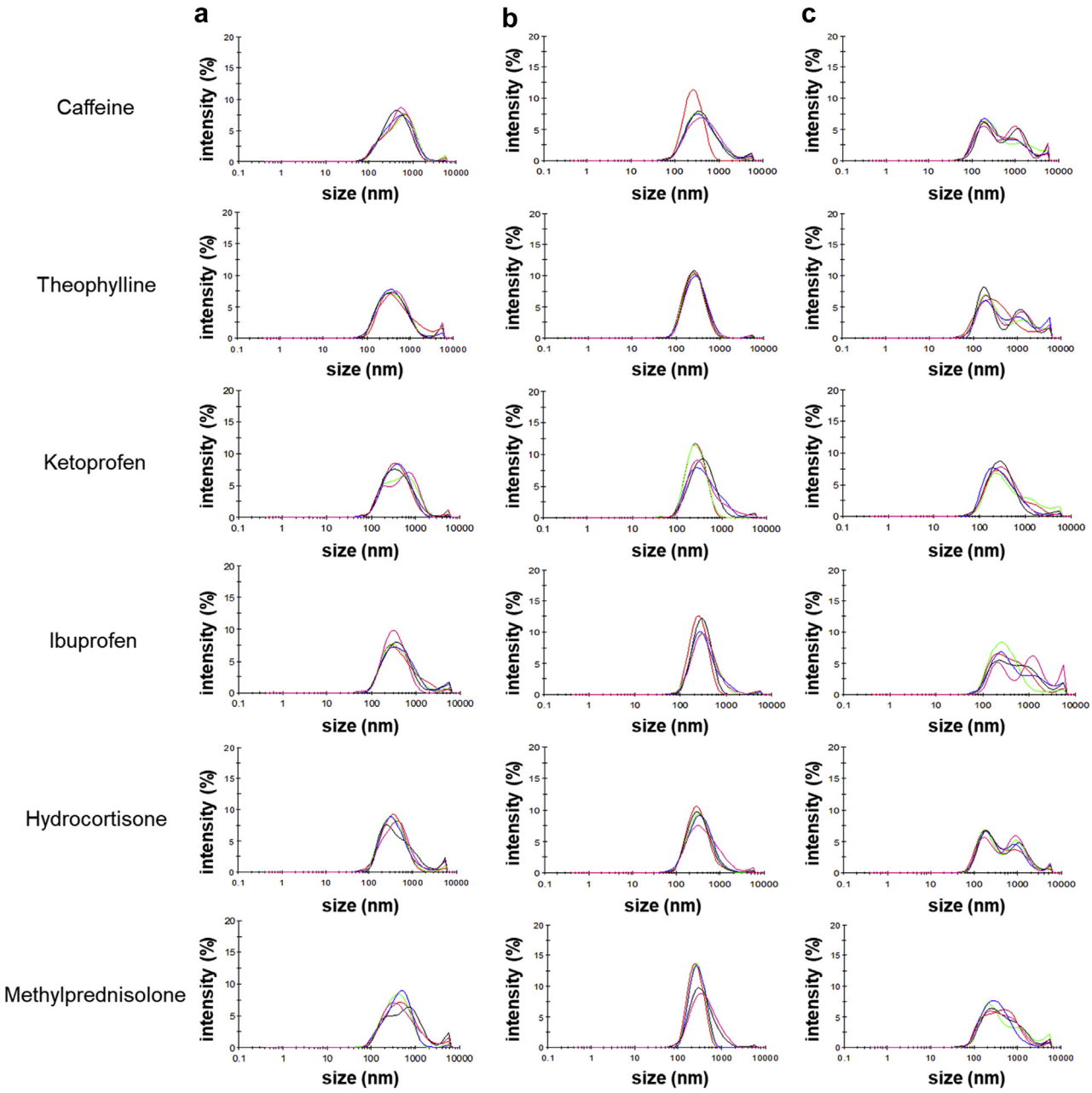

Figure 2. Size distributional changes for drug-loaded LUVs in (a) isotonic condition (ΔmOsm/kg of 3 ± 2 mOsm/kg), (b) low-hypotonic condition (ΔmOsm/kg of 414 ± 19 mOsm/kg), and (c) hypotonic condition (ΔmOsm/kg of 648 ± 19 mOsm/kg). Each line represents the mean size distribution ($n = 2$) measured at 5 different time points within 90 min.

dispersions suitable for nasal administration.[21,22] In relation to liposomal sizes, PI and ZP, the prepared LUV formulations exhibited suitable profiles when compared with other liposomal formulations intended for nasal administration.[13,14,42,43] In agreement with our previous findings,[30] the ZP was found to be slightly more negative for the LUVs prepared in PBS65 compared with PBS300 (Table 3). Although the neutral ZP at higher ionic strength can be expected because of the formation of a thicker ion shell surrounding the liposomes,[44] the larger sizes of LUVs prepared in PBS65 in comparison with PBS300 are difficult to explain. It could be argued that this discrepancy is related to small changes in elasticity of the phospholipid bilayers in environments of different ionic strengths. The prepared LUVs were also found to be suitable carriers to entrap all the drugs with different magnitude of loading. In accordance with their distribution coefficients at pH 7.4 ($\log D_{7.4}$, Table 1) and the literature, hydrophobic drugs (hydrocortisone and methylprednisolone) reached the highest EE into liposomes (between 74% and 85%, respectively), whereas the entrapment was much lower for hydrophilic drugs (close to 25% for caffeine and theophylline).[45] The lipophilic drugs (ibuprofen and ketoprofen) showed a medium-high EE ranging between 41% and 56% (similarly to what has been reported previously by Nii and Ishii).[46] The entrapment was significantly enhanced for LUVs with hydrophilic drugs prepared in PBS65 when compared with PBS300 (caffeine $p = 0.040$, theophylline $p = 0.014$, respectively). This might be related to the increased size of liposomal carriers when prepared in different PBS (Table 3). In our previous study, we

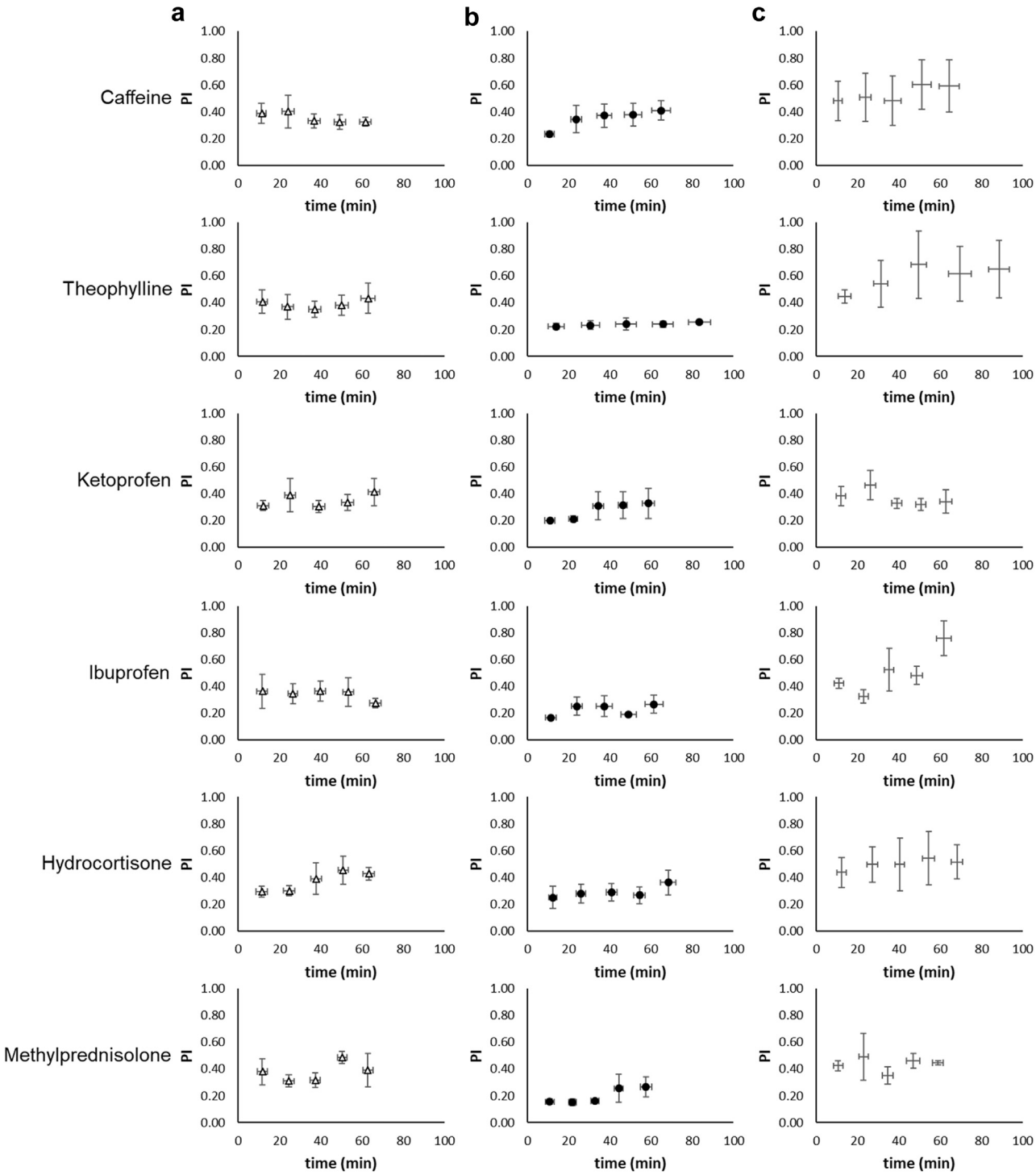

Figure 3. Polydispersity index (PI) changes for drug-loaded LUVs in (a) isotonic condition (ΔmOsm/kg of 3 ± 2 mOsm/kg), (b) low-hypotonic condition (ΔmOsm/kg of 414 ± 19 mOsm/kg), and (c) hypotonic condition (ΔmOsm/kg of 648 ± 19 mOsm/kg). Results represent mean ± SD ($n = 2$).

assumed, due to the lack of available literature on the topic, that the total tonicity of the liposomal formulation should have been primarily influenced by the ionic strength of the solution.[30] In the present work, we measured the tonicity of each of the LUV dispersions (Table 3), and surprisingly, a significant discrepancy in tonicity for LUV dispersions in comparison to plain buffer (Table 2) was found for all formulation tested. As the drug alone did not affect the buffer's tonicity at the experimental condition (Table 4), assuming that at the equilibrium, the tonicity of the inner core of liposomes is equal to the measured tonicity of the LUV dispersion (i.e., external environment), it appears that liposomes themselves acted as strong tonicity agents (the influence on total tonicity accounts for more than 300 mOsm/kg). A very similar trend was observed for empty liposomes (measured tonicity of 718 ± 34 mOsm/kg and 448 ± 22 mOsm/kg when prepared in PBS300 or PBS65, respectively). To the best of our knowledge, this phenomenon has not been described earlier and it might be of extreme importance in liposomal drug research.

Table 4
Regenerated Cellulose Barrier's Resistance to Drug Transport (R_B) of Drug Solutions in Phosphate Buffered Saline

Drugs	Buffer Solution	Drug Concentration (mM)	Tonicity (mOsm/kg)	R_B (10^4 s/cm)
Caffeine	PBS65	2.04 ± 0.03	65 ± 1	1.64 ± 0.03
	PBS300	2.00 ± 0.00	300 ± 2	1.64 ± 0.05
Theophylline	PBS65	1.92 ± 0.03	65 ± 1	1.58 ± 0.05
	PBS300	1.99 ± 0.02	297 ± 1	1.60 ± 0.07
Ketoprofen	PBS65	2.00 ± 0.04	66 ± 2	2.26 ± 0.08
	PBS300	2.00 ± 0.00	298 ± 0	2.08 ± 0.11
Ibuprofen	PBS65	2.03 ± 0.00	68 ± 4	2.14 ± 0.14
	PBS300	2.01 ± 0.00	308 ± 10	2.18 ± 0.15
Hydrocortisone	PBS65	1.02 ± 0.01	66 ± 1	1.92 ± 0.23
	PBS300	1.03 ± 0.02	298 ± 0	2.22 ± 0.17
Methylprednisolone	PBS65	0.26 ± 0.00	64 ± 0	2.03 ± 0.18
	PBS300	0.25 ± 0.00	301 ± 5	2.27 ± 0.34

Results represent mean ± SD ($n = 4$).

Effect of the Ionic Strength on LUVs Sizes

It has been reported previously that LUV sizes can be affected by changes in tonicity of the surrounding environment.[30,47] If the environment surrounding liposomes is hypotonic in comparison to the liposomal core, liposomes have a tendency to increase in size as a result of water influx into the liposomes.[27-29] Photon correlation spectroscopy is a powerful technique applied to quantify liposomal sizes and PI in a dispersion. However, in these experiments, it was difficult to determine an accurate size of the

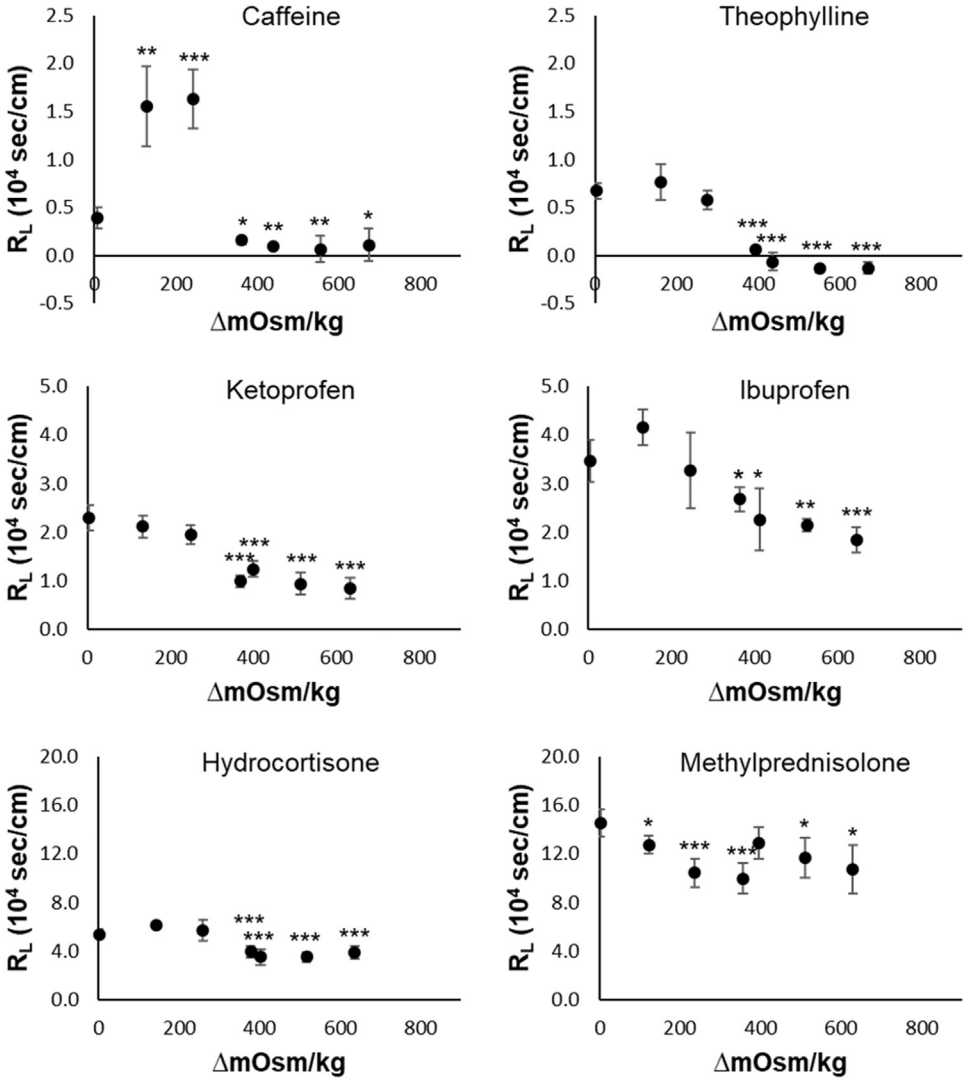

Figure 4. Liposomal bilayer resistance (R_L) to drug transport under the influence of hypotonic environmental changes. The tonicity difference between the inner core and external environment of liposomes are shown as ΔmOsm/kg. Results represent mean ± SD ($n = 4$), and significant difference ($^{*}p \leq 0.050$, $^{**}p \leq 0.010$, $^{***}p \leq 0.001$) in R_L is determined between the hypotonic compared with isotonic condition.

LUVs under the influence of tonicity perturbations. To have a better and clear picture of the effect that hypotonic surrounding environments had on the formulations, LUV dispersions (approx. 710 mOsm/kg) were exposed to 2 buffers of different ionic strengths (300 mOsm/kg and 65 mOsm/kg) and sizes of the liposomes were measured at approximately 15-min intervals for a total period of 90 min. The size distribution of all formulations was rather homogenous (Fig. 2). Interestingly, the dispersions were more homogeneous in the low-hypotonic conditions rather than isotonic conditions (Figs. 2a and 2b). Because ions are capable of neutralizing liposomal surface charges due to ion-shell formation,[44,48-51] it is reasonable to assume that liposomal aggregation is more significant in isotonic conditions than in low-hypotonic conditions because of the surface charge neutralization of liposomes (see also Table 3). When the surrounding liposomal environment was highly hypotonic (ΔmOsm/kg of 648 ± 19 mOsm/kg, Fig. 2c), the size distribution became very heterogeneous. The same trend could be observed for the PI that was significantly increased over time just at the high tonicity gradient (Fig. 3c). The combination of these results clearly indicates that LUVs grew in sizes when exposed to hypotonic environments at the difference of approximately 648 mOsm/kg, whereas smaller differences were not apparent because of the disturbances on the liposomal surfaces, which might have affected the LUVs behavior and the size measurements.

Resistance to Drug Transport Through Regenerated Cellulose Barrier (R_B)

In this work, the kinetics of transport for the investigated drugs through barrier(s) were described by calculating the resistance of each single barrier involved. This was done to better differentiate the role of each barrier involved in the total net transport of drug (Eq. 3) and is essential for a correct interpretation of transport studies that involve liposomes. The R_B was determined by measuring the drug's permeability (Eq. 2) from drug solutions, or in the case of very poorly soluble drugs (hydrocortisone and methylprednisolone), employing aqueous drug suspensions (no liposomes present). As can be seen in Table 4, the lowest R_B was found for caffeine and theophylline, whereas the highest was found for hydrocortisone and methylprednisolone. The reason for the significant discrepancy could to be attributed to the different size (i.e., molecular weight, Table 1) of the molecules. In fact, Equation 5 (adaptation of Fick's first law) can describe the permeability of a drug through a regenerated cellulose barrier as

$$P = \frac{D}{C_d} \cdot \frac{dc}{dx} \tag{5}$$

where D represents the diffusion coefficient and dc/dx is the gradient of concentration between donor and acceptor compartments. From this equation, it is evident that, normalizing the concentration and assuming same thickness of the barrier in all experiments, the differences in permeability (and therefore in resistance to transport) within different drugs through cellulose barriers are solely given by the different diffusion coefficients of each drug. Indeed, D is higher for small compounds such as caffeine (measured diffusivity in similar conditions, 9×10^{-6} cm^2/s[52]) and lower for larger compounds such as ketoprofen (measured diffusivity in similar conditions, 6×10^{-6} cm^2/s[52]).

Resistance to Passive Transport Through Liposomal Barrier (R_L)

The liposomal bilayer of LUVs represents an additive barrier that drug molecules need to cross to reach the acceptor compartment (Fig. 1). To calculate the resistance to drug transport through the phospholipid bilayer (R_L), the permeability of drugs through the regenerated cellulose barrier of LUVs loaded with drug (R_T) needed to be measured and subtracted from R_B (Eq. 4). In isotonic conditions (Fig. 4, ΔmOsm/kg of approx. 0 mOsm/kg), hydrophilic compounds (caffeine and theophylline) exhibit a R_L of approximately 0.4 to 0.7 $\times$ 10^4 s/cm and this resistance rises with the lipophilicity of the compounds (Table 1) up to 14.6 $\times$ 10^4 s/cm for a very hydrophobic compound, methylprednisolone. The higher resistance to transport through the lipid bilayer expressed by hydrophobic compounds in comparison with hydrophilic is not surprising and is due to the fact that the lipophilic compounds are tightly embedded in the lipid bilayers and cannot escape (be released) easily. These results are in agreement with previous findings.[18] Interestingly, for the hydrophilic compounds (caffeine and theophylline) and to a minor but substantial extent, lipophilic acidic drugs (ketoprofen and ibuprofen), a strong reduction in R_L was measured with reduced external ionic strength (increased ΔmOsm/kg, Fig. 4). This is a clear evidence that exposure of drug-loaded LUVs to hypotonic environment is a powerful trigger of drug release. This can be attributed to the stretching of the phospholipid bilayers induced by LUV size enlargements that makes the barrier leakier and drugs can permeate more easily.[29,53] This phenomenon is in agreement with previous findings.[54-56] An alternative hypothesis to explain the increased drug release in hypotonic conditions is the pore formation during liposomes swelling, which can cause a pulsating release of entrapped content.[47,57-59] For caffeine and theophylline, the R_L becomes practically zero (i.e., no resistance to drug transport caused by phospholipid bilayers) when the tonicity differences between the inner core and external environment of LUVs reached around 350 mOsm/kg. Interestingly, R_L increases at the lowest tonicity gradient for caffeine (below 300 mOsm/kg, Fig. 4 upper-left). It can be argued that at low tonicity gradients, the stretching of phospholipid bilayers might be compensated (if not overdriven in the case of caffeine) by the water flux directed inward (i.e., against drug flux), causing therefore an increasing in R_L. For ibuprofen and ketoprofen, the reduction in R_L seemed to be more proportional and reaching a minimum of approximately half of the initial R_L at the highest tonicity gradient (ΔmOsm/kg above 600 mOsm/kg). Interestingly, the release of hydrophobic compounds (hydrocortisone and methylprednisolone) was also positively affected by the hypotonic surrounding environment, however, to a minor extent in comparison with the other compounds tested. At a tonicity gradient above 600 mOsm/kg, the R_L for hydrophobic hydrocortisone and methylprednisolone is reduced by approximately 27% in comparison with isotonic condition. These results are in agreement with our previous findings where we demonstrated that the kinetic of calcein release (hydrophilic marker) from LUVs was more affected by tonicity perturbation in comparison with the lipophilic marker (rhodamine).[30] It is clear that the effect of the environmental tonicity on the release of liposomal drugs needs to be studied to assist in optimization of liposomal formulations destined for nasal administration.

Conclusions

In this work, we have proven that the tonicity of the environment surrounding liposomes plays a crucial role in LUVs' physical characteristics (i.e., size, polydispersity, and surface charge) and drug release profiles. First, we have showed that liposomes themselves significantly affect the total tonicity of the dispersions. Second, we have demonstrated that LUV size and polydispersity increase after exposing liposomes to hypotonic

environment proven them osmotically active. Finally, we have proven that the exposure of drug-loaded LUVs to hypotonic environments reduces R_L and therefore enhances drug release kinetics of both hydrophilic and lipophilic/hydrophobic drugs. The findings have clear implications in the development and optimization of liposomal formulations targeting nasal administration. Moreover, the observed effects can be utilized to tailor the release of liposomal drugs within nasal environment.

Acknowledgment

The authors thank Lipoid (Ludwigshafen, Rheinland-Pfalz, Germany) for their donation of lipids. This project was financed by the University of Tromsø—The Arctic University of Norway. This research did not receive any specific grant from funding agencies in the public, commercial, or not-for-profit sectors.

References

1. Alam MI, Beg S, Samad A, et al. Strategy for effective brain drug delivery. *Eur J Pharm Sci*. 2010;40(5):385-403.
2. Pardridge WM. Drug transport across the blood—brain barrier. *J Cereb Blood Flow Metab*. 2012;32(11):1959-1972.
3. Patel MM, Patel BM. Crossing the blood-brain barrier: recent advances in drug delivery to the brain. *CNS Drugs*. 2017;31(2):109-133.
4. Pardridge WM. The blood-brain barrier: bottleneck in brain drug development. *NeuroRx*. 2005;2(1):3-14.
5. Bourganis V, Kammona O, Alexopoulos A, Kiparissides C. Recent advances in carrier mediated nose-to-brain delivery of pharmaceutics. *Eur J Pharm Biopharm*. 2018;128:337-362.
6. Selvaraj K, Gowthamarajan K, Karri V. Nose to brain transport pathways an overview: potential of nanostructured lipid carriers in nose to brain targeting. *Artif Cells Nanomed Biotechnol*. 2018;46(8):2088-2095.
7. Sood S, Jain K, Gowthamarajan K. Intranasal therapeutic strategies for management of Alzheimer's disease. *J Drug Target*. 2014;22(4):279-294.
8. Chow HS, Chen Z, Matsuura GT. Direct transport of cocaine from the nasal cavity to the brain following intranasal cocaine administration in rats. *J Pharm Sci*. 1999;88(8):754-758.
9. Illum L. Nasal drug delivery-possibilities, problems and solutions. *J Control Release*. 2003;87(1—3):187-198.
10. Agrawal M, Ajazuddin, Tripathi DK, et al. Recent advancements in liposomes targeting strategies to cross blood-brain barrier (BBB) for the treatment of Alzheimer's disease. *J Control Release*. 2017;260:61-77.
11. Bangham AD, Horne RW. Negative staining of phospholipids and their structural modification by surface-active agents as observed in the electron microscope. *J Mol Biol*. 1964;8:660-668.
12. New RRC. Chapter 1: introduction. In: *Liposomes: A Practical Approach*. Oxford: IRL Press; 1990:1-32.
13. Salade L, Wauthoz N, Deleu M, et al. Development of coated liposomes loaded with ghrelin for nose-to-brain delivery for the treatment of cachexia. *Int J Nanomedicine*. 2017;12:8531-8543.
14. Zheng X, Shao X, Zhang C, et al. Intranasal H102 peptide-loaded liposomes for brain delivery to treat Alzheimer's disease. *Pharm Res*. 2015;32(12):3837-3849.
15. Vieira D, Gamarra L. Getting into the brain: liposome-based strategies for effective drug delivery across the blood-brain barrier. *Int J Nanomedicine*. 2016;11:5381-5414.
16. Migliore MM, Ortiz R, Dye S, Campbell RB, Amiji MM, Waszczak BL. Neurotrophic and neuroprotective efficacy of intranasal GDNF in a rat model of Parkinson's disease. *Neuroscience*. 2014;274:11-23.
17. Salade L, Wauthoz N, Vermeersch M, Amighi K, Goole J. Chitosan-coated liposome dry-powder formulations loaded with ghrelin for nose-to-brain delivery. *Eur J Pharm Biopharm*. 2018;129:257-266.
18. di Cagno M, Luppi B. Drug "supersaturation" states induced by polymeric micelles and liposomes: a mechanistic investigation into permeability enhancements. *Eur J Pharm Sci*. 2013;48(4-5):775-780.
19. Goren D, Horowitz AT, Zalipsky S, Woodle MC, Yarden Y, Gabizon A. Targeting of stealth liposomes to erbB-2 (Her/2) receptor: in vitro and in vivo studies. *Br J Cancer*. 1996;74(11):1749-1756.
20. Vingerhoeds MH, Steerenberg PA, Hendriks J, et al. Immunoliposome-mediated targeting of doxorubicin to human ovarian carcinoma in vitro and in vivo. *Br J Cancer*. 1996;74:1023.
21. Homer JJ, Dowley AC, Condon L, El-Jassar P, Sood S. The effect of hypertonicity on nasal mucociliary clearance. *Clin Otolaryngol Allied Sci*. 2000;25(6):558-560.
22. Ohwaki T, Ando H, Kakimoto F, et al. Effects of dose, pH, and osmolarity on nasal absorption of secretin in rats II: histological aspects of the nasal mucosa in relation to the absorption variation due to the effects of pH and osmolarity. *J Pharm Sci*. 1987;76(9):695-698.
23. Majima Y, Harada T, Shimizu T, et al. Effect of biochemical components on rheologic properties of nasal mucus in chronic sinusitis. *Am J Respir Crit Care Med*. 1999;160(2):421-426.
24. Bangham AD, De Gier J, Greville GD. Osmotic properties and water permeability of phospholipid liquid crystals. *Chem Phys Lipids*. 1967;1(3):225-246.
25. Paula S, Volkov AG, Van Hoek AN, Haines TH, Deamer DW. Permeation of protons, potassium ions, and small polar molecules through phospholipid bilayers as a function of membrane thickness. *Biophys J*. 1996;70(1):339-348.
26. Pencer J, White GF, Hallett FR. Osmotically induced shape changes of large unilamellar vesicles measured by dynamic light scattering. *Biophys J*. 2001;81(5):2716-2728.
27. Mui BL, Cullis PR, Evans EA, Madden TD. Osmotic properties of large unilamellar vesicles prepared by extrusion. *Biophys J*. 1993;64(2):443-453.
28. Rutkowski CA, Williams LM, Haines TH, Cummins HZ. The elasticity of synthetic phospholipid vesicles obtained by photon correlation spectroscopy. *Biochemistry*. 1991;30(23):5688-5696.
29. Sun S-T, Milon A, Tanaka T, Ourisson G, Nakatani Y. Osmotic swelling of unilamellar vesicles by the stopped-flow light scattering method. Elastic properties of vesicles. *Biochim Biophys Acta Biomembr*. 1986;860(3):525-530.
30. Wu IY, Škalko-Basnet N, di Cagno MP. Influence of the environmental tonicity perturbations on the release of model compounds from large unilamellar vesicles (LUVs): a mechanistic investigation. *Colloids Surf B Biointerfaces*. 2017;157:65-71.
31. PubChem. pKa value for caffeine. Available at: https://pubchem.ncbi.nlm.nih.gov/compound/2519. Accessed August 8, 2018.
32. Zhu C, Jiang L, Chen T-M, Hwang K-K. A comparative study of artificial membrane permeability assay for high throughput profiling of drug absorption potential. *Eur J Med Chem*. 2002;37(5):399-407.
33. PubChem. pKa value for theophylline. Available at: https://pubchem.ncbi.nlm.nih.gov/compound/2153. Accessed August 8, 2018.
34. PubChem. pKa value for ketoprofen. Available at: https://pubchem.ncbi.nlm.nih.gov/compound/3825. Accessed August 8, 2018.
35. Stein PC, di Cagno M, Bauer-Brandl A. A novel method for the investigation of liquid/liquid distribution coefficients and interface permeabilities applied to the water-octanol-drug system. *Pharm Res*. 2011;28(9):2140-2146.
36. PubChem. pKa value for ibuprofen. Available at: https://pubchem.ncbi.nlm.nih.gov/compound/3672. Accessed August 8, 2018.
37. McCaulley ME, Grush KA. Alzheimer's disease: exploring the role of inflammation and implications for treatment. *Int J Alzheimers Dis*. 2015;2015:515248.
38. Onatibia-Astibia A, Franco R, Martinez-Pinilla E. Health benefits of methylxanthines in neurodegenerative diseases. *Mol Nutr Food Res*. 2017;61(6):1-14.
39. Brodin B, Steffansen B, Uhd Nielsen C. Chapter 3.2: passive diffusion of drug substances: the concepts of flux and permeability. In: *Molecular Biopharmaceutics: Aspects of Drug Characterisation, Drug Delivery and Dosage Form Evaluation*. London: Pharmaceutical Press; 2010:135-152.
40. di Cagno M, Bibi HA, Bauer-Brandl A. New biomimetic barrier Permeapad™ for efficient investigation of passive permeability of drugs. *Eur J Pharm Sci*. 2015;73:29-34.
41. Ghartey-Tagoe EB, Morgan JS, Neish AS, Prausnitz MR. Increased permeability of intestinal epithelial monolayers mediated by electroporation. *J Control Release*. 2005;103(1):177-190.
42. Illum L. Nanoparticulate systems for nasal delivery of drugs: a real improvement over simple systems? *J Pharm Sci*. 2007;96(3):473-483.
43. Yang Z-Z, Zhang Y-Q, Wang Z-Z, Wu K, Lou J-N, Qi X-R. Enhanced brain distribution and pharmacodynamics of rivastigmine by liposomes following intranasal administration. *Int J Pharm*. 2013;452(1-2):344-354.
44. Sabin J, Prieto G, Ruso JM, Hidalgo-Alvarez R, Sarmiento F. Size and stability of liposomes: a possible role of hydration and osmotic forces. *Eur Phys J E Soft Matter*. 2006;20(4):401-408.
45. Xu X, Khan MA, Burgess DJ. Predicting hydrophilic drug encapsulation inside unilamellar liposomes. *Int J Pharm*. 2012;423(2):410-418.
46. Nii T, Ishii F. Encapsulation efficiency of water-soluble and insoluble drugs in liposomes prepared by the microencapsulation vesicle method. *Int J Pharm*. 2005;298(1):198-205.
47. Ahumada M, Calderon C, Alvarez C, Lanio ME, Lissi EA. Response of unilamellar DPPC and DPPC:SM vesicles to hypo and hyper osmotic shocks: a comparison. *Chem Phys Lipids*. 2015;188:54-60.
48. Bordi F, Cametti C. Salt-induced aggregation in cationic liposome aqueous suspensions resulting in multi-step self-assembling complexes. *Colloids Surf B Biointerfaces*. 2002;26(4):341-350.
49. Carrión FJ, De La Maza A, Parra JL. The influence of ionic strength and lipid bilayer charge on the stability of liposomes. *J Colloid Interface Sci*. 1994;164(1):78-87.
50. Helm CA, Laxhuber L, Lösche M, Möhwald H. Electrostatic interactions in phospholipid membranes I: influence of monovalent ions. *Colloid Polym Sci*. 1986;264(1):46-55.
51. Narenji M, Talaee MR, Moghimi HR. Investigating the effects of size, charge, viscosity and bilayer flexibility on liposomal delivery under convective flow. *Int J Pharm*. 2016;513(1-2):88-96.

52. di Cagno MP, Clarelli F, Våbenø J, et al. Experimental determination of drug diffusion coefficients in unstirred aqueous environments by temporally resolved concentration measurements. *Mol Pharm*. 2018;15(4):1488-1494.
53. Borochov A, Borochov H. Increase in membrane fluidity in liposomes and plant protoplasts upon osmotic swelling. *Biochim Biophys Acta Biomembr*. 1979;550(3):546-549.
54. Ertel A, Marangoni AG, Marsh J, Hallett FR, Wood JM. Mechanical properties of vesicles. I. Coordinated analysis of osmotic swelling and lysis. *Biophys J*. 1993;64(2):426-434.
55. Kure T, Sakai H. Transmembrane difference in colloid osmotic pressure affects the lipid membrane fluidity of liposomes encapsulating a concentrated protein solution. *Langmuir*. 2017;33(6):1533-1540.
56. Polozov IV, Anantharamaiah GM, Segrest JP, Epand RM. Osmotically induced membrane tension modulates membrane permeabilization by class L amphipathic helical peptides: nucleation model of defect formation. *Biophys J*. 2001;81(2):949-959.
57. Alam Shibly Sayed U, Ghatak C, Sayem Karal Mohammad A, Moniruzzaman M, Yamazaki M. Experimental estimation of membrane tension induced by osmotic pressure. *Biophys J*. 2016;111(10):2190-2201.
58. Oglecka K, Rangamani P, Liedberg B, Kraut RS, Parikh AN. Oscillatory phase separation in giant lipid vesicles induced by transmembrane osmotic differentials. *Elife*. 2014;3:e03695.
59. Taupin C, Dvolaitzky M, Sauterey C. Osmotic pressure induced pores in phospholipid vesicles. *Biochemistry*. 1975;14(21):4771-4775.

Paper III

European Journal of Pharmaceutical Sciences 138 (2019) 105026

Contents lists available at ScienceDirect

European Journal of Pharmaceutical Sciences

journal homepage: www.elsevier.com/locate/ejps

Interpreting non-linear drug diffusion data: Utilizing Korsmeyer-Peppas model to study drug release from liposomes

Iren Yeeling Wu[a], Sonali Bala[a], Nataša Škalko-Basnet[a], Massimiliano Pio di Cagno[a,b,*]

[a] Drug Transport and Delivery Research Group, Department of Pharmacy, University of Tromsø The Arctic University of Norway, Universitetsvegen 57, 9037 Tromsø, Norway

[b] Department of Pharmacy, Faculty of Mathematics and Natural Sciences, University of Oslo, Sem Sælands vei 3, 0371 Oslo, Norway

ARTICLE INFO

Keywords:
Large unilamellar vesicles
Cholesterol
Drug release kinetics
Osmotic stress
Permepad®
Korsmeyer-Peppas model

ABSTRACT

The aim of this work was to clarify the dynamics behind the influence of ionic strength on the changes in drug release from large unilamellar vesicles (LUVs). For this purpose, we have investigated the transport of two different model drugs (caffeine and hydrocortisone) formulated into liposomes through different types of barriers with different retention properties (regenerated cellulose and the newly introduced biomimetic barrier, Permeapad®). Drug release from liposomes was studied utilizing the standard Franz diffusion cells. LUV dispersions were exposed to the isotonic, hypotonic and hypertonic environment (difference of 300 mOsm/kg between the initial LUVs and the environment) and experimental data treated with both linear and non-linear (Korsmeyer-Peppas) regression models. To alter the rigidity of the liposomal membranes, cholesterol was introduced in the liposomal barriers (up to 25% w/w). Korsmeyer-Peppas model was proven to be suited to analyse experimental data throughout the experimental time frame, providing important additive information in comparison to standard linear approximation. The obtained results are highly relevant as they improve the interpretation of drug release kinetics from LUVs under osmotic stress. Moreover, the findings can be utilized in the development of liposomal formulations intended for nose-to-brain targeted drug delivery.

1. Introduction

Liposomes are lipid-based vesicles with a nanometric size range (Bangham and Horne, 1964; New, 1990). Since liposomes were first described in the 1960s (Bangham and Horne, 1964), they have been extensively studied as drug delivery systems for both hydrophilic and lipophilic drugs (Allen and Cullis, 2013; Li et al., 2019). Nasally administered liposomal drug formulations have shown promising potentials for the treatment of some brain diseases such as Alzheimer's and Parkinson's disease (Lai et al., 2013; Vieira and Gamarra, 2016). However, to achieve maximal therapeutic benefits, controlled release from the liposomes in the nasal cavity is required to obtain optimal available dose at the target site *in vivo* (Bourganis et al., 2018; Lai et al., 2013).

One important parameter that is often underestimated in the development of formulations for nasal drug delivery is the variability of physiological conditions at the administration site. For example, under normal physiological conditions, the nasal mucus tonicity is approximately 300 mOsm/kg (Pedersen et al., 2007). However, this value can change considerably as the nasal mucosa is rather sensitive to the external environment such as air humidity and temperature (Quraishi et al., 1998). For instance, hyperventilation in dry air can increase the human nasal tonicity up to 450 mOsm/kg (Pedersen et al., 2007). Variation in the ionic strength at the administration site is highly relevant for liposomes since they consist of semi-permeable membrane, and are therefore, highly sensitive to osmosis (Bangham et al., 1967; Paula et al., 1996; Pencer et al., 2001). To predict performance of liposomes *in vivo*, good *in vitro* models that can determine the release kinetics from liposomes at the early stage of the liposomal drug development process are necessary (Solomon et al., 2017; Wacker, 2017).

Abbreviations: EE, entrapment efficiency; hypo, hypotonic environment; hyper, hypertonic environment; iso, isotonic environment; K, transport constant; LUVs, large unilamellar vesicles; M_t/M_∞, fractional permeated drug; n, transport exponent; PBS, phosphate buffered saline; PI, polydispersity index; P_L, permeability through the liposomal bilayer; R^2adj, adjusted correlation coefficient; R_B, resistance to drug transport through the barrier; R_L, resistance to drug transport through liposomal bilayer; R_T, total resistance to drug transport; SD, standard deviation; SPC, soy-phosphatidylcholine; t, time; ZP, ζ-potential

* Corresponding author at: Drug Transport and Delivery Research Group, Department of Pharmacy, University of Tromsø The Arctic University of Norway, Universitetsvegen 57, 9037 Tromsø, Norway.

E-mail address: m.p.d.cagno@farmasi.uio.no (M.P. di Cagno).

https://doi.org/10.1016/j.ejps.2019.105026
Received 6 June 2019; Received in revised form 10 July 2019; Accepted 29 July 2019
Available online 30 July 2019

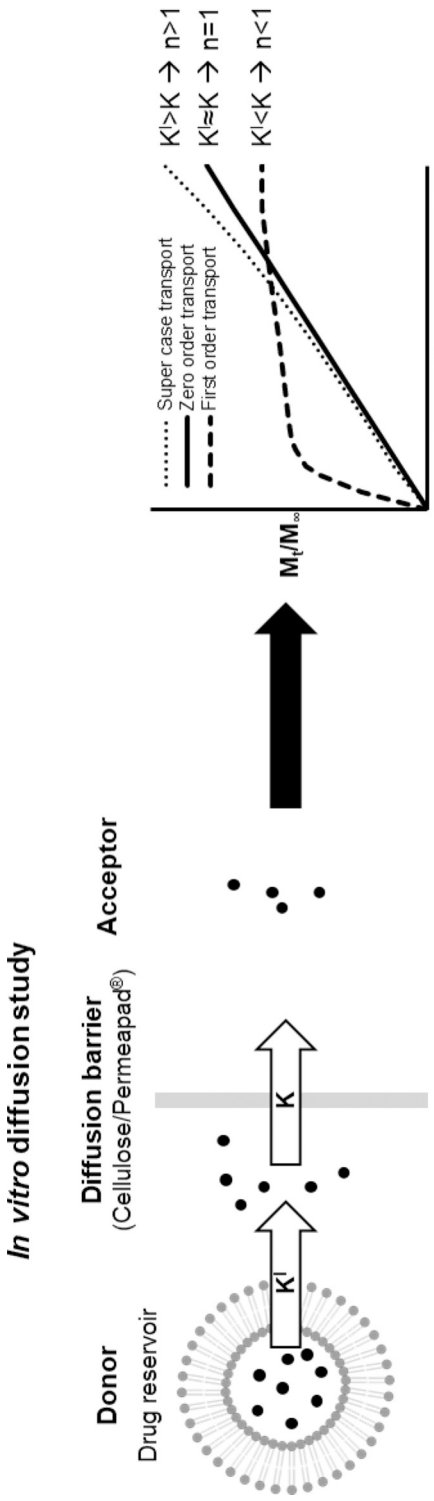

Fig. 1. Schematic representation of the *in vitro* diffusion study using the dynamic dialysis method. The amount of drug accumulated in the acceptor compartment is directly influenced by the drug release rate from liposome (K^l) and the drug transport rate through a diffusion barrier (K). The mechanism of drug release from liposomes can be defined by the transport exponent (n), obtained from the order of the fitted curve according to the Korsmeyer-Peppas equation.

Currently, there are no standard methods for studying drug release from liposomes *in vitro* (Nothnagel and Wacker, 2018; Solomon et al., 2017; Wacker, 2017). The proposed methods are based on separating the dissolved fraction (released drug) from the undissolved fraction (liposomal drug) (Nothnagel and Wacker, 2018). Some of the most common methods applied to liposomes are filtration, ultracentrifugation, solid phase extraction, and dialysis-based methods (Nothnagel and Wacker, 2018). The dialysis-based methods utilize the drug's diffusion across barriers to separate liposomal drug from released drug (Solomon et al., 2017). The liposomal formulation is placed in the donor compartment which is separated from the acceptor compartment by a barrier that can exhibit low retention (*e.g.* dialysis barrier) or high retention (*e.g.* biomimetic, biologic barrier) to drug permeation (Nothnagel and Wacker, 2018). Disadvantages regarding the dialysis-based methods are related to violation of sink condition (Solomon et al., 2017), and the fact that drug released from liposomes needs to cross an additional barrier before being quantified (Fig. 1) (Nothnagel and Wacker, 2018; Wacker, 2017). On the other hand, dialysis-based methods are convenient, cost-effective and simple. Consequently, the dialysis-based devices have been implemented into USP dissolution apparatuses (*e.g.* glass basket, dispersion releaser, flow-through), and used in the development of *in situ* methods (Nothnagel and Wacker, 2018; Solomon et al., 2017; Tang et al., 2019; Yuan et al., 2017). It has to be mentioned that the improved dialysis-based methods are still limited by the barrier properties that separates the liposomal drug from released drug. Therefore, more processing of the diffusion data is still required for correct interpretation of the release mechanism from liposomes (Jain and Jain, 2016; Wacker, 2017).

The most common way to treat diffusion data is by simple zero order mass transport kinetic (Brandl et al., 2007; Brodin et al., 2010; Nothnagel and Wacker, 2018). In both previous studies (Wu et al., 2017; Wu et al., 2019), we applied a zero order model to interpret the mass transport data. The release from liposomes was calculated by using a reference experiment of free drug solution (Wu et al., 2019). We observed that the release kinetics from liposomes were altered due to tonicity perturbations in the external environments (*i.e.* uneven ionic strength within inner core and external environment of liposomes). Moreover, we noticed that when the osmotic stress was applied, the drug transport profiles through regenerated cellulose barrier showed deviations from linearity, indicating possible modifications of the drug release kinetics from the liposomes over time. In such situations, the non-linear regression models for data fitting could have been applied to analyse the diffusion data (Jain and Jain, 2016).

The non-linear regression models such as Higuchi and Korsmeyer-Peppas are the two most applied mathematical models to interpret non-linear diffusion profiles (Costa and Sousa Lobo, 2001; Jain and Jain, 2016). The Korsmeyer-Peppas model has previously been successfully used to describe the drug release kinetics from liposomes (Haghiralsadat et al., 2018; Jain and Jain, 2016). In this study, experimental data from the dynamic dialysis studies are fitted to Eq. (1) (named the Korsmeyer-Peppas equation);

$$\frac{M_t}{M_\infty} = K \bullet t^n \tag{1}$$

In this equation, M_t/M_∞ represents the fractional permeated drug, t is the time, K is the transport constant (dimension of time^{-1}), and n is the transport exponent (dimensionless). The release constant K provides mostly information on the drug formulation such as structural characteristics of the nanocarriers, whereas n is important since it is related to the drug release mechanism (*i.e.* Fickian diffusion or non-Fickian diffusion). In the case of liposomes and assuming sink conditions, the flux of the drug (j) through a low retention barrier (*e.g.* regenerated cellulose) of constant thickness (x) can be described by Eq. (2) (simplified Fick's first law);

$$j = D\frac{(c_d^0 - c_a)}{x} \quad (2)$$

In this equation, c_d^0 is the freely dissolved unentrapped drug concentration outside liposomes in the donor compartment, c_a the acceptor drug concentration and D is the diffusion coefficient. According to this model, the net flux of drug through the barrier is the result of two diffusion mechanisms (Fig. 1). One is the diffusion of drug molecules from the donor compartment to the acceptor compartment (experimentally measured K, Fig. 1). The second is the diffusion through the phospholipid bilayer of liposomes that is dependent on the liposomal release rate (K^I, Fig. 1). In the case where $K \approx K^I$, the gradient of concentration (driving force of the diffusion) should be constant, giving as result of data fitting an n equal (or close) to 1 (zero-order transport kinetic, non-Fickian diffusion). If n is lower than 1 ($n < 1$), this indicates a reduced concentration gradient over time (first-order/pseudo first-order kinetic, Fig. 1). In the last scenario possible, the gradient of concentration ($(c_d^0\text{-}c_a)/x$) is increasing over time, producing a positive deviation from linearity of mass transport profiles. This anomalous behaviour (associated to $n > 1$) is generally called "super case" (Costa and Sousa Lobo, 2001; Jain and Jain, 2016).

Under these premises, in this work, caffeine and hydrocortisone (hydrophilic and a lipophilic drug, respectively) were the chosen drugs to be formulated into large unilamellar vesicle (LUV) dispersions of controlled size and tonicity. Drug transport studies were performed employing two different types of barriers; one with a low retention (regenerated cellulose) and another with a high retention (Permeapad® (Di Cagno et al., 2015)). Moreover, LUV compositions were altered by the addition of different amount of cholesterol (from 0 up to 25% w/w) to increase liposomal barrier rigidity. To evaluate the influence of osmotic stress on drug release kinetics from liposomes, liposomal dispersions were exposed to environment of different ionic strengths. The obtained experimental data were analysed by the means of linear and non-linear (Korsmeyer-Peppas) regression models. The results obtained from this study might provide a new insight into the drug release mechanism from liposomes, and might be relevant for the development of liposomal drug formulations intended for nose-to-brain drug delivery.

2. Materials and methods

2.1. Materials

Caffeine, hydrocortisone, disodium hydrogen phosphate dihydrate ($Na_2HPO_4{\cdot}2H_2O$), sodium chloride (NaCl), sodium hydroxide (NaOH), sodium dihydrogen phosphate monohydrate ($NaH_2PO_4{\cdot}H_2O$), chloroform and methanol were purchased from Sigma-Aldrich Chemie GmbH (Steinheim, Germany). Lipoid S100 (SPC, soy-phosphatidylcholine > 94%) was kindly provided from Lipoid GmbH (Ludwigshafen, Germany) and Permeapad® barriers from InnoME GmbH (Espelkamp, Germany).

2.2. Preparation of phosphate buffered saline (PBS)

PBS of pH 7.4 and 65 mOsm/kg (namely PBS65) was prepared according to Wu et al. (2017). The measured osmolality (Semi-Micro Osmometer Model 4602, Knauer, Berlin, Germany) and pH (SensION™ + PH31 pH meter, Hach, Barcelona, Spain) of the different PBS used in this study are represented in Table 1. To create isotonic PBS (namely PBSiso that exhibited same tonicity as the LUVs, approx. 400 mOsm/kg), 0.05 g of NaCl was dissolved in1 L of PBS65. For the preparation of hypertonic PBS (PBShyper), 0.10 g of NaCl was dissolved into 1 L of PBS65 (tonicity of approx. 700 mOsm/kg). Droplets of NaCl dissolved in PBS65 (concentration of 200 g/L) were added to PBS65 in order to adjust its tonicity to PBShypo's tonicity (approx. 100 mOsm/kg).

2.3. Preparation of LUVs

LUV dispersions were prepared following a method previously described (Wu et al., 2017). In the case of cholesterol-LUVs (11 and 25% w/w), solutions of SPC/cholesterol (ratio of 9:1 w/w or 4:1 w/w) in chloroform were used as organic phase. LUV formulations containing caffeine were prepared by dissolving the drug in the PBS65 (2 mM), whereas in the case of hydrocortisone, the drug was dissolved in the organic phase together with lipids.

2.4. Size, zeta potential and entrapment efficiency characterization

LUV dispersions were diluted with PBS65 (same buffer used to prepare the LUVs) 1:100 (v/v) and filtered through polyether sulfone membranes (0.2 µm pore size, VWR International, Radnor, USA) prior to size measurement. For the determination of the electrokinetic potential (ZP) on liposomes surface, LUV dispersions were diluted 1:20 (v/v) with freshly filtrated deionized water (0.2 µm pore size filter) and analysis conducted at room temperature (23–25 °C) using the DTS1070 cell (Malvern, Worcestershire, UK). The liposomal size and ZP were measured using a Zetasizer Nano Zen 2600 (25 °C, Malvern, Worcestershire, UK) as previously described (Wu et al., 2019). To determine the entrapment efficiency (EE), drug-loaded LUVs were separated from the unentrapped drug by ultracentrifugation (200,000g, 10 °C, 30 min, Beckman model L8-70M with SW 60 Ti rotor, Beckman Instruments, California, USA) (Wu et al., 2019). The drug concentrations in both LUVs and supernatant (representing unentrapped drug concentration) were quantified spectroscopically (Spectra Max 190 Microplate, Spectrophotometer Molecular devices, Sunnyvale, USA) using wavelengths at 273 and 247 nm for caffeine and hydrocortisone, respectively. Two samples for each batch of formulations were measured minimum three times. Experiments were repeated in minimum duplicates ($n \geq 2$).

2.5. In vitro diffusion study

The *in vitro* diffusion studies of caffeine and hydrocortisone were performed using standard Franz diffusion cells (0.64 cm^2 diffusion area jacketed flat ground joint, PermeGear diffusion cells and systems, Hellertown, USA) following a previously described method (Wu et al., 2019). The acceptor compartment was filled with 5 mL PBS following Table 1. Regenerated cellulose (Visking dialysis tubing MWCO 12–14 kDa, Medicell Membranes Ltd., London, UK), or alternatively, Permeapad® (InnoME GmbH, Espelkamp, Germany) was used as diffusion barrier and experiments were conducted at 35 °C (Julabo 200F heating circulator, Julabo Inc., Allentown, USA). At time zero (start of the experiment), 0.3 mL of PBS (same composition as acceptor buffer) was topped with 0.5 mL of LUV dispersion (2 mM total drug concentration) in the donor compartment. As reference experiments, drug solution (caffeine, 2 mM) or suspension (hydrocortisone, 1 mM, thermodynamic solubility) in PBS65 were also analysed. Aliquots of 0.5 mL were withdrawn from the acceptor compartment and replaced with equal volumes of the respective PBS (with same tonicity) every 30 min over a period of 4 h.

2.6. Data analysis

2.6.1. Resistance to drug transport determination (R)

The resistance to drug transport through liposomal bilayer (R_L,) was calculated according to Wu et al. (2019). In brief, the initial part of diffusional curves (up to 2.5 h) was used to calculate the drug flux (j) through the diffusion barrier, which was supposed to be constant during the experiment since the sink conditions were kept. The apparent permeability (P) was determined by normalizing the flux over the total initial concentration (c_d) (see Eq. (3)):

Table 1
Experimentally determined osmolality and pH for all LUV dispersions and PBS solutions used in the *in vitro* study. Results represent mean ± standard deviation ($n = 2$).

LUVs	Cholesterol (% of lipid weight)	Initial LUVs osmolality (mOsm/kg)	Buffer type	PBS osmolality (mOsm)	PBS pH
Caffeine	0	420 ± 11	PBShypo	119 ± 10	7.5 ± 0.1
			PBSiso	418 ± 10	7.3 ± 0.0
			PBShyper	718 ± 12	7.2 ± 0.0
	11	392 ± 12	PBShypo	95 ± 16	7.6 ± 0.0
			PBSiso	386 ± 5	7.3 ± 0.0
			PBShyper	693 ± 23	7.2 ± 0.0
	25	388 ± 4	PBShypo	88 ± 8	7.5 ± 0.0
			PBSiso	393 ± 4	7.3 ± 0.0
			PBShyper	692 ± 8	7.2 ± 0.0
Hydrocortisone	0[a]	383 ± 5	PBShypo	83 ± 5	7.6 ± 0.0
			PBSiso	384 ± 5	7.3 ± 0.0
			PBShyper	683 ± 5	7.2 ± 0.0
	11	405 ± 5	PBShypo	105 ± 5	7.6 ± 0.0
			PBSiso	405 ± 5	7.3 ± 0.0
			PBShyper	705 ± 5	7.2 ± 0.0
	25	383 ± 19	PBShypo	86 ± 16	7.6 ± 0.0
			PBSiso	385 ± 16	7.3 ± 0.0
			PBShyper	687 ± 15	7.2 ± 0.0

[a] n = 3.

$$P = \frac{j}{c_d} \quad (3)$$

The resistance to drug transport through liposomal bilayer (R_L) (*i.e.* the reciprocal function of permeability through the liposomal bilayer, $1/P_L$) was calculated from the total resistance to drug transport (R_T, measured in the liposomal dispersion experiments) and from the resistance to drug transport through the barrier (R_B, measured in drug solution experiments) by Eq. (4):

$$R_L = R_T - R_B \quad (4)$$

2.6.2. Non-linear regression analysis (Korsmeyer-Peppas model)

Drug transport constants (K) and transport exponents (n) of the different liposomal formulations were determined by fitting of the *in vitro* diffusion data to the Korsmeyer-Peppas equation (see Eq. (1)) using the add-in DDSolver program (China Pharmaceutical University, Nanjing, China). Microsoft Office Excel (Microsoft Corporation, Redmond, USA) was used as built-in module of the DDSolver. The K and n were determined in the range of M_t/M_∞ 0–60% (Costa and Sousa Lobo, 2001).

2.7. Stability study

LUVs containing 0, 11 and 25% w/w cholesterol were prepared for both model drugs (caffeine and hydrocortisone) in duplicates ($n = 2$) as described in Section 2.3. Each batch was divided into two aliquots and stored in the fridge (at 6 °C) and at room temperature (at 22 °C) away from light sources for 65 days in clear polypropylene tubes (VWR® High-Performance centrifuge tubes, VWR International, Radnor, USA). Samples were periodically withdrawn (72 h, 14, 35 and 65 days after preparation) and analysed. The stability of liposomal dispersions was evaluated in terms of tonicity, vesicle size distribution, ZP and EE (analysis performed as described in Sections 2.2 and 2.4). Each sample was measured minimum four times.

2.8. Statistical data evaluation

Student's *t*-test was used to determine the significance of difference between means of different data sets. Differences were considered significant for $p \leq 0.050$.

3. Results

3.1. Liposome characterization

The general characteristics of liposomes used in the *in vitro* study are presented in Tables 1 and 2. The LUV dispersions exhibited total initial tonicity of around 400 mOsm/kg (Table 1). The mean sizes of liposomes were between 236 and 374 nm (Table 2). Incorporation of cholesterol into the LUVs increased the mean sizes and polydispersity for caffeine-LUVs ($p \leq 0.010$ and 0.001, respectively), and similarly for hydrocortisone-LUVs with 25% w/w cholesterol (PI, $p = 0.000$). All LUVs

Table 2
Measured size (average diameter), polydispersity index (PI), ζ-potential (ZP) and entrapment efficiency (EE) for LUV dispersions used in the *in vitro* release study. Results represent mean ± standard deviation (n = 2).

LUVs	Cholesterol (% of lipid weight)	Size (nm)	PI	ZP (mV)	EE (%)
Caffeine	0	236 ± 36	0.25 ± 0.02	−3.7 ± 1.0	12 ± 1
	11	289 ± 55*	0.34 ± 0.04*	−3.0 ± 1.0	11 ± 2
	25	374 ± 80**	0.45 ± 0.05**	−3.5 ± 1.1	10 ± 1**
Hydrocortisone	0[a]	246 ± 30	0.25 ± 0.01	−3.5 ± 1.0	68 ± 5
	11	248 ± 38	0.24 ± 0.02	−4.1 ± 1.1	60 ± 3**
	25	261 ± 47	0.35 ± 0.03**	−5.2 ± 1.1	51 ± 3**

* $p \leq 0.050$.
** $p \leq 0.001$ when compared to the respective formulation without cholesterol.
[a] n = 3.

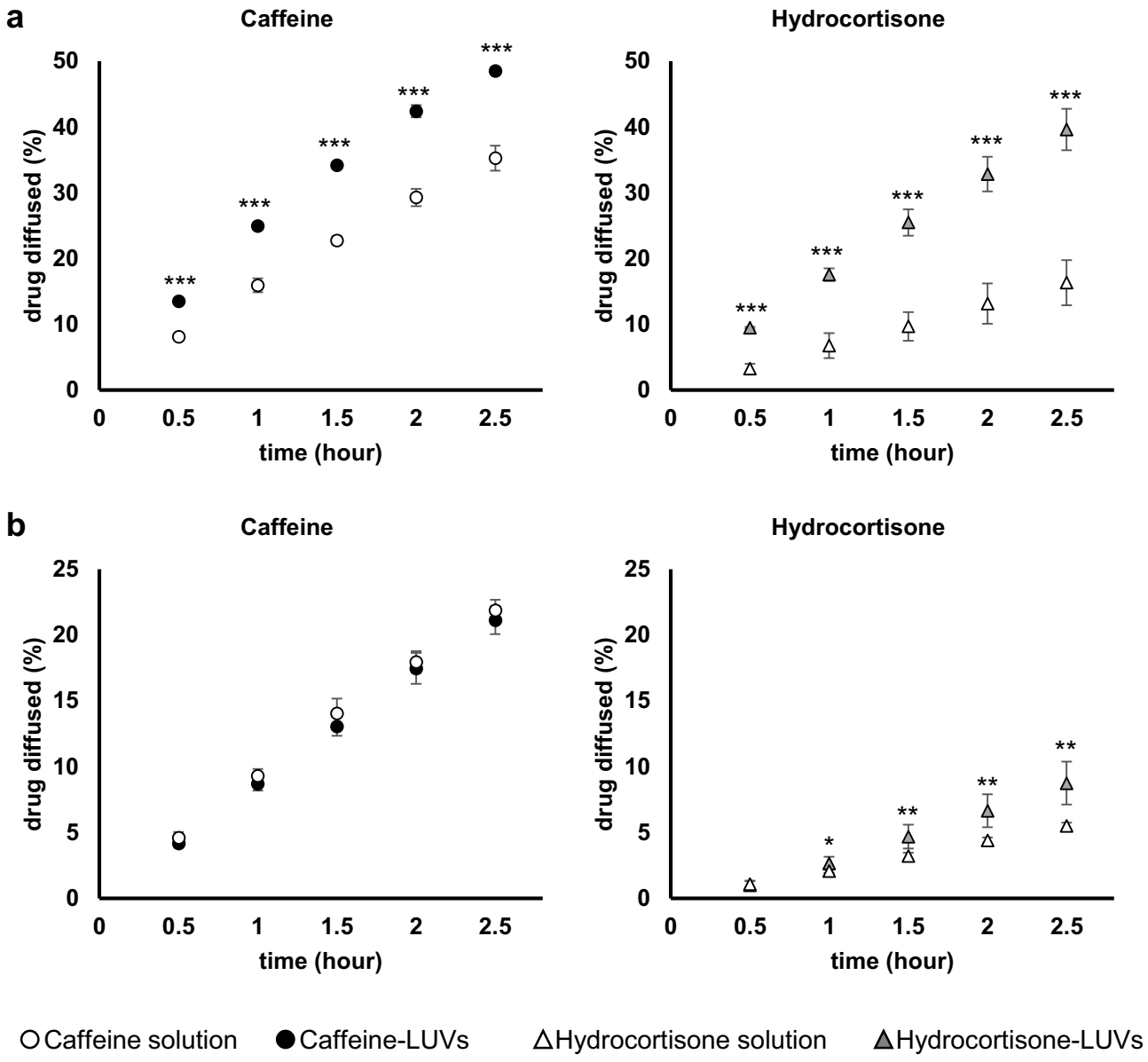

Fig. 2. *In vitro* diffusion study of caffeine (○) and hydrocortisone (Δ) from solutions (filled symbols) and LUV dispersions (0% w/w cholesterol, empty symbols) through regenerated cellulose (a) or, alternatively, Permeapad® (b) as barriers in isotonic conditions. Results represent the mean ± standard deviation ($n = 3$, $^{*}p \leq 0.050$, $^{**}p \leq 0.010$, $^{***}p \leq 0.001$).

exhibited almost neutral surface charges. The EE was approximately 11% for caffeine-LUVs and considerably higher for hydrocortisone-LUVs (51–68%). The EE decreased significantly with increased amount of incorporated cholesterol especially for hydrocortisone-LUVs ($p \leq 0.001$).

3.2. *In vitro diffusion study*

3.2.1. *Drug diffusion studies*

In Fig. 2, the diffusion profiles of caffeine and hydrocortisone in aqueous solution as well as in liposomal dispersions (0% w/w cholesterol) are reported for both regenerated cellulose and Permeapad® barriers. As it can be seen, the drug diffusion profiles through the different barriers varied accordingly to the drug used; the formulation (aqueous solution or liposomal dispersion) and the barrier (regenerated cellulose or Permeapad®). Specifically, the amount of diffused drug was significantly higher for caffeine than for hydrocortisone for both barriers. For both drugs, the total amount of diffused drug after 2.5 h was significantly higher ($p < 0.000$) from solution in comparison to LUV dispersion when regenerated cellulose was employed as the barrier (Fig. 2a, 49 ± 1 *vs* 35 ± 2% for caffeine and 40 ± 3 *vs* 16 ± 3% for hydrocortisone, respectively). Similarly, the total amount of accumulated hydrocortisone in the acceptor medium was significantly higher for drug solutions in comparison to the liposomal formulations (cumulative diffused after 2.5 h, 9 ± 2 *vs* 6%, $p = 0.004$) when Permeapad® was employed as barrier (Fig. 2b right). Interestingly, when Permeapad® was employed (Fig. 2b, lower-left), the amount of caffeine accumulated in the acceptor medium from solution and liposomal dispersion was the same.

3.2.2. *R_L under the influence of changed external environments*

In Fig. 3, the resistances to drug transport through liposomal bilayer (R_L) are reported for all the formulations prepared, for both drugs (caffeine in Fig. 3a and hydrocortisone in Fig. 3b, respectively) and two different types of barriers (regenerated cellulose and Permeapad®). From these data, it appeared that the ionic strength of external

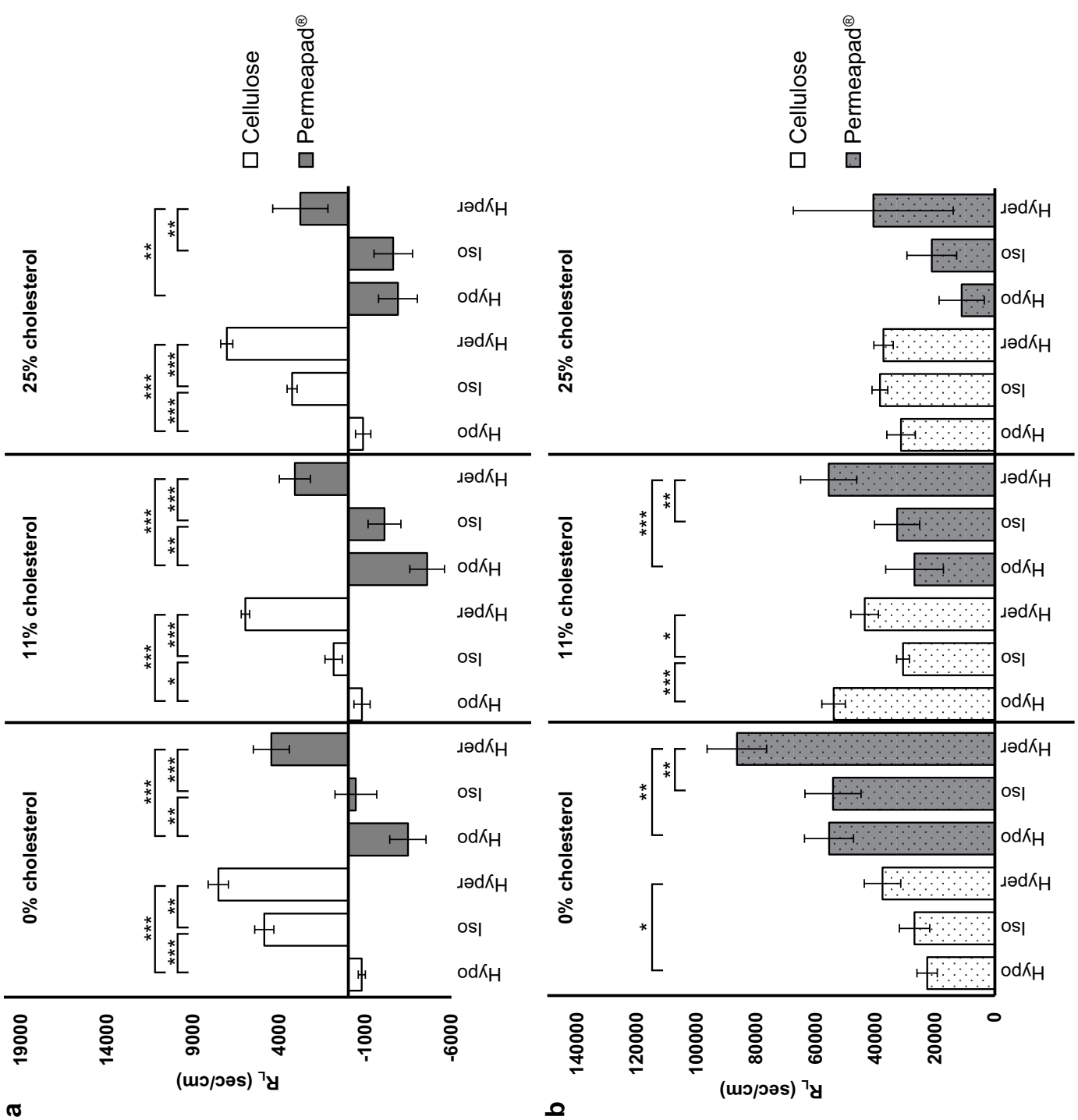

(caption on next page)

Fig. 3. Resistance to drug transport through liposomal bilayers (R_L) containing various amount of cholesterol (0, 11 and 25% w/w) for caffeine (a) or hydrocortisone (b). Diffusion experiments were carried out employing regenerated cellulose (white bars) or, alternatively, Permeapad® (grey bars) barriers and exposing the LUV dispersions to isotonic, hypotonic and hypertonic environments (tonicity difference of 0 and ± 300 mOsm/kg within inner core of liposomes and external environment), respectively. Results represent the mean ± standard deviation (n = 3, *$p \leq 0.050$, **$p \leq 0.010$, ***$p \leq 0.001$).

environment had a remarkable impact on R_L. Specifically, R_L was lowest when caffeine-LUVs were exposed to hypotonic environments, medium in isotonic and significantly higher level for hypertonic environment (Fig. 3a). For hydrocortisone-LUVs (Fig. 3b), the R_L values were considerably higher in comparison to the caffeine-LUVs in all circumstances. Similarly to caffeine-LUVs, the R_L was found to be lower for hypotonic/isotonic environment and significantly ($p < 0.050$) higher in hypertonic environment. The incorporation of cholesterol into the liposomal membrane seemed not to significantly affect R_L of hydrocortisone, whereas, for caffeine, a trend indicating reduction of R_L with growing concentration of cholesterol was observed (white bars). The employment of a biomimetic barrier such as Permeapad® (grey bars) resulted in a slight reduction in R_L absolute values for caffeine in comparison to regenerated cellulose even though the trend at different external environmental tonicity was respected. The same was observed for hydrocortisone, but in this case, a significant reduction of R_L was observed with increasing concentration of cholesterol (Fig. 3a–b).

3.2.3. Non-linear data fitting using Korsmeyer-Peppas model

The *in vitro* diffusion data obtained in this study were fitted according to the Korsmeyer-Peppas equation, Eq. (1). For all data sets, the correlation coefficient (R^2) was rather high (min. 0.96 up to 1.00, data are shown in Supplementary material, Figs. A.1–2) indicating a good correlation within experimental data and Eq. (1). From the data fitting, the transport constants (K, Fig. 4) and transport exponents (n, Fig. 5) were determined. The K values were much higher for caffeine (ranged between 8 and 25, Fig. 4a) in comparison to hydrocortisone (from 1 to 8, Fig. 4b). It is worth mentioning that K values were significantly different for regenerated cellulose (white bars) and Permeapad® (grey bars) and these differences were higher for hydrocortisone than for caffeine.

As already observed for R_L, a clear correlation between K and environmental ionic strength was found. Specifically, the higher ionic strength in the external environment, the lower were the K value (Fig. 4, 0% w/w cholesterol). This phenomenon was more evident when using regenerated cellulose (white bars) as a barrier rather than Permeapad® (grey bars). In fact, no significant difference was determined in K values between the hypotonic and isotonic environments employing Permeapad® as barrier for both drugs. Interestingly, the experiments carried out on the regenerated cellulose barrier maintained a similar trend for caffeine-LUVs, even though increasing amounts of cholesterol were incorporated into LUV's lipid bilayer (Fig. 4a, 0–25% w/w cholesterol). Differently, hydrocortisone seemed to somehow be less affected to the environmental ionic strength by the presence of cholesterol in the liposome's membrane (Fig. 4b, 0–25% w/w cholesterol).

The n values determined for caffeine-LUVs using regenerated cellulose as barrier at all tonicity conditions (Fig. 5a, white bars) ranged between 0.74 and 0.92. The n in hypotonic environment was significantly ($p \leq 0.001$) and consistently lowest in comparison to both isotonic and hypertonic values (Fig. 5a). For the caffeine-LUV experiments carried out with biomimetic Permeapad® barrier (Fig. 5a, grey bars), n values were closer to 1, ranging between 0.83 and 0.97. For hydrocortisone-LUVs (Fig. 5b), n values were generally higher than caffeine-LUVs and in case of Permeapad®, they were even superior than 1. Moreover, an increasing trend in n values with increased cholesterol amount was detected employing regenerated cellulose. This trend was not evident for Permeapad® where the highest n values were detected at 11% w/w cholesterol.

3.3. Liposomal stability

The stability data obtained for the different liposomal dispersions stored at two different temperatures (6 °C and 22 °C) are reported in Table 3. As it can be seen, the tonicity of all the LUV dispersions was relatively stable over the 65 days period. The mean sizes and PI of caffeine-LUVs were relatively stable when stored up to 65 days at 6 °C. The caffeine-LUVs formulations stored at room temperature (22 °C) exhibited significant shifts in size distribution to smaller sizes ($p \leq 0.016$) and narrower PI ($p \leq 0.031$) after approx. 14 days for the formulations with 0 and 11% w/w cholesterol. For the hydrocortisone-LUVs, the mean sizes and PI varied quite remarkably at both storage temperatures.

All LUV dispersions exhibited rather neutral zeta potentials right after formation, but became significantly more negative ($p < 0.05$) after storage. For the caffeine-LUVs, the increase in ZP was more significant for the samples stored at 22 °C, especially for the LUVs with no cholesterol (change up to 40 mV). For the hydrocortisone-LUVs, the samples stored in the fridge (6 °C) exhibited significant variation in ZP as well as those stored at room temperature ($p \leq 0.050$). However, in this case, the ZP changes were rather small in magnitude (maximum variation of 5 mV).

The EE of caffeine-LUVs with various amount of cholesterol incorporated in the phospholipid bilayer (0, 11 and 25% w/w) showed a mean EE of 13% and maximum variation of 6% during a period of 65 days of storage at 6 °C. Surprisingly, when the same formulations were stored at 22 °C, increase of EE up to 40, 30 and 19% could be found for caffeine-LUVs with 0, 11 and 25% w/w cholesterol, respectively. Those results indicated that the liposomal integrity probably changed during storage and for these reasons, as an additive information, pictures of all the different LUV dispersions prepared for the stability study were taken at 65 days to better discriminate differences in the sample appearance (see Supplementary material, Fig. B.1). As it can be seen, the visual perception of caffeine-LUVs dispersions with 0% w/w cholesterol stored at 22 °C had a more transparent/opaque colour than those stored at 6 °C with a more white colour (Fig. B.1a, upper-right compared to upper-left). On the contrary, the hydrocortisone-LUVs (0–25% w/w cholesterol) showed more stable EE with a maximum variation of 4% (Table 3). These results emphasize the relevance of investigating LUV dispersion's stability as changes in size, surface charge and drug entrapment might have an impact on the drug release kinetics from the liposomes.

4. Discussion

4.1. Liposome characterization

LUV dispersions used in this work were prepared aiming to be suited for nasal delivery. For optimal transport through the nasal epithelium, the vesicles should exhibit a size of 10–400 nm, neutral ZP and tonicity around 300 mOsm (Bourganis et al., 2018; Homer et al., 2000; Illum, 2007; Ohwaki et al., 1987). LUVs' tonicity, sizes, PI, ZP and EE were found to be in the same order of magnitude as those employed in previous studies (Wu et al., 2019).

As expected, the incorporation of the neutrally charged cholesterol into the lipid bilayer (consisting of neutrally charged SPC) did not induce any significant change in the surface charge of the liposomes.

In comparison to hydrocortisone-LUVs, the sizes and PI of caffeine-LUVs, were more affected by the cholesterol incorporation in the phospholipid bilayer, which might be related to the drugs localization inside the LUVs (Briuglia et al., 2015; Leite et al., 2018).

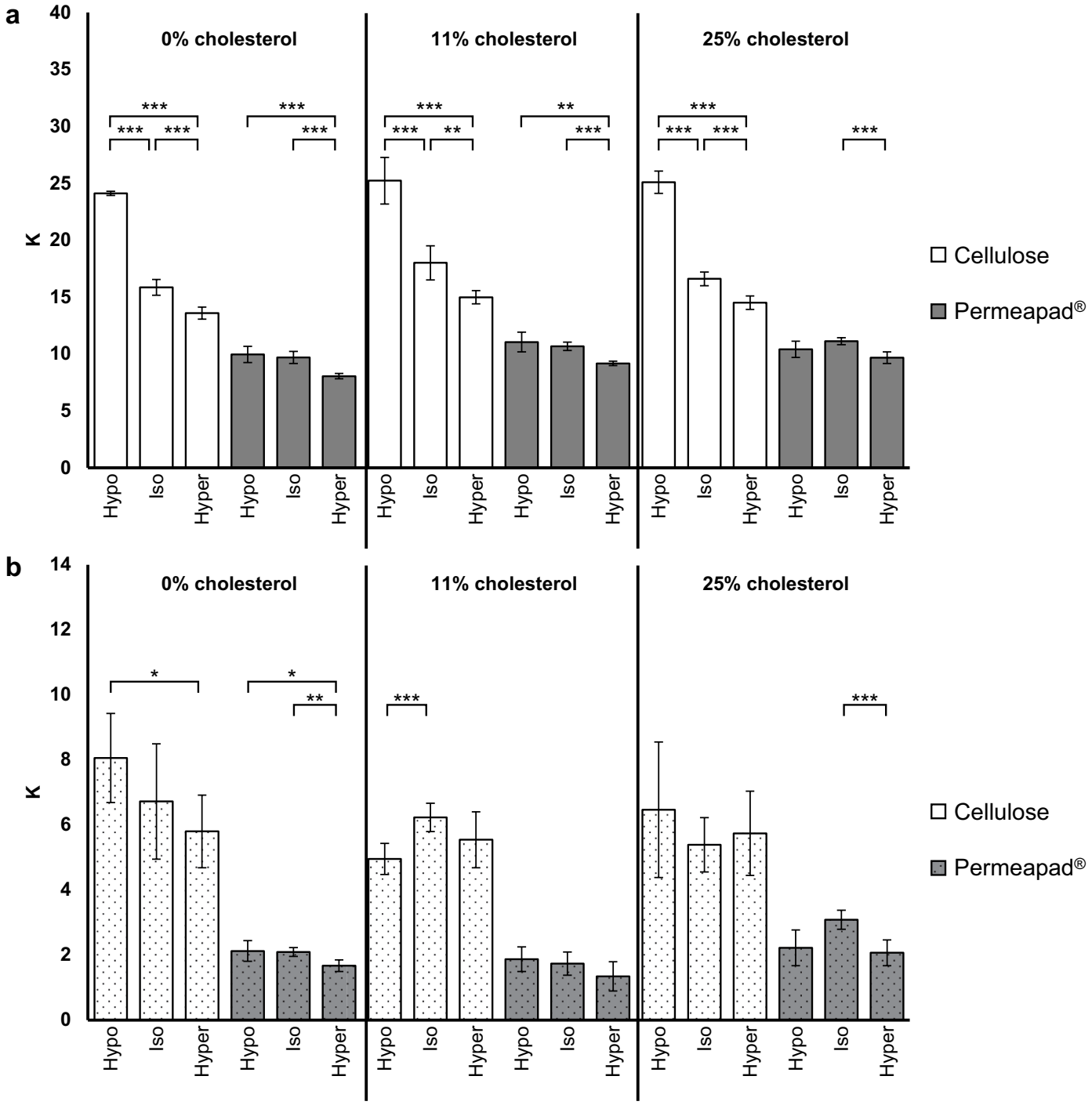

Fig. 4. Transport constant (K) obtained from non-linear data fitting of diffusion experimental data for caffeine- (a) or hydrocortisone- (b) LUV dispersions with various amount of cholesterol incorporated in the phospholipid bilayer (0, 11 and 25% w/w). Diffusion experiments were carried out employing regenerated cellulose (white bars) or alternatively, Permeapad® (grey bars) as barriers. LUV formulations were exposed to isotonic, hypotonic, and hypertonic environments (tonicity difference between inner core and external environment of liposomes of 0 and ± 300 mOsm/kg), respectively. Results represent the mean ± standard deviation (n = 3, *$p \leq 0.050$, **$p \leq 0.010$, ***$p \leq 0.001$).

The incorporation of cholesterol into liposomal membranes significantly affected the EE of hydrocortisone, whereas the caffeine-LUVs were not affected. This might be explained by the different affinity of drugs for the liposomal bilayer (Di Cagno and Stein, 2019) and cholesterol's affinity for the lipid bilayer. In fact, the negative effect of cholesterol on EE for lipophilic compounds is well-documented (Ali et al., 2010; Mohammed et al., 2004). From the obtained results, it was evident that cholesterol prevented, to a certain degree, hydrocortisone embedding into the liposomal bilayers by reducing the space available for hydrocortisone (Table 2).

4.2. In vitro diffusion study

The current methods used to determine the release from liposomes are the filtration, ultracentrifugation, solid phase extraction and dialysis-based methods. The filtration and ultracentrifugation are two methods that with the help of mechanical forces separate the nanocarriers from the released drug. However, these methods are not

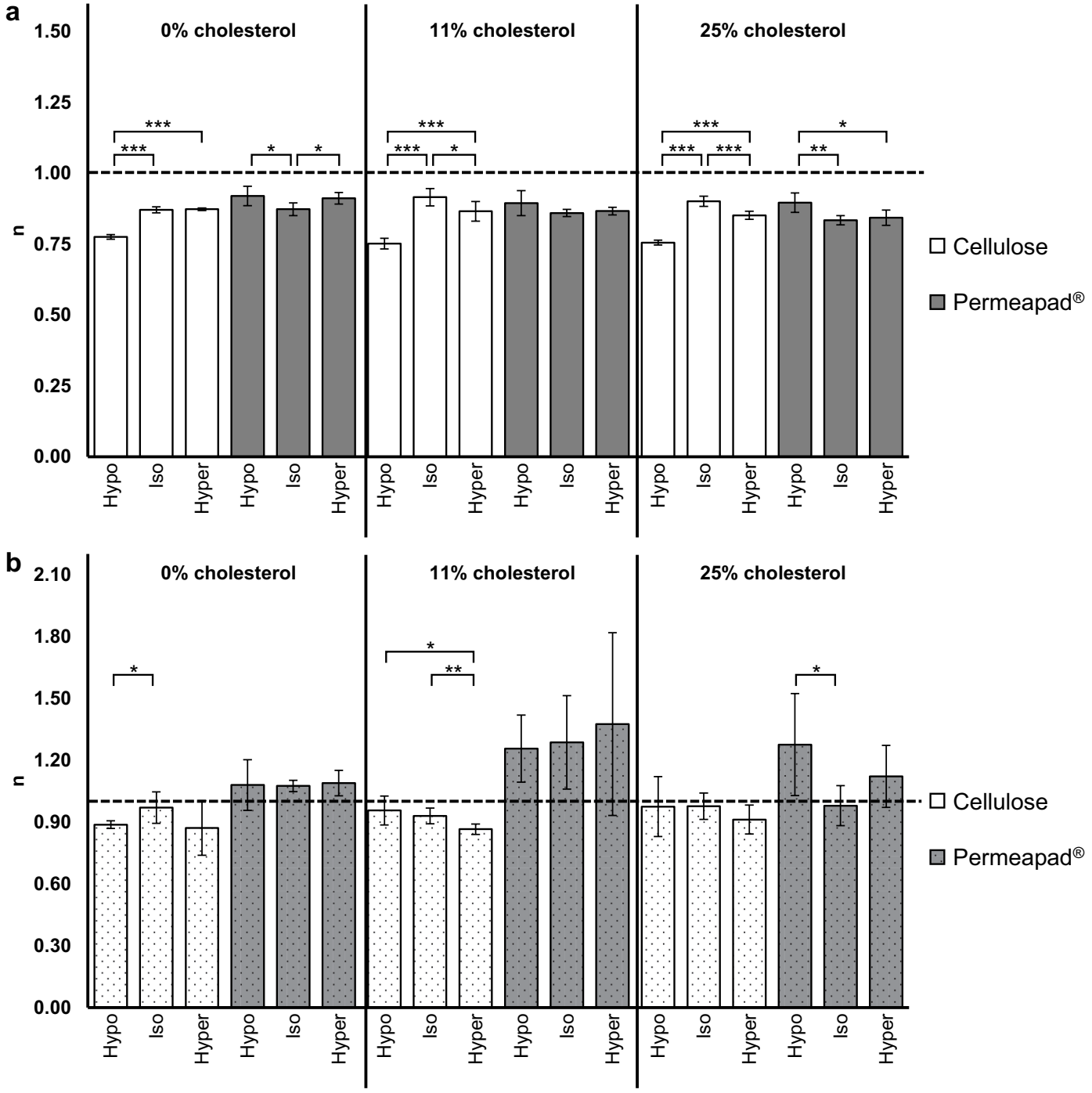

Fig. 5. Transport exponent (n) obtained from non-linear data fitting of diffusion experimental results for caffeine- (a) or hydrocortisone- (b) LUV dispersions with various amount of cholesterol incorporated in the phospholipid bilayer (0, 11 and 25% w/w). Diffusion experiments were carried out employing regenerated cellulose (white bars) or, alternatively, Permeapad® (grey bars) as barriers. LUV formulations were exposed to isotonic, hypotonic, and hypertonic environments (tonicity difference between inner core and external environment of liposomes of 0 and ± 300 mOsm/kg), respectively. Results represent the mean ± standard deviation (n = 3, $*p \leq 0.050$, $**p \leq 0.010$, $***p \leq 0.001$).

suitable for easily deformable nanocarriers such as liposomes, as the separation procedure might disrupt the nanocarrier leading to overrated release (Solomon et al., 2017). For this reason, solid phase extraction is considered to be a more gentle method, and has been successfully applied to separate free drug from liposomes (Xie et al., 2018). However, some of the limitations with this method are that it is not suitable for all types of release medium, and is dependent on the medium composition (*i.e.* bile salts, ions, proteins), therefore the efficiency of separation can be influenced (Nothnagel and Wacker, 2018). Probably that is why the dialysis-based methods are more favoured, and in this study, we used the classical Franz diffusion cell set up to monitor the release from liposomes because of its convenience, cost-effectiveness and simplicity.

4.2.1. Drug diffusion from drug solution and drug-loaded LUVs

The dialysis-based method used in this study allowed us to quantify the amount of drug that diffused through a diffusion barrier. However, this method does not measure the direct release from the liposomal

carrier. For correct interpretation, it has been proposed to use reference experiment of free drug solution (Wacker, 2017). For this reason, we have presented here the drug diffusion profiles from solution and LUVs through two different diffusion barriers.

The regenerated cellulose barrier is highly permeable to small and neutrally charged molecules and the drug diffusion rate through the barrier is highly controlled by the drug concentration gradient between the both sides of the barrier (Bartels et al., 2005; Benavente, 1984; Nothnagel and Wacker, 2018). On the other hand, the biomimetic Permeapad® barrier consists of a lipid layer in between two support sheets (Di Cagno and Bauer-Brandl, 2014). In contact with aqueous solution, the lipid layer is assumed to create tightly packed vesicles mimicking the structure of biological membranes (Di Cagno et al., 2015). In other words, the Permeapad® barrier represents a biomimetic barrier capable of discriminating drug permeability according to the physicochemical property of drug molecules. Consequently, the drug distribution coefficient at neutral pH ($LogD_{7.4}$) plays a key role in the net drug mass transport through the barrier (Brandl et al., 2007; Nothnagel and Wacker, 2018).

As represented in Fig. 2, the total amount of diffused drug from caffeine formulations was much lower (37–57% according to the formulation tested) when studied with Permeapad® in comparison to regenerated cellulose barriers (Fig. 2a–b). On the other hand, for hydrocortisone formulations, a reduction of 63–78% could be observed. As expected, hydrocortisone was more retained by Permeapad® in comparison to caffeine, due to its higher lipophilicity ($logD_{7.4}$ of 1.6 for hydrocortisone in comparison to 0.0 for caffeine) (Zhu et al., 2002).

As reported in previous studies (Di Cagno et al., 2015; Fadda et al., 1998; Wu et al., 2017; Wu et al., 2019), the drug diffusion rate was lower for liposomal dispersions in comparison to drug solutions when analysed on regenerated cellulose barrier (Fig. 2). Surprisingly, this difference was not evident when Permeapad® was employed. This interesting finding indicates that, when biomimetic barrier was employed, the differences in drug transport properties within different formulations were reduced if not annulled. This can be by reason of the biomimetic barrier is the limiting step of the permeation in this case, reducing the impact of the formulation on the total drug transport kinetic. However, for hydrocortisone, a small difference between diffusion from drug solution or liposomal formulation was detectable, indicating that this phenomena is highly drug dependent.

To evaluate better the liposomal bilayer's contribution to changed drug diffusion profiles across the different barriers, we decided to report the R_L as shown in the next sections. We also incorporated various amount of cholesterol into the liposomal bilayer (0–25% w/w) to study the relationship between liposomal rigidity and drug release. Moreover, we exposed the LUVs to different environmental tonicity to see if this could affect the drug release.

4.2.2. Influence of cholesterol on R_L

Liposomes containing hydrophilic molecules might experience leakage due to cholesterol induced lipid bilayer reconstruction (Briuglia et al., 2015; Schullery, 1977). The effect cholesterol has on the SPC liposomes and the release properties from them can be translated from the calculated R_L values. The decreasing R_L values indicated that more drug was diffusing out of the nanocarrier. In agreement with the literature, the R_L was found decreasing for both caffeine- (Fig. 3a) and hydrocortisone-LUVs (Fig. 3b) when the amount of incorporated cholesterol increased from 0 to 25% w/w.

On the other hand, it has also been argued that liposomes containing cholesterol should exhibit higher liposomal bilayer rigidity and the resistance to drug transport (R_L) should increase as compared to liposomes made of plain SPC (Leite et al., 2018; Milon et al., 1986). Surprisingly, the findings from this study seem to deviate from the reported literature. This fact can be explained by the variations of unentrapped drug concentration in the different formulations. As shown in Table 2, the hydrocortisone entrapment was strongly affected by the presence of cholesterol, whereas this was not found for the caffeine-LUVs. Specifically, only minimal changes in the unentrapped drug concentration for caffeine-LUVs with various amount of cholesterol could be measured (ranged between 1758 and 1773 μM), whereas hydrocortisone-LUVs showed unentrapped drug concentrations of 798, 838 and 992 μM for 0, 11 and 25% w/w cholesterol, respectively. The higher the unentrapped drug concentration, the higher the concentration gradient (Eq. (2)) and therefore the flux through the membrane. It should be underlined that these data are in agreement with previous reports of supersaturation induced by liposomal formulations (Di Cagno and Luppi, 2013).

4.2.3. Influence of ionic strength on R_L

Early works have shown that large unilamellar vesicles are susceptible to osmotic stress induced vesicle size changes (Mui et al., 1993; Sun et al., 1986). Liposomes have the tendency to swell when exposed to hypotonic environments. As a result of the swelling, the liposomal membrane becomes thinner and this can contribute to increased release from liposomes (*i.e.* reduced R_L) (Ahumada et al., 2015; Alam et al., 2016; Polozov et al., 2001). On the contrary, when liposomes are exposed to hypertonic environments, liposomes shrink and the liposomal membrane might become less permeable to drug permeation (*i.e.* higher R_L) (Ahumada et al., 2015; Fujiwara and Yanagisawa, 2014; Ohno et al., 2009). Our results were in agreement with the literature (Ahumada et al., 2015; Alam et al., 2016; Fujiwara and Yanagisawa, 2014; Ohno et al., 2009; Polozov et al., 2001). For almost all caffeine-LUV formulations, the R_L was significantly lower in hypotonic environment and highest for the hypertonic environment (Fig. 3a). Similar trend was also observed for hydrocortisone to a lower extent (Fig. 3b).

As it can be seen in Fig. 3a, the R_L values were negative for the caffeine-LUVs when experiments were conducted using Permeapad® barriers. This result indicates that, in some cases, linear regression applied for data treatment and R_L calculation, even though feasible, might lead to incomplete- or miss-interpretation of the data. This might be due to the experimental set up conditions where the drug release is highly influenced by the equilibrium across the diffusion barrier.

One upcoming apparatus for drug release study from liposomes is the flow-through USP 4 (Tang et al., 2019; Yuan et al., 2017). This apparatus provides continuous flow of the release medium into a cell containing the drug formulation. The release medium with instant released drug is then pumped through a separation device (*e.g.* dialysis-based device) to remove liposomal drug, and the collected sample can be measured *in situ* at predetermined time points. The advantages with this method include its continuous renewal of the release medium, and the easily varied medium composition according to the solubility of the drug. Moreover, the apparatus can easily adjust variables such as temperature, flow rate, and detection wavelength. Sample measurements can be automatic, and relatively little manual work is required. However, due to the fact that relatively few companies develop the flow-through cells, and the complexity of the apparatus, this method is still not mainstream (Solomon et al., 2017).

The main purpose of this study was not to improve the experimental set up conditions, but to better interpret the obtained diffusion data collected from available equipment in our laboratory. It has to be mentioned that even though the flow-through USP 4 drug release assay might be a superior method, and has shown some promising results for studying release from liposomes (Tang et al., 2019; Yuan et al., 2017), this method is still limited by the barrier properties that separates the liposomal drug from released drug. Therefore, more processing of the diffusion data is still required for correct interpretation of the release mechanism from liposomes (Jain and Jain, 2016; Solomon et al., 2017; Wacker, 2017).

Two of the most common mathematical methods used to study non-linear diffusion profiles are the Higuchi and Korsmeyer-Peppas model. In this study, we investigated the diffusion data employing the

Table 3
Liposomes characteristics under storage at 6 and 22 °C over a period of 65 days. Changes were monitored by measuring the tonicity of the LUV dispersions (osmolality), liposomal size (average diameter), polydispersity index (PI), ζ-potential (ZP), and entrapment efficiency (EE). Results represent mean ± standard deviation (n = 2).

LUVs	Cholesterol (% w/w)	Day	6 °C					22 °C				
			Osmolality (mOsm/kg)	Size (nm)	PI	ZP (mV)	EE	Osmolality (mOsm/kg)	Size (nm)	PI	ZP (mV)	EE
Caffeine	0	3	400 ± 0	255 ± 41	0.27 ± 0.03	−2.7 ± 0.9	13 ± 1	–	–	–	–	–
		14	398 ± 5	266 ± 44	0.28 ± 0.03	−2.1 ± 0.8*	14 ± 0	400 ± 0	245 ± 36	0.23 ± 0.02	−6.5 ± 1.0***	15 ± 1*
		35	395 ± 6	291 ± 52	0.30 ± 0.03	−3.2 ± 0.9*	15 ± 0*	403 ± 5	318 ± 60**	0.34 ± 0.04*	−14.7 ± 1.4***	31 ± 6**
		65	390 ± 12	266 ± 43	0.29 ± 0.03	−6.2 ± 1.0***	13 ± 2	405 ± 6	158 ± 28***	0.34 ± 0.03*	−43.1 ± 1.2***	40 ± 5***
	11	3	376 ± 6	381 ± 82	0.48 ± 0.05	−3.1 ± 1.0	9 ± 1	–	–	–	–	–
		14	375 ± 9	342 ± 69	0.39 ± 0.04*	−4.4 ± 1.0**	13 ± 1***	374 ± 10	318 ± 62*	0.41 ± 0.04	−10.0 ± 1.23***	16 ± 2***
		35	374 ± 8	358 ± 75	0.43 ± 0.04	−7.7 ± 1.3***	16 ± 3***	365 ± 9	302 ± 58**	0.38 ± 0.04*	−9.0 ± 1.2***	20 ± 1***
		65	364 ± 8*	350 ± 73	0.46 ± 0.04	−10.7 ± 1.3***	16 ± 4***	360 ± 4**	313 ± 62*	0.37 ± 0.04*	−19.3 ± 1.3***	30 ± 5***
	25	3	398 ± 21	373 ± 82	0.48 ± 0.05	−4.9 ± 1.0	10 ± 1	–	–	–	–	–
		14	395 ± 24	382 ± 83	0.48 ± 0.05	−5.0 ± 1.1	11 ± 1	390 ± 18	339 ± 67	0.43 ± 0.04	−9.5 ± 1.3***	12 ± 1*
		35	390 ± 23	387 ± 83	0.50 ± 0.05	−9.3 ± 1.2***	11 ± 1	390 ± 23	352 ± 73	0.47 ± 0.04	−8.4 ± 1.3***	15 ± 1***
		65	391 ± 10	327 ± 68	0.46 ± 0.04	−11.1 ± 1.3***	13 ± 1*	390 ± 12	372 ± 80	0.48 ± 0.05	−9.8 ± 1.2***	19 ± 1***
Hydrocortisone	0	3	365 ± 17	238 ± 33	0.21 ± 0.02	−3.5 ± 1.0	74 ± 1	–	–	–	–	–
		14	370 ± 12	251 ± 37*	0.23 ± 0.02*	−5.0 ± 1.1***,[a]	71 ± 1**	370 ± 12	259 ± 37*	0.22 ± 0.02	−7.2 ± 1.2***,[a]	69 ± 2**
		35	370 ± 7	291 ± 51**	0.32 ± 0.03***	−5.1 ± 1.1***	70 ± 1**	370 ± 7	322 ± 59**	0.35 ± 0.03***	−5.5 ± 1.1***	70 ± 2**
		65	355 ± 6	304 ± 57**	0.34 ± 0.04***	−7.8 ± 1.1***	78 ± 1**	358 ± 21	262 ± 41**	0.26 ± 0.02*	−6.2 ± 1.1***	71 ± 2*
	11	3	410 ± 18	333 ± 67	0.41 ± 0.04	−4.2 ± 1.0	64 ± 2	–	–	–	–	–
		14	415 ± 6	335 ± 68	0.41 ± 0.04	−5.4 ± 1.1**,[a]	61 ± 1*	418 ± 10	260 ± 42***	0.28 ± 0.03***	−5.7 ± 1.2**,[a]	63 ± 1
		35	410 ± 12	255 ± 44**	0.29 ± 0.03**	−6.8 ± 1.2***	63 ± 1	408 ± 15	294 ± 52*	0.35 ± 0.03	−4.6 ± 1.2	65 ± 1
		65	410 ± 12	283 ± 50*	0.34 ± 0.03	−8.8 ± 1.2***	65 ± 2	413 ± 10	295 ± 55*	0.36 ± 0.04	−6.7 ± 1.2***	67 ± 3
	25	3	438 ± 10	330 ± 66	0.41 ± 0.04	−5.4 ± 1.1	55 ± 2	–	–	–	–	–
		14	430 ± 12	386 ± 81*	0.48 ± 0.04*	−7.8 ± 1.2***,[a]	53 ± 0	438 ± 5	358 ± 74	0.46 ± 0.04	−7.1 ± 1.2***,[a]	54 ± 1
		35	423 ± 10	333 ± 69	0.43 ± 0.04	−5.7 ± 1.3	53 ± 1	428 ± 10	303 ± 58	0.40 ± 0.04	−8.8 ± 1.2***	58 ± 2
		65	423 ± 21	323 ± 64	0.42 ± 0.04	−10.1 ± 1.3***	53 ± 0	423 ± 5*	382 ± 84*	0.51 ± 0.05*	−7.6 ± 1.3***	54 ± 1

* $p \leq 0.050$.
** $p \leq 0.010$.
*** $p \leq 0.001$ when compared to the control (measurement on day 3).
[a] Measured on day 22 instead of day 14.

Korsmeyer-Peppas model.

4.2.4. Data fitting to the Korsmeyer-Peppas model

Since the aim of this study was to investigate the contributing alterations in liposomal bilayer properties relevant for drug release, the Korsmeyer-Peppas model was chosen due to its ability to provide the descriptive information on both release kinetics and mechanism of drug release. It should be underlined that the data we have been fitting to the model refer to the diffusion through low retention/high retention barriers, however, the data also reflect (as described in Fig. 1) the release kinetics from the nanocarriers.

The parameter K indicated the constant drug transport that can be seen intuitively as directly proportional to the drug release kinetics from LUVs. In fact, higher K indicated faster drug release. On a contrary, lower value of K indicated a low transport kinetic and therefore poor drug release from nanocarriers. Interestingly, caffeine-LUVs generally expressed higher K values in comparison to hydrocortisone-LUVs (Fig. 4a and b). This was expected, since caffeine is known for its high permeability through phospholipid barriers (Di Cagno et al., 2015; Flaten et al., 2006). It should be underlined that K and R_L were in rather good agreement; the higher the R_L, the lower value of K, and *vice versa*. As seen before for R_L, K also seemed to be highly influenced by changes in the ionic strengths of external environments. Specifically, the higher the increase in the external ionic strength (consequently shrinkage of liposomes) the K became lower, indicating a clear reduction of drug release from liposomes.

The K changed more drastically in response to the environment when the regenerated cellulose barriers were employed in comparison to the Permeapad® barriers. This implies that, when biomimetic barriers were employed (*i.e.* higher retention barrier), the drug formulation plays a minor role in the net final drug transported through the barrier. This was also an interesting finding, highlighting the fact that dialysis barriers were extremely efficient to measure formulation kinetics but not necessarily predictive for *in vitro-in vivo* correlations.

The advantage with the non-linear fitting approach was that a larger part of the experimental data was efficiently fitted (M_t/M_∞ up to 60%) and seemed to better represent the drug diffusion kinetics from liposomes. Moreover, using this data treatment approach, there was no need to measure reference sample (*i.e.* drug solution). The application of Korsmeyer-Peppas model resulted in the time-efficient and precise method for interpreting diffusion data from nanocarriers.

Under the influence of osmotic stress, the drug release kinetics of both caffeine (Fig. 4a) and hydrocortisone (Fig. 4b) from liposomes exhibited less variations in K when cholesterol was incorporated in the bilayers (0 *vs* 25% w/w). The more stable K values in different environmental ionic strengths indicated that the liposomal sensitivity to osmotic influences decreased. Possible explanation could be that cholesterol embedment into the liposomal bilayer decreases its flexibility (Leite et al., 2018).

The advantage with the Korsmeyer-Peppas model was the mechanistic considerations this model permitted, describing the drug release mechanism from liposomes by providing the transport exponent, n. In order to have a Fickian diffusion process, when no boundaries are present, n should be equal to 0.5, whereas values of n between 0.5 and 1 indicates non-Fickian diffusion and are indications of boundary region affecting the passive drug diffusion (Costa and Sousa Lobo, 2001). For the regenerated cellulose experiments (Fig. 5), n values for caffeine were always lower than 1. The lowest value of n measured for the diffusion of caffeine was in hypotonic environment (0.75–0.78) when the lipid bilayers should be the most stretched and therefore with the lowest resistance (Fig. 3) (Ahumada et al., 2015; Alam et al., 2016; Polozov et al., 2001). Interestingly, when liposomes were exposed to isotonic and hypertonic environments, the n value increased remarkably (between 0.83 and 0.92). This variation in n indicated that the diffusion of caffeine was moving even further from a Fickian behaviour. This can be very well explained by the increasing resistance of caffeine transport through liposomal bilayers induced by vesicles' shrinkage (Ahumada et al., 2015; Fujiwara and Yanagisawa, 2014; Ohno et al., 2009). Considering the experiments with regenerated cellulose barrier, in the case of hydrocortisone, n values were higher than for caffeine ranging between 0.86 and 0.98. This finding suggests that hydrocortisone was from the start diffusing in a more controlled manner from the liposomal bilayer. The release profile of hydrocortisone seemed to be less affected by the changes in ionic strengths of liposomal surrounding environment (as observed in previous studies (Wu et al., 2017, 2019)).

For the Permeapad® experiments, the n were found relatively more stable and were less affected by changes in the external environment of LUVs. As mentioned previously, it was plausible that the higher retention of Permeapad® in comparison to regenerated cellulose overrules the liposomal effect ($K \ll K^I$).

4.3. Formulation stability

All LUV formulations prepared in this study retained a stable tonicity upon storage at both 6 and 22 °C (Table 3). Stable tonicity is an important parameter considering the overall stability of liposomal suspensions (Grit and Crommelin, 1993).

The more stable LUV dispersions in terms of size, PI and EE were the ones stored at 6 rather than at 22 °C, as expected. Moreover, low temperatures (4–6 °C) are the recommendable storage conditions for liposomes (Grit and Crommelin, 1993).

Instability of LUV dispersions in terms of drug loading can be described as the leakage of originally-associated liposomal content during storage. As expected, the hydrocortisone-LUVs exhibited stable EE up to 65 days at both 6 and 22 °C independently of the amount of incorporated cholesterol. Surprisingly, the EE of caffeine-LUVs stored at 22 °C seemed to increase over time. Similar increase in drug loading upon storage has been reported for other small hydrophilic compound such as rivastigmine (MW of 250 g/mol (Pubchem, 2019b)). Caffeine has MW of 194 g/mol (Pubchem, 2019a). In the study carried out by Arumugam et al., an increase in EE of rivastigmine in liposomes was measured after 3 months of storage in comparison to freshly prepared drug-loaded liposomes (Arumugam et al., 2008). This might be an indication that the liposomal bilayer structure is permitting drug to pass through the liposomal membrane considering that we did not remove the unentrapped drug from the formulation. Analysing the samples visually, the caffeine-LUV dispersions without cholesterol had a more transparent/opaque colour in comparison to the formulations with cholesterol (11–25% w/w). The increase in the EE for those formulations was probably due to drug migration to equilibrium in the samples as if the liposomal bilayers were no longer present. However, it could be observed that the changes in caffeine entrapment were not evident when cholesterol was in the lipid bilayer; it is well known that cholesterol stabilizes phospholipid bilayers (Briuglia et al., 2015; Grit and Crommelin, 1993).

Taking into account all the variables measured, LUVs with 11% w/w cholesterol seemed to be the most stable formulation and exhibited suitable storage profiles in terms of size distribution, ZP and EE for the development of drug-loaded LUVs intended for nose-to-brain targeted drug delivery.

We are currently testing several drugs with different lipophilicity as well as charge to confirm the applicability of proposed approach.

5. Conclusions

Drug release from LUVs was significantly affected by the ionic strengths of the external environment confirmed by both linear (zero order) and non-linear (Korsmeyer-Peppas) regression models. Korsmeyer-Peppas model was proven to be suitable to analyse all drug transport data obtained in this study, providing important information on the release mechanism from the carrier in addition to being time

efficient (less controls needed) unlike the zero order approximation. The drug release from LUVs could be tailored by the incorporation of cholesterol, and LUVs with 11% w/w cholesterol seemed to be the optimal liposomal composition in terms of stability and responsiveness to osmotic stress. In spite of the fact that regenerated cellulose is considered to be a standard, simpler and cheaper barrier used for the transport study, the Permeapad® appeared a more reliable when it comes to *in vitro-in vivo* correlation due to closer similarities to biological membranes. The results obtained in this work are rather relevant as the data can be utilized for the development of liposomal formulations intended for nose-to-brain targeted drug delivery.

Acknowledgements

The authors are grateful to Lipoid GmbH (Ludwigshafen, Germany) and InnoME GmbH (Espelkamp, Germany) for their donation of lipids and Permeapad® barriers, respectively. This project was financed by the University of Tromsø - The Arctic University of Norway. This research did not involve funding from any specific grant in the public, commercial, or not-for-profit sectors.

Declaration of competing interest

No conflict of interest is declared by the authors.

Appendix A. Supplementary data

Supplementary data to this article can be found online at https://doi.org/10.1016/j.ejps.2019.105026.

References

Ahumada, M., Calderon, C., Alvarez, C., Lanio, M.E., Lissi, E.A., 2015. Response of unilamellar DPPC and DPPC:SM vesicles to hypo and hyper osmotic shocks: a comparison. Chem. Phys. Lipids 188, 54–60. https://doi.org/10.1016/j.chemphyslip.2015.05.001.

Alam shibly, Sayed, U., Ghatak, C., Karal, Sayem, Mohammad, A., Moniruzzaman, M., Yamazaki, M., 2016. Experimental estimation of membrane tension induced by osmotic pressure. Biophys. J. 111, 2190–2201. https://doi.org/10.1016/j.bpj.2016.09.043.

Ali, M.H., Kirby, D.J., Mohammed, A.R., Perrie, Y., 2010. Solubilisation of drugs within liposomal bilayers: alternatives to cholesterol as a membrane stabilising agent. J. Pharm. Pharmacol. 62, 1646–1655. https://doi.org/10.1111/j.2042-7158.2010.01090.x.

Allen, T.M., Cullis, P.R., 2013. Liposomal drug delivery systems: from concept to clinical applications. Adv. Drug Deliv. Rev. 65, 36–48. https://doi.org/10.1016/j.addr.2012.09.037.

Arumugam, K., Subramanian, G.S., Mallayasamy, S.R., Averineni, R.K., Reddy, M.S., Udupa, N., 2008. A study of rivastigmine liposomes for delivery into the brain through intranasal route. Acta Pharma. 58, 287–297. https://doi.org/10.2478/v10007-008-0014-3.

Bangham, A.D., Horne, R.W., 1964. Negative staining of phospholipids and their structural modification by surface-active agents as observed in the electron microscope. J. Mol. Biol. 8, 660–668. https://doi.org/10.1016/S0022-2836(64)80115-7.

Bangham, A.D., De Gier, J., Greville, G.D., 1967. Osmotic properties and water permeability of phospholipid liquid crystals. Chem. Phys. Lipids 1, 225–246. https://doi.org/10.1016/0009-3084(67)90030-8.

Bartels, C., Franks, R., Rybar, S., Schierach, M., Wilf, M., 2005. The effect of feed ionic strength on salt passage through reverse osmosis membranes. Desalination 184, 185–195. https://doi.org/10.1016/j.desal.2005.04.032.

Benavente, J., 1984. A study of membrane potentials across a cellophane membrane for different electrolytes. J Non-Equilib Thermodyn 9, 217–224. https://doi.org/10.1515/jnet.1984.9.3.217.

Bourganis, V., Kammona, O., Alexopoulos, A., Kiparissides, C., 2018. Recent advances in carrier mediated nose-to-brain delivery of pharmaceutics. Eur. J. Pharm. Biopharm. 128, 337–362. https://doi.org/10.1016/j.ejpb.2018.05.009.

Brandl, M., Eide Flaten, G., Bauer-Brandl, A., Begley, T.P., 2007. Passive diffusion across membranes. In: Wiley Encyclopedia of Chemical Biology. John Wiley & Sons, Inc..

Briuglia, M.L., Rotella, C., Mcfarlane, A., Lamprou, D.A., 2015. Influence of cholesterol on liposome stability and on in vitro drug release. Drug Deliv Transl Res 5, 231–242. https://doi.org/10.1007/s13346-015-0220-8.

Brodin, B., Steffansen, B., Uhd Nielsen, C., 2010. Chapter 3.2 passive diffusion of drug substances: the concepts of flux and permeability. In: Molecular Biopharmaceutics: Aspects of Drug Characterisation, Drug Delivery and Dosage Form Evaluation. Pharmaceutical Press, London, pp. 135–152.

Costa, P., Sousa Lobo, J.M., 2001. Modeling and comparison of dissolution profiles. Eur. J. Pharm. Sci. 13, 123–133. https://doi.org/10.1016/S0928-0987(01)00095-1.

Di Cagno, M., Bauer-Brandl, A., 2014. Assembly for Assessing Drug Permeability With Adjustable Biomimetic Properties. WO 2016/078667 A1.

Di Cagno, M.P., Stein, P.C., 2019. Studying the effect of solubilizing agents on drug diffusion through the unstirred water layer (UWL) by localized spectroscopy. Eur. J. Pharm. Biopharm. 139, 205–212. https://doi.org/10.1016/j.ejpb.2019.04.005.

Di Cagno, M., Bibi, H.A., Bauer-Brandl, A., 2015. New biomimetic barrier Permeapad™ for efficient investigation of passive permeability of drugs. Eur. J. Pharm. Sci. 73, 29–34. https://doi.org/10.1016/j.ejps.2015.03.019.

di Cagno, M., Luppi, B., 2013. Drug "supersaturation" states induced by polymeric micelles and liposomes: A mechanistic investigation into permeability enhancements. Eur. J Pharm. Sci. 48, 775–780.

Fadda, A.M., Baroli, B.M., Maccioni, A.M., Sinico, C., Valenti, D., Alhaique, F., 1998. Phospholipid-detergent systems: effects of polysorbates on the release of liposomal caffeine. Farmaco 53, 650–654. https://doi.org/10.1016/S0014-827X(98)00081-0.

Flaten, G.E., Dhanikula, A.B., Luthman, K., Brandl, M., 2006. Drug permeability across a phospholipid vesicle based barrier: a novel approach for studying passive diffusion. Eur. J. Pharm. Sci. 27, 80–90. https://doi.org/10.1016/j.ejps.2005.08.007.

Fujiwara, K., Yanagisawa, M., 2014. Generation of giant unilamellar liposomes containing biomacromolecules at physiological intracellular concentrations using hypertonic conditions. ACS Synth. Biol. 3, 870–874. https://doi.org/10.1021/sb4001917.

Grit, M., Crommelin, D.J.A., 1993. Chemical stability of liposomes: implications for their physical stability. Chem. Phys. Lipids 64, 3–18. https://doi.org/10.1016/0009-3084(93)90053-6.

Haghiralsadat, F., Amoabediny, G., Helder, M.N., Naderinezhad, S., Sheikhha, M.H., Forouzanfar, T., Zandieh-Doulabi, B., 2018. A comprehensive mathematical model of drug release kinetics from nano-liposomes, derived from optimization studies of cationic PEGylated liposomal doxorubicin formulations for drug-gene delivery. Artif Cells Nanomed Biotechnol 46, 169–177. https://doi.org/10.1080/21691401.2017.1304403.

Homer, J.J., Dowley, A.C., Condon, L., El-Jassar, P., Sood, S., 2000. The effect of hypertonicity on nasal mucociliary clearance. Clin Otolaryngol Allied Sci 25, 558–560. https://doi.org/10.1046/j.1365-2273.2000.00420.x.

Illum, L., 2007. Nanoparticulate systems for nasal delivery of drugs: a real improvement over simple systems? J. Pharm. Sci. 96, 473–483. https://doi.org/10.1002/jps.20718.

Jain, A., Jain, S.K., 2016. In vitro release model fitting of liposomes: an insight. Chem. Phys. Lipids 201, 28–40. https://doi.org/10.1016/j.chemphyslip.2016.10.005.

Lai, F., Fadda, A.M., Sinico, C., 2013. Liposomes for brain delivery. Expert Opin Drug Deliv 10, 1003–1022. https://doi.org/10.1517/17425247.2013.766714.

Leite, N.B., Martins, D.B., Fazani, V.E., Vieira, M.R., Dos Santos Cabrera, M.P., 2018. Cholesterol modulates curcumin partitioning and membrane effects. Biochim. Biophys. Acta Biomembr. 1860, 2320–2328. https://doi.org/10.1016/j.bbamem.2018.05.018.

Li, M., Du, C., Guo, N., Teng, Y., Meng, X., Sun, H., Li, S., Yu, P., Galons, H., 2019. Composition design and medical application of liposomes. Eur. J. Med. Chem. 164, 640–653. https://doi.org/10.1016/j.ejmech.2019.01.007.

Milon, A., Lazrak, T., Albrecht, A.-M., Wolff, G., Weill, G., Ourisson, G. & Nakatani, Y. 1986. Osmotic swelling of unilamellar vesicles by the stopped-flow light scattering method. Influence of vesicle size, solute, temperature, cholesterol and three α,ω-dihydroxycarotenoids. Biochim. Biophys. Acta Biomembr., 859, 1–9. doi:https://doi.org/10.1016/0005-2736(86)90311–1.

Mohammed, A.R., Weston, N., Coombes, A.G.A., Fitzgerald, M., Perrie, Y., 2004. Liposome formulation of poorly water soluble drugs: optimisation of drug loading and ESEM analysis of stability. Int. J. Pharm. 285, 23–34. https://doi.org/10.1016/j.ijpharm.2004.07.010.

Mui, B.L., Cullis, P.R., Evans, E.A., Madden, T.D., 1993. Osmotic properties of large unilamellar vesicles prepared by extrusion. Biophys. J. 64, 443–453. https://doi.org/10.1016/S0006-3495(93)81385-7.

New, R.R.C., 1990. Chapter 1: Introduction. Liposomes: A Practical Approach. vol. 58. IRL Press, Oxford, pp. 1–32.

Nothnagel, L., Wacker, M.G., 2018. How to measure release from nanosized carriers? Eur. J. Pharm. Sci. 120, 199–211. https://doi.org/10.1016/j.ejps.2018.05.004.

Ohno, M., Hamada, T., Takiguchi, K., Homma, M., 2009. Dynamic behavior of giant liposomes at desired osmotic pressures. Langmuir 25, 11680–11685. https://doi.org/10.1021/la900777g.

Ohwaki, T., Ando, H., Kakimoto, F., Uesugi, K., Watanabe, S., Miyake, Y., Kayano, M., 1987. Effects of dose, pH, and osmolarity on nasal absorption of secretin in rats II: histological aspects of the nasal mucosa in relation to the absorption variation due to the effects of pH and osmolarity. J. Pharm. Sci. 76, 695–698. https://doi.org/10.1002/jps.2600760905.

Paula, S., Volkov, A.G., Van Hoek, A.N., Haines, T.H., Deamer, D.W., 1996. Permeation of protons, potassium ions, and small polar molecules through phospholipid bilayers as a function of membrane thickness. Biophys. J. 70, 339–348. https://doi.org/10.1016/s0006-3495(96)79575-9.

Pedersen, P.S., Braunstein, T.H., Jorgensen, A., Larsen, P.L., Holstein-Rathlou, N.H., Frederiksen, O., 2007. Stimulation of aquaporin-5 and transepithelial water permeability in human airway epithelium by hyperosmotic stress. Pflugers Arch. 453, 777–785. https://doi.org/10.1007/s00424-006-0157-3.

Pencer, J., White, G.F., Hallett, F.R., 2001. Osmotically induced shape changes of large unilamellar vesicles measured by dynamic light scattering. Biophys. J. 81, 2716–2728. https://doi.org/10.1016/s0006-3495(01)75914-0.

Polozov, I.V., Anantharamaiah, G.M., Segrest, J.P., Epand, R.M., 2001. Osmotically induced membrane tension modulates membrane permeabilization by class L amphipathic helical peptides: nucleation model of defect formation. Biophys. J. 81, 949–959. https://doi.org/10.1016/s0006-3495(01)75753-0.

Pubchem National Center for Biotechnology Information Compound Database, 2019a. Caffeine, CID = 2519 [Online] Available from: https://pubchem.ncbi.nlm.nih.gov/compound/2519 (Accessed on: May 14, 2019).

Pubchem National Center for Biotechnology Information Compound Database, 2019b. Rivastigmine, CID = 77991 [Online] Available from: https://pubchem.ncbi.nlm.nih.gov/compound/77991, Accessed date: 14 May 2019.

Quraishi, M.S., Jones, N.S., Mason, J., 1998. The rheology of nasal mucus: a review. Clin Otolaryngol Allied Sci 23, 403–413. https://doi.org/10.1046/j.1365-2273.1998.00172.x.

Schullery, S.E., 1977. Permeability of iodide in multilamellar liposomes modeled by two compartments and a reservoir. Biochim. Biophys. Acta Biomembr. 468, 238–244. https://doi.org/10.1016/0005-2736(77)90117-1.

Solomon, D., Gupta, N., Mulla, N.S., Shukla, S., Guerrero, Y.A., Gupta, V., 2017. Role of in vitro release methods in liposomal formulation development: challenges and regulatory perspective. AAPS J. 19, 1669–1681. https://doi.org/10.1208/s12248-017-0142-0.

Sun, S.-T., Milon, A., Tanaka, T., Ourisson, G., Nakatani, Y., 1986. Osmotic swelling of unilamellar vesicles by the stopped-flow light scattering method. Elastic properties of vesicles. Biochim. Biophys. Acta Biomembr. 860, 525–530. https://doi.org/10.1016/0005-2736(86)90549-3.

Tang, J., Srinivasan, S., Yuan, W., Ming, R., Liu, Y., Dai, Z., Noble, C.O., Hayes, M.E., Zheng, N., Jiang, W., Szoka, F.C., Schwendeman, A., 2019. Development of a flow-through USP 4 apparatus drug release assay for the evaluation of amphotericin B liposome. Eur. J. Pharm. Biopharm. 134, 107–116. https://doi.org/10.1016/j.ejpb.2018.11.010.

Vieira, D., Gamarra, L., 2016. Getting into the brain: liposome-based strategies for effective drug delivery across the blood-brain barrier. Int. J. Nanomedicine 11, 5381–5414. https://doi.org/10.2147/IJN.S117210.

Wacker, M.G., 2017. Challenges in the drug release testing of next-generation nanomedicines – what do we know? Mater Today Proc 4, S214–S217. https://doi.org/10.1016/j.matpr.2017.09.189.

Wu, I.Y., Škalko-Basnet, N., Di Cagno, M.P., 2017. Influence of the environmental tonicity perturbations on the release of model compounds from large unilamellar vesicles (LUVs): a mechanistic investigation. Colloids Surf B 157, 65–71. https://doi.org/10.1016/j.colsurfb.2017.05.062.

Wu, I.Y., Nikolaisen, T.E., Škalko-Basnet, N., Di Cagno, M.P., 2019. The hypotonic environmental changes affect liposomal formulations for nose-to-brain targeted drug delivery. J. Pharm. Sci. https://doi.org/10.1016/j.xphs.2019.03.006.

Xie, Y., Shao, N., Jin, Y., Zhang, L., Jiang, H., Xiong, N., Su, F., Xu, H., 2018. Determination of non-liposomal and liposomal doxorubicin in plasma by LC–MS/MS coupled with an effective solid phase extraction: in comparison with ultrafiltration technique and application to a pharmacokinetic study. J. Chromatogr. B 1072, 149–160. https://doi.org/10.1016/j.jchromb.2017.11.020.

Yuan, W., Kuai, R., Dai, Z., Yuan, Y., Zheng, N., Jiang, W., Noble, C., Hayes, M., Szoka, F.C., Schwendeman, A., 2017. Development of a flow-through USP-4 apparatus drug release assay to evaluate doxorubicin liposomes. AAPS J. 19, 150–160. https://doi.org/10.1208/s12248-016-9958-2.

Zhu, C., Jiang, L., Chen, T.-M., Hwang, K.-K., 2002. A comparative study of artificial membrane permeability assay for high throughput profiling of drug absorption potential. Eur. J. Med. Chem. 37, 399–407. https://doi.org/10.1016/S0223-5234(02)01360-0.

Supplementary material

Interpreting non-linear drug diffusion data: Utilizing Korsmeyer-Peppas model to follow drug release from liposomes

Iren Yeeling Wu[1], Sonali Bala[1], Nataša Škalko-Basnet[1], Massimiliano Pio di Cagno[1,2,*]

[1]*Drug Transport and Delivery Research Group, Department of Pharmacy, University of Tromsø The Arctic University of Norway, Universitetsvegen 57, 9037 Tromsø, Norway.*

[2]*Department of Pharmacy, Faculty of Mathematics and Natural Sciences, University of Oslo, Sem Sælands vei 3, 0371 Oslo, Norway.*

[*]*Corresponding author. Tel.: +47 22856598; e-mail: m.p.d.cagno@farmasi.uio.no*

Content:

1. Fitting the *in vitro* diffusion data to the Korsmeyer-Peppas model for caffeine-LUVs (Fig.A.1) and hydrocortisone-LUVs (Fig.A.2).
2. Picture of drug-loaded LUVs after 65 days of storage at 6 and 22°C (Fig.B.1).

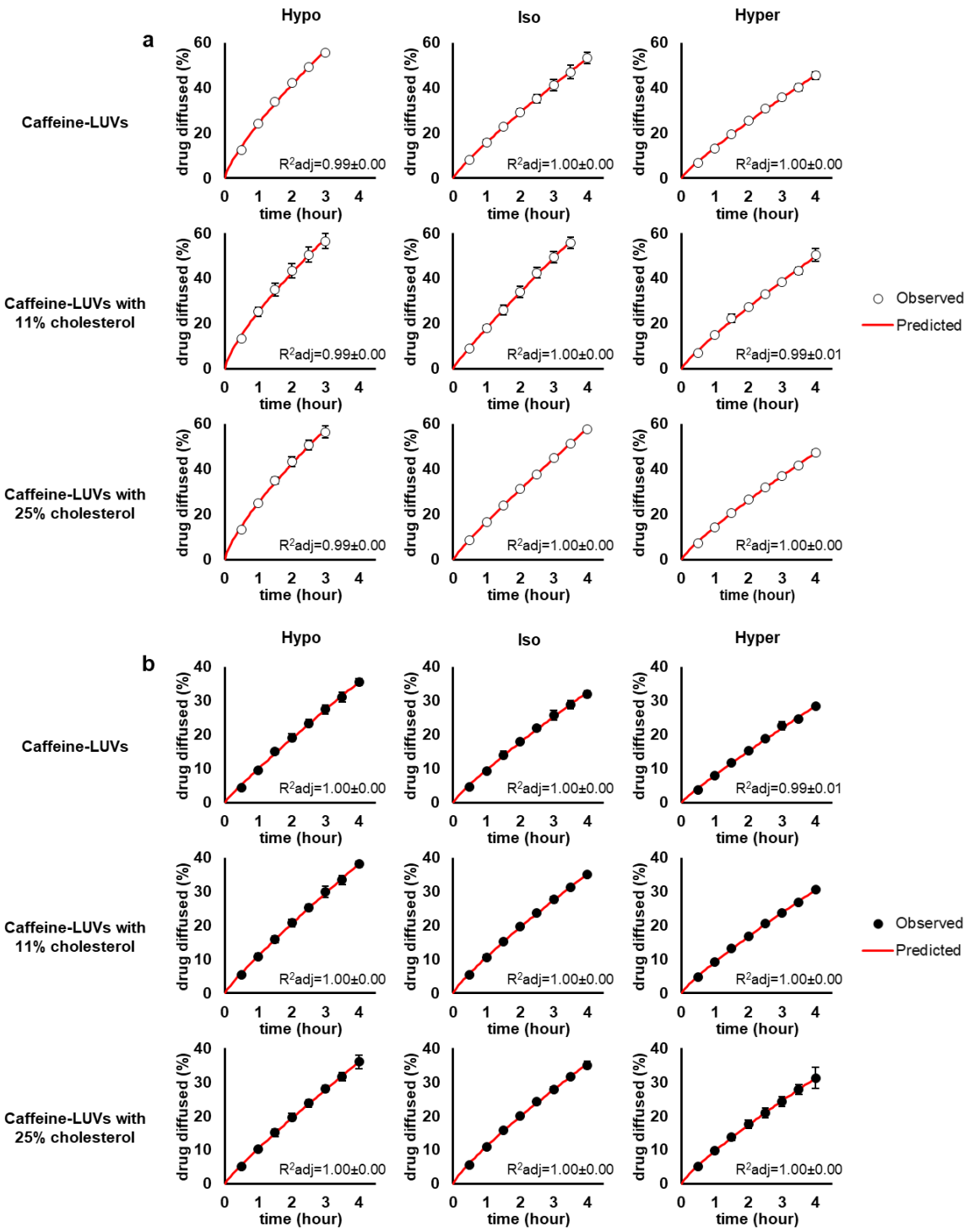

Fig.A.1: Fitting of caffeine diffusion experimental results to the Korsmeyer-Peppas model. Diffusion experiments were carried out employing regenerated cellulose (a) or alternatively, Permeapad® (b) as the barriers. The drugs were formulated in LUV dispersions with various amount of cholesterol incorporated in the phospholipid bilayers (0, 11 and 25% w/w) and the LUV dispersions were exposed to isotonic, hypotonic and hypertonic environments (tonicity difference of 0 and ±300 mOsm/kg within inner core of liposomes and external environment). Results represent the mean ± standard deviation of three parallel experiments (n=3, *p≤0.050, **p≤0.010, ***p≤0.001).

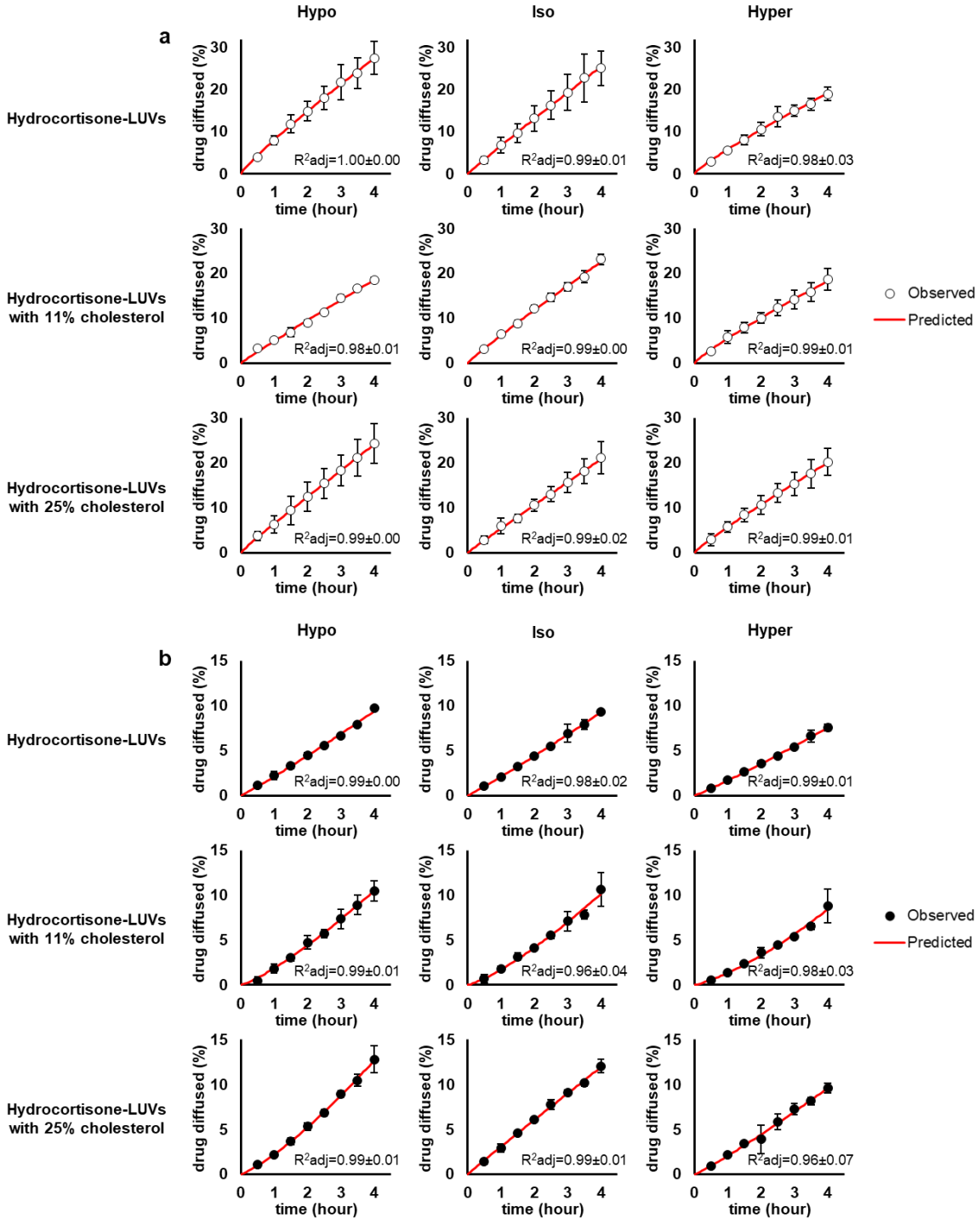

Fig.A.2: Fitting of hydrocortisone diffusion experiment results to the Korsmeyer-Peppas model. Diffusion experiments were carried out employing regenerated cellulose (a) or alternatively, Permeapad® (b) as barriers. The drugs were formulated in LUV dispersions with various amount of cholesterol incorporated in the phospholipid bilayers (0, 11 and 25% w/w) and the LUV dispersions were exposed to isotonic, hypotonic and hypertonic environments (tonicity difference of 0 and ±300 mOsm/kg within inner core of liposomes and external environment). Results represent the mean ± standard deviation of three parallel experiments (n=3, **p*≤0.050, ***p*≤0.010, ****p*≤0.001).

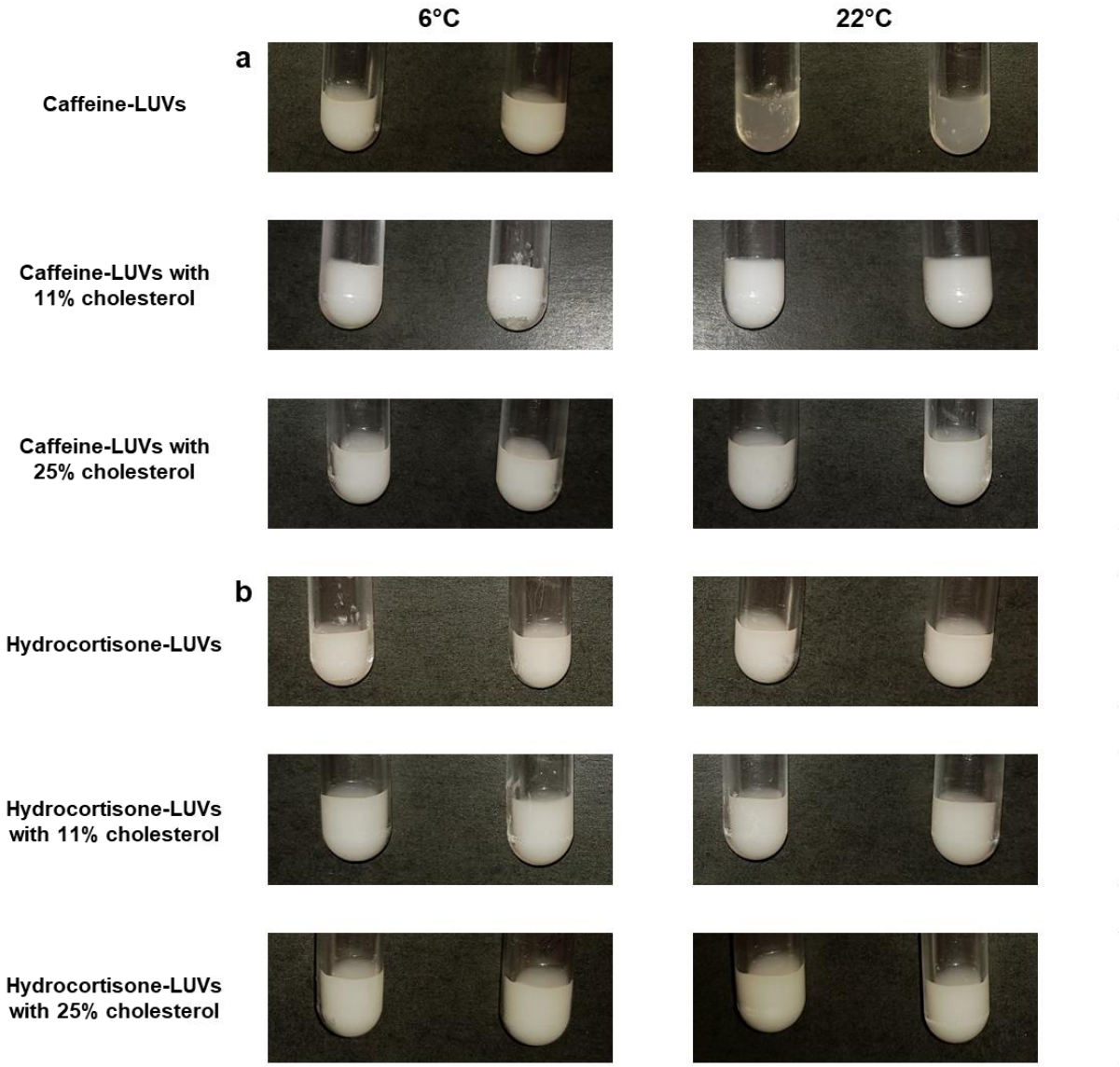

Fig.B.1: Photographs of LUV-dispersions with caffeine (a) or hydrocortisone (b) and various amount of cholesterol incorporated in the phospholipid bilayers (0, 11 and 25% w/w) after 65 days storage at 6 and 22°C. Each tube represents one replicate out of total two replicates (n=2).